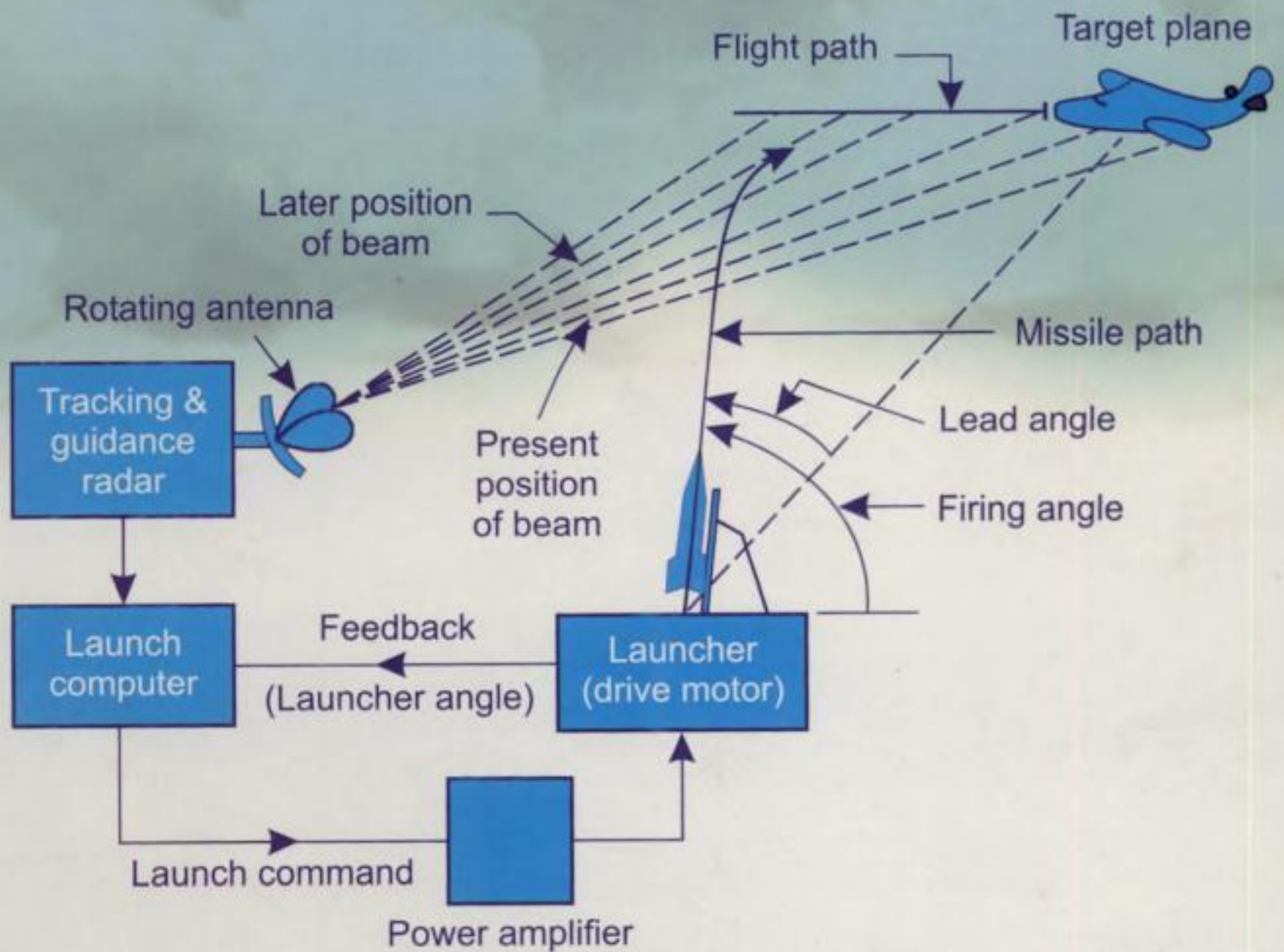


Control Systems Engineering

I.J. NAGRATH • M. GOPAL



Copyright © 2006, 1998, 1982, 1975, New Age International (P) Ltd., Publishers
Published by New Age International (P) Ltd., Publishers
First Edition : 1975
Fourth Edition : 2006

All rights reserved.

No part of this book may be reproduced in any form, by photostat, microfilm, xerography, or any other means, or incorporated into any information retrieval system, electronic or mechanical, without the written permission of the copyright owner.

ISBN : 81-224-1775-2

Rs. 695.00

C-05-07-261

Printed in India at Ajit Printers, Delhi.

Typeset at Goswami Printers, Delhi.

PUBLISHING FOR ONE WORLD

NEW AGE INTERNATIONAL (P) LIMITED, PUBLISHERS

(formerly Wiley Eastern Limited)

4835/24, Ansari Road, Daryaganj, New Delhi - 110002

Visit us at www.newagepublishers.com

CONTENTS

| | |
|----------------------------------------------------------------------|----------------|
| <i>Preface to the Fourth Edition</i> | v |
| <i>Preface to the Third Edition</i> | vii |
| 1. INTRODUCTION | 1-20 |
| 1.1 The Control System | 2 |
| 1.2 Servomechanisms | 6 |
| 1.3 History and Development of Automatic Control | 10 |
| 1.4 Digital Computer Control | 14 |
| 1.5 Application of Control Theory in Non-engineering Fields | 18 |
| 1.6 The Control Problem | 19 |
| 2. MATHEMATICAL MODELS OF PHYSICAL SYSTEMS | 21-90 |
| 2.1 Introduction | 22 |
| 2.2 Differential Equations of Physical Systems | 24 |
| 2.3 Dynamics of Robotic Mechanisms | 42 |
| 2.4 Transfer Functions | 46 |
| 2.5 Block Diagram Algebra | 54 |
| 2.6 Signal Flow Graphs | 62 |
| 2.7 Illustrative Examples | 72 |
| Problems | 83 |
| 3. FEEDBACK CHARACTERISTICS OF CONTROL SYSTEMS | 91-129 |
| 3.1 Feedback and Non-feedback Systems | 92 |
| 3.2 Reduction of Parameter Variations by Use of Feedback | 93 |
| 3.3 Control Over System Dynamics by Use of Feedback | 97 |
| 3.4 Control of the Effects of Disturbance Signals by Use of Feedback | 100 |
| 3.5 Linearizing Effect of Feedback | 102 |
| 3.6 Regenerative Feedback | 103 |
| 3.7 Illustrative Examples | 104 |
| Problems | 119 |
| 4. CONTROL SYSTEMS AND COMPONENTS | 131-192 |
| 4.1 Introduction | 132 |
| 4.2 Linear Approximation of Nonlinear Systems | 133 |

- 4.3 Controller Components 134
- 4.4 Stepper Motors 154
- 4.5 Hydraulic Systems 163
- 4.6 Pneumatic Systems 177
- Problems 185

5. TIME RESPONSE ANALYSIS, DESIGN SPECIFICATIONS AND PERFORMANCE INDICES **193–268**

- 5.1 Introduction 194
- 5.2 Standard Test Signals 195
- 5.3 Time Response of First-order Systems 197
- 5.4 Time Response of Second-order Systems 199
- 5.5 Steady-state Errors and Error Constants 210
- 5.6 Effect of Adding a Zero to a System 214
- 5.7 Design Specifications of Second-order Systems 215
- 5.8 Design Considerations for Higher-order Systems 221
- 5.9 Performance Indices 223
- 5.10 Illustrative Examples 227
- 5.11 Robotic Control Systems 237
- 5.12 State Variable Analysis—Laplace Transform Technique 245
- 5.13 The Approximation of Higher-order Systems by Lower-order 248
- Problems 261

6. CONCEPTS OF STABILITY AND ALGEBRAIC CRITERIA **269–295**

- 6.1 The Concept of Stability 270
- 6.2 Necessary Conditions for Stability 275
- 6.3 Hurwitz Stability Criterion 277
- 6.4 Routh Stability Criterion 278
- 6.5 Relative Stability Analysis 287
- 6.6 More on the Routh Stability Criterion 290
- 6.7 Stability of Systems Modelled in State Variable Form 291
- Problems 293

7. THE ROOT LOCUS TECHNIQUE **297–343**

- 7.1 Introduction 298
- 7.2 The Root Locus Concepts 299
- 7.3 Construction Foot Loci 302
- 7.4 Root Contours 327
- 7.5 Systems with Transportation Lag 332
- 7.6 Sensitivity of the Roots of the Characteristic Equation 334
- 7.7 MATLAB: Tool for Design and Analysis of Control Systems—Appendix III 340
- Problems 340

| | |
|---------------------------------------------------------------------------------|----------------|
| 8. FREQUENCY RESPONSE ANALYSIS | 345–376 |
| 8.1 Introduction | 346 |
| 8.2 Correlation between Time and Frequency Response | 347 |
| 8.3 Polar Plots | 352 |
| 8.4 Bode Plots | 355 |
| 8.5 All-pass and Minimum-phase Systems | 366 |
| 8.6 Experimental Determination of Transfer Functions | 367 |
| 8.7 Log-magnitude versus Phase Plots | 370 |
| 8.8 MATLAB: Tool for Design and Analysis of Control Systems—Appendix III | 371 |
| Problems | 374 |
| 9. STABILITY IN FREQUENCY DOMAIN | 377–423 |
| 9.1 Introduction | 378 |
| 9.2 Mathematical Preliminaries | 378 |
| 9.3 Nyquist Stability Criterion | 381 |
| 9.4 Assessment of Relative Stability Using Nyquist Criterion | 394 |
| 9.5 Closed-loop Frequency Response | 409 |
| 9.6 Sensitivity Analysis in Frequency Domain | 417 |
| Problems | 420 |
| 10. INTRODUCTION TO DESIGN | 425–511 |
| 10.1 The Design Problem | 426 |
| 10.2 Preliminary Considerations of Classical Design | 428 |
| 10.3 Realization of Basic Compensators | 435 |
| 10.4 Cascade Compensation in Time Domain | 440 |
| 10.5 Cascade Compensation in Frequency Domain | 459 |
| 10.6 Tuning of PID Controllers | 477 |
| 10.7 Feedback Compensation | 483 |
| 10.8 Robust Control System Design | 490 |
| Problems | 506 |
| 11. DIGITAL CONTROL SYSTEMS | 513–568 |
| 11.1 Introduction | 514 |
| 11.2 Spectrum Analysis of Sampling Process | 517 |
| 11.3 Signal Reconstruction | 519 |
| 11.4 Difference Equations | 519 |
| 11.5 The z -transform | 521 |
| 11.6 The z -transfer Function (Pulse Transfer Function) | 531 |
| 11.7 The Inverse z -transform and Response of Linear Discrete Systems | 535 |
| 11.8 The z -transform Analysis of Sampled-data Control Systems | 538 |
| 11.9 The z- and s-domain Relationship | 548 |

| | | | |
|------------|------------------------------------------------------------------|-----|----------------|
| 11.10 | Stability Analysis | 549 | |
| 11.11 | Compensation Techniques | 558 | |
| | Problems | 564 | |
| 12. | STATE VARIABLE ANALYSIS AND DESIGN | | 569–640 |
| 12.1 | Introduction | 570 | |
| 12.2 | Concepts of State, State Variables and State Model | 571 | |
| 12.3 | State Models for Linear Continuous-Time Systems | 578 | |
| 12.4 | State Variables and Linear Discrete-Time Systems | 596 | |
| 12.5 | Diagonalization | 599 | |
| 12.6 | Solution of State Equations | 604 | |
| 12.7 | Concepts of Controllability and Observability | 617 | |
| 12.8 | Pole Placement by State Feedback | 625 | |
| 12.9 | Observer Systems | 632 | |
| | Problems | 634 | |
| 13. | LIAPUNOV'S STABILITY ANALYSIS | | 641–662 |
| 13.1 | Introduction | 642 | |
| 13.2 | Liapunov's Stability Criterion | 646 | |
| 13.3 | The Direct Method of Liapunov and the Linear System | 650 | |
| 13.4 | Methods of Constructing Liapunov Functions for Nonlinear Systems | 652 | |
| | Problems | 660 | |
| 14. | OPTIMAL CONTROL SYSTEMS | | 663–712 |
| 14.1 | Introduction | 664 | |
| 14.2 | Parameter Optimization: Servomechanisms | 665 | |
| 14.3 | Optimal Control Problems: Transfer Function Approach | 673 | |
| 14.4 | Optimal Control Problems: State Variable Approach | 684 | |
| 14.5 | The State Regulator Problem | 688 | |
| 14.6 | The Infinite-time Regulator Problem | 697 | |
| 14.7 | The Output Regulator and the Tracking Problems | 702 | |
| 14.8 | Parameter Optimization: Regulators | 704 | |
| | Problems | 707 | |
| 15. | ADVANCES IN CONTROL SYSTEMS | | 713–763 |
| 15.1 | Introduction | 714 | |
| 15.2 | Adaptive Control | 715 | |
| 15.3 | Fuzzy Logic Control | 731 | |
| 15.4 | Neural Networks | 749 | |
| | Problems | 760 | |

APPENDICES

Appendix-I Fourier and Laplace Transforms and Partial Fractions 766

Appendix-II Element of Matrix Analysis 775

Appendix-IV MATLAB : Tool for Design and Analysis of Control Systems 784

Appendix-V Final Value Theorem 796

Appendix-VI Proof of a Transformation 797

Appendix-VII Answers to Problems 800

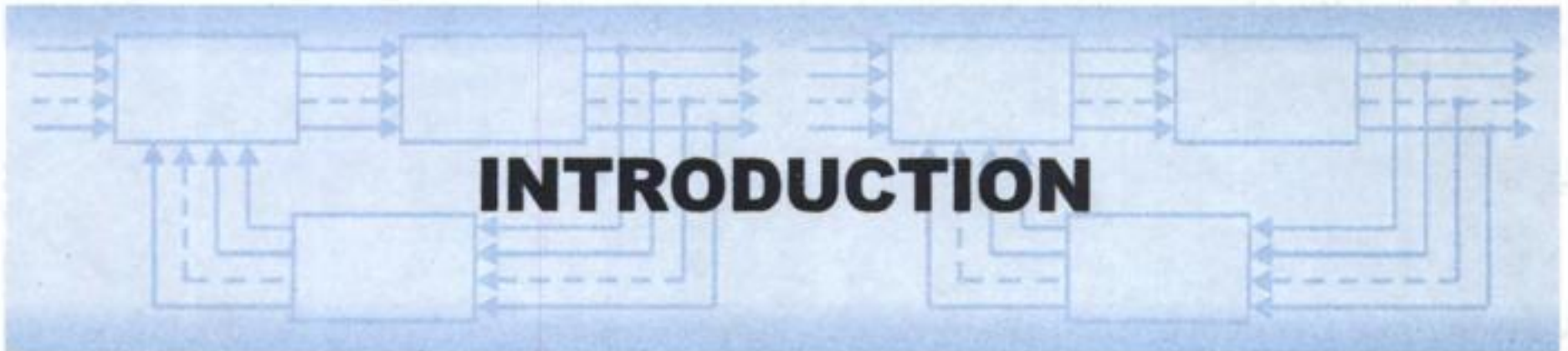
Bibliography 817-833

Index 835-843

1

INTRODUCTION

1



1.1 THE CONTROL SYSTEM

The control system is that means by which any quantity of interest in a machine, mechanism or other equipment is maintained or altered in accordance with a desired manner. Consider, for example, the driving system of an automobile. Speed of the automobile is a function of the position of its accelerator. The desired speed can be maintained (or a desired change in speed can be achieved) by controlling pressure on the accelerator pedal. This automobile driving system (accelerator, carburettor and engine-vehicle) constitutes a control system. Figure 1.1 shows the general diagrammatic representation of a typical control system. For the automobile driving system the input (command) signal is the force on the accelerator pedal which through linkages causes the carburettor valve to open (close) so as to increase or decrease fuel (liquid form) flow to the engine bringing the engine-vehicle speed (controlled variable) to the desired value.

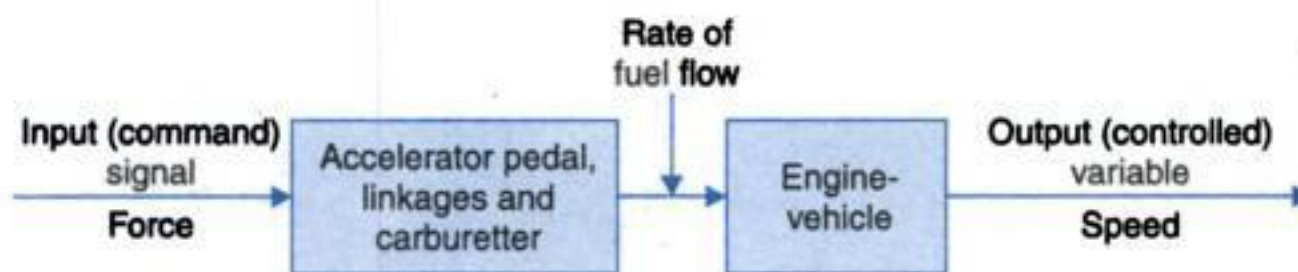


Fig. 1.1. The basic control system.

The diagrammatic representation of Fig. 1.1 is known as *block diagram* representation wherein each block represents an element, a plant, mechanism, device etc., whose inner details are not indicated. Each block has an input and output signal which are linked by a relationship characterizing the block. It may be noted that the signal flow through the block is unidirectional.

Closed-Loop Control

Let us reconsider the automobile driving system. The route, speed and acceleration of the automobile are determined and controlled by the driver by observing traffic and road conditions and by properly manipulating the accelerator, clutch, gear-lever, brakes and steering wheel, etc. Suppose the driver wants to maintain a speed of 50 km per hour (desired output). He accelerates the automobile to this speed with the help of the accelerator and then maintains it by holding the accelerator steady. No error in the speed of the automobile occurs so long as there are no gradients or other disturbances along the road. The actual speed of the automobile is measured by the speedometer and indicated on its dial. The driver reads the speed dial visually and compares the actual speed with the desired one mentally. If there is a deviation of speed from the desired speed, accordingly he takes the decision to increase or decrease the speed. The decision is executed by change in pressure of his foot (through muscular power) on the accelerator pedal.

These operations can be represented in a diagrammatic form as shown in Fig. 1.2. In contrast to the sequence of events in Fig. 1.1, the events in the control sequence of Fig. 1.2 follow a closed-loop, *i.e.*, the information about the instantaneous state of the output is feedback to the input and is used to modify it in such a manner as to achieve the desired output. It is on account of this basic difference that the system of Fig. 1.1 is called an *open-loop system*, while the system of Fig. 1.2 is called a *closed-loop system*.

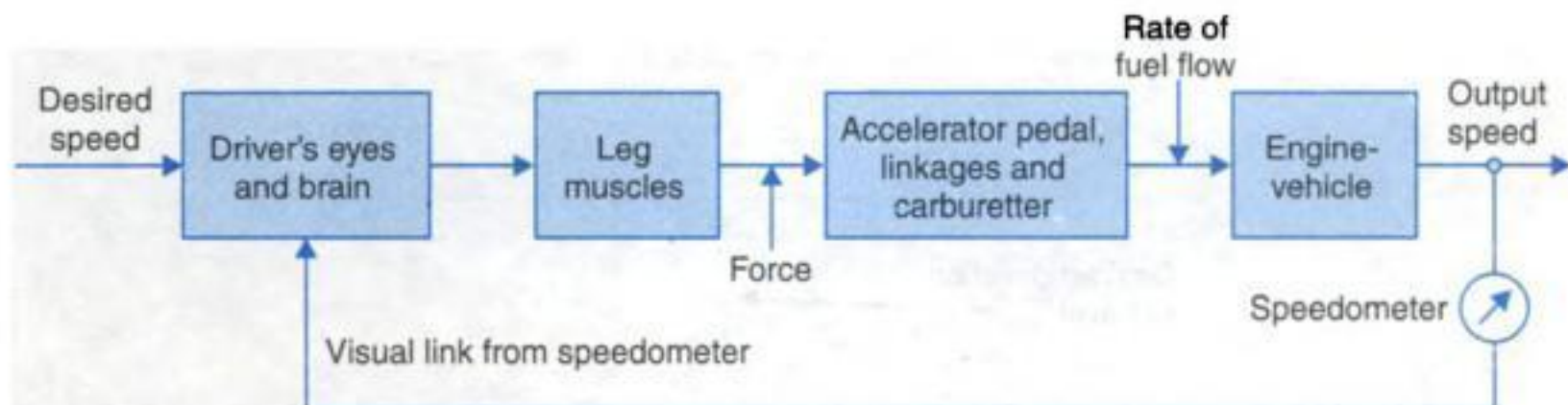


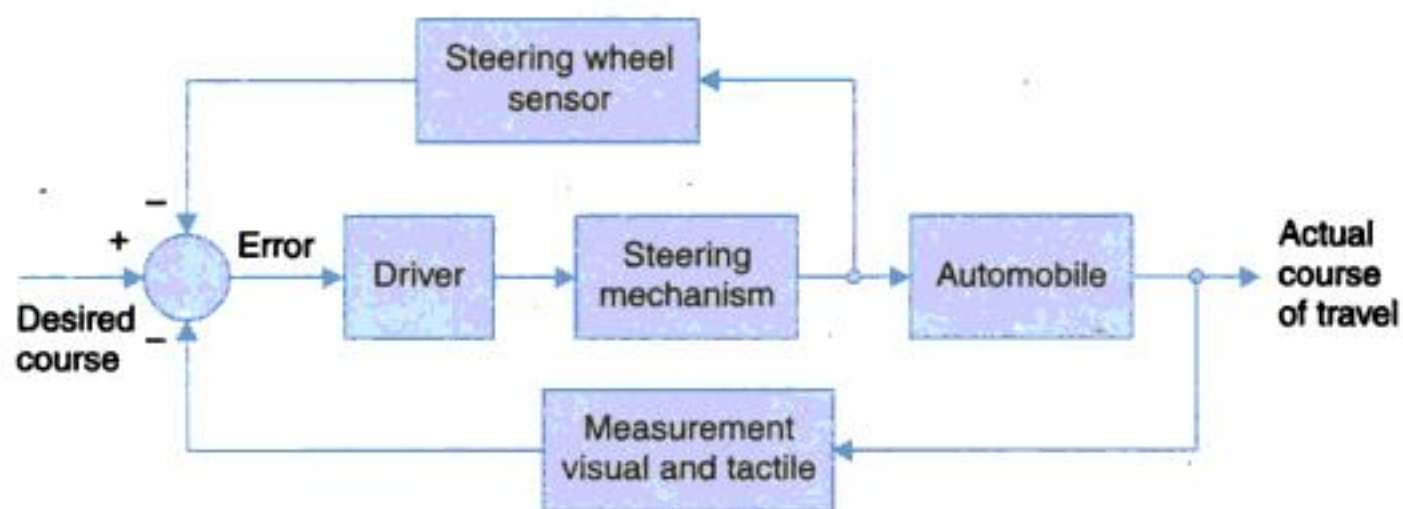
Fig. 1.2. Schematic diagram of a manually controlled closed-loop system.

Let us investigate another control aspect of the above example of an automobile (engine vehicle) say its steering mechanism. A simple block diagram of an automobile steering mechanism is shown in Fig. 1.3(a). The driver senses visually and by tactile means (body movement) the error between the actual and desired directions of the automobile as in Fig. 1.3(b). Additional information is available to the driver from the feel (sensing) of the steering wheel through his hand(s), these informations constitute the feedback signal(s) which are interpreted by driver's brain, who then signals his hand to adjust the steering wheel accordingly. This again is an example of a closed-loop system where human visual and tactile measurements constitute the feedback loop.

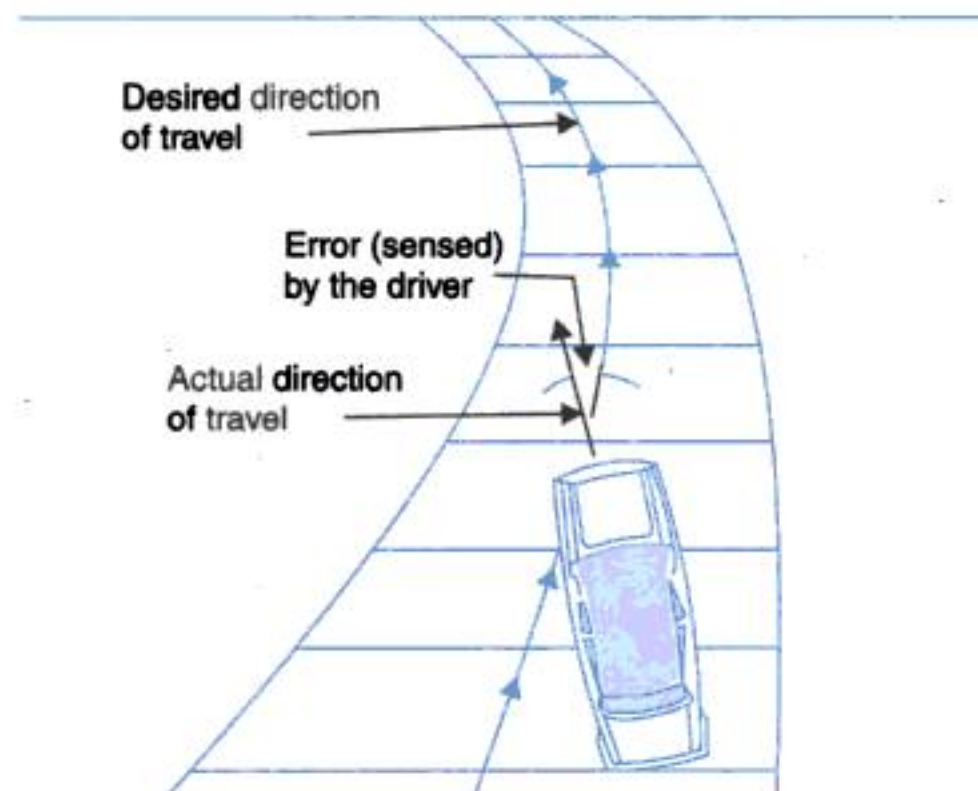
In fact unless human being(s) are not left out of in a control system study practically all control systems are a sort of closed-loop system (with intelligent measurement and sensing loop or there may indeed be several such loops).

Systems of the type represented in Figs. 1.2 and 1.3 involve continuous manual control by a human operator. These are classified as *manually controlled systems*. In many complex

and fast-acting systems, the presence of human element in the control loop is undesirable because the system response may be too rapid for an operator to follow or the demand on operator's skill may be unreasonably high. Furthermore, some of the systems, e.g., missiles, are self-destructive and in such systems human element must be excluded. Even in situations where manual control could be possible, an economic case can often be made out for reduction of human supervision. Thus in most situations the use of some equipment which performs the same intended function as a continuously employed human operator is preferred. A system incorporating such an equipment is known as *automatic control system*. In fact in most situations an automatic control system could be made to perform intended functions better than a human operator, and could further be made to perform such functions as would be impossible for a human operator.



(a)



(b)

Fig. 1.3. (a) Automobile steering control system. (b) The driver uses the difference between the actual and desired direction of travel to adjust the steering wheel accordingly.

The general block diagram of an automatic control system which is characterised by a feedback loop, is shown in Fig. 1.4. An error detector compares a signal obtained through

feedback elements, which is a function of the output response, with the reference input. Any difference between these two signals constitutes an error or actuating signal, which actuates the control elements. The control elements in turn alter the conditions in the plant (controlled member) in such a manner as to reduce the original error.

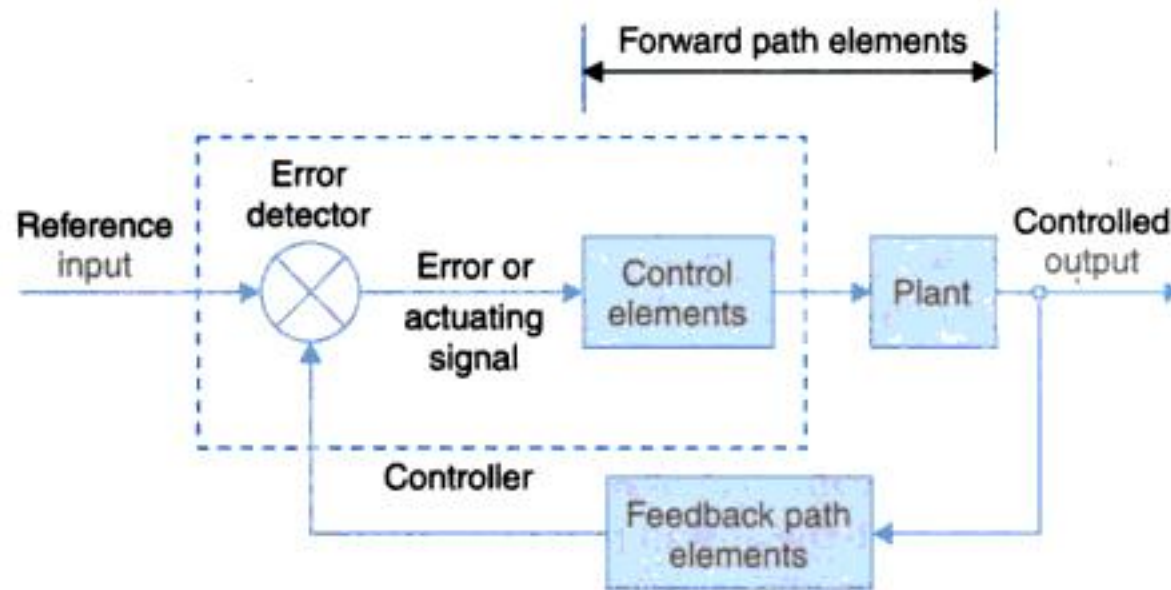


Fig. 1.4. General block diagram of an automatic control system.

In order to gain a better understanding of the interactions of the constituents of a control system, let us discuss a simple tank level control system shown in Fig. 1.5. This control system can maintain the liquid level h (controlled output) of the tank within accurate tolerance of the

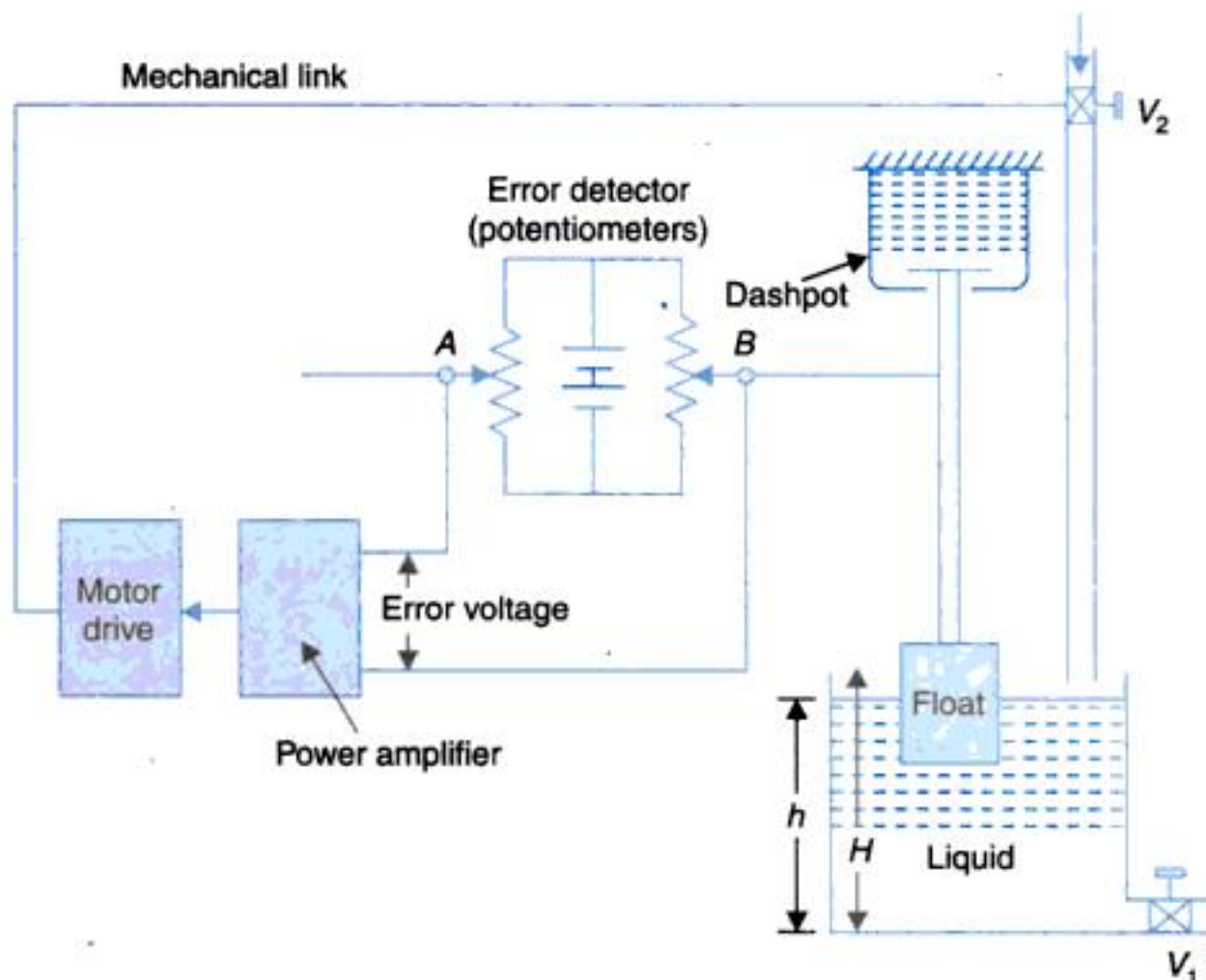


Fig. 1.5. Automatic tank-level control system.

desired liquid level even though the output flow rate through the valve V_1 is varied. The liquid level is sensed by a float (feedback path element), which positions the slider arm B on a

potentiometer. The slider arm A of another potentiometer is positioned corresponding to the desired liquid level H (the reference input). When the liquid level rises or falls, the potentiometers (error detector) give an error voltage (error or actuating signal) proportional to the change in liquid level. The error voltage actuates the motor through a power amplifier (control elements) which in turn conditions the plant (*i.e.*, decreases or increases the opening of the valve V_2) in order to restore the desired liquid level. Thus the control system automatically attempts to correct any deviation between the actual and desired liquid levels in the tank.

Open-Loop Control

As stated already, any physical system which does not automatically correct for variation in its output, is called an open-loop system. Such a system may be represented by the block diagram of Fig. 1.6. In these systems the output remains constant for a constant input signal provided the external conditions remain unaltered. The output may be changed to any desired value by appropriately changing the input signal but variations in external conditions or internal parameters of the system may cause the output to vary from the desired value in an uncontrolled fashion. The open-loop control is, therefore, satisfactory only if such fluctuations can be tolerated or system components are designed and constructed so as to limit parameter variations and environmental conditions are well-controlled.

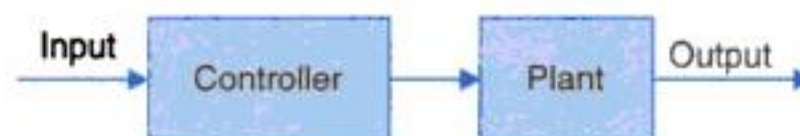


Fig. 1.6. General block diagram of open-loop system.

It is important to note that the fundamental difference between an open and closed-loop control system is that of feedback action. Consider, for example, a traffic control system for regulating the flow of traffic at the crossing of two roads. The system will be termed open-loop if red and green lights are put on by a timer mechanism set for predetermined fixed intervals of time. It is obvious that such an arrangement takes no account of varying rates of traffic flowing to the road crossing from the two directions. If on the other hand a scheme is introduced in which the rates of traffic flow along both directions are measured (some distance ahead of the crossing) and are compared and the difference is used to control the timings of red and green lights, a closed-loop system (feedback control) results. Thus the concept of feedback can be usefully employed to traffic control.

Unfortunately, the feedback which is the underlying principle of most control systems, introduces the possibility of undesirable system oscillations (hunting). Detailed discussion of feedback principle and the linked problem of stability are dealt with later in the book.

1.2 SERVOMECHANISMS

In modern usage the term *servomechanism* or servo is restricted to feedback control systems in which the controlled variable is mechanical position or time derivatives of position, *e.g.*, velocity and acceleration.

A servo system used to position a load shaft is shown in Fig. 1.7 in which the driving motor is geared to the load to be moved. The output (controlled) and desired (reference) positions θ_C and θ_R respectively are measured and compared by a potentiometer pair whose output voltage v_E is proportional to the error in angular position $\theta_E = \theta_R - \theta_C$. The voltage $v_E = K_p \theta_E$ is amplified and is used to control the field current (excitation) of a dc generator which supplies the armature voltage to the drive motor.

To understand the operation of the system assume $K_p = 100$ volts/rad and let the output shaft position be 0.5 rad. Corresponding to this condition, the slider arm B has a voltage of +50 volts. Let the slider arm A be also set at +50 volts. This gives zero actuating signal ($v_E = 0$). Thus the motor has zero output torque so that the load stays stationary at 0.5 rad.

Assume now that the new desired load position is 0.6 rad. To achieve this, the arm A is placed at +60 volts position, while the arm B remains instantaneously at +50 volts position. This creates an actuating signal of +10 volts, which is a measure of lack of correspondence between the actual load position and the commanded position. The actuating signal is amplified and fed to the servo motor which in turn generates an output torque which repositions the load. The system comes to a standstill only when the actuating signal becomes zero, *i.e.*, the arm B and the load reach the position corresponding to 0.6 rad (+60 volts position).

Consider now that a load torque T_L is applied at the output as indicated in Fig. 1.7. This will require a steady value of error voltage v_E which acting through the amplifier, generator, motor and gears will counterbalance the load torque. This would mean that a steady error will exist between the input and output angles. This is unlike the case when there is no load torque and consequently the angle error is zero. In control terminology, such loads are known as load disturbances and system has to be designed to keep the error to these disturbances within specified limits.

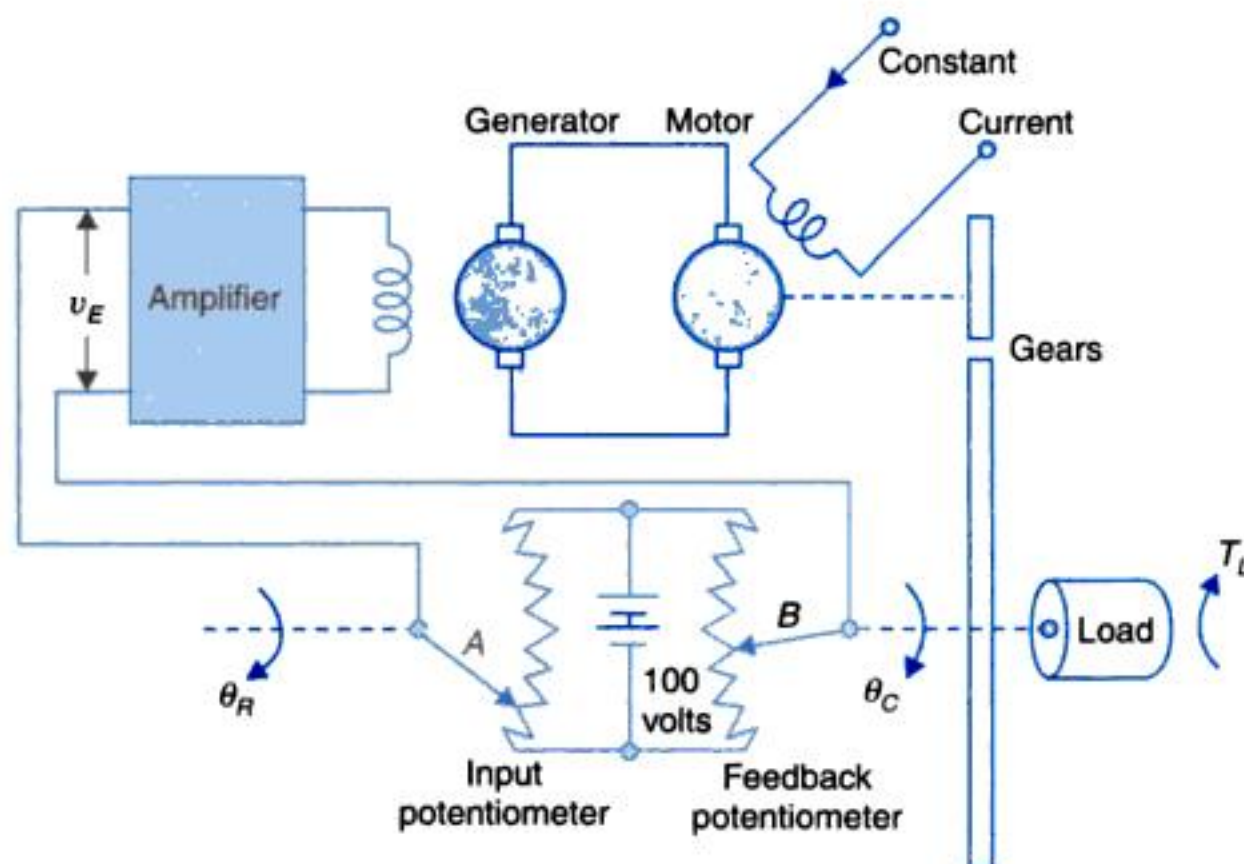


Fig. 1.7. A position control system.

By opening the feedback loop *i.e.*, disconnecting the potentiometer B , the reader can easily verify that any operator acting as part of feedback loop will find it very difficult to adjust θ_c to a desired value and to be able to maintain it. This further demonstrates the power of a negative feedback (hardware) loop.

The position control systems have innumerable applications, namely, machine tool position control, constant-tension control of sheet rolls in paper mills, control of sheet metal thickness in hot rolling mills, radar tracking systems, missile guidance systems, inertial guidance, roll stabilization of ships, etc. Some of these applications will be discussed in this book.

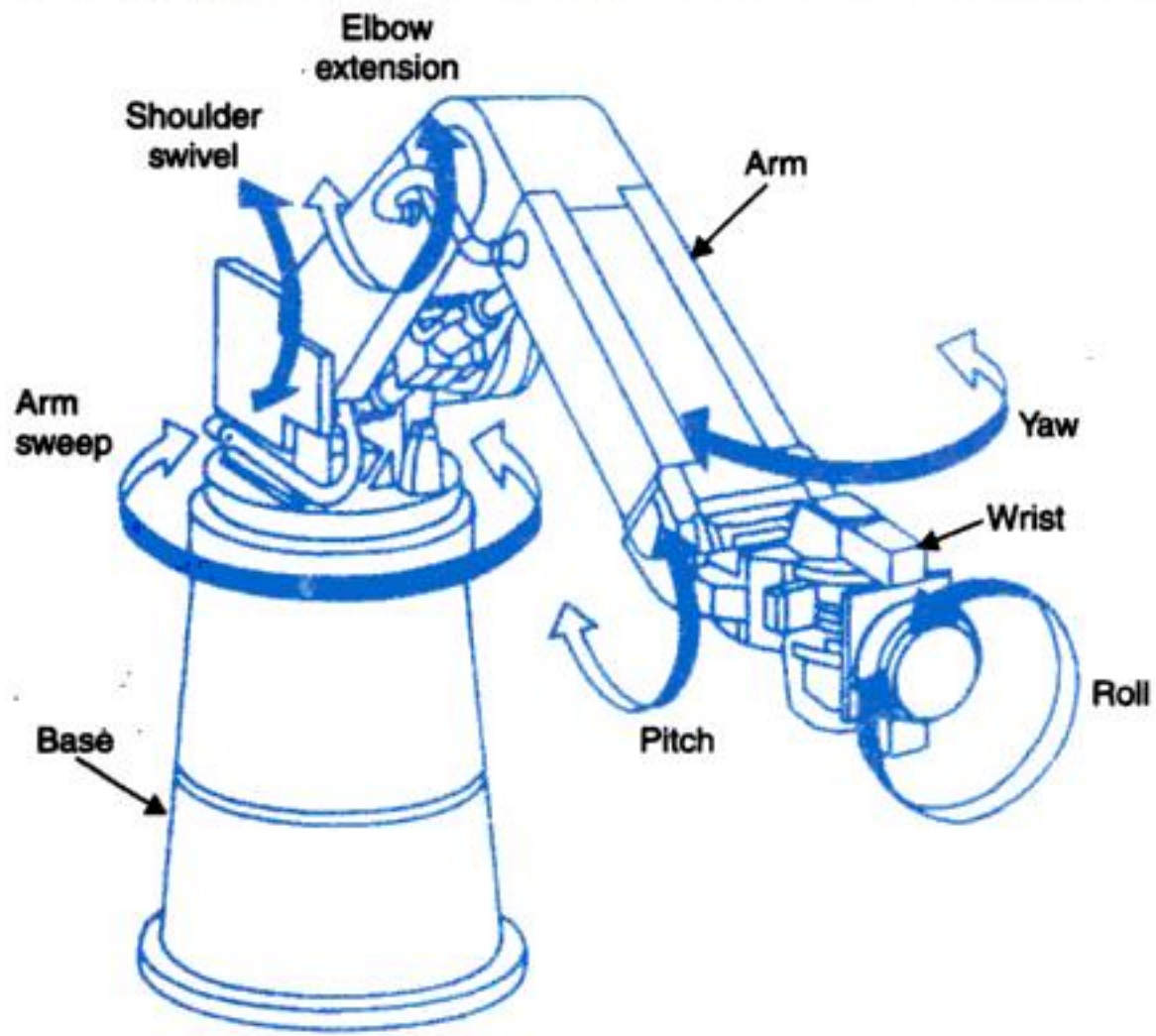
Robotics

Advances in servo mechanism has led to the development of the new field of control and automation, the robots and robotology. A robot is a mechanism devised to perform repetitive tasks which are tiresome for a human being or tasks to be performed in a hazardous environment say in a radioactive area. Robots are as varied as the tasks that can be imagined to be performed by them. Great strides are being made in this field with the explosion in the power of digital computer, interfacing and software tools which have brought to reality the application of vision and artificial intelligent for devising more versatile robots and increased applications of robotology in industrial automation. In fact in replacing a human being for a repetitive and/or hazardous task the robots can perform the task at a greater speed (so increased productivity) and higher precision (better quality and higher reliability of the product or service).

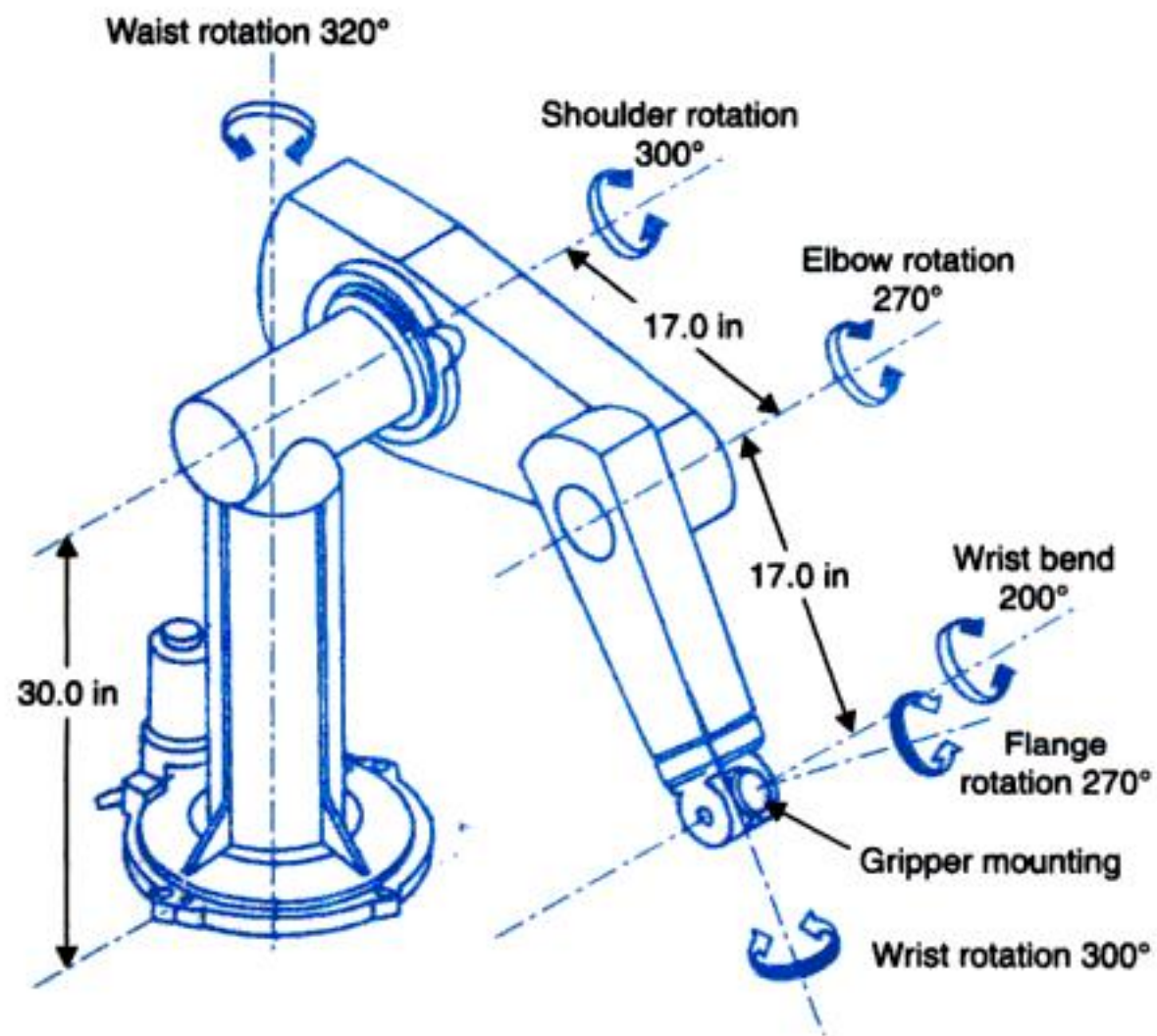
We shall describe here a robot manipulator arm as an example. The arm is devised to preform some of the tasks performed by a human arm (shoulder, elbow and wrist). Imitation of some of the elementary functions of hand is carried out by an end effector with three degrees of freedom in general (roll, yaw and pitch). The robot arm is a set of serial links with the beginning of each link jointed with the end of the preceeding link in form of a revolute joint (for relative rotary motion between the two links) or a prismatic joint (for relative translatory motion). The number of joints determine the degrees of freedom of the arm.

Figures 1.8 (a) and (b) show the schematic diagrams of two kinds of manipulator arms. To reduce joint inertia and gravity loading the drive motors are located in the base and the joints are belt driven. For a programmed trajectory of the manipulator tip, each joint requires not only a controlled angular (or translatory) motion but also controlled velocity, acceleration and torque. Further the mechanism complexity is such that the effective joint inertia may change by as much as 300% during a trajectory traversal. The answer to such control complexity is the computer control. The versatility of high-speed on-line computer further permits the sophistication of control through computer vision, learning of new tasks and other intelligent functions. Manipulators can perform delicate (light) as well as heavy tasks; for example, manipulator can pick up objects weighing hundreds of kilograms and position them with an accuracy of a centimeter or better.

Using robots (specially designed for broken-down tasks) an assembly line in a manufacturing process can be speeded up with added quality and reliability of the end product. Example can be cited of watch industry in Japan where as many as 150 tasks on the assembly are robot executed.



(a)



(b)

Fig. 1.8. (a) Cincinnati Milacron T³ robot arm (b) PUMA 560 series robot arm.

For flexible manufacturing units mobile automations (also called AGV (automated guided vehicle)) have been devised and implemented which are capable of avoiding objects while travelling through a room or industrial plant.

1.3 HISTORY AND DEVELOPMENT OF AUTOMATIC CONTROL

It is instructive to trace brief historical development of automatic control: Automatic control systems did not appear until the middle of eighteenth century. The first automatic control system, the fly-ball governor, to control the speed of steam engines, was invented by James Watt in 1770. This device was usually prone to hunting. It was about hundred years later that Maxwell analyzed the dynamics of the fly-ball governor.

The schematic diagram of a speed control system using a fly-ball governor is shown in Fig. 1.9. The governor is directly geared to the output shaft so that the speed of the fly-balls is proportional to the output speed of the engine. The position of the throttle lever sets the desired speed. The lever pivoted as shown in Fig. 1.9 transmits the centrifugal force from the fly-balls to the bottom of the lower seat of the spring. Under steady conditions, the centrifugal force of the fly-balls balances the spring force* and the opening of flow control valve is just sufficient to maintain the engine speed at the desired value.

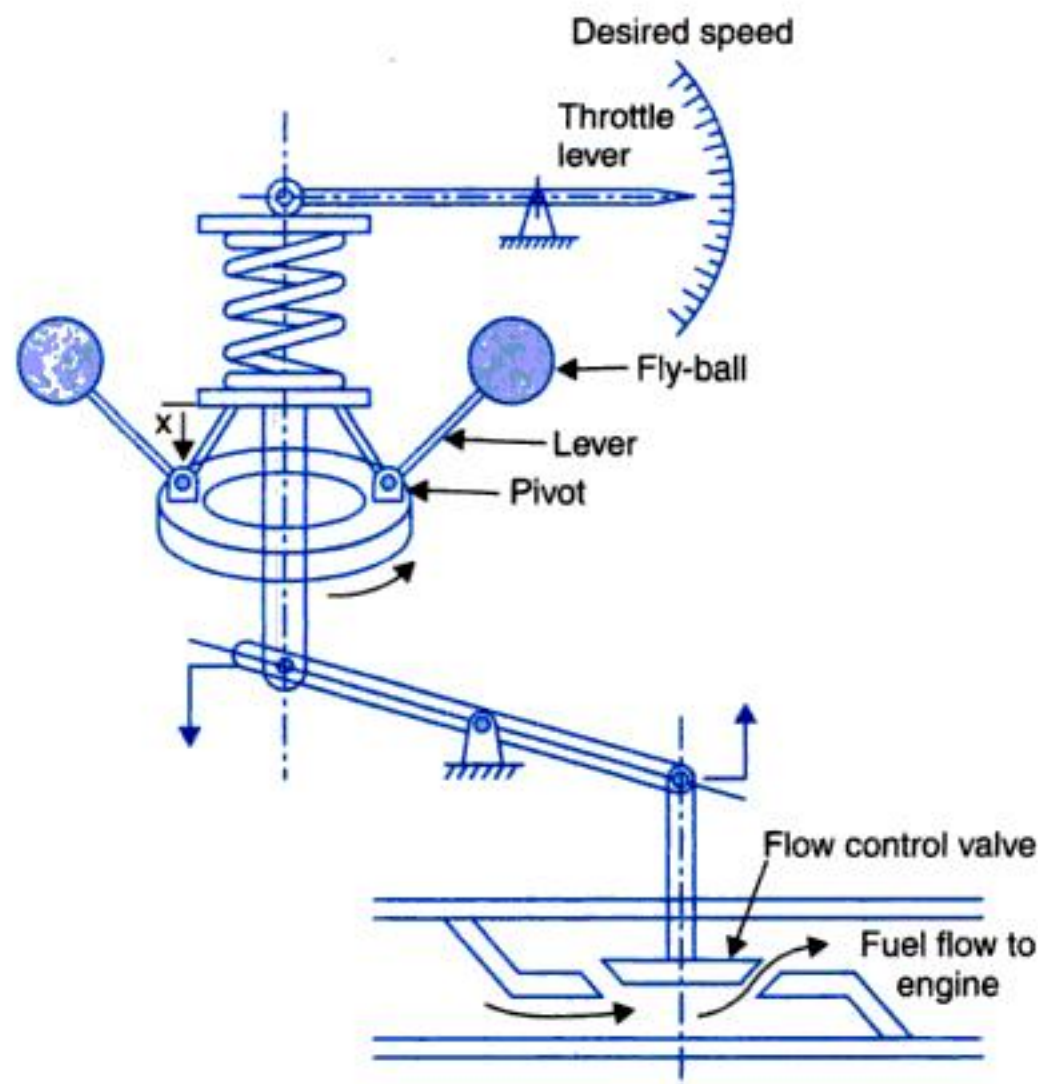


Fig. 1.9. Speed control system.

* The gravitational forces are normally negligible compared to the centrifugal force.

If the engine speed drops below the desired value, the centrifugal force of the fly-balls decreases, thus decreasing the force exerted on the bottom of the spring, causing x to move downward. By lever action, this results in wider opening of the control valve and hence more fuel supply which increases the speed of the engine until equilibrium is restored. If the speed increases, the reverse action takes place.

The change in desired engine speed can be achieved by adjusting the setting of throttle lever. For a higher speed setting, the throttle lever is moved up which in turn causes x to move downward resulting in wider opening of the fuel control valve with consequent increase of speed. The lower speed setting is achieved by reverse action.

The importance of positioning heavy masses like ships and guns quickly and precisely was realized during the World War I. In early 1920, Minorsky performed the classic work on the automatic steering of ships and positioning of guns on the shipboards.

A date of significance in automatic control systems is that of Hazen's work in 1934. His work may possibly be considered as a first struggling attempt to develop some general theory for servomechanisms. The word 'servo' has originated with him.

Prior to 1940 automatic control theory was not much developed and for most cases the design of control systems was indeed an art. During the decade of 1940's, mathematical and analytical methods were developed and practised and control engineering was established as an engineering discipline in its own rights. During the World War II it became necessary to design and construct automatic aeroplane pilots, gun positioning systems, radar tracking systems and other military equipments based on feedback control principle. This gave a great impetus to the automatic control theory.

The missile launching and guidance system of Fig. 1.10 is a sophisticated example of military applications of feedback control. The target plane is sighted by a rotating radar antenna which then locks in and continuously tracks the target. Depending upon the position and velocity of the plane as given by the radar output data, the launch computer calculates the firing angle in terms of a launch command signal, which when amplified through a power amplifier drives the launcher (drive motor). The launcher angular position is feedback to the launch computer and the missile is triggered as soon as the error between the launch command signal and the missile firing angle becomes zero. After being fired the missile enters the radar beam which is tracking the target. The control system contained within the missile now receives a guidance signal from the beam which automatically adjusts the control surface of the missile such that the missile rides along the beam, finally homing on to the target.

It is important to note that the actual missile launching and guidance system is far more complex requiring control of gun's bearing as well as elevation. The simplified case discussed above illustrates the principle of feedback control.

The industrial use of automatic control has tremendously increased since the World War II. Modern industrial processes such as manufacture and treatment of chemicals and metals are now automatically controlled.

A simple example of an automatically controlled industrial process is shown in Fig. 1.11. This is a scheme employed in paper mills for reeling paper sheets. For best results the paper sheet must be pulled on to the wind-up roll at nearly constant tension. A reduction in tension

will produce a loose roll, while an increase in tension may result in tearing of the paper sheet. If reel speed is constant, the linear velocity of paper and hence its tension increases, as the wind-up roll diameter increases. Tension control may be achieved by suitably varying the reel speed.

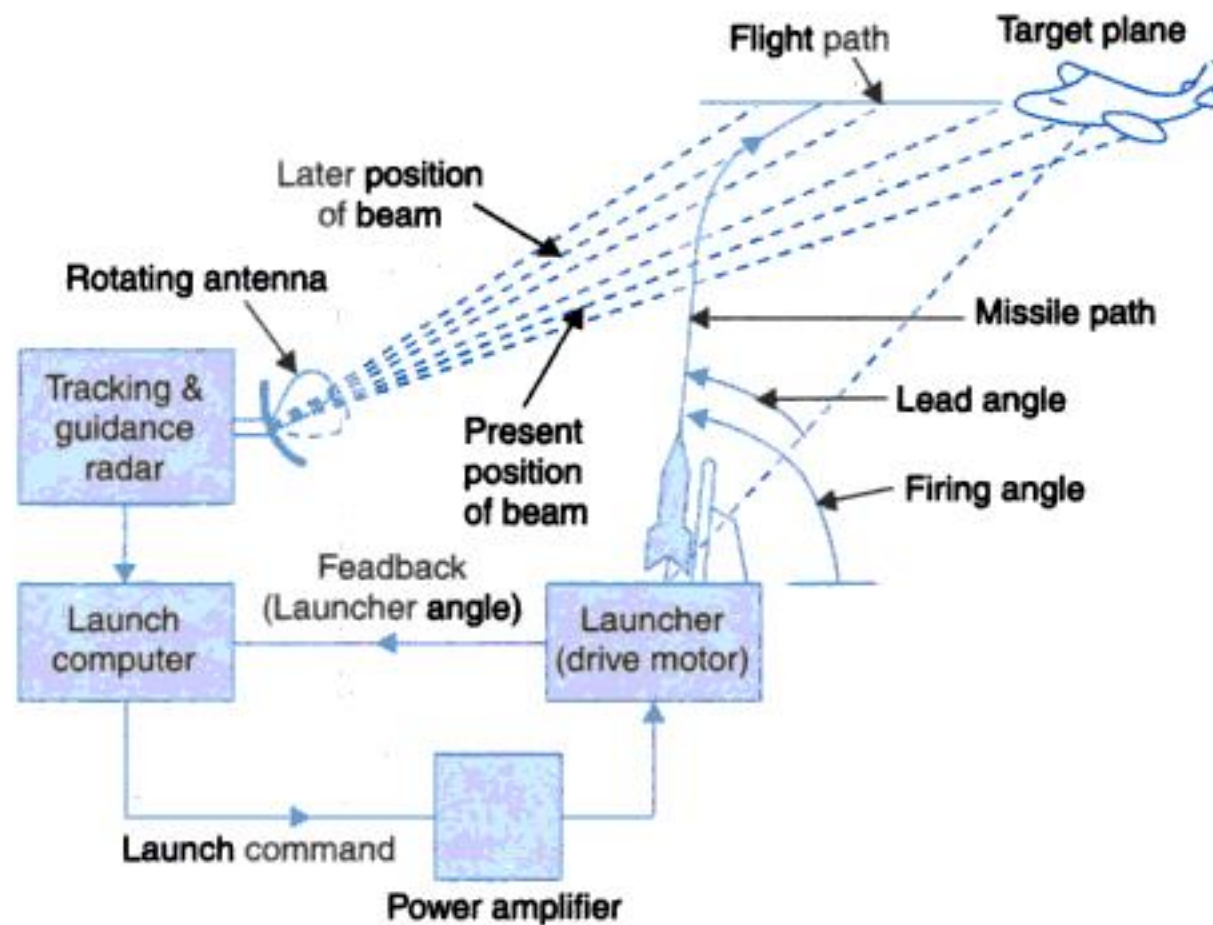


Fig. 1.10. Missile launching and guidance system.

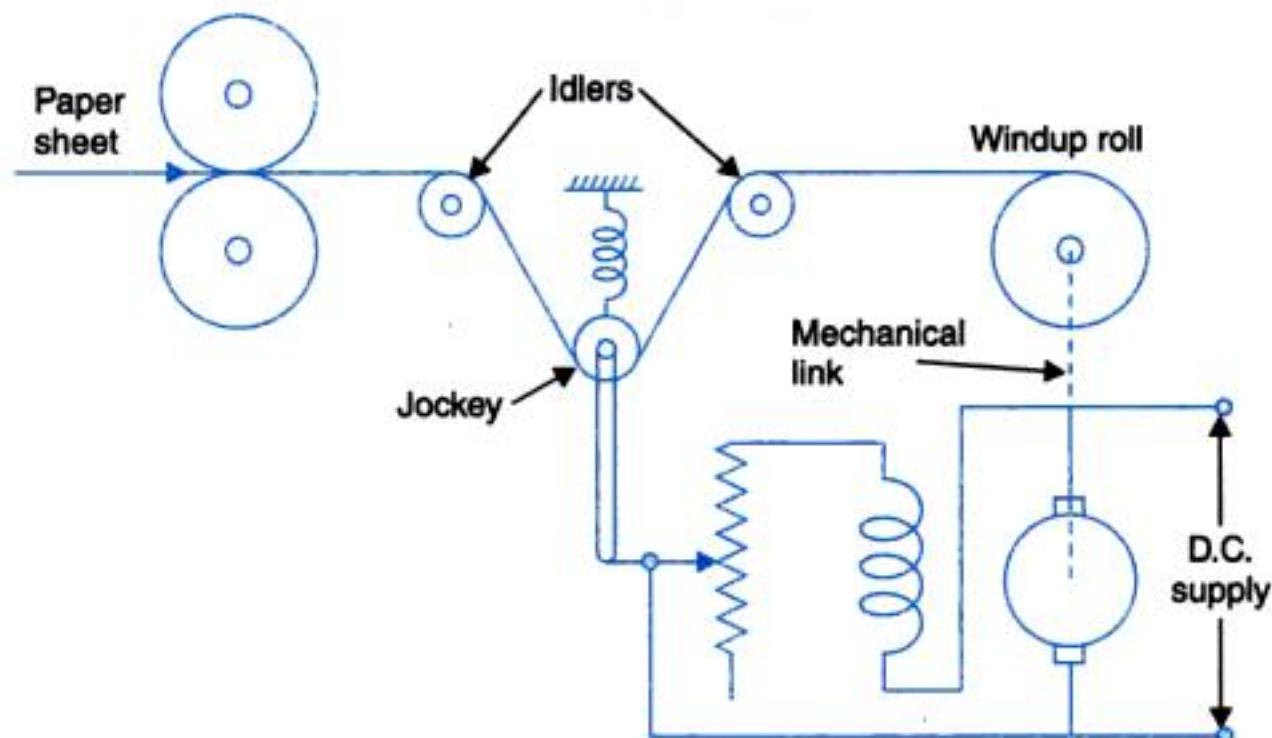


Fig. 1.11. A constant tension reeling system.

In the scheme shown in Fig. 1.11 the paper sheet passes over two idling and one jockey roll. The jockey roll is constrained to vertical motion only with its weight supported by paper tension and spring. Any change in tension moves the jockey in vertical direction, upward for increased tension and downward for decreased tension. The vertical motion of the jockey is used to change the field current of the drive motor and hence the speed of wind-up roll which adjusts the tension.

Another example of controlled industrial processes is a batch chemical reactor shown in Fig. 1.12. The reactants are initially charged into the reaction vessel of the batch reactor and are then agitated for a certain period of time to allow the reaction to take place. Upon completion of the reaction, the products are discharged.

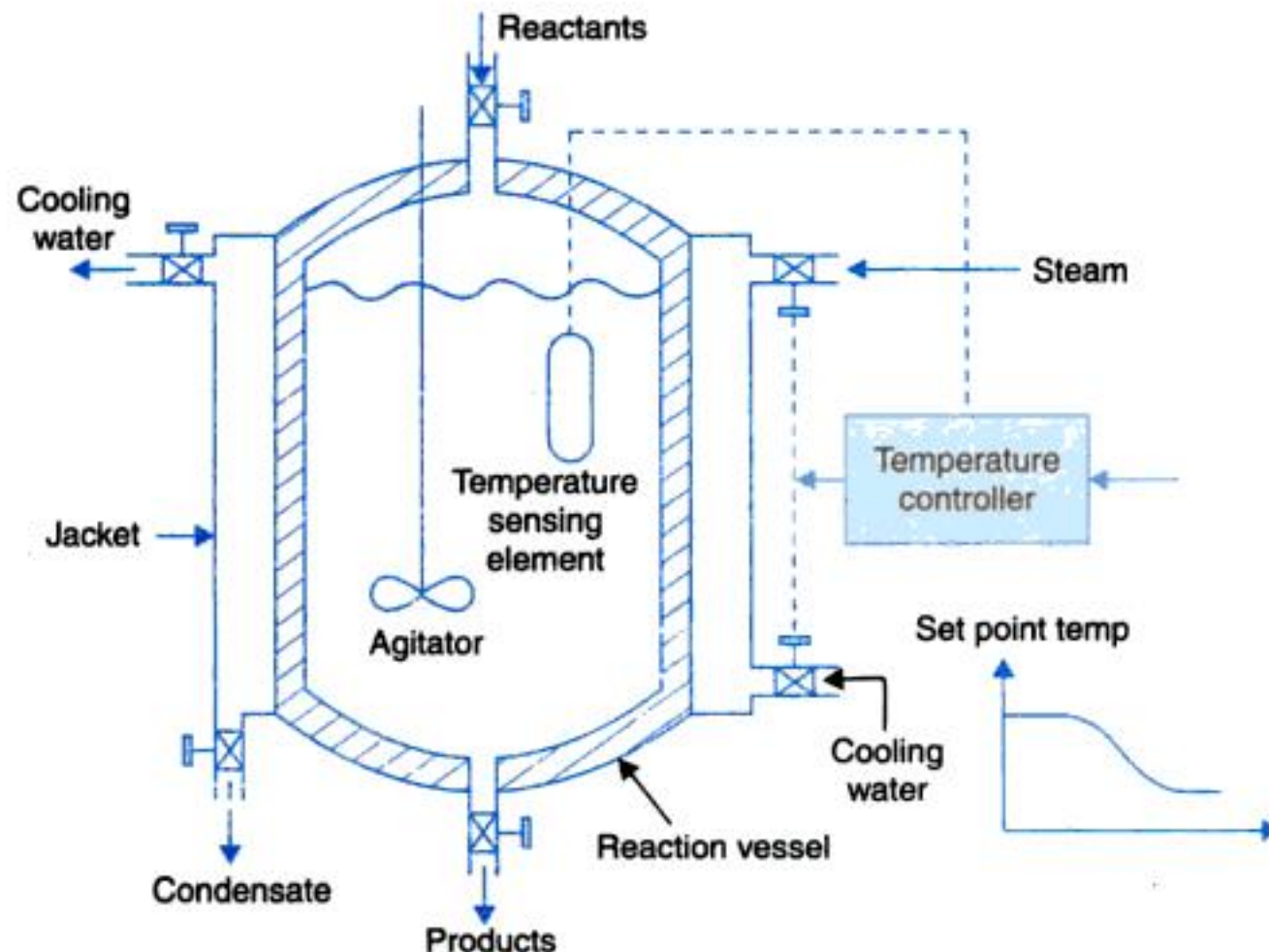


Fig. 1.12. A batch chemical process.

For a specific reaction there is an optimum temperature profile according to which the temperature of the reactor mass should be varied to obtain best results. Automatic temperature control is achieved by providing both steam and cooling water jackets for heating or cooling the reactor mass (cooling is required to remove exothermic heat of reaction during the period the reaction proceeds vigorously). During the heating phase, the controller closes the water inlet valve and opens and controls the steam inlet valve while the condensate valve is kept open. Reverse action takes place during the cooling phase.

Control engineering has enjoyed tremendous growth during the years since 1955. Particularly with the advent of analog and digital computers and with the perfection achieved in computer field, highly sophisticated control schemes have been devised and implemented. Furthermore, computers have opened up vast vistas for applying control concepts to non-engineering fields like business and management. On the technological front fully automated computer control schemes have been introduced for electric utilities and many complex industrial processes with several interacting variables particularly in the chemical and metallurgical processes.

A glorious future lies ahead for automation wherein computer control can run our industries and produce our consumer goods provided we can tackle with equal vigour and success the socio-economic and resource depletion problems associated with such sophisticated degree of automation.

1.4 DIGITAL COMPUTER CONTROL

In some of the examples of control systems of high level of complexity (robot manipulator of Fig. 1.9 and missile launching and guidance system of Fig. 1.11) it is seen that such control systems need a digital computer as a control element to digitally process a number of input signals to generate a number of control signals so as to manipulate several plant variables. In these control systems signals in certain parts of the plant are in analog form *i.e.*, continuous functions of the time variable, while the control computer handles data only in digital (or discrete) form. This requires signal discretization and analog-to-digital interfacing in form of *A/D* and *D/A* converters.

To begin with we will consider a simple form the digital control system known as sampled-data control system. The block diagram of such a system with single feedback loop is illustrated in Fig. 1.13 wherein the sampler samples the error signal $e(t)$ every T seconds. The sampler is an electronic switch whose output is the discretized version of the analog error signal and is a train of pulses of the sampling frequency with the strength of each pulse being that of the error signal at the beginning of the sampling period. The sampled signal is passed through a data hold and is then filtered by a digital filter in accordance with the control algorithm. The smoothed out control signal $u(t)$ is then used to manipulate the plant.

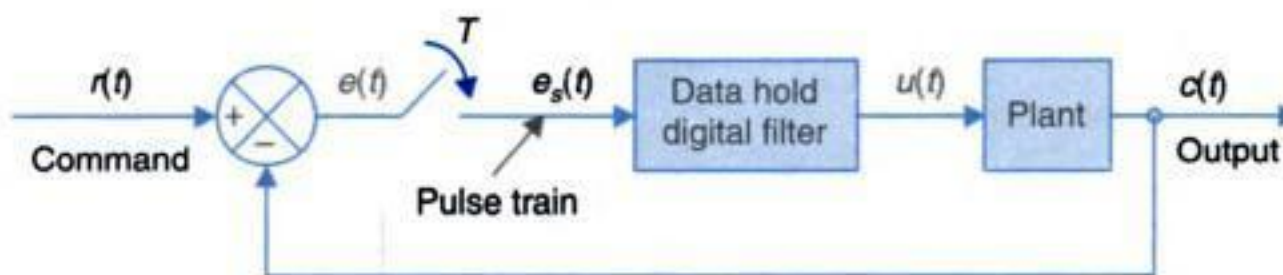


Fig. 1.13. Block diagram of a sampled-data control system.

It is seen above that computer control is needed in large and complex control schemes dealing with a number of input, output variables and feedback channels. This is borne out by the examples of Fig. 1.9 and 1.11. Further in chemical plants, a number of variables like temperatures, pressures and fluid flows have to be controlled after the information on throughput, its quality and its constitutional composition has been analyzed on-line. Such systems are referred to as multivariable control systems whose general block diagram is shown in Fig. 1.14.

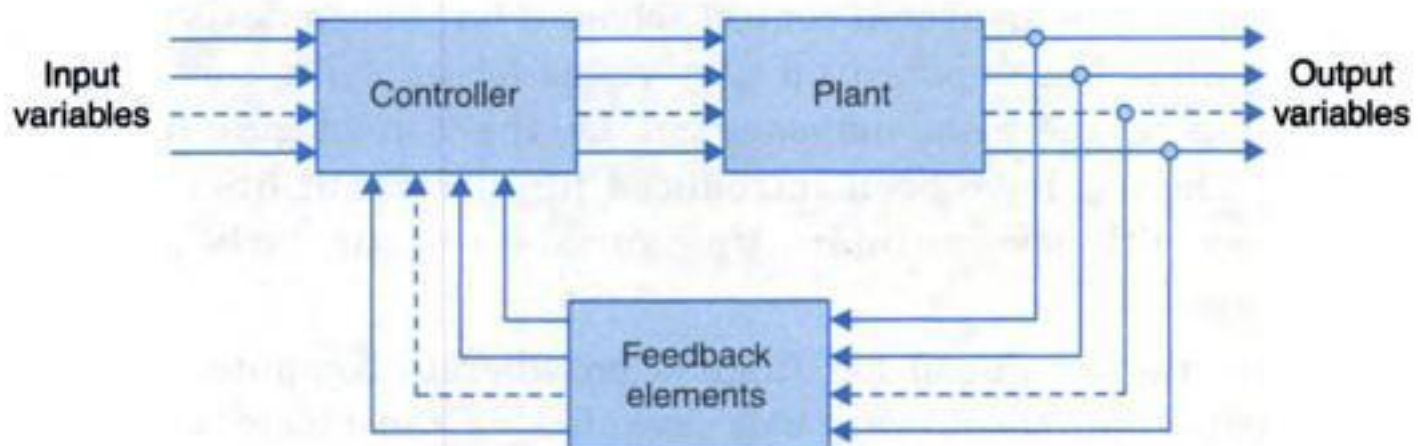


Fig. 1.14. General block diagram of a multivariable control system.

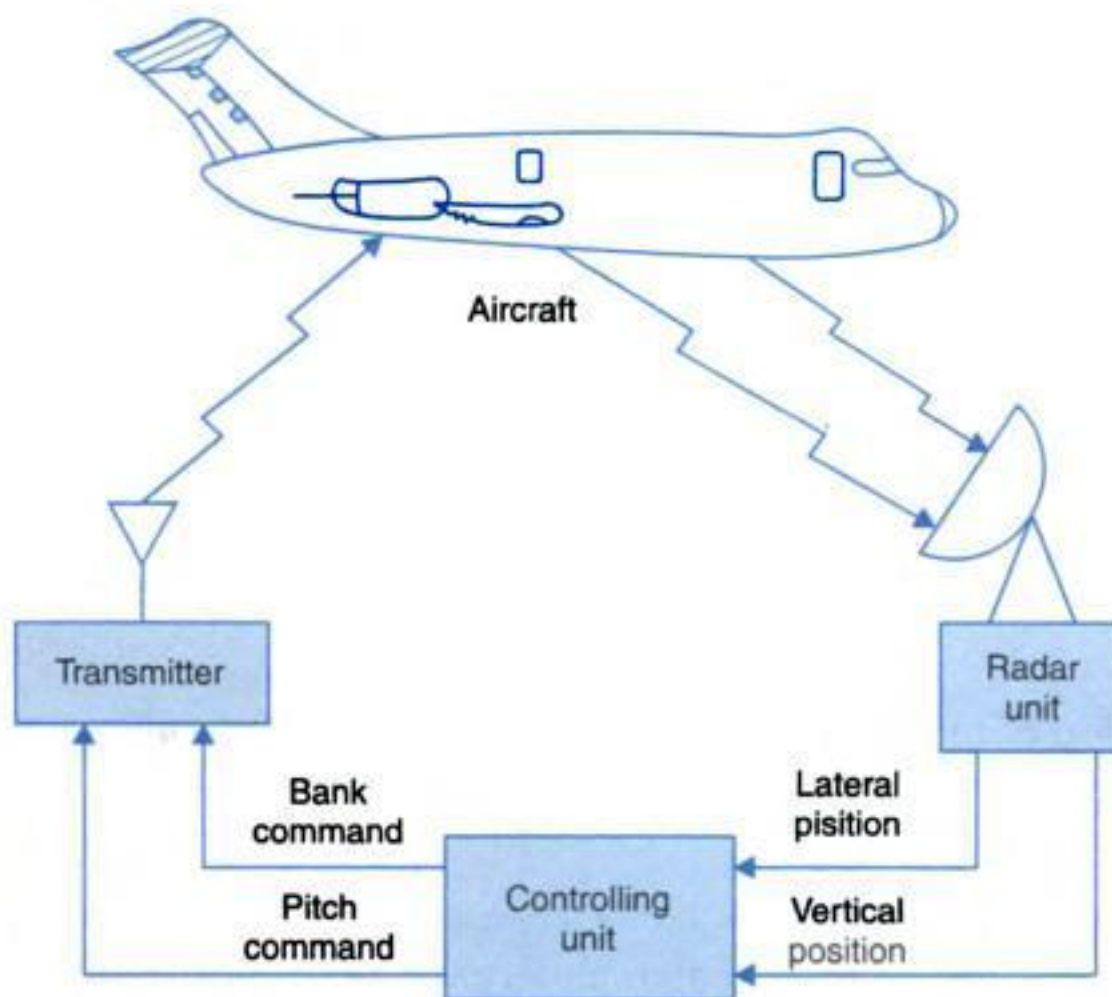
Where a few variables are to be controlled with a limited number of commands and the control algorithm is of moderate complexity and the plant process to be controlled is at a given physical location, a general purpose computer chip, the microprocessor (μP) is commonly employed. Such systems are known as μP -based control systems. Of course at the input/output interfacing A/D and D/A converter chips would be needed.

For large systems a central computer is employed for simultaneous control of several subsystems wherein certain hierarchies are maintained keeping in view the overall system objectives. Additional functions like supervisory control, fault recording, data logging etc, also become possible. We shall advance three examples of central computer control.

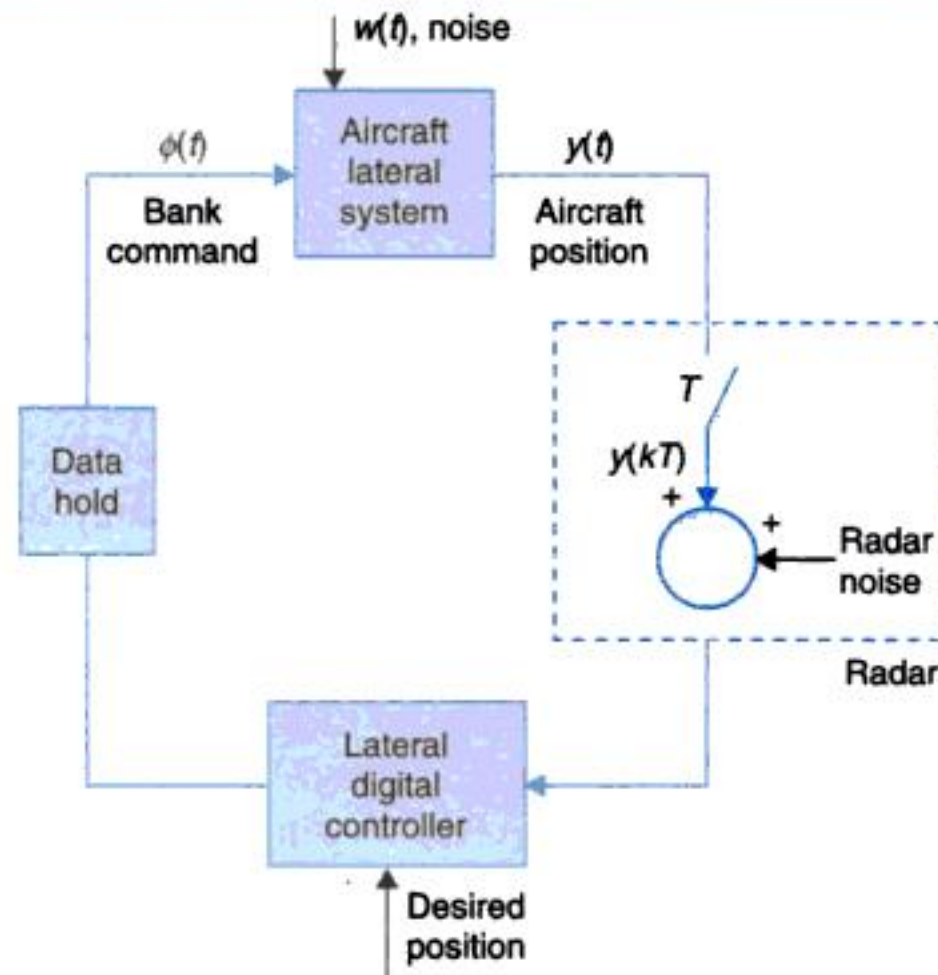
Automatic Aircraft Landing System

The automatic aircraft landing system in a simplified form is depicted in Fig. 1.15(a). The system consists of three basic parts: the aircraft, the radar unit and the controlling unit. The radar unit measures the approximate vertical and lateral positions of the aircraft, which are then transmitted to the controlling unit. From these measurements, the controlling unit calculates appropriate pitch and bank commands. These commands are then transmitted to the aircraft autopilots which in turn cause the aircraft to respond.

Assuming that the lateral control system and the vertical control system are independent (decoupled), we shall consider only the lateral control system whose block diagram is given in Fig. 1.15(b). The aircraft lateral position, $y(t)$, is the lateral distance of the aircraft from the extended centerline of the landing area on the deck of the aircraft carrier. The control system attempts to force $y(t)$ to zero. The radar unit measures $y(kT)$ is the sampled value of $y(t)$, with



(a) Schematic



(b) Lateral landing system.

Fig. 1.15. Automatic aircraft landing system.

$T = 0.05\text{s}$ and $k = 0, 1, 2, 3 \dots$. The digital controller processes these sampled values and generates the discrete bank command constant at the last value received until the next value is received. Thus the bank commands is updated every $t = 0.05\text{s}$, which is called the sampling period. The aircraft responds to the bank command, which changes the lateral position $y(t)$.

It may be noted here that the lateral digital controller must be able to compute the control signal within one sampling period. This is the computational stringency imposed on the central computer in all on-line computer control schemes.

Two unwanted inputs called **disturbances** appear into the system. These are (i) wind gust affecting the position of the aircraft and (ii) radar noise present in measurement of aircraft position. These are labelled as disturbance input in Figure 1.15(b). The system has to be designed to mitigate the effects of disturbance input so that the aircraft lands within acceptable limits of lateral accuracy.

Rocket Autopilot System

As another illustration of computer control, let us discuss an autopilot system which steers a rocket vehicle in response to radioed command. Figure 1.16 shows a simplified block diagram representation of the system.

The state of motion of the vehicle (velocity, acceleration) is fed to the control computer by means of motion sensors (gyros, accelerometers). A position pick-off feeds the computer with the information about rocket engine angle displacement and hence the direction in which the vehicle is heading. In response to heading-commands from the ground, the computer generates a signal which controls the hydraulic actuator and in turn moves the engine.

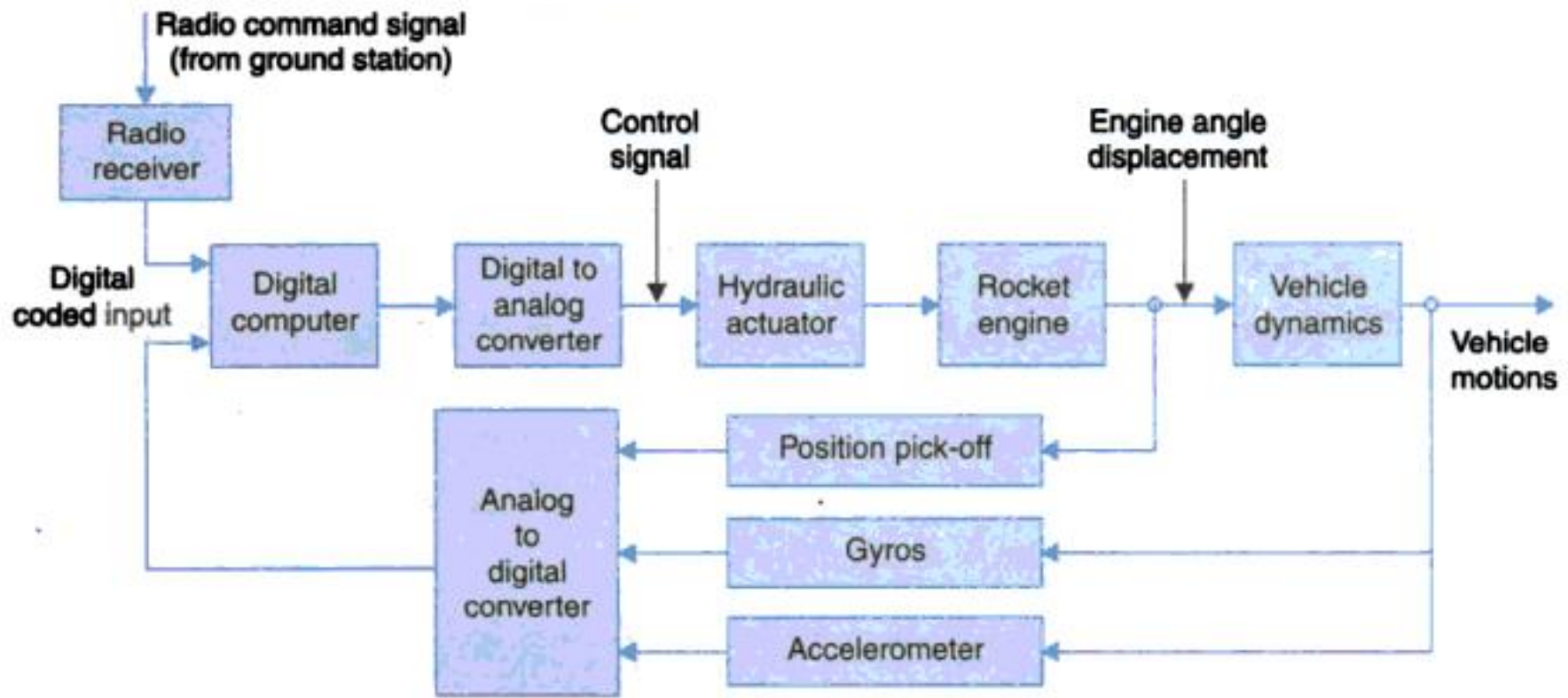


Fig. 1.16. A typical autopilot system.

Coordinated Boiler-Generator Control

Coordinated control system for a boiler-generator unit by a central computer is illustrated by the simplified schematic block diagram of Fig. 1.17. Various signal inputs to the control computer from suitable sensor blocks are:

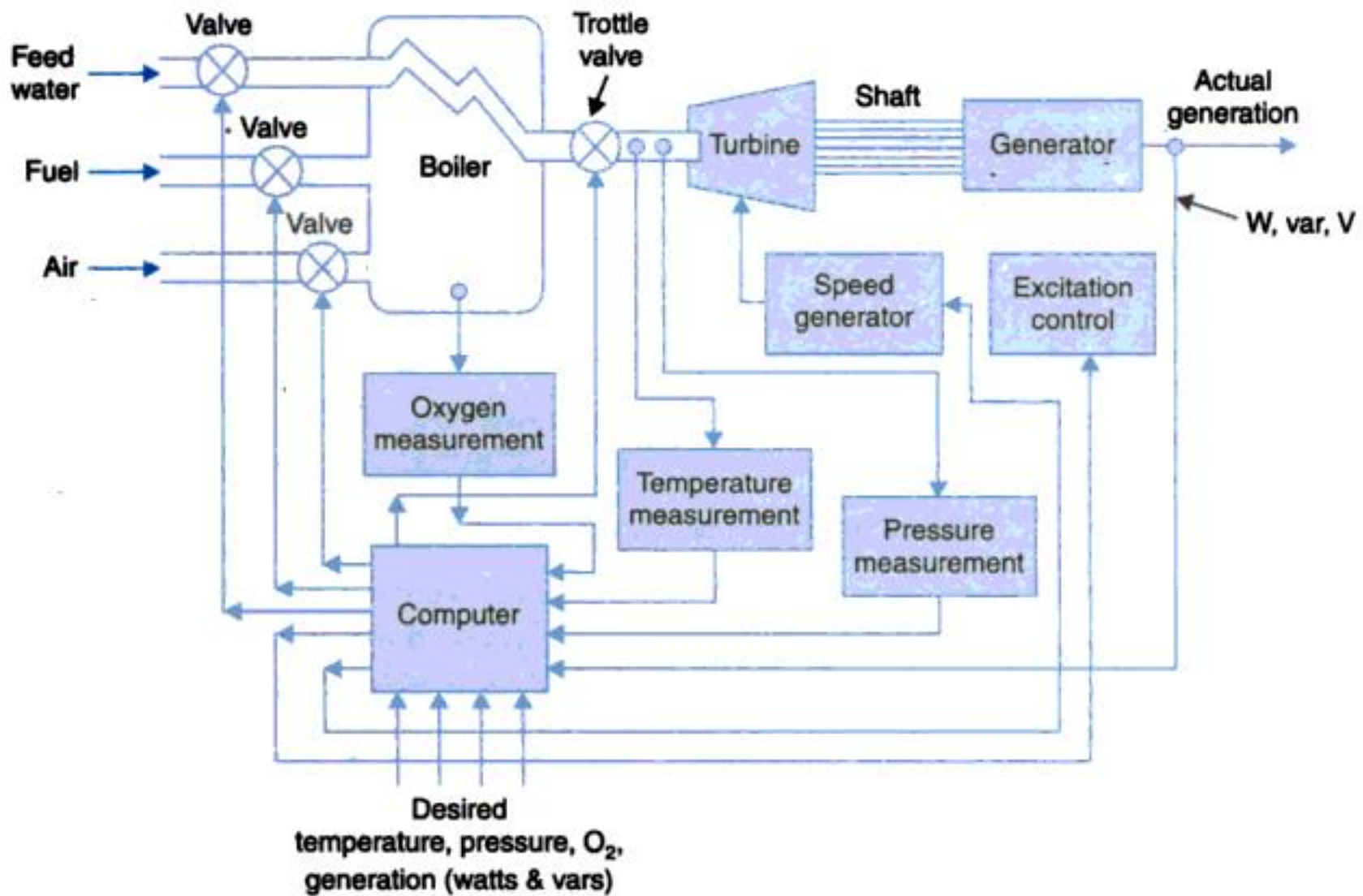


Fig. 1.17. Coordinated control for a boiler-generator.

- Watts, vars, line voltage.
- Temperature and pressure of steam inlet to turbine.
- Oxygen content in furnace air.

These inputs are processed by the control computer by means of a coordinated control algorithm to produce control signals as below:

- Signal to adjust throttle valve. This controls the rate of steam input to turbine and so controls the generator output.
- Signals to adjust fuel, feed water and air in accordance with the throttle valve opening.
- Signals which adjust generator excitation so as to control its var output (which indirectly controls the terminal voltage of the generator).

1.5 APPLICATION OF CONTROL THEORY IN NON-ENGINEERING FIELDS

We have considered in previous sections a number of applications which highlight the potentialities of automatic control to handle various engineering problems. Although control theory originally evolved as an engineering discipline, due to universality of the principles involved it is no longer restricted to engineering confines in the present state of art. In the following paragraphs we shall discuss some examples of control theory as applied to fields like economics, sociology and biology.

Consider an economic inflation problem which is evidenced by continually rising prices. A model of the vicious price-wage inflationary cycle, assuming simple relationship between wages, product costs and cost of living is shown in Fig 1.18. The economic system depicted in this figure is found to be a positive feedback system.

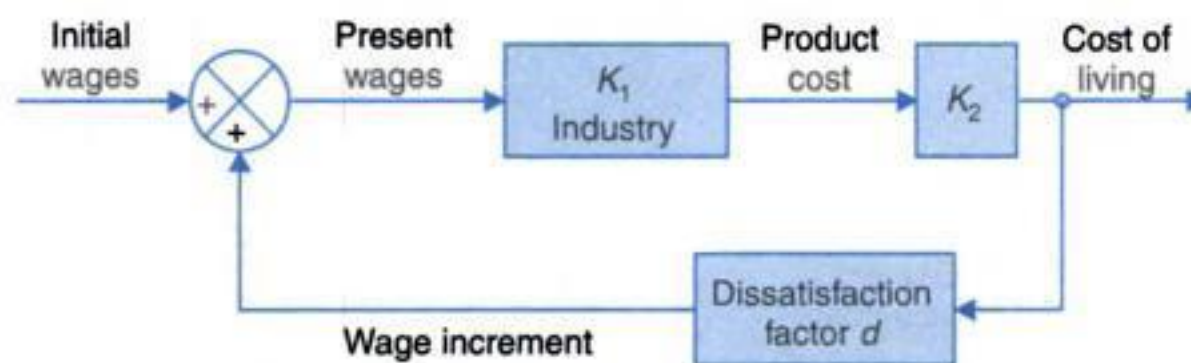


Fig. 1.18. Economic inflation dynamics.

To introduce yet another example of non-engineering application of control principles, let us discuss the dynamics of epidemics in human beings and animals. A normal healthy community has a certain rate of daily contacts C . When an epidemic disease affects this community the social pattern is altered as shown in Fig. 1.19. The factor K_1 contains the

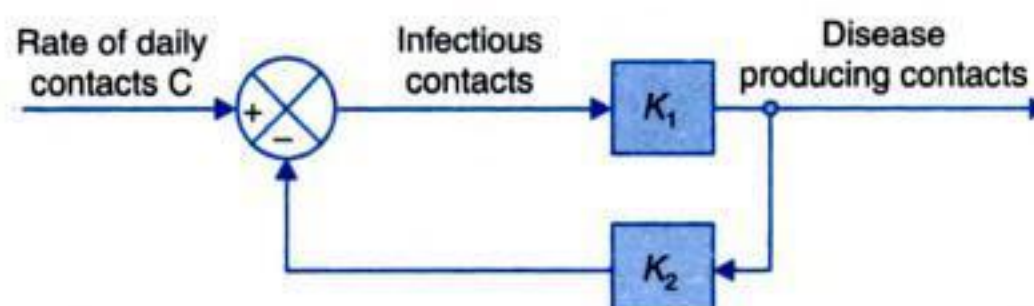


Fig. 1.19. Block diagram representation of epidemic dynamics.

statistical fraction of infectious contacts that actually produce the disease, while the factor K_2 accounts for the isolation of the sick people and medical immunization. Since the isolation and immunization reduce the infectious contacts, the system has a negative feedback loop.

In medical field, control theory has wide applications, such as temperature regulation, neurological, respiratory and cardiovascular controls. A simple example is the automatic anaesthetic control. The degree of anaesthesia of a patient undergoing operation can be measured from encephalograms. Using control principles anaesthetic control can be made completely automatic, thereby freeing the anaesthetist from observing constantly the general condition of the patient and making manual adjustments.

The examples cited above are somewhat over-simplified and are introduced merely to illustrate the universality of control principles. More complex and complete feedback models in various non-engineering fields are now available. This area of control is under rapid development and has a promising future.

1.6 THE CONTROL PROBLEM

In the above account the field of control systems has been surveyed with a wide variety of illustrative examples including those of some nonphysical systems. The basic block diagram of a control system given in Fig. 1.3 is reproduced in Fig. 1.20 wherein certain alternative block and signal nomenclature are introduced.

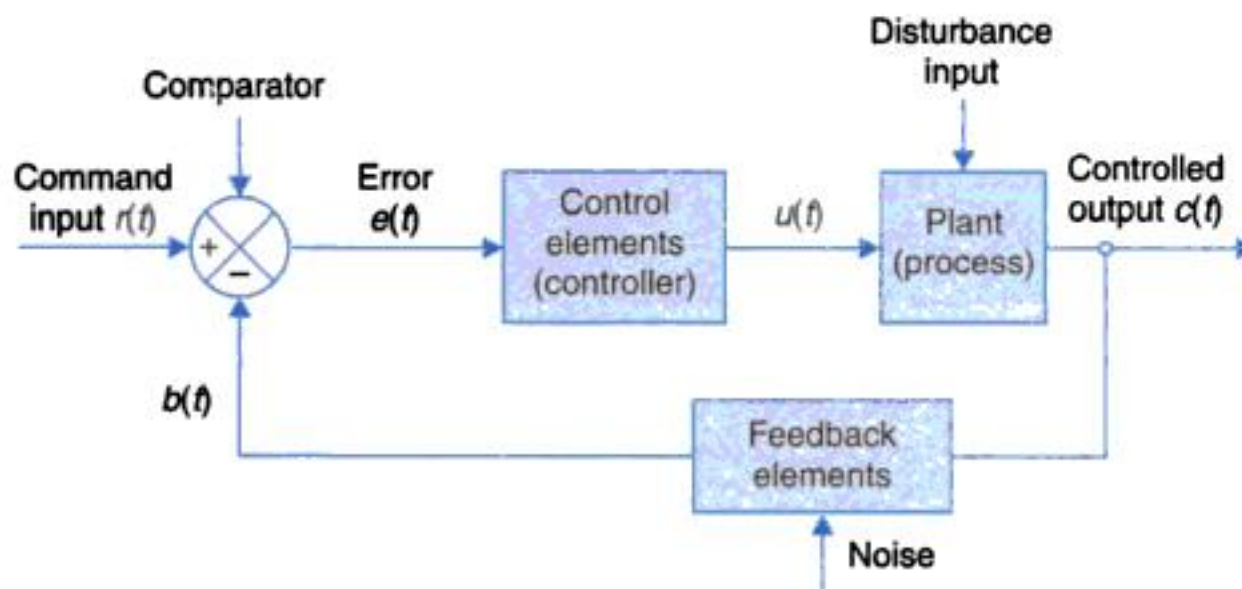


Fig. 1.20. The basic control loop.

Further the figure also indicates the presence of the disturbance input (load disturbance) in the plant and noise input in feedback element (noise enters in the measurement process; see example of automatic aircraft landing system in Fig. 1.15). This basic control loop with negative feedback responds to reduce the error between the command input (desired output) and the controlled output.

Further as we shall see in later chapters that negative feedback has several benefits like reduction in effects of disturbances input, plant nonlinearities and changes in plant parameters. A multivariable control system with several feedback loops essentially follows the same logic. In some mechanical systems and chemical processes a certain signal also is directly

input to the controller elements particularly to counter the effect of load disturbance (not shown in the figure).

Generally, a controller (or a filter) is required to process the error signal such that the overall system satisfies certain criteria specifications. Some of these criteria are:

1. Reduction in effect of disturbance signal.
2. Reduction in steady-state errors.
3. Transient response and frequency response performance.
4. Sensitivity to parameter changes.

Solving the control problem in the light of the above criteria will generally involve following steps:

1. Choice of feedback sensor(s) to get a measure of the controlled output.
2. Choice of actuator to drive (manipulate) the plant like opening or closing a valve, adjusting the excitation or armature voltage of a motor.
3. Developing mathematical models of plant, sensor and actuator.
4. Controller design based on models developed in step 3 and the specified criteria.
5. Simulating system performance and fine tuning.
6. Iterate the above steps, if necessary.
7. Building the system or its prototype and testing.

The criteria and steps involved in system design and implementation and tools of analysis needed of this, form the subject matter of the later chapters.

2

MATHEMATICAL MODELS OF PHYSICAL SYSTEMS

2

MATHEMATICAL MODELS OF PHYSICAL SYSTEMS

2.1 INTRODUCTION

A *physical system* is a collection of physical objects connected together to serve an objective. Examples of a physical system may be cited from laboratory, industrial plant or utility services—an electronic amplifier composed of many components, the governing mechanism of a steam turbine or a communications satellite orbiting the earth are all examples of physical systems. A more general term *system* is used to describe a combination of components which may not all be physical, e.g., biological, economic, socio-economic or management systems. Study in this book will be mainly restricted to physical systems though a few examples of general type systems will also be introduced.

No physical system can be represented in its full physical intricacies and therefore idealizing assumptions are always made for the purpose of analysis and synthesis of systems. An idealized physical system is called a *physical model*. A physical system can be modelled in a number of ways depending upon the specific problem to be dealt with and the desired accuracy. For example, an electronic amplifier may be modelled as an interconnection of linear lumped elements, or some of these may be pictured as nonlinear elements in case the stress is on distortion analysis. A communication satellite may be modelled as a point, a rigid body or a flexible body depending upon the type of study to be carried out. As idealizing assumptions are gradually removed for obtaining a more accurate model, a point of diminishing return is reached, i.e., the gain in accuracy of representation is not commensurate with the increased complexity of the computation required. In fact, beyond a certain point there may indeed be an undetermined loss in accuracy of representation due to flow of errors in the complex computations.

Once a physical model of a physical system is obtained, the next step is to obtain a *mathematical model* which is the mathematical representation of the physical model through

use of appropriate physical laws. Depending upon the choice of variables and the coordinate system, a given physical model may lead to different mathematical models. A network, for example, may be modelled as a set of nodal equations using Kirchhoff's current law or a set of mesh equations using Kirchhoff's voltage law. A control system may be modelled as a scalar differential equation describing the system or state variable vector-matrix differential equation. The particular mathematical model which gives a greater insight into the dynamic behaviour of physical system is selected.

When the mathematical model of a physical system is solved for various input conditions, the result represents the dynamic response of the system. The mathematical model of a system is *linear*, if it obeys the *principle of superposition and homogeneity*. This principle implies that if a system model has responses $y_1(t)$ and $y_2(t)$ to any two inputs $x_1(t)$ and $x_2(t)$ respectively, then the system response to the linear combination of these inputs

$$\alpha_1 x_1(t) + \alpha_2 x_2(t)$$

is given by the linear combination of the individual outputs, *i.e.*,

$$\alpha_1 y_1(t) + \alpha_2 y_2(t)$$

where α_1 and α_2 are constants.

Mathematical models of most physical systems are characterized by differential equations. A mathematical model is linear, if the differential equation describing it has coefficients, which are either functions only of the independent variable or are constants. If the coefficients of the describing differential equations are functions of time (the independent variable), then the mathematical model is *linear time-varying*. On the other hand, if the coefficients of the describing differential equations are constants, the model is *linear time-invariant*.

The differential equation describing a linear time-invariant system can be reshaped into different forms for the convenience of analysis. For example, for transient response or frequency response analysis of single-input-single-output linear systems, *the transfer function representation* (to be discussed later in this chapter) forms a useful model. On the other hand, when a system has multiple inputs and outputs, the *vector-matrix notation* (discussed in Chapter 12) may be more convenient. The mathematical model of a system having been obtained, the available mathematical tools can then be utilized for analysis or synthesis of the system.

Powerful mathematical tools like the Fourier and Laplace transforms are available for use in linear systems. Unfortunately no physical system in nature is perfectly linear. Therefore certain assumptions must always be made to get a linear model which, as pointed out earlier, is a compromise between the simplicity of the mathematical model and the accuracy of results obtained from it. However, it may not always be possible to obtain a valid linear model, for example, in the presence of a strong nonlinearity or in presence of distributive effects which can not be represented by lumped parameters.

A commonly adopted approach for handling a new problem is: first build a simplified model, linear as far as possible, by ignoring certain nonlinearities and other physical properties which may be present in the system and thereby get an approximate idea of the dynamic response of a system; a more complete model is then built for more complete analysis.

2.2 DIFFERENTIAL EQUATIONS OF PHYSICAL SYSTEMS

This section presents the method of obtaining differential equation models of physical systems by utilizing the physical laws of the process. Depending upon the system well-known physical laws like Newton's laws, Kirchhoff's laws, etc. will be used to build mathematical models.

We shall in first step build the physical model of the system as interconnection of idealized system elements and describe these in form of elemental laws. These idealized elements are sort of building blocks of the system. An ideal element results by making two basic assumptions.

1. Spatial distribution of the element is ignored and it is regarded as a point phenomenon. Thus mass which has physical dimensions, is considered concentrated at a point and temperature in a room which is distributed out into the whole room space is replaced by a representative temperature as if of a single point in the room.

The process of ignoring the spatial dependence by choosing a representative value is called lumping and the corresponding modelling is known as lumped-parameter modelling as distinguished from the distributed parameter modelling which accounts for space distribution.

2. We shall assume that the variables associated with the elements lie in the range that the element can be described by simple linear law of (i) a constant of proportionality or (ii) a first-order derivative or (iii) a first-order integration.

The last two forms are in fact alternatives and can be interconverted by a single differentiation or integration.

To begin with we shall consider ideal elements which have a single-port or two-terminal representation and so have two variables associated with it as shown in Fig. 2.1. These variables are identified as

1. **Through variable** V_T which sort of passes through the element and so has the same value in at one port and out at the other. For example, current through an electrical resistance.
2. **Across variable** V_A which appears across the two terminals of the element. For example, voltage across an electrical resistance.

Another classification of the element variables is

1. **Input variable** or independent variable (V_i)
2. **Output variable** or dependent (response) variable (V_o)

Thus V_i could be V_T or V_A and corresponding V_o would be V_A or V_T . The element is then represented in *block diagram* form (**cause-effect form**) as in Fig. 2.2 wherein the signal V_i flows into the block and flows out of it (V_o) suitably modified by the law represented by the block.

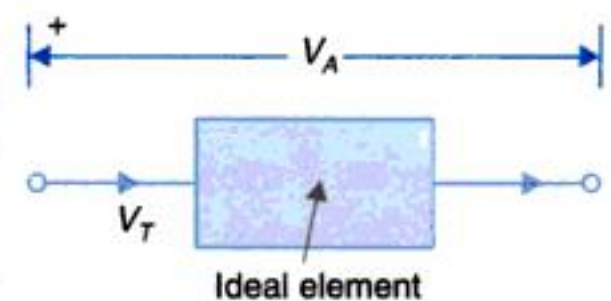


Fig. 2.1

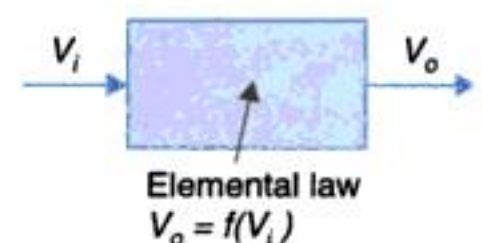


Fig. 2.2. Block diagram of element.

Mechanical Systems

Mechanical systems and devices can be modelled by means of three* ideal translatory and three ideal rotary elements. Their diagrammatic representation and elemental relationships are given in Fig. 2.3. In case of mass/inertia elements it may be noted that one terminal is always the inertial reference frame with respect to which the free terminal moves/rotates.

Through and Across variables for ideal mechanical elements* of Fig. 2.3 are indentified in Table 2.1 along with their units.

Table 2.1. Variables of Mechanical Elements

| | <i>Through variable</i> | <i>Integrated through variable</i> | <i>Across variable</i> | <i>Integrated across variable</i> |
|------------------------|-------------------------------------------------------|------------------------------------------------------------------------------------|------------------------------------------------------------------------------------------|-------------------------------------------------------------------------------------|
| Translational elements | Force, F $N = \text{kg}\cdot\text{m}/\text{s}^2$ | Translational momentum $p = \int_{-\infty}^t F dt$ $(N\cdot\text{s})$ | Velocity difference $v = v_1 - v_2$ (m/s) | Displacement difference $x = x_1 - x_2$ (m) |
| Rotational elements | Torque, T $(N\cdot\text{m})$ | Angular momentum $h = \int_{-\infty}^t T dt$ $(N\cdot\text{m}\cdot\text{s})$ | Angular velocity difference $\omega = \omega_1 - \omega_2$ (rad/s) | Angular Displacement difference $\theta = \theta_1 - \theta_2$ (rad) |

Mass/inertia and the two kinds of springs are the energy storage elements where in energy can be stored and retrieved without loss and so these are called conservative elements. Energy stored in these elements in expressed as:

Mass : $E = (1/2) Mv^2 = \text{kinetic energy } (J) ; \text{ motional energy}$

Inertia : $E = (1/2) J\omega^2 = \text{kinetic energy } (J) ; \text{ motional energy}$

Spring (translatory) : $E = 1/2 Kx^2 = \text{potential energy } (J) ; \text{ deformation energy}$

Spring (torsional) : $E = 1/2 K\theta^2 = \text{potential energy } (J) ; \text{ deformation energy}$

Damper is a **dissipative** element and power it consumes (lost in form of heat) is given as

$$P = fv^2 (W)$$

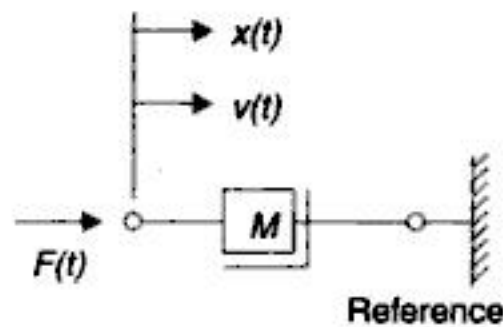
$$= f\omega^2 (W)$$

The elemental relationships in Fig. 2.3 are not expressed in momentum form (which is used mainly in **impulse excitation**). For illustration the relationship of mass can be integrated and expressed as

$$\int_{-\infty}^t F dt = M \int_{-\infty}^t (dv / dt) dt \quad \text{or} \quad p = Mv ; \text{ if } v(-\infty) = 0$$

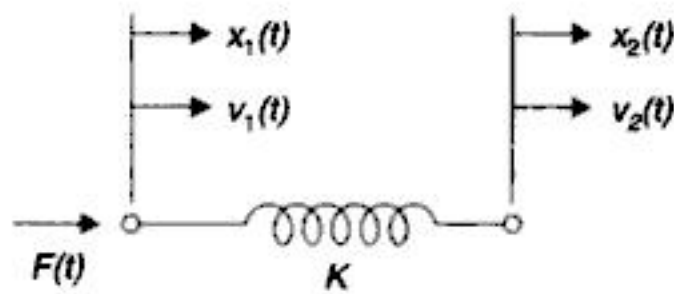
*Another element generally needed is the gear train which will be considered later in this Section.

(1) The mass element



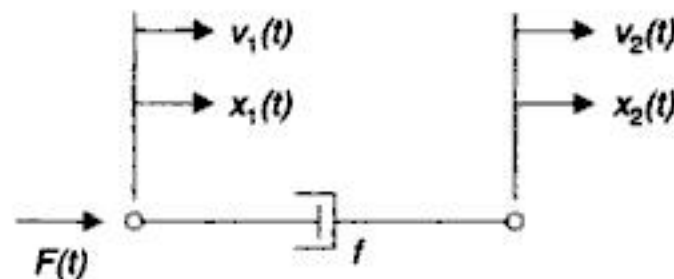
$$F = M \frac{dv}{dt} = M \frac{d^2x}{dt^2}$$

(2) The spring element



$$F = K(x_1 - x_2) = Kx = K \int_{-\infty}^t (v_1 - v_2) dt = K \int_{-\infty}^t v dt$$

(3) The damper element

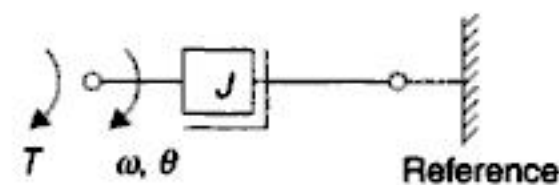


$$F = f(v_1 - v_2) = fv = f(\dot{x}_1 - \dot{x}_2) = f\dot{x}$$

x (m), v (m/sec), M (kg), F (newton), K (newton/m), f (newton per m/sec)

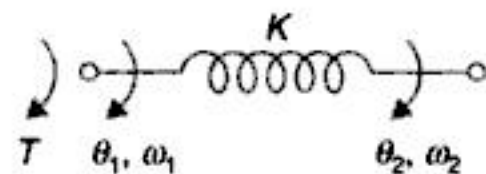
Rotational Elements

(4) The inertia element



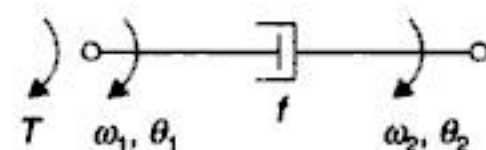
$$T = J \frac{d\omega}{dt} = J \frac{d^2\theta}{dt^2}$$

(5) The torsional spring element



$$T = K(\theta_1 - \theta_2) = K\theta = K \int_{-\infty}^t (\omega_1 - \omega_2) dt = K \int_{-\infty}^t \omega dt$$

(6) The damper element



$$T = f(\omega_1 - \omega_2) = f\omega = f(\dot{\theta}_1 - \dot{\theta}_2) = f\dot{\theta}$$

θ (rad), ω (rad/sec), J (kg-m²), T (newton-m)

K (newton-m/rad), f (newton-m per rad/sec)

Fig. 2.3. Ideal elements for mechanical systems.

A mechanical system which is modelled using the three ideal elements presented above would yield a mathematical model which is an ordinary differential equation. Before we advance examples of this type of modelling, we will examine in some detail the friction which has been modelled as a linear element, the damper.

Friction

The friction exists in physical systems whenever mechanical surfaces are operated in sliding contact. The friction encountered in physical systems may be of many types:

- (i) **Coulomb friction force:** The force of sliding friction between dry surfaces. This force is substantially constant.
- (ii) **Viscous friction force:** The force of friction between moving surfaces separated by viscous fluid or the force between a solid body and a fluid medium. This force is approximately linearly proportional to velocity over a certain limited velocity range.
- (iii) **Stiction:** The force required to initiate motion between two contacting surfaces (which is obviously more than the force required to maintain them in relative motion).

In most physical situations of interest, the viscous friction predominates. The ideal relation given in Fig. 2.3 is based on this assumption.

The friction force acts in a direction opposite to that of velocity. However, it should be realised that friction is not always undesirable in physical systems. Sometimes it may even be necessary to introduce friction intentionally to improve the dynamic response of the system (discussed in Chapter 5). Friction may be introduced intentionally in a system by use of a dashpot shown in Fig. 2.4. It consists of a piston and oil filled cylinder with a narrow annular passage between piston and cylinder. Any relative motion between piston and cylinder is resisted by oil with a friction force (fv).

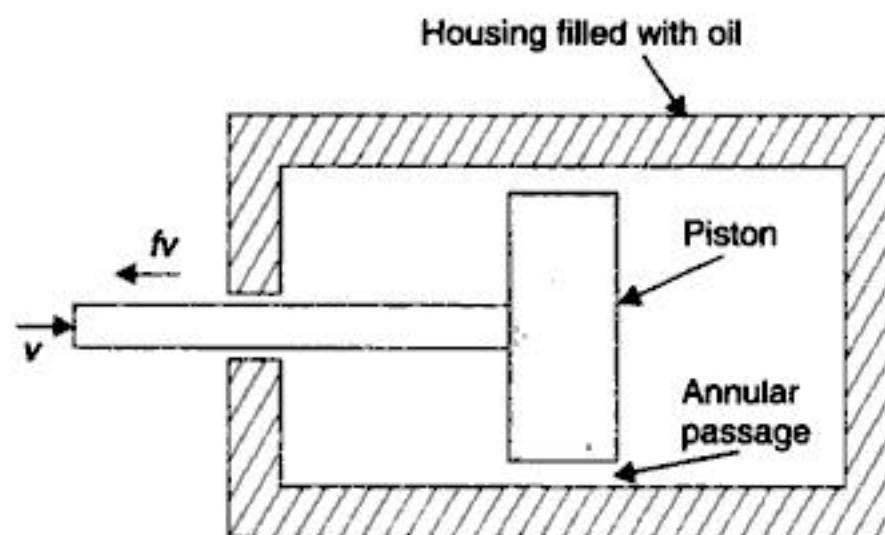


Fig. 2.4. Dashpot construction.

Translational Systems

Let us consider now the mechanical system shown in Fig. 2.5 (a). It is simply a mass M attached to a spring (stiffness K) and a dashpot (viscous friction coefficient f) on which the force F acts. Displacement x is positive in the direction shown. The zero position is taken to be at the point where the spring and mass are in static equilibrium.*

*Note that the gravitational effect is eliminated by this choice of zero position.

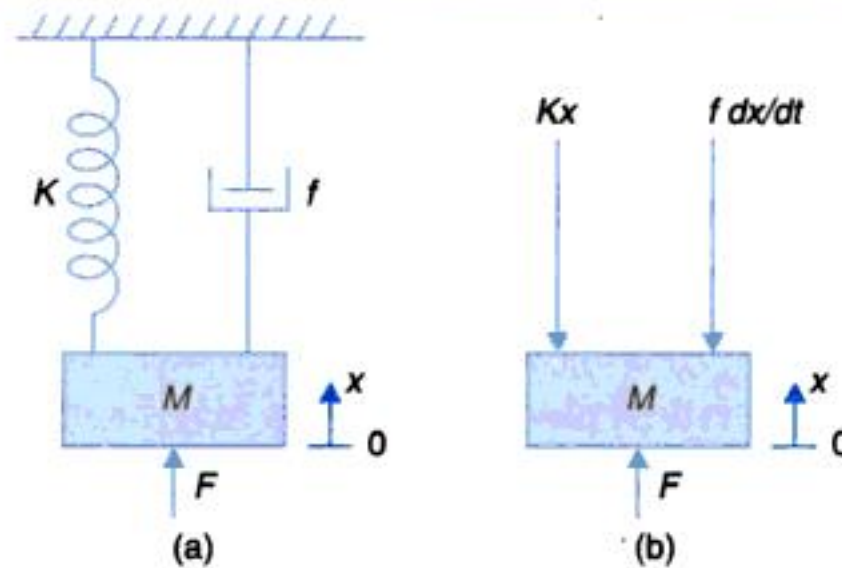


Fig. 2.5. (a) A mass-spring-dashpot system; (b) Free-body diagram.

The systematic way of analyzing such a system is to draw a free-body diagram* as shown in Fig. 2.5 (b). Then by applying Newton's law of motion to the free-body diagram, the force equation can be written as

$$F - f \frac{dx}{dt} - Kx = M \frac{d^2x}{dt^2} \quad \text{or} \quad F = M \frac{d^2x}{dt^2} + f \frac{dx}{dt} + Kx \quad \dots(2.1)$$

Equation (2.1) is a linear, constant coefficient differential equation of second-order. Also observe that the system has two storage elements (mass M and spring K).

Mechanical Accelerometer

In this simplest form, an accelerometer consists of a spring-mass-dashpot system shown in Fig. 2.6. The frame of the accelerometer is attached to the moving vehicle.

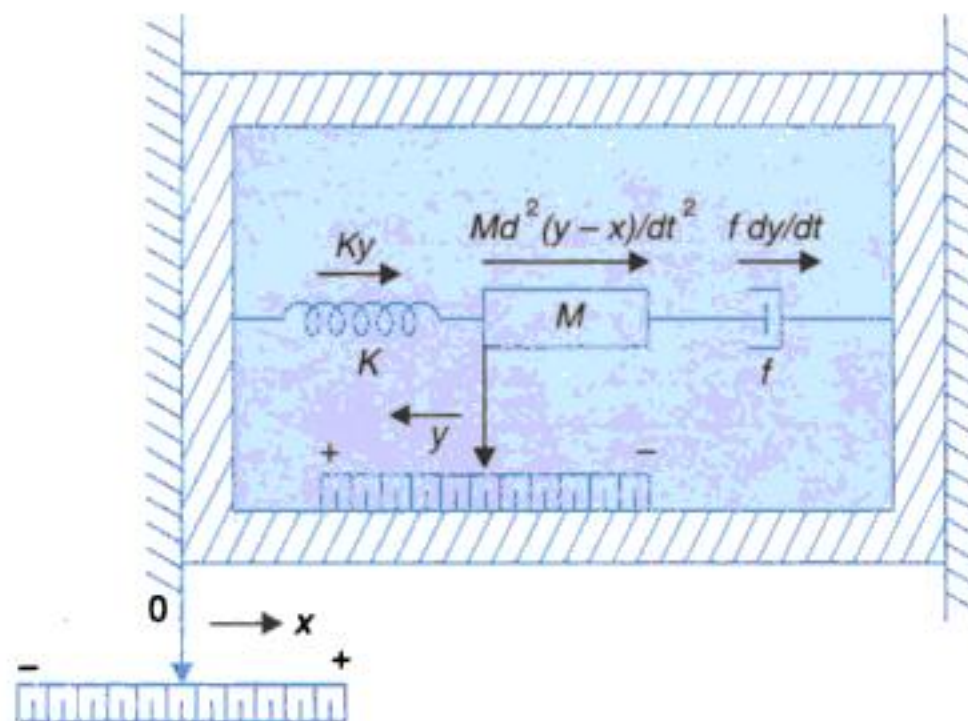


Fig. 2.6. Simplified diagram of an accelerometer.

Whenever the moving vehicle and hence the frame of the accelerometer is accelerated, the spring deflects until it produces enough force to accelerate the mass at the same rate as the

* In example (2.1), we shall see that there is one to one correspondence between free-body diagram approach and nodal method of analysis.

frame. The deflection of the spring which may be measured by a linear-motion potentiometer is a direct measure of acceleration.

Let

x = displacement of the moving vehicle (or frame) with respect to a fixed reference frame.

y = displacement of the mass M with respect to the accelerometer frame.

The positive directions for x and y are indicated on the diagram. Since y is measured with respect to the frame, the force on the mass due to spring is $-Ky$ and due to viscous friction is $-f\frac{dy}{dt}$. The motion of the mass with respect to the fixed reference frame in the positive direction of y is $(y - x)$.

The force equation for the system becomes

$$M\frac{d^2(y - x)}{dt^2} + f\frac{dy}{dt} + Ky = 0$$

or
$$M\frac{d^2y}{dt^2} + f\frac{dy}{dt} + Ky = M\frac{d^2x}{dt^2} = Ma \quad \dots(2.2)$$

where a is the input acceleration.

If a constant acceleration is applied to the accelerometer, the output displacement y becomes constant under steady-state as the derivatives by y become zero, i.e.,

$$Ma = Ky \quad \text{or} \quad a = \left(\frac{K}{M}\right)y$$

The steady-state displacement y is thus a measure of the constant input acceleration. This instrument can also be used for displacement measurements as explained later in Section 2.3.

Nonlinear Spring

No spring is linear over an arbitrary range of extensions—in fact that is true of all physical as well as nonphysical systems. The linear spring elemental law

$$F = Ky$$

is applicable within a limited range of extension y measured beyond the unstretched end of the spring as in Fig. 2.7. Where large extensions are encountered the spring law changes to

$$F = Ky^2 \quad \dots(2.3)$$

which is graphically represented in Fig. 2.8. This law does not obey the principle of superposition as shown below:

$$F_{S_1} = Ky_1 ; y_1 = \text{spring extension in linear range}$$

$$F_{S_2} = Ky_2^2 ; y_2 = \text{spring extension in nonlinear range}$$

$$F_{S_2} = F_{S_1} + F_{S_2}, y = y_1 + y_2 = \text{total spring extension}$$

$$F_S = Ky_1 + Ky_2^2 \neq Ky^2$$

So this behaviour (response) of the spring is not linear (**nonlinear**)

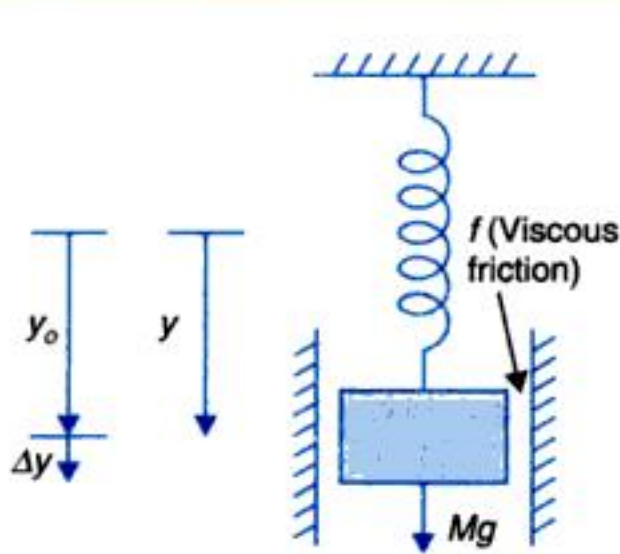


Fig. 2.7

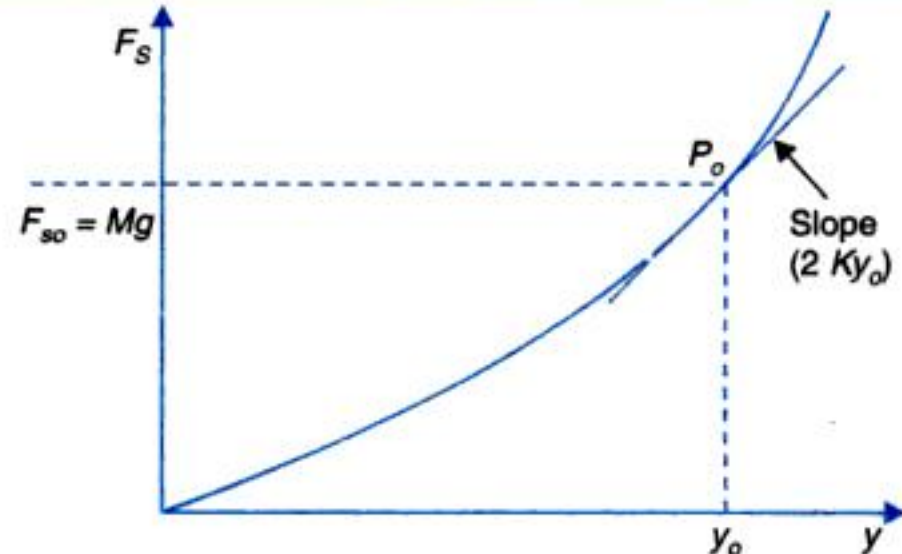


Fig. 2.8

Linearization

Consider the mass-spring system of Fig. 2.7, under gravitational force Mg which when large pushes the spring to nonlinear region of operation. From the freebody diagram we can write the describing equation of the system as

$$Mg = M\ddot{y} + f\dot{y} + Ky^2 \quad \dots(2.4)$$

Under steady condition (rest position of the mass) all derivatives of y are zero. So eqn. (2) gives

$$Mg = Ky_0^2 \text{ or } y_0 = \sqrt{Mg/K} \quad \dots(2.5)$$

Consider now that the system moves through a small value Δy about y_0 . Equation (2.4) can then be written as

$$Mg = M\frac{d^2}{dt^2}(y_0 + \Delta y) + f\frac{d}{dt}(y_0 + \Delta y) + K(y_0 + \Delta y)^2 \quad \dots(2.6)$$

The nonlinear spring term can be approximated by retaining the first derivative term in Taylor series, i.e.,

$$y = K(y_0 + \Delta y)^2 = Ky_0 + \left. \frac{d}{dy}(Ky^2) \right|_{y=y_0} \Delta y = Ky_0 + (2Ky_0)\Delta y$$

Substituting this approximated value we get

$$Mg = M\frac{d^2}{dt^2}(y_0 + \Delta y) + f\frac{d}{dt}(y_0 + \Delta y) + Ky_0 + (2Ky_0)\Delta y$$

$$\text{or } 0 = M\frac{d^2}{dt^2}(\Delta y) + f\frac{d}{dt}(\Delta y) + (2Ky_0)\Delta y \quad \dots(2.7)$$

It is seen from eqn. (2.7) that the spring behaviour for small movement around $P_0(F_0 = Mg, y_0)$ in Fig. 2.8 is linear with spring constant modified to $(2Ky_0)$, the slope of the spring characteristic at the point P_0 , called the **operating point**.

If we relabel $x = \Delta y$ and also apply an external force F in positive direction of x (i.e., downwards), eqn. (2.7) becomes

$$F = Mx + fx + K_0x; K_0 = 2K/y_0 \quad \dots(2.8)$$

The technique of linearization presented above is also known as **small-signal** modelling. This is commonly used in **automatic regulating systems** which operate in a narrow range

around the set point. It will be used in this section in modelling of hydraulic and pneumatic systems which are otherwise nonlinear. The technique of small-signal linearization will be elaborated in Section 2.4 for multivariable components/devices.

Levered Systems

An ideal (mass and friction less) lever is shown in Fig. 2.9 (a) so long as the rotation θ about the axis of the lever is small

$$x = a\theta \text{ and } y = b\theta$$

so that $\frac{x}{y} = \frac{a}{b}$; displacement ratio ... (2.9a)

also $aF_1 = bF_2$... (2.9b)

or $\frac{F_1}{F_2} = \frac{b}{a}$; force advantage

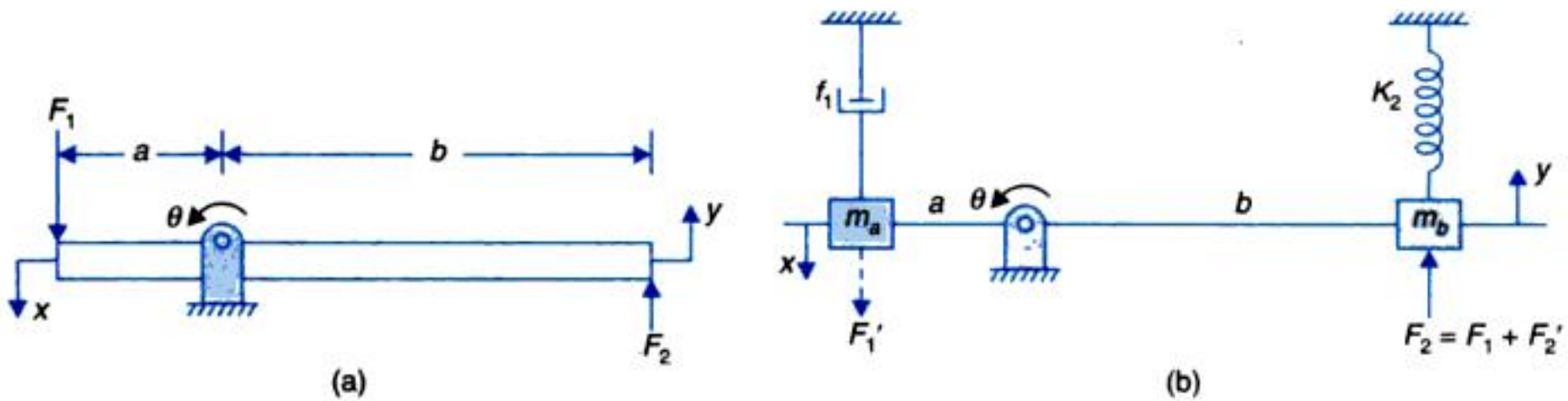


Fig. 2.9. Levered systems.

Consider now the levered system of Fig. 2.9 (b). External force F_2 acting on m_b comprises two components, i.e.,

$$F_2 = F_1 + F_2'$$

F_2' acts on (m_b, K_2) subsystem and F_1' the reflection of F_1 at a -end of the lever acts on (m_a, f_1) subsystem. The dynamical equations for the two systems are written as

$$F_2' = m_b \ddot{y} + K_2 y \quad \dots(2.10a)$$

$$F_1' = m_a \ddot{x} + f_1 \dot{x} \quad \dots(2.10b)$$

But $F_1' = (b/a) F_1$ and $x = (a/b)y$. Substituting in eqn. (2.10b), we get

$$(b/a) F_1 = (a/b) m_a \ddot{y} + (a/b) f_1 \dot{y}$$

or $F_1 = (a/b)^2 m_a \ddot{y} + (a/b)^2 f_1 \dot{y} = m_a' \ddot{y} + f_1' \dot{y} \quad \dots(2.11)$

where $m_a' = (a/b)^2 m_a$; mass at end 'a' reflected at end 'b' of the lever.

$f_1' = (a/b)^2 f_1$ friction at end 'a' reflected at end 'b' of the lever

Adding eqns. (2.10a) and (2.10b), we have

$$F_2 = F_1 + F_2' = (m_a' + m_b) \ddot{y} + f_1' \dot{y} + K_2 y \quad \dots(2.12)$$

Equation (2.12) can be written down directly by reflecting the parameters from one end of the lever to the other in the inverse square displacement ratio of the lever.

Rotational Systems

Mechanical systems involving fixed-axis rotation occur in the study of machinery of many types and are very important. The modelling procedure is very close to that used in translation. In these systems, the variables of interest are the torque and angular velocity (or displacement). The three basic components for rotational systems are: moment of inertia, torsional spring and viscous friction.

The three ideal rotational elements with their relevant properties and conventions are shown in Fig. 2.3.

Let us consider now, the rotational mechanical system shown in Fig. 2.10 (a) which consists of a rotatable disc of moment of inertia J and a shaft of stiffness K . The disc rotates in a viscous medium with viscous friction coefficient f .

Let T be the applied torque which tends to rotate the disc. The free-body diagram is shown in Fig. 2.10 (b).

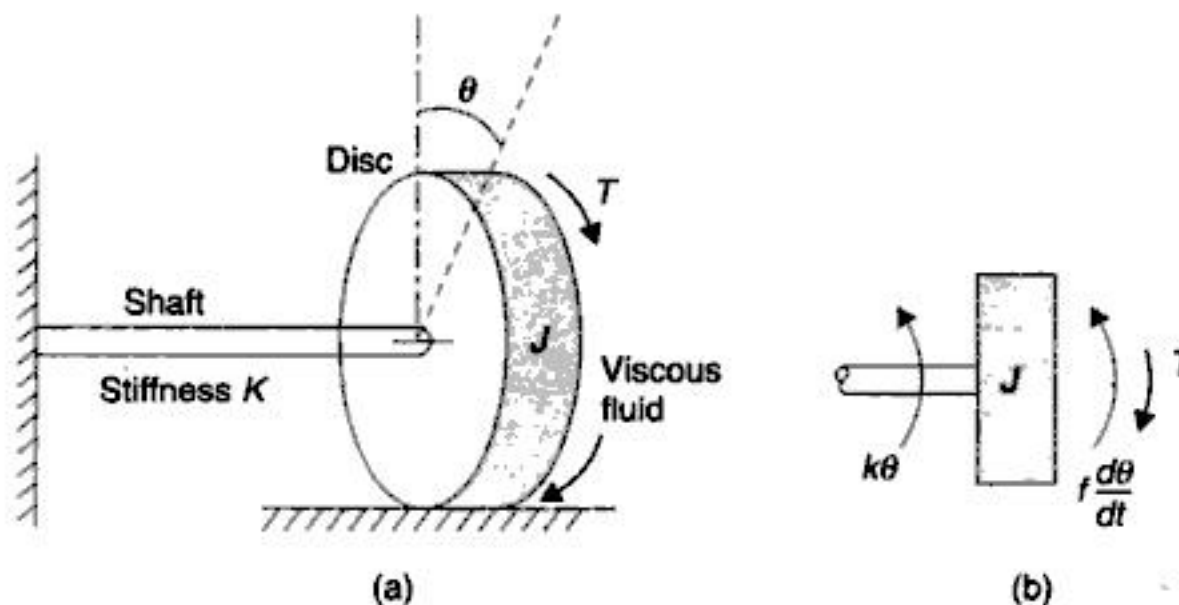


Fig. 2.10. (a) Rotational mechanical system; (b) Free-body diagram.

The torque equation obtained from the free-body diagram is

$$T - f \frac{d\theta}{dt} - K\theta = J \frac{d^2\theta}{dt^2} \quad \text{or} \quad T = J \frac{d^2\theta}{dt^2} + f \frac{d\theta}{dt} + K\theta \quad \dots(2.13)$$

Equation (2.13) is a linear constant coefficient differential equation describing the dynamics of the system shown in Fig. 2.10 (a). Again observe that the system has two storage elements, inertia J and shaft of stiffness K .

Gear Trains

Gear trains are used in control systems to attain the mechanical matching of motor to load. Usually a servomotor operates at high speed but low torque. To drive a load with high torque and low speed by such a motor, the torque magnification and speed reduction are achieved by gear trains. Thus in mechanical systems gear trains act as matching devices like transformers in electrical systems.

Figure 2.11 shows a motor driving a load through a gear train which consists of two gears coupled together. The gear with N_1 teeth is called the primary gear (analogous to primary winding of a transformer) and gear with N_2 teeth is called the secondary gear.

Angular displacements of shafts 1 and 2 are denoted by θ_1 and θ_2 respectively. The moment of inertia and viscous friction of motor and gear 1 are denoted by J_1 and f_1 and those of gear 2 and load are denoted by J_2 and f_2 respectively.

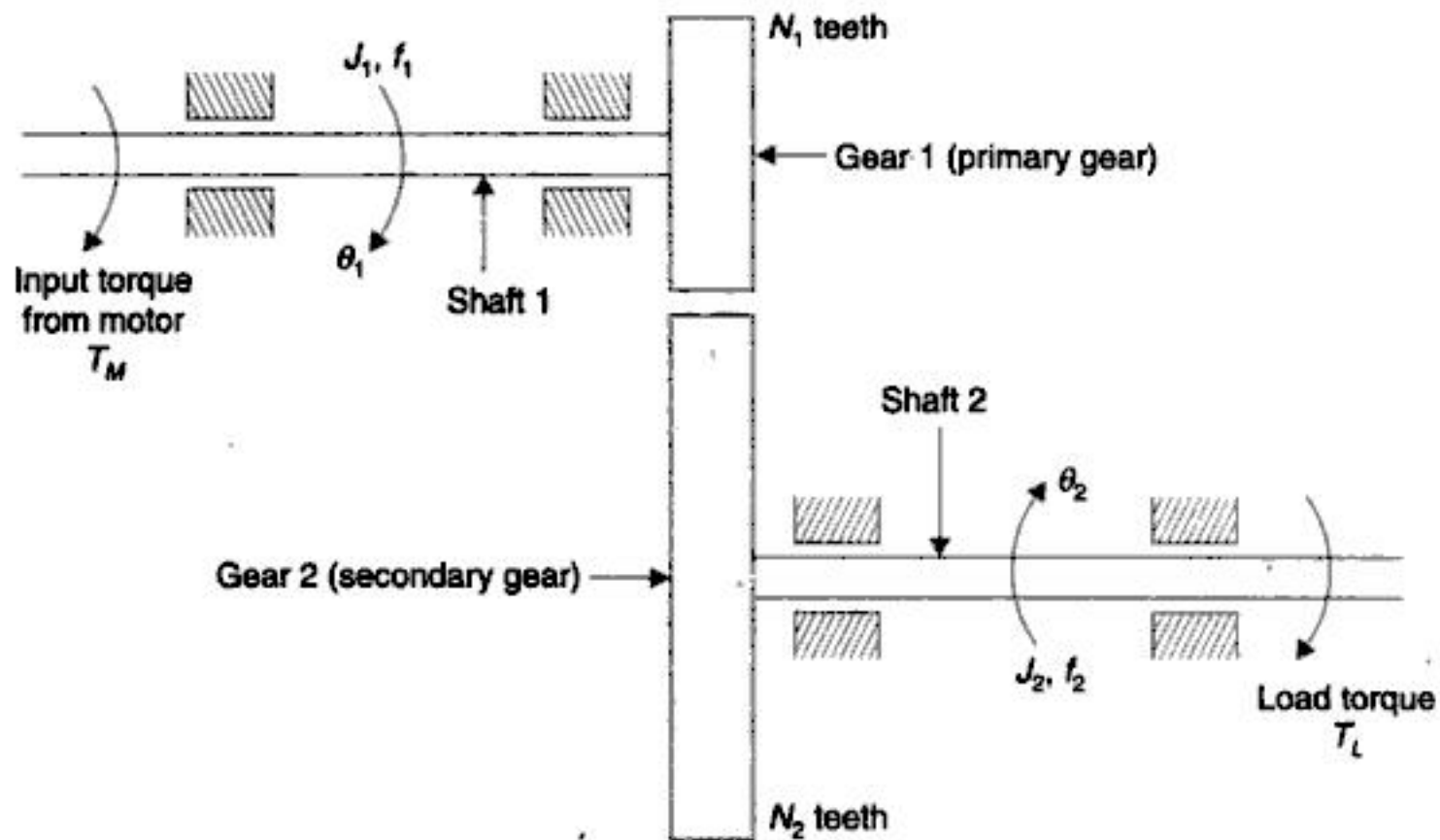


Fig. 2.11. Gear train system.

For the first shaft, the differential equation is

$$J_1 \ddot{\theta}_1 + f_1 \dot{\theta}_1 + T_1 = T_M \quad \dots(2.14)$$

where T_m is the torque developed by the motor and T_1 is the load torque on gear 1 due to the rest of the gear train.

For the second shaft $J_2 \ddot{\theta}_2 + f_2 \dot{\theta}_2 + T_L = T_2 \quad \dots(2.15)$

where T_2 is the torque transmitted to gear 2 and T_L is the load torque.

Let r_1 be the radius of gear 1 and r_2 be that of gear 2. Since the linear distance travelled along the surface of each gear is same, $\theta_1 r_1 = \theta_2 r_2$. The number of teeth on gear surface being proportional to gear radius, we obtain

$$\frac{\theta_2}{\theta_1} = \frac{N_1}{N_2} \quad \dots(2.16)$$

Here the stiffness of the shafts of the gear train is assumed to be infinite. In an ideal case of no loss in power transfer, the work done by gear 1 is equal to that of gear 2. Therefore,

$$T_1 \theta_1 = T_2 \theta_2 \quad \dots(2.17)$$

Combining eqns. (2.16) and (2.17) we have

$$\frac{T_1}{T_2} = \frac{\theta_2}{\theta_1} = \frac{N_1}{N_2} \quad \dots(2.18)$$

Differentiating θ_1 and θ_2 in eqn. (2.18) twice, we have the following relation for speed and acceleration.

$$\frac{\ddot{\theta}_2}{\ddot{\theta}_1} = \frac{\dot{\theta}_2}{\dot{\theta}_1} = \frac{N_1}{N_2} \quad \dots(2.19)$$

Thus if $N_1/N_2 < 1$, from eqns. (2.18) and (2.19) it is found that the gear train reduces the speed and magnifies the torque.

Eliminating T_1 and T_2 from eqns. (2.14) and (2.15) with the help of eqns. (2.18) and (2.19), we obtain

$$J_1 \ddot{\theta}_1 + f_1 \dot{\theta}_1 + \frac{N_1}{N_2} (J_2 \ddot{\theta}_2 + f_2 \dot{\theta}_2 + T_L) = T_M \quad \dots(2.20)$$

Elimination of θ_2 from eqn. (2.20) with the help of eqn. (2.19) yields,

$$\left[J_1 + \left(\frac{N_1}{N_2} \right)^2 J_2 \right] \ddot{\theta}_1 + \left[f_1 + \left(\frac{N_1}{N_2} \right)^2 f_2 \right] \dot{\theta}_1 + \left(\frac{N_1}{N_2} \right) T_L = T_M \quad \dots(2.21)$$

Thus the equivalent moment of inertia and viscous friction of gear train referred to shaft 1 are

$$J_{1eq} = J_1 + \left(\frac{N_1}{N_2} \right)^2 J_2 ; f_{1eq} = f_1 + \left(\frac{N_1}{N_2} \right)^2 f_2$$

In terms of equivalent moment of inertia and friction, eqn. (2.21) may be written as

$$J_{1eq} \ddot{\theta}_1 + f_{1eq} \dot{\theta}_1 + \left(\frac{N_1}{N_2} \right) T_L = T_M$$

Here $(N_1/N_2) T_L$ is the load torque referred to shaft 1.

Similarly, expressing θ_1 in terms of θ_2 in eqn. (2.20) with the help of eqn. (2.19), the equivalent moment of inertia and viscous friction of gear train referred to load shaft are

$$J_{2eq} = J_2 + \left(\frac{N_2}{N_1} \right)^2 J_1 ; f_{2eq} = f_2 + \left(\frac{N_2}{N_1} \right)^2 f_1$$

Torque equation referred to the load shaft may then be expressed as

$$J_{2eq} \ddot{\theta}_2 + f_{2eq} \dot{\theta}_2 + T_L = \left(\frac{N_2}{N_1} \right) T_M$$

It is observed that inertia and friction parameters are referred from one shaft of the gear train to the other in the direct square ratio of the gear teeth. The same will hold for shaft stiffness when present.

Electrical Systems

The resistor, inductor and capacitor are the three basic elements of electrical circuits. These circuits are analyzed by the application of Kirchhoff's voltage and current laws.

Let us analyze the L - R - C series circuit shown in Fig. 2.7 by using Kirchhoff's voltage law. The governing equations of the system are

$$L \frac{di}{dt} + Ri + \frac{1}{C} \int_{-\infty}^t i dt = e \quad \dots(2.22)$$

$$\frac{1}{C} \int_{-\infty}^t i dt = e_o ; e_o = e_c \quad \dots(2.23)$$

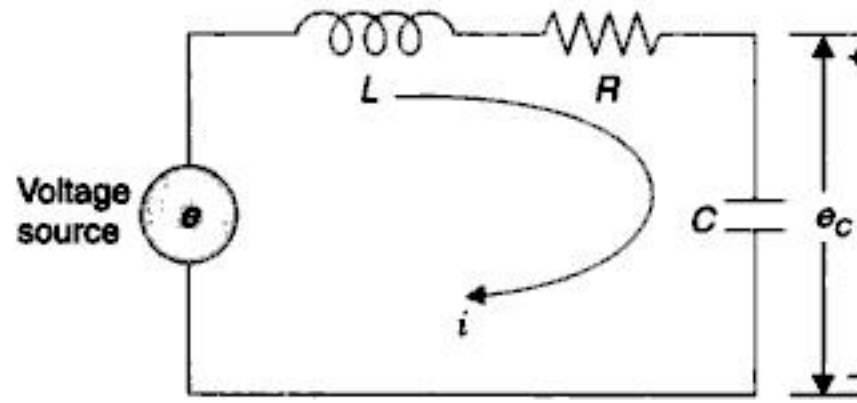


Fig. 2.12. L-R-C series circuit.

Elemental relationships are obvious from these equations. It is also to be noted that inductor and capacitor are the storage elements and resistor is the dissipative element. In terms of electric charge $q = \int idt$, eqn. (2.12) becomes

$$L \frac{d^2q}{dt^2} + R \frac{dq}{dt} + \frac{1}{C}q = e \quad \dots(2.24)$$

Similarly, using Kirchhoff's current law, we obtain the following equations for L-R-C parallel circuit shown in Fig. 2.13.

$$C \frac{de}{dt} + \frac{1}{L} \int_{-\infty}^t e dt + \frac{e}{R} = i \quad \dots(2.25)$$

In terms of magnetic flux linkage $\phi = \int edt$, eqn. (2.25) may be written as

$$C \frac{d^2\phi}{dt^2} + \frac{1}{R} \frac{d\phi}{dt} + \frac{1}{L}\phi = i \quad \dots(2.26)$$

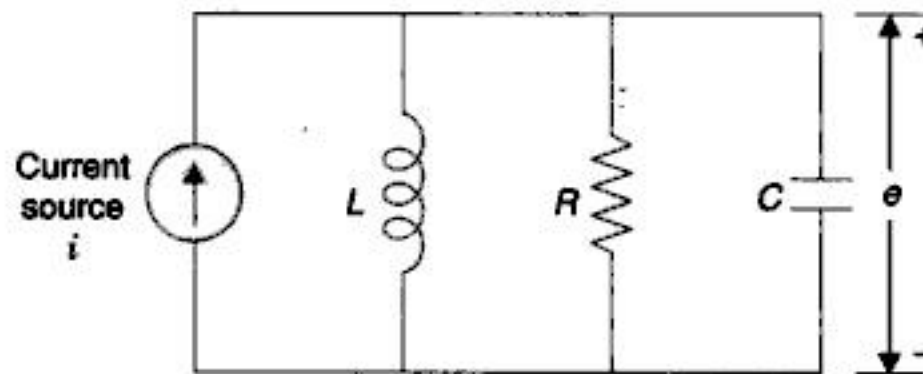


Fig. 2.13. L-R-C parallel circuit.

Analogous System

Comparing eqn. (2.1) for the mechanical translational system shown in Fig. 2.5 (a) or eqn. (2.13) for the mechanical rotational system shown in Fig. 2.10 (a) and eqn. (2.24) for the electrical system shown in Fig. 2.11, it is seen that they are of identical form. Such systems whose differential equations are of identical form are called *analogous systems*. The force F (torque T) and voltage e are the analogous variables here. This is called the Force (Torque)-Voltage analogy. A list of analogous variables in this analogy is given in Table 2.2.

Table 2.2. Analogous Quantities In Force (Torque)-Voltage Analogy

| <i>Mechanical translational systems</i> | <i>Mechanical rotational systems</i> | <i>Electrical systems</i> |
|-----------------------------------------|--------------------------------------|---------------------------------|
| Force F | Torque T | Voltage e |
| Mass M | Moment of inertia J | Inductance L |
| Viscous friction coefficient f | Viscous friction coefficient f | Resistance R |
| Spring stiffness K | Torsional spring stiffness K | Reciprocal of capacitance $1/C$ |
| Displacement x | Angular displacement θ | Charge q |
| Velocity \dot{x} | Angular velocity $\dot{\theta}$ | Current i |

Similarly eqns. (2.1) and (2.3) referred above and eqn. (2.26) for the electrical system shown in Fig. 2.13 are also identical. In this case force F (torque T) and current i are the analogous variables. This is called the Force (Torque)-Current analogy. A list of analogous quantities in this analogy is given in Table 2.3.

Table 2.3. Analogous Quantities In Force (Torque)-current Analogy

| <i>Mechanical translational systems</i> | <i>Mechanical rotational systems</i> | <i>Electrical systems</i> |
|-----------------------------------------|--------------------------------------|---------------------------------|
| Force F | Torque T | Voltage i |
| Mass M | Moment of inertia J | Capacitance C |
| Viscous friction coefficient f | Viscous friction coefficient f | Reciprocal of resistance $1/R$ |
| Spring stiffness K | Torsional spring stiffness K | Reciprocal of inductance $1/L$ |
| Displacement x | Angular displacement θ | Magnetic flux linkage λ |
| Velocity \dot{x} | Angular velocity $\dot{\theta}$ | Voltage e |

The concept of analogous system is a useful technique for the study of various systems like electrical, mechanical, thermal, liquid-level, etc. If the solution of one system is obtained, it can be extended to all other systems analogous to it. Generally it is convenient to study a non-electrical system in terms of its electrical analog as electrical systems are more easily amenable to experimental study.

Thermal Systems

The basic requirement for the representation of thermal systems by linear models is that the temperature of the medium be uniform which is generally not the case. Thus for precise analysis a distributed parameter model must be used. Here, however, in order to simplify the analysis, uniformity of temperature is assumed and thereby the system is represented by a lumped parameter model.

Consider the simple thermal system shown in Fig. 2.14. Assume that the tank is insulated to eliminate heat loss to the surrounding air, there is no heat storage in the insulation and liquid in the tank is kept at uniform temperature by perfect mixing with the help of a stirrer. Thus a single temperature may be used to describe the thermal state of the entire liquid. (If complete mixing is not present, there is a complex temperature distribution throughout the liquid and the problem becomes one of the distributed parameters, requiring the use of partial differential equations). Assume that the steady-state temperature of the inflowing liquid is θ_1 and that of the outflowing liquid is θ . The steady-state heat input rate from the heater is H . The liquid flow rate is of course assumed constant. To obtain a linear model we shall use small-signal analysis already illustrated for a nonlinear spring.

Let ΔH (J/min) be a small increase in the heat input rate from its steady-state value. This increase in heat input rate will result in increase of the heat outflow rate by an amount ΔH_1 and a heat storage rate of the liquid in the tank by an amount ΔH_2 . Consequently the temperature of the liquid in the tank and therefore of the outflowing liquid rises by $\Delta\theta$ (°C). Since the insulation has been regarded as perfect, the increase in heat outflow rate is only due to the rise in temperature of the outflowing liquid and is given by

$$\Delta H_1 = Qs \Delta\theta$$

where Q = steady liquid flow rate in kg/min; and s = specific heat of the liquid in J/kg °C.

The above relationship can be written in the form

$$\Delta H_1 = \Delta\theta/R \quad \dots(2.27)$$

where $R = 1/Qs$, is defined as the *thermal resistance* and has the units of °C/J/min.

The rate of heat storage in the tank is given by

$$\Delta H_2 = Ms \frac{d(\Delta\theta)}{dt}$$

where M = mass of liquid in the tank in kg; and $\frac{d(\Delta\theta)}{dt}$ = rate of rise of temperature in the tank.

The above equation can be expressed in the form

$$\Delta H_2 = C \frac{d(\Delta\theta)}{dt} \quad \dots(2.28)$$

where $C = Ms$, is defined as the *thermal capacitance* and has the units of J/°C. For the system of Fig. 2.14, the heat flow balance equation is

$$\Delta H = \Delta H_1 + \Delta H_2 = \frac{\Delta\theta}{R} + C \frac{d(\Delta\theta)}{dt}$$

or
$$RC \frac{d(\Delta\theta)}{dt} + \Delta\theta = R(\Delta H) \quad \dots(2.29)$$

Equation (2.29) describes the dynamics of the thermal system with the assumption that the temperature of the inflowing liquid is constant.

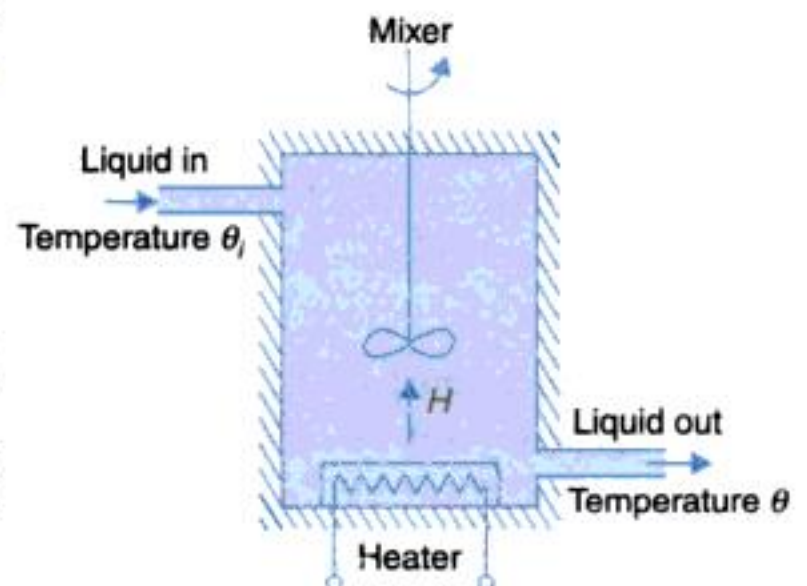


Fig. 2.14. Thermal system.

In practice, the temperature of the inflowing liquid fluctuates. Thus along with a heat input signal from the heater, there is an additional signal due to change in the temperature of the inflowing liquid which is known as the *disturbance signal*.

Let $\Delta\theta_i$ be change in the temperature of the inflowing liquid from its steady-state value. Now in addition to the change in heat input from the heater, there is a change in heat carried by the inflowing liquid. The heat flow equation, therefore, becomes

$$\Delta H + \frac{\Delta\theta_i}{R} = \frac{\Delta\theta}{R} + C \frac{d}{dt}(\Delta\theta)$$

or
$$RC \frac{d}{dt}(\Delta\theta) + \Delta\theta = \Delta\theta_i + R(\Delta H) \quad \dots(2.30)$$

Let us now relax the assumption that the tank insulation is perfect. As the liquid temperature increases by $\Delta\theta$, the rate of heat flow through the tank walls to the ambient medium increases by

$$\Delta H_3 = \frac{\Delta\theta}{R_t}$$

where R_t is the thermal resistance of the tank walls. Equation (2.30) is then modified to

$$\Delta H + \frac{\Delta\theta_i}{R} = \left(\frac{\Delta\theta}{R} + \frac{\Delta\theta}{R_t} \right) + C \frac{d}{dt}(\Delta\theta)$$

or
$$R'C \frac{d}{dt}(\Delta\theta) + \Delta\theta = \left(\frac{R'}{R} \right) \Delta\theta_i + R'(\Delta H)$$

where $R' = \frac{RR_t}{R + R_t}$ = effective thermal resistance due to liquid outflow and tank walls (it is a parallel combination of R and R_t).

It is still being assumed above that there is no heat storage in the tank walls. Relaxing this assumption will simply add to the thermal capacitance C .

Fluid Systems

The dynamics of the fluid systems can be represented by ordinary linear differential equations only if the fluid is incompressible and fluid flow is laminar. Industrial processes often involve fluid flow through connecting pipes and tanks where the flow is usually turbulent resulting in nonlinear equations describing the system.

Velocity of sound is a key parameter in fluid flow to determine the compressibility property. If the fluid velocity is much less than the velocity of sound, compressibility effects are usually small. As the velocity of sound in liquids is about 1500 m/s, compressibility* effects are rarely of importance in liquids and the treatment of compressibility is generally restricted to gases, where the velocity of sound is about 350 m/s.

Another important fluid property is the type of fluid flow-laminar or turbulent. Laminar flow is characterized by smooth motion of one laminar of fluid past another, while turbulent flow is characterized by an irregular and nearly random motion superimposed on the main

*The tendency of so-called incompressible fluids to compress slightly under pressure is called *fluid compliance*. This type of effect is accounted for in hydraulic pumps and motors discussed in Section 4.5.

motion of fluid. The transition from laminar to turbulent flow was first investigated by Osborne Reynolds, who after experimentation found that for pipe flow the transition conditions could be correlated by a dimensionless group which is now known as *Reynolds number*, Re .

From his experiments, Reynolds found that pipe flow will be laminar for Re less than 2,000 and turbulent for Re greater than 3,000. When Re is between 2,000 and 3,000, the type of flow is unpredictable and often changes back and forth between the laminar and turbulent states because of flow disturbances and pipe vibrations.

The pressure drop across a pipe section is given by

$$P = \frac{128l\mu}{\pi D^4} Q ; \text{ for laminar flow} \quad \dots(2.31a)$$

$$= RQ$$

$$P = \frac{8K_t\rho l}{\pi^2 D^5} Q^2 ; \text{ for turbulent flow} \quad \dots(2.31b)$$

$$= K_T Q^2$$

where l = length of pipe section (m); D = diameter of pipe (m); μ = viscosity (Ns/m²); Q = volumetric flow rate (m³/s); K_t = a constant (to be determined experimentally); and ρ = mass density (kg/m³).

Equation (2.31a) representing laminar flow is linear, *i.e.*,

$$P = RQ$$

where $R = \frac{128l\mu}{\pi D^4} \left(\frac{N/m^2}{m^3/s} \right)$ is the *fluid resistance*.

Equation (2.31b) representing turbulent flow is nonlinear, *i.e.*,

$$P = K_T Q^2$$

where $K_T = \frac{8K_t\rho l}{\pi^2 D^5}$.

This equation can be linearized about the operating point (P_o, Q_o) by techniques discussed earlier in this section (See Nonlinear Spring). At the operating point,

$$P_o = K_T Q_o^2$$

Expanding the turbulent flow equation (2.31b) in Taylor series about the operating point and retaining first-order term only, we have

$$P = P_o + \left. \frac{dP}{dQ} \right|_{(P_o, Q_o)} (Q - Q_o)$$

It follows that $P - P_o = 2K_T Q_o (Q - Q_o)$

or $\Delta P = R \Delta Q \quad \dots(2.32)$

where $R = 2K_T Q_o$ is the *turbulent flow resistance*.

Equation (2.32) relates the incremental fluid flow to incremental pressure around the operating point in the case of turbulent flow.

Large pipes even when long offer small resistance while short devices that contain some contractions (orifices, nozzles, valves, etc.) offer large resistance to fluid flow. For these dissipation devices, head loss

$$P = \frac{8K\rho}{\pi^2 D^4} Q^2$$

where K is a constant. Experimentally determined values of K for various dissipation devices can be found in handbooks. This equation is analogous to eqn. (2.31b) and can be linearized about the operating point to obtain resistance offered by a dissipation device.

The other ideal element used in modelling fluid systems is the *fluid capacitance*. Consider a tank with cross-sectional area = $A(m^2)$.

$$\text{The rate of fluid storage in the tank} = A \frac{dH}{dt} = \frac{A}{\rho g} \frac{dP}{dt} = C \frac{dP}{dt} \quad \dots(2.33)$$

where H = fluid head in the tank (m); $P = \rho gH$ (N/m^2) = pressure at tank bottom; and

$$C = \frac{A}{\rho g} \left(\frac{m^3}{N/m^2} \right) = \text{capacitance of the tank.}$$

Inertial effect of fluid in a pipe line is modelled as *inertance* defined below.

$$\Delta P = L \frac{dQ}{dt}$$

where ΔP = pressure drop as on the pipe

Q = rate of fluid flow through pipe

$$L = \frac{\rho l}{A} = \text{inertance (Ns}^2/\text{m}^5\text{)}.$$

For small fluid accelerations, the inertance effect is usually neglected to obtain a simple mathematical model of the system. This is really true of hydraulic components used in control systems.

Liquid Level Systems

In terms of head $H(m)$, the fluid pressure is given by

$$P = \rho gH$$

The pressure-flow rate relations given by eqns. (2.32a) and (2.32b) may be expressed as the following head-flow rate relations:

$$H = RQ; \text{ for laminar flow} \quad (2.34a)$$

$$\text{where } R = \frac{128lu}{\pi D^2 \rho g}$$

$$\Delta H = R\Delta Q; \text{ for turbulent flow} \quad (2.34b)$$

$$\text{where } R = \frac{2K_T Q_o}{\rho g}$$

The parameter R in eqns. (2.34) is referred to as *hydraulic resistance*.

$$\text{The rate of fluid storage in a tank} = A \frac{dH}{dt} = C \frac{dH}{dt}$$

where $C = A (m^2) = \text{hydraulic capacitance of the tank.}$

Consider a simple liquid-level system shown in Fig. 2.15 where a tank is supplying liquid through an outlet. Under steady conditions, let Q_i be the liquid flow rate into the tank and Q_o be the outflow rate, while H_o is the steady liquid head in the tank. Obviously $Q_i = Q_o$.

Let ΔQ_i be a small increase in the liquid inflow rate from its steady-state value. This increase in liquid inflow rate causes increase of head of the liquid in the tank by ΔH , resulting in increase of liquid outflow rate by

$$\Delta Q_o = \Delta H/R$$

The system dynamics is described by the liquid flow rate balance equation:

Rate of liquid storage in the tank = rate of liquid inflow-rate of liquid outflow

Therefore

$$C \frac{d(\Delta H)}{dt} = \Delta Q_i - \frac{\Delta H}{R}$$

or
$$RC \frac{d(\Delta H)}{dt} + \Delta H = R(\Delta Q_i) \tag{2.35}$$

where C is the capacitance of the tank and R is the total resistance offered by the tank outlet and pipe.

Pneumatic Systems

We shall assume in our discussion that velocities of gases are a small fraction of the velocity of sound, which is true in a number of engineering applications. With this assumption, we treat pneumatic flow also as nearly incompressible. Therefore, the results presented earlier are directly applicable to this class of pneumatic systems.

Consider a simple pneumatic system shown in Fig. 2.16. A pneumatic source is supplying air to the pressure vessel through a pipe line.



Fig. 2.16. Simple pneumatic system.

Let us define:

P_i = air pressure of the source at steady-state (N/m^2).

P_o = air pressure in the vessel at steady-state (N/m^2).

ΔP_i = small change in air pressure of the source from its steady-state value.

ΔP_o = small change in air pressure of the vessel from its steady-state value.

System dynamics is described by the equation:

Rate of gas storage in vessel = rate of gas inflow

or
$$C \frac{d(\Delta P_o)}{dt} = \frac{\Delta P}{R} = \frac{\Delta P_i - \Delta P_o}{R}$$

or
$$RC \frac{d(\Delta P_o)}{dt} + \Delta P_o = \Delta P_i \tag{2.36}$$

Table 2.4 summarizes the variables and parameters of the thermal, liquid level and pneumatic systems which are analogous to those of electrical systems.

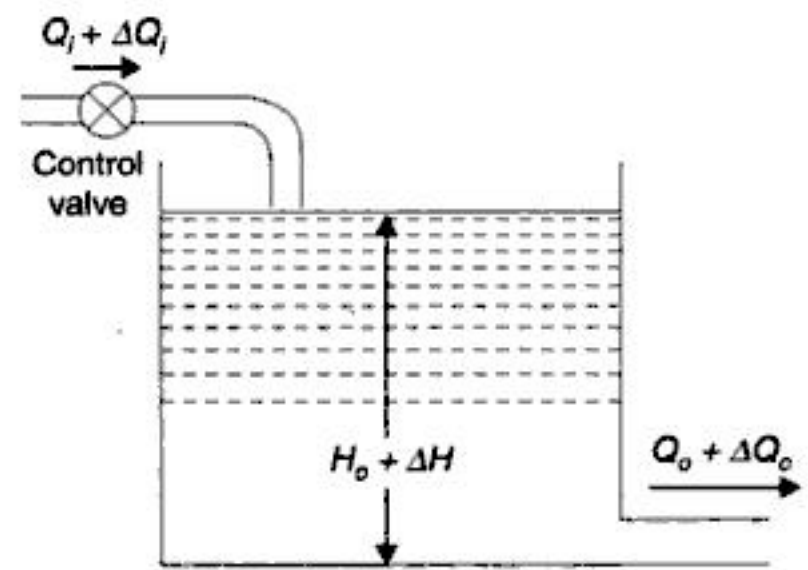


Fig. 2.15. Liquid-level system.

Table 2.4. Analogous Quantities

| Electrical systems | Thermal systems | Liquid-level systems | Pneumatic systems |
|----------------------|-----------------------------------------------------|----------------------------------------------------------|----------------------------------------------------------|
| Charge, q | Heat flow, J | Liquid flow, m^3 | Air flow, m^3 |
| Current, A | Heat flow rate, J/min | Liquid flow rate, m^3/min | Air flow rate, m^3/min |
| Voltage, V | Temperature, $^{\circ}\text{C}$ | Head, m | Pressure, N/m^2 |
| Resistance, Ω | Resistance, $\frac{^{\circ}\text{C}}{J/\text{min}}$ | Resistance, $\frac{\text{N}/\text{m}^2}{m^3/\text{min}}$ | Resistance, $\frac{\text{N}/\text{m}^2}{m^3/\text{min}}$ |
| Capacitance, C | Capacitance, $J/^{\circ}\text{C}$ | Capacitance, m^2 | Capacitance, $\frac{m^3}{\text{N}/\text{m}^2}$ |

2.3 DYNAMICS OF ROBOTIC MECHANISMS

Dynamical equations for robotic serial links will be illustrated here by means of two simple examples of two-link mechanisms.

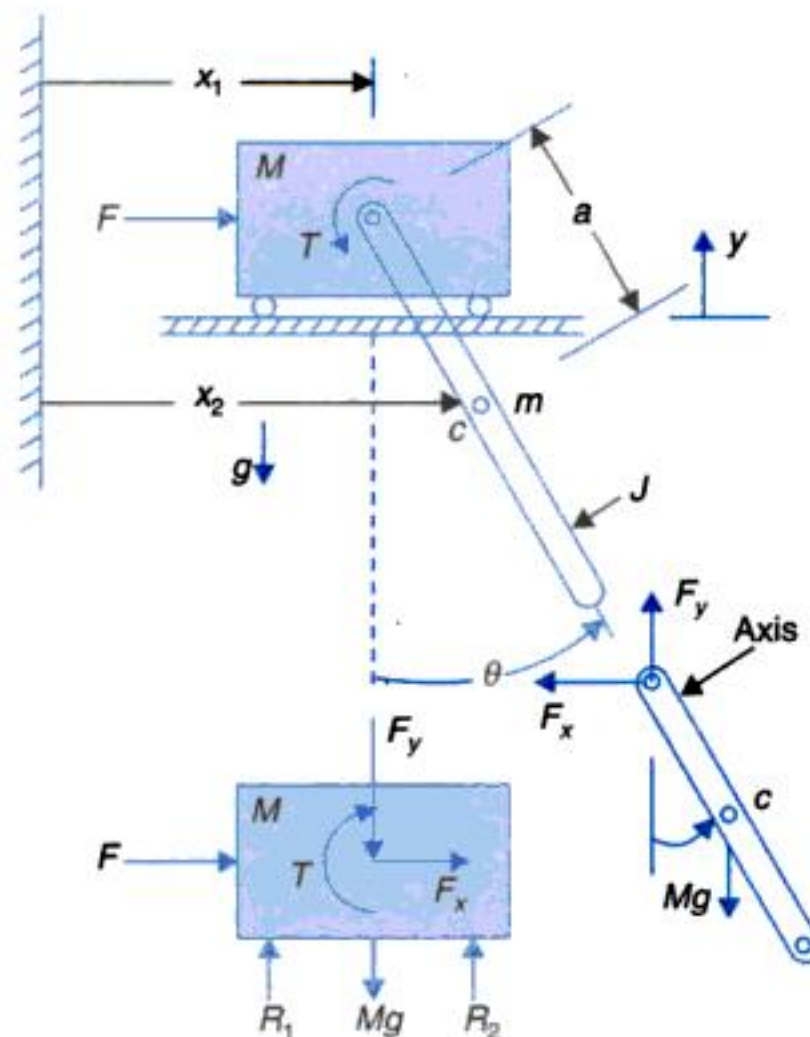


Fig. 2.17. Simplified model of a gantry robot.

Gantry Robot

A simple gantry robot mechanism is shown in Fig. 2.17(a) wherein the main body the crane is propelled by traction force, F . To the body is attached a rotating arm (mass m , and moment of

inertia J about the axis of rotation) driven by an actuator located on the crane body. At the end of the arm a hand (**end effector**) would be attached for picking up objects (not shown in figure).

The free-body diagrams of the masses M and m are drawn in Figs. 2.17(b) and (c).

For mass M

$$M\ddot{x}_1 = F_x + F \quad \dots(i)$$

$$M\ddot{y}_1 = R_1 + R_2 - F_y - Mg \quad \dots(ii)$$

Equation (ii) is needed to be used only if reaction R_1 and R_2 are to be calculated.

For mass m

$$m\ddot{x}_2 = -F_x \quad \dots(iii)$$

$$m\ddot{y}_2 = F_y - mg \quad \dots(iv)$$

$$J\ddot{\theta} = aF_x \cos \theta - F_y \sin \theta + T \quad \dots(v)$$

Eliminating F_x in eqns. (i) and (iii), we get

$$M\ddot{x}_1 + m\ddot{x}_2 = F \quad \dots(vi)$$

Eliminating F_y in eqns. (iv) and (v), we have

$$J\ddot{\theta} = m\ddot{x}_2 a \cos \theta + ma(\ddot{y}_2 + g) = T \quad \dots(vii)$$

The displacements x_2 and y_2 are related to θ as follows:

$$x_2 = x_1 + a \sin \theta$$

$$y_2 = -a \cos \theta$$

Differentiating twice

$$\ddot{x}_2 = \ddot{x}_1 - a \sin \theta \dot{\theta}^2 + \cos \theta \ddot{\theta} \quad \dots(viii)$$

$$\ddot{y}_2 = a \cos \theta \dot{\theta}^2 + a \sin \theta \ddot{\theta} \quad \dots(ix)$$

Substituting \ddot{x}_2 and \ddot{y}_2 into eqns. (vi) and (vii), we get

$$(J + ma^2)\ddot{\theta} + ma \cos \theta \ddot{x}_1 + mga \sin \theta = T \quad \dots(x)$$

$$(M + m)\ddot{x}_1 + ma \cos \theta \ddot{\theta} - ma \sin \theta \dot{\theta}^2 = F \quad \dots(xi)$$

It is observed that the dynamic equations are nonlinear and coupled. Serial link manipulator is too complex a mechanism to be modelled by the free-body technique. It is much simpler to use energy method which employs generalized coordinates.

Lagrangian Mechanics

The Lagrangian L is defined as the difference between the kinetic energy K and the potential energy P of the system

$$L = K - P \quad \dots(2.37)$$

The kinetic potential energy of the system may be expressed in any convenient coordinate system that will simplify the problem. It is not necessary to use Cartesian coordinates.

The dynamics equations, in terms of the coordinates used to express the kinetic and potential energy, are obtained as

$$F_i = \frac{d}{dt} \frac{\partial L}{\partial \dot{q}_i} - \frac{\partial L}{\partial q_i} \quad \dots(2.38)$$

where q_i are the coordinates in which the kinetic and potential energy are expressed \dot{q}_i is the corresponding velocity, and F_i the corresponding force or torque; F_i is either a force or a torque i , depending upon whether q_i is a linear or an angular coordinate. These factors, torques, and coordinates are referred to as generalized forces, torques, and coordinates.

Illustrative Example

We shall derive the dynamic equations for a two-link serial manipulator as shown in Fig. 2.18. Here the link masses are represented by point masses at the end of the link. The manipulator hangs down in a field of gravity g . As indicated in the figure θ_1 and θ_2 are chosen as the generalized coordinates.

The Kinetic and Potential Energy

The kinetic energy of a mass is $K = 1/2 mv^2$. So far the mass m_1 the kinetic energy is expressed as

$$K_1 = (1/2)m_1 d_1^2 \dot{\theta}_1^2 \quad \dots(i)$$

The potential energy with reference to the coordinate frame is expressed by the y -coordinate as

$$P_1 = -m_1 g d_1 \cos(\theta_1) \quad \dots(ii)$$

In the case of the second mass let us first write expressions for its Cartesian position coordinates. These are

$$x_2 = d_1 \sin(\theta_1) + d_2 \sin(\theta_1 + \theta_2) \quad \dots(iii)$$

$$y_2 = -d_1 \cos(\theta_1) - d_2 \cos(\theta_1 + \theta_2) \quad \dots(iv)$$

Differentiating these we get the velocity components of the mass m_2 as

$$\dot{x}_2 = d_1 \cos(\theta_1) \dot{\theta}_1 + d_2 \cos(\theta_1 + \theta_2) (\dot{\theta}_1 + \dot{\theta}_2)$$

$$\dot{y}_2 = d_1 \sin(\theta_1) \dot{\theta}_1 + d_2 \sin(\theta_1 + \theta_2) (\dot{\theta}_1 + \dot{\theta}_2)$$

The magnitude of the velocity squared is then

$$\begin{aligned} v_2^2 &= d_1^2 \dot{\theta}_1^2 + d_2^2 (\dot{\theta}_1^2 + 2\dot{\theta}_1 \dot{\theta}_2 + \dot{\theta}_2^2) \\ &\quad + 2d_1 d_2 \cos(\theta_1) \cos(\theta_1 + \theta_2) (\dot{\theta}_1^2 + \dot{\theta}_1 \dot{\theta}_2) \\ &\quad + 2d_1 d_2 \sin(\theta_1) \sin(\theta_1 + \theta_2) (\dot{\theta}_1^2 + \dot{\theta}_1 \dot{\theta}_2) \\ &= d_1^2 \dot{\theta}_1^2 + d_2^2 (\dot{\theta}_1^2 + 2\dot{\theta}_1 \dot{\theta}_2 + \dot{\theta}_2^2) + 2d_1 d_2 \cos(\theta_2) (\dot{\theta}_1^2 + \dot{\theta}_1 \dot{\theta}_2) \end{aligned}$$

and the kinetic energy of the mass m_2 is then

$$K_2 = 1/2 m_2 d_1^2 \dot{\theta}_1^2 + 1/2 m_2 d_2^2 (\dot{\theta}_1^2 + 2\dot{\theta}_1 \dot{\theta}_2 + \dot{\theta}_2^2) + m_2 d_1 d_2 \cos(\theta_2) (\dot{\theta}_1^2 + \dot{\theta}_1 \dot{\theta}_2)$$

From eqn. (iv) the potential energy of the mass m_2 is

$$P_2 = -m_2 g d_1 \cos(\theta_1) - m_2 g d_2 \cos(\theta_1 + \theta_2) \quad \dots(v)$$

The Lagrangian

The Lagrangian for the two-link system is

$$L = (K_1 + K_2) - (P_1 + P_2)$$

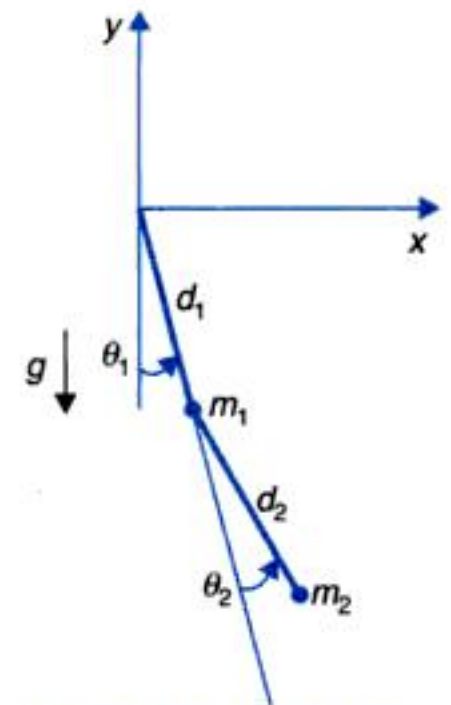


Fig. 2.18. A two link manipulator.

Substituting the values we get

$$\begin{aligned}
 L = & 1/2(m_1 + m_2)d_1^2\dot{\theta}_1^2 + 1/2m_2d_2^2(\dot{\theta}_1^2 + 2\dot{\theta}_1\dot{\theta}_2 + \dot{\theta}_2^2) \\
 & + m_2d_1d_2 \cos(\theta_2)(\dot{\theta}_1^2 + \dot{\theta}_1\dot{\theta}_2) \\
 & + (m_1 + m_2)gd_1 \cos(\theta_1) + m_2gd_2 \cos(\theta_1 + \theta_2) \quad \dots(vi)
 \end{aligned}$$

The Dynamic Equations

The dynamic equations are derived below using the Lagrangian of eqn. (vi)

$$\begin{aligned}
 \frac{\partial L}{\partial \dot{\theta}_1} &= (m_1 + m_2)d_1^2\dot{\theta}_1 + m_2d_2^2\dot{\theta}_1 + m_2d_1d_2 \cos(\theta_2)\dot{\theta}_1 \\
 &+ 2m_2d_1d_2 \cos(\theta_2)\dot{\theta}_1 + m_2d_1d_2 \cos(\theta_2)\dot{\theta}_2 \\
 \frac{d}{dt} \frac{\partial L}{\partial \dot{\theta}_1} &= [(m_1 + m_2)d_1^2 + m_2d_2^2 + 2m_2d_1d_2 \cos(\theta_2)]\ddot{\theta}_1 \\
 &+ [m_2d_2^2 + m_2d_1d_2 \cos(\theta_2)]\ddot{\theta}_2 \\
 &- 2m_2d_1d_2 \sin(\theta_2)\dot{\theta}_1\dot{\theta}_2 - m_2d_1d_2 \sin(\theta_2)\dot{\theta}_2^2 \\
 \frac{\partial L}{\partial \theta_1} &= -(m_1 + m_2)gd_1 \sin(\theta_1) - m_2gd_2 \sin(\theta_1 + \theta_2)
 \end{aligned}$$

These equations yield the torque at joint 1 as

$$\begin{aligned}
 T_1 = & [(m_1 + m_2)d_1^2 + m_2d_2^2 + 2m_2d_1d_2 \cos(\theta_2)]\ddot{\theta}_1 \\
 & + [m_2d_2^2 + m_2d_1d_2 \cos(\theta_2)]\ddot{\theta}_2 \\
 & - 2m_2d_1d_2 \sin(\theta_2)\dot{\theta}_1\dot{\theta}_2 - m_2d_1d_2 \sin(\theta_2)\dot{\theta}_2^2 \\
 & + (m_1 + m_2)gd_1 \sin(\theta_1) + m_2gd_2 \sin(\theta_1 + \theta_2) \quad \dots(vii)
 \end{aligned}$$

Performing similar operations at joint 2, we have

$$\begin{aligned}
 \frac{\partial L}{\partial \dot{\theta}_2} &= m_2d_1d_2 \cos(\theta_2)\dot{\theta}_1 + m_2d_2^2\dot{\theta}_2 \\
 \frac{d}{dt} \frac{\partial L}{\partial \dot{\theta}_2} &= m_2d_1d_2 \cos(\theta_2)\ddot{\theta}_1 + m_2d_2^2\ddot{\theta}_2 - m_2d_1d_2 \sin(\theta_2)\dot{\theta}_1\dot{\theta}_2 \\
 \frac{\partial L}{\partial \theta_2} &= -m_2d_1d_2 \sin(\theta_2)\dot{\theta}_1\dot{\theta}_2 - m_2gd_2 \sin(\theta_1 + \theta_2)
 \end{aligned}$$

The torque at joint 2 is then given by

$$\begin{aligned}
 T_2 = & [m_2d_1d_2 \cos(\theta_2)]\ddot{\theta}_1 + m_2d_2^2\ddot{\theta}_2 - 2m_2d_1d_2 \sin(\theta_2)\dot{\theta}_1\dot{\theta}_2 \\
 & - m_2d_1d_2 \sin(\theta_2)\dot{\theta}_1^2 + m_2gd_2 \sin(\theta_1 + \theta_2) \quad \dots(viii)
 \end{aligned}$$

The torques at joint 1 and 2 (eqns. (vii) and (viii)), can be rewritten in the general form

$$T_1 = D_{11}\ddot{\theta}_1 + D_{12}\ddot{\theta}_2 + D_{111}\dot{\theta}_1^2 + D_{122}\dot{\theta}_2^2 + D_{112}\dot{\theta}_1\dot{\theta}_2 + D_{121}\dot{\theta}_2\dot{\theta}_1 + D_1 \quad \dots(ix)$$

$$T_2 = D_{12}\ddot{\theta}_1 + D_{22}\ddot{\theta}_2 + D_{211}\dot{\theta}_1^2 + D_{222}\dot{\theta}_2^2 + D_{212}\dot{\theta}_1\dot{\theta}_2 + D_{221}\dot{\theta}_2\dot{\theta}_1 + D_2 \quad \dots(x)$$

Various coefficients in the torque expressions of eqns. (x) and (xi) are defined below:

$$\begin{aligned}
 D_{11} &= [(m_1 + m_2)d_1^2 + m_2d_2^2 + 2m_2d_1d_2 \cos(\theta_2)] \\
 D_{22} &= m_2d_2^2
 \end{aligned}$$

Coupling inertias

$$D_{12} = D_{21} = m_2 d_2^2 + m_2 d_1 d_2 \cos(\theta_2)$$

Centripetal acceleration coefficients

$$D_{111} = 0$$

$$D_{122} = D_{211} = -m_2 d_1 d_2 \sin(\theta_2)$$

$$D_{222} = 0$$

Coriolis acceleration coefficients

$$D_{112} = D_{121} = -m_2 d_1 d_2 \sin(\theta_2)$$

$$D_{212} = D_{221} = -m_2 d_1 d_2 \sin(\theta_2)$$

Gravity terms

$$D_1 = (m_1 + m_2)gd_1 \sin(\theta_1) + m_2gd_2 \sin(\theta_1 + \theta_2)$$

$$D_2 = m_2gd_2 \sin(\theta_1 + \theta_2).$$

2.4 TRANSFER FUNCTIONS

The transfer function of a linear time-invariant system is defined to be the ratio of the Laplace transform of the output variable to the Laplace transform of the input variable under the assumption that all initial conditions are zero.

Consider the mass-spring-dashpot system shown in Fig. 2.5 (a), whose dynamics is described by the second-order differential equation (2.1).

Taking the Laplace transform of each term of this equation (assuming zero initial conditions), we obtain

$$F(s) = Ms^2X(s) + fsX(s) + KX(s)$$

Then the transfer function is

$$G(s) = \frac{X(s)}{F(s)} = \frac{1}{Ms^2 + fs + K} \quad \dots(2.39)$$

The highest power of the complex variable s in the denominator of the transfer function determines the *order of the system*. The mass-spring-dashpot system under consideration is thus a second-order system, a fact which is already recognized from its differential equation.

The transfer function of the L - R - C circuits shown in Fig. 2.12 is similarly obtained by taking the Laplace transform of eqns. (2.22) and (2.23), with zero initial conditions. The resulting equations are

$$sLI(s) + RI(s) + \frac{1}{s} \frac{I(s)}{C} = E(s)$$

$$\frac{1}{s} \frac{I(s)}{C} = E_0(s)$$

If e is assumed to be the input variable and e_0 the output variable, the transfer function of the system is

$$\frac{E_0(s)}{E(s)} = \frac{1}{LCs^2 + RCs + 1} \quad \dots(2.40)$$

Equation (2.39) and (2.40) reveal that the transfer function is an expression in s -domain, relating the output and input of the linear time-invariant system in terms of the system parameters and is independent of the input. It describes the input output behaviour of the system and does not give any information concerning the internal structure of the system. Thus, when the transfer function of a physical system is determined, the system can be represented by a *block*, which is a shorthand pictorial representation of the cause and effect relationship between input and output of the system. The signal flowing into the block (called input) flows out of it (called output) after being processed by the transfer function characterizing the block, see Fig. 2.19 (a). Functional operation of a system can be more readily visualized by examination of a block diagram rather than by the examination of the equations describing the physical system. Therefore, when working with a linear time-invariant system, we can think of a system or its sub-systems simply as interconnected blocks with each block described by a transfer function.

Laplace transforming eqn. (2.29), the transfer function of the thermal system shown in Fig. 2.14 is

$$\frac{\Delta\theta(s)}{\Delta H(s)} = \frac{R}{RCs + 1} \quad \dots(2.41)$$

The block diagram representation of the system is shown in Fig. 2.19 (a). When this system is subjected to a disturbance, the dynamics is described by eqn. (2.30). Taking the Laplace transformation of this equation, we get

$$(RCs + 1) \Delta\theta(s) = \Delta\theta_i(s) + R\Delta H(s) \quad \dots(2.42)$$

The corresponding block diagram representation is given in Fig. 2.19 (b).

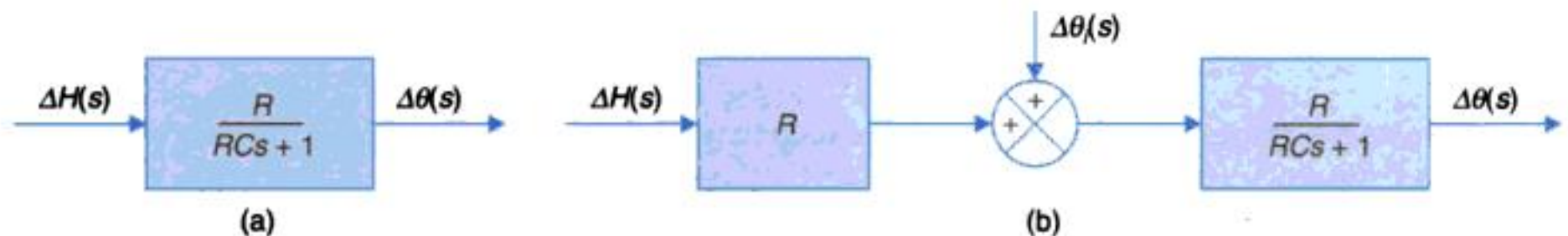


Fig. 2.19. Block diagram of the thermal system shown in Fig. 2.14.

Sinusoidal Transfer Functions

The steady-state response of a control system to a sinusoidal input is obtained by replacing s with $j\omega$ in the transfer function of the system.

Transfer function of the mechanical accelerometer shown in Fig. 2.6, obtained from eqn. (2.2), is

$$\frac{Y(s)}{X(s)} = \frac{Ms^2}{Ms^2 + fs + K} = \frac{s^2}{s^2 + \frac{f}{M}s + \frac{K}{M}}$$

Its sinusoidal transfer function becomes

$$\frac{Y(j\omega)}{X(j\omega)} = \frac{(j\omega)^2}{(j\omega)^2 + \frac{f}{M}(j\omega) + \frac{K}{M}} \quad \dots(2.43)$$

Equation (2.43) represents the behaviour of the accelerometer when used as a device to measure sinusoidally varying displacement. If the frequency of the sinusoidal input signal $X(j\omega)$ is very low, *i.e.*, $\omega \ll \omega_n = \sqrt{(K/M)}$, then the transfer function given by eqn. (2.43) may be approximated by

$$\frac{Y(j\omega)}{X(j\omega)} \approx \frac{-\omega^2}{K/M}$$

The output signal is very weak for values of frequency $\omega \ll \omega_n$. Weak output signal coupled with the fact that some inherent noise may always be present in the system, makes the displacement measurement by the accelerometer in the low frequency range as quite unreliable.

For $\omega \gg \omega_n$, the transfer function given by eqn. (2.43) may be approximated by

$$\frac{Y(j\omega)}{X(j\omega)} \approx 1$$

Thus, at very high frequencies the accelerometer output follows the sinusoidal displacement input. For this range of frequencies the basic accelerometer system can be used for displacement measurement particularly in seismographic studies.

For a sinusoidal input acceleration, the steady-state sinusoidal response of the accelerometer is given by

$$\frac{Y(j\omega)}{A(j\omega)} = \frac{1}{(j\omega)^2 + \frac{f}{M}(j\omega) + \frac{K}{M}}$$

As long as $\omega \ll \omega_n = \sqrt{(K/M)}$,

$$\frac{Y(j\omega)}{A(j\omega)} \approx \frac{M}{K}$$

The accelerometer is thus suitable for measurement of sinusoidally varying acceleration from zero frequency (constant acceleration) to a frequency which depends upon the choice of ω_n for the accelerometer. The sinusoidal behaviour of this type of transfer functions will be studied in greater details in Chapter 8.

Procedure for Deriving Transfer Functions

The following assumptions are made in deriving transfer functions of physical systems.

1. It is assumed that there is no loading, *i.e.*, no power is drawn at the output of the system. If the system has more than one nonloading elements in tandem, then the transfer function of each element can be determined independently and the overall transfer function of the physical system is determined by multiplying the individual transfer functions. In case of systems consisting of elements which load each other, the overall transfer function should be derived by basic analysis without regard to the individual transfer functions.
2. The system should be approximated by a linear lumped constant parameters model by making suitable assumptions.

To illustrate the point (1) above, let us consider two identical RC circuits connected in cascade so that the output from the first circuit is fed as input to the second as shown in Fig. 2.20.

The describing equations for this system are

$$\frac{1}{C} \int_{-\infty}^t (i_1 - i_2) dt + Ri_1 = e_i \quad \dots(2.44a)$$

$$\frac{1}{C} \int_{-\infty}^t (i_2 - i_1) dt + Ri_2 = -\frac{1}{C} \int_{-\infty}^t i_2 dt = -e_o \quad \dots(2.44b)$$

Taking the Laplace transforms of eqns. (2.44 (a)) and (2.44 (b)), assuming zero initial conditions, we obtain

$$\frac{1}{sC} [I_1(s) - I_2(s)] + RI_1(s) = E_i(s)$$

$$\frac{1}{sC} [I_2(s) - I_1(s)] + RI_2(s) = -\frac{1}{sC} [I_2(s)] = -E_o(s)$$

The transfer function obtained by eliminating $I_1(s)$ and $I_2(s)$ from the above equation is

$$\frac{E_o(s)}{E_i(s)} = \frac{1}{\tau^2 s^2 + 3\tau s + 1} \quad \dots(2.45)$$

where $\tau = RC$.

The transfer function of each of the individual RC circuits is $1/(1 + s\tau)$. From eqn. (2.45) it is seen that overall transfer function of the two RC circuits connected in cascades is not equal to $[1/(\tau s + 1)] [1/(\tau s + 1)]$ but instead it is $1/(\tau^2 s^2 + 3\tau s + 1)$.

This difference is explained by the fact that while deriving the transfer function of a single RC circuits, it is assumed that the output is unloaded. However, when the input of second circuit is obtained from the output of first, a certain amount of energy is drawn from the first circuit and hence its original transfer function is no longer valid. The degree to which the overall transfer function is modified from the product of individual transfer functions depends upon the amount of loading.

As an example to illustrate the point (2) above, let us derive the transfer function of a d.c. servomotor. In servo applications, a d.c. motor is required to produce rapid accelerations from standstill. Therefore the physical requirements of such a motor are low inertia and high starting torque. Low inertia is attained with reduced armature diameter with a consequent increase in armature length such that the desired power output is achieved. Thus, except for minor differences in constructional features, a d.c. servomotor is essentially an ordinary d.c. motor.

In control systems, the d.c. motors are used in two different control modes: armature-control mode with fixed field current, and field-control mode with fixed armature current.

Armature-control

Consider the armature-controlled d.c. motor shown in Fig. 2.21.

In this system,

R_a = resistance of armature (Ω).

L_a = inductance of armature winding (H).

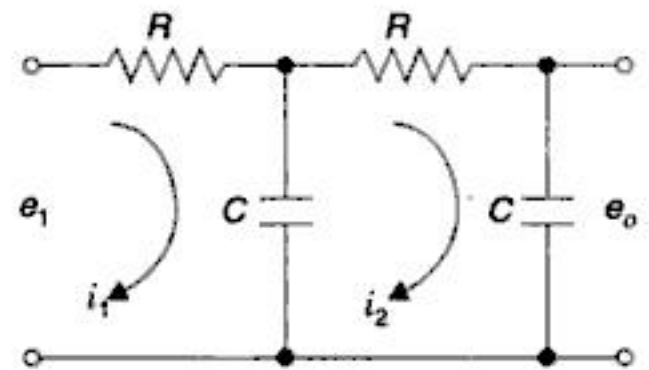


Fig. 2.20. RC circuits in cascade.

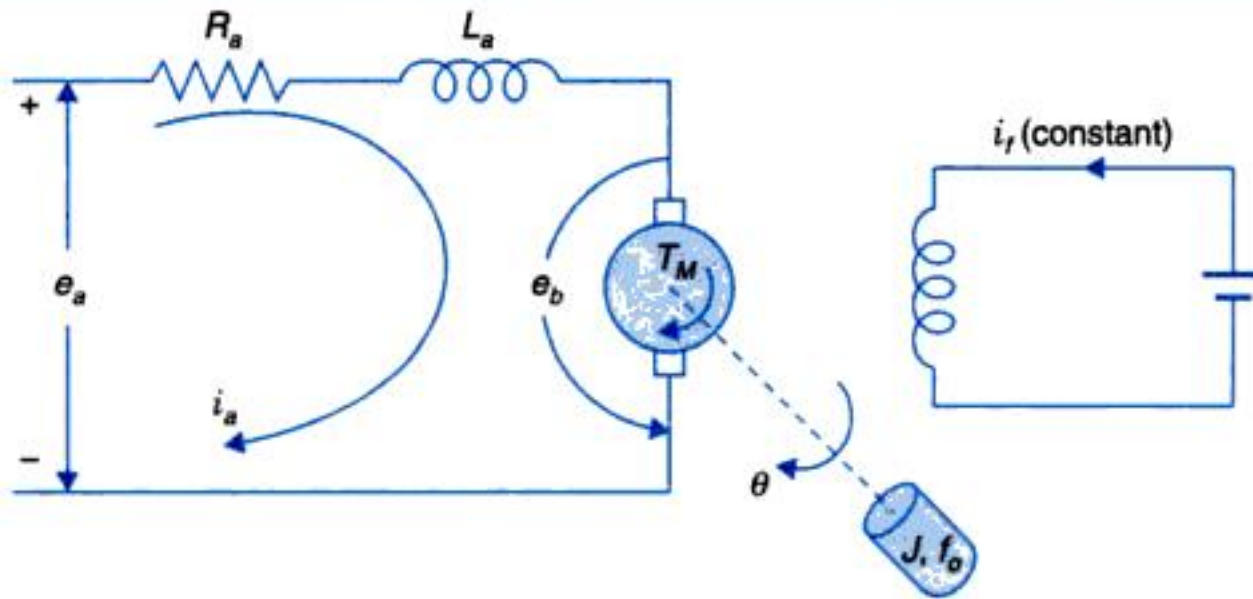


Fig. 2.21. Armature-controlled d.c. motor.

i_a = armature current (A).

i_f = field current (A).

e_a = applied armature voltage (V).

e_b = back emf (volts).

T_M = torque developed by motor (Nm).

θ = angular displacement of motor-shaft (rad).

J = equivalent moment of inertia of motor and load referred to motor shaft (kg-m^2).

f_0 = equivalent viscous friction coefficient of motor and load referred to motor shaft

$$\left(\frac{\text{Nm}}{\text{rad/s}} \right).$$

In servo applications, the d.c. motors are generally used in the linear range of the magnetization curve. Therefore, the air gap flux ϕ is proportional of the field current, *i.e.*,

$$\phi = K_f i_f \quad \dots(2.46)$$

where K_f is a constant.

The torque T_M developed by the motor is proportional to the product of the armature current and air gap flux, *i.e.*,

$$T_M = K_1 K_f i_f i_a \quad \dots(2.47)$$

where K_1 is a constant.

In the armature-controlled d.c. motor, the field current is kept constant, so that eqn. (2.46) can be written as

$$T_M = K_T i_a \quad \dots(2.48)$$

where K_T is known as the motor torque constant.

The motor back emf being proportional to speed is given as

$$e_b = K_b \frac{d\theta}{dt} \quad \dots(2.49)$$

where K_b is the back emf constant.

The differential equation of the armature circuit is

$$L_a \frac{di_a}{dt} + R_a i_a + e_b = e_a \quad \dots(2.50)$$

The torque equation is

$$J \frac{d^2\theta}{dt^2} + f_0 \frac{d\theta}{dt} = T_M = K_T i_a \quad \dots(2.51)$$

Taking the Laplace transforms of eqns. (2.48) to (2.50), assuming zero initial conditions, we get

$$E_b(s) = K_b s \theta(s) \quad \dots(2.52)$$

$$(L_a s + R_a) I_a(s) = E_a(s) - E_b(s) \quad \dots(2.53)$$

$$(J s^2 + f_0 s) \theta(s) = T_M(s) = K_T I_a(s) \quad \dots(2.54)$$

From eqns. (2.51) to (2.53), the transfer function of the system is obtained as

$$G(s) = \frac{\theta(s)}{E_a(s)} = \frac{K_T}{s[(R_a + sL_a)(Js + f_0) + K_T K_b]} \quad \dots(2.55)$$

The block diagram representation of eqn. (2.53) is shown in Fig. 2.22 (a) where the circular block representing the differencing action is known as the *summing point*. Equation (2.54) is represented by a block shown in Fig. 2.22 (b).

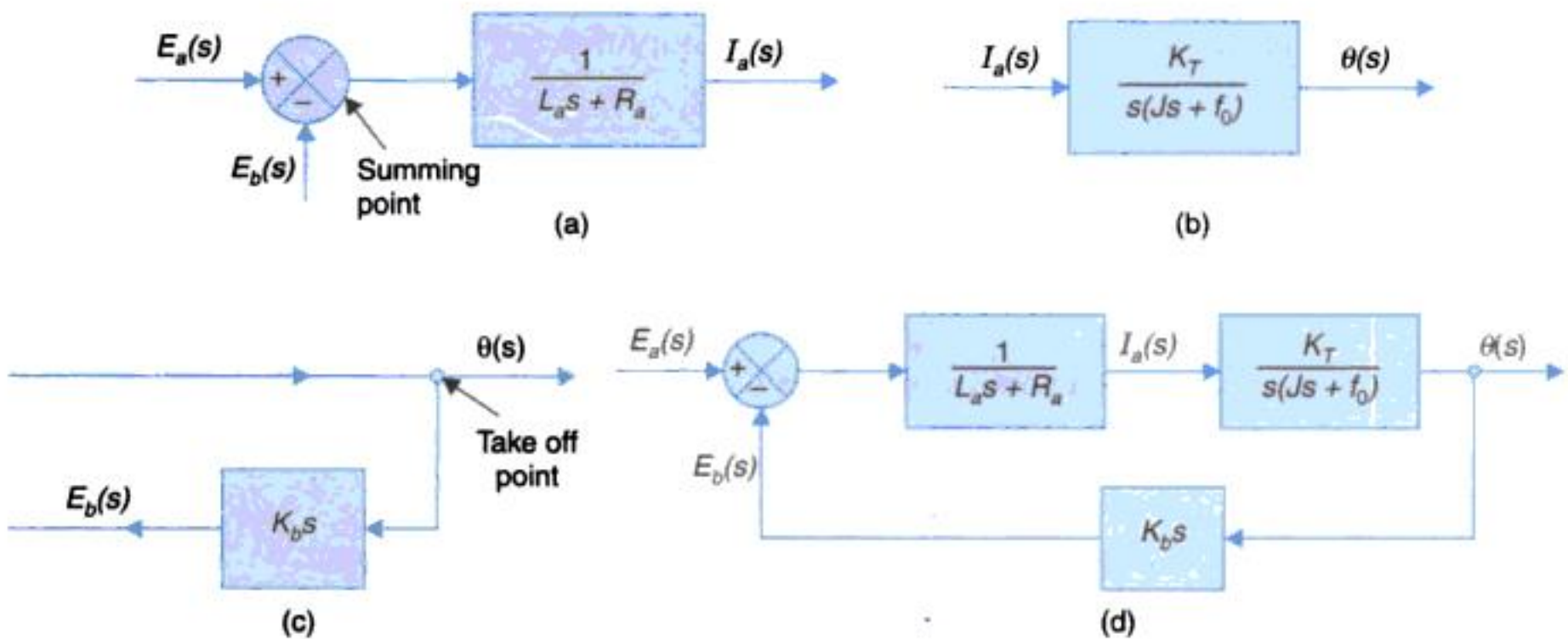


Fig. 2.22. Block diagram of armature-controlled d.c. motor.

Figure 2.22 (c) represents eqn. (2.52) where a signal is taken off from a *take-off point* and fed to the feedback block ($K_b s$). Fig. 2.22 (d) is the complete block diagram of the system under consideration, obtained by connecting the block diagram shown in Fig. 2.22 (a), (b) and (c). It may be pointed out here that when a signal is taken from the output of a block, this does not affect the output as per assumption 1 of the procedure for driving transfer functions advanced earlier.

However, it should be noted that the block diagram of the system under consideration can be directly obtained from the physical system of Fig. 2.21 by using the transfer functions of simple electrical and mechanical networks derived already. The voltage applied to the armature circuit is $E_a(s)$ which is opposed by the back emf ($E_b(s)$). The net voltage ($E_a - E_b$) acts on a linear circuit comprised of resistance and inductance in series, having the transfer function $1/(sL_a + R_a)$. The result is an armature current $I_a(s)$. For fixed field, the torque developed by

the motor is $K_T I_a(s)$. This torque rotates the load at a speed $\dot{\theta}(s)$ against the moment of inertia J and viscous friction with coefficient f_0 [the transfer function is $1/(Js + f_0)$]. The back emf signal $E_b = K_b \dot{\theta}(s)$ is taken off from the shaft speed and fed back negatively to the summing point. The angle signal $\theta(s)$ is obtained by integrating (i.e., $1/s$) the speed $\dot{\theta}(s)$. This results in the block diagram of Fig. 2.23, which is equivalent to that of Fig. 2.22 as can be seen by shifting the take off point from $\dot{\theta}(s)$ to $\theta(s)$.

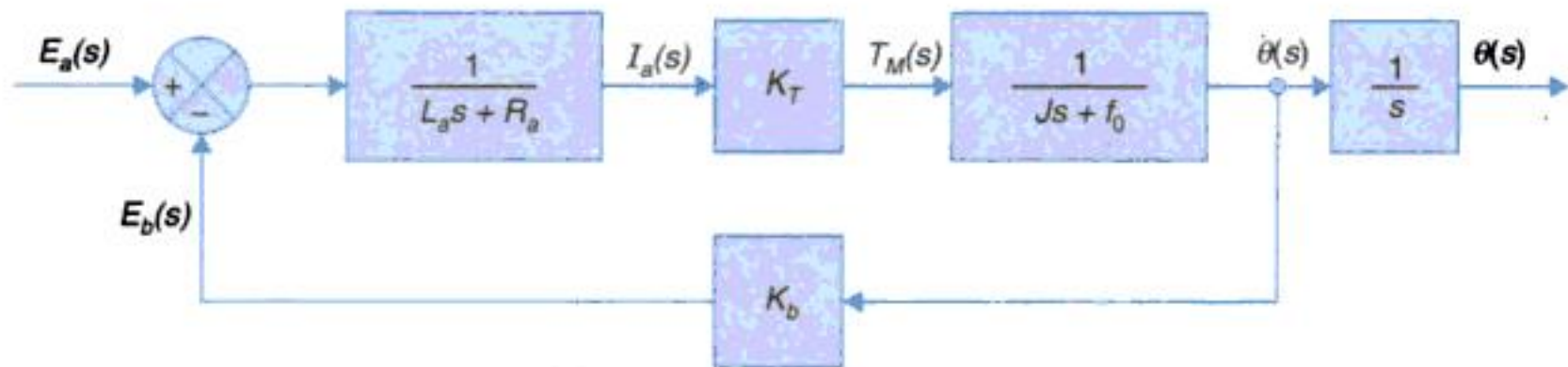


Fig. 2.23. Block diagram of armature-controlled d.c. motor.

The *armature circuit inductance* L_a is usually negligible. Therefore from eqn. (2.55), the transfer function of the armature controlled motor simplifies to

$$\frac{\theta(s)}{E_a(s)} = \frac{K_T/R_a}{Js^2 + s(f_0 + K_T K_b/R_a)} \quad \dots(2.56)$$

The term $(f_0 + K_T K_b/R_a)$ indicates that the back emf of the motor effectively increases the viscous friction of the system. Let

$$f = f_0 + K_T K_b/R_a$$

be the effective viscous friction coefficient. Then from eqn. (2.56)

$$\frac{\theta(s)}{E_a(s)} = \frac{K_T/R_a}{s(Js + f)} \quad \dots(2.57)$$

The transfer function given by eqn. (2.56) may be written in the form

$$\frac{\theta(s)}{E_a(s)} = \frac{K_m}{s(s\tau_m + 1)} \quad \dots(2.58)$$

where $K_m = K_T/R_a f =$ motor gain constant, and $\tau_m = J/f =$ motor time constant.

The motor torque and back emf constants K_T, K_b are interrelated. Their relationship is deduced below. In metric units, K_b is in V/rad/s and K_T is in Nm/A.

Electrical power converted to mechanical form = $e_b i_a = K_b \dot{\theta} i_a$ W

Power at shaft (in mechanical form) = $T \dot{\theta} = K_T i_a \dot{\theta}$ W

At steady speed these two powers balance. Hence

$$K_b \dot{\theta} i_a = K_T i_a \dot{\theta} \quad \text{or} \quad K_b = K_T \text{ (in MKS units)}$$

This result can be used to advantage in practice as K_b can be measured more easily and with greater accuracy than K_T .

Field-control

A field-controlled d.c. motor is shown in Fig. 2.24 (a).

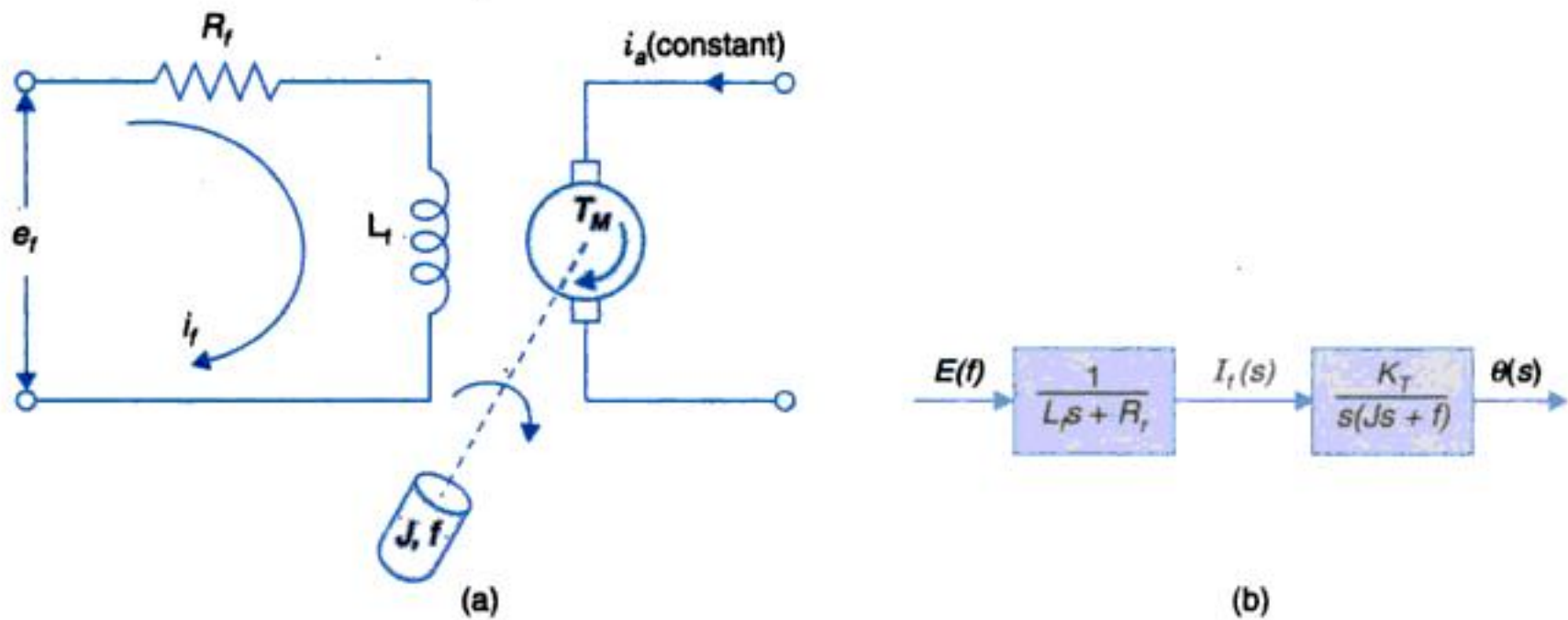


Fig. 2.24. (a) Field-controlled d.c. motor, (b) Block diagram of field-controlled motor.

In this system,

R_f = field winding resistance (Ω).

L_f = field winding inductance (H).

e = field control voltage (V).

i_f = field current (A).

T_M = torque developed by motor (Nm).

J = equivalent moment of inertia of motor and load referred to motor shaft ($\text{kg}\cdot\text{m}^2$).

f = equivalent viscous friction coefficient of motor and load referred to motor shaft $\frac{\text{Nm}}{\text{rad/s}}$.

θ = angular displacement of motor shaft (rad).

In the field-controlled motor, the armature current is fed from a constant current source.

Therefore, from eqn. (2.36)

$$T_M = K_1 K_f i_f i_a = K_T' i_f$$

where K_T' is a constant.

The equation for the field circuit is

$$L_f \frac{di_f}{dt} + R_f i_f = e_f \tag{2.59}$$

The torque equation is

$$J \frac{d^2\theta}{dt^2} = f \frac{d\theta}{dt} = T_M = K_T' i_f \tag{2.60}$$

Taking the Laplace transform of eqns. (2.48) and (2.49), assuming zero initial conditions, we get

$$(L_f s + R_f) I_f(s) = E_f(s) \tag{2.61}$$

$$(Js^2 + fs) \theta(s) = T_M(s) = K_T' I_f(s) \tag{2.62}$$

From the above equations, the transfer function of the motor is obtained as

$$\frac{\theta(s)}{E_f(s)} = \frac{K_T'}{s(L_f s + R_f)(Js + f)} = \frac{K_m}{s(\tau_f s + 1)(\tau_{me} s + 1)} \quad \dots(2.63)$$

where $K_m = K_T'/R_f f =$ motor gain constant; $\tau_f = L_f/R_f =$ time constant of field circuit; and $\tau_{me} = J/f$; mechanical time constant.

The block diagram of the field-controlled d.c. motor obtained from eqns. (2.61) and (2.62) is given in Fig. 2.24 (b).

For small size motors field-control is advantageous because only a low power servo amplifier is required while the armature current which is not large can be supplied from an expensive constant current amplifier. For large size motors it is on the whole cheaper to use armature-control scheme. Further in armature-controlled motor, back emf contributes additional damping over and above that provided by load friction. With the advances made in permanent magnet materials, permanent magnet armature-controlled d.c. servomotor are now universally adopted (see Chapter 5).

2.5 BLOCK DIAGRAM ALGEBRA

As introduced earlier, the input-output behaviour of a linear system or element of a linear system is given by its transfer function

$$G(s) = C(s)/R(s)$$

where $R(s) =$ Laplace transformation of the input variable; and $C(s) =$ Laplace transform of the output variable.

A convenient graphical representation of this behaviour is the *block diagram* as shown in Fig. 2.25 (a) wherein the signal into the block represents the input $R(s)$ and the signal out of the block represents the output $C(s)$, while the block itself stands for the transfer function $G(s)$. The flow of information (signal) is unidirectional from the input to the output with the output being equal to the input multiplied by the transfer function of the block. A complex system comprising of several non-loading elements is represented by the interconnection of the blocks for individual elements. The blocks are connected by lines with arrows indicating the unidirectional flow of information from the output of one block to the input of the other. In addition to this, *summing* or *differencing* of signals is indicated by the symbols shown in Fig. 2.25 (b), while the *take-off* point of a signal is represented by Fig. 2.25 (c).

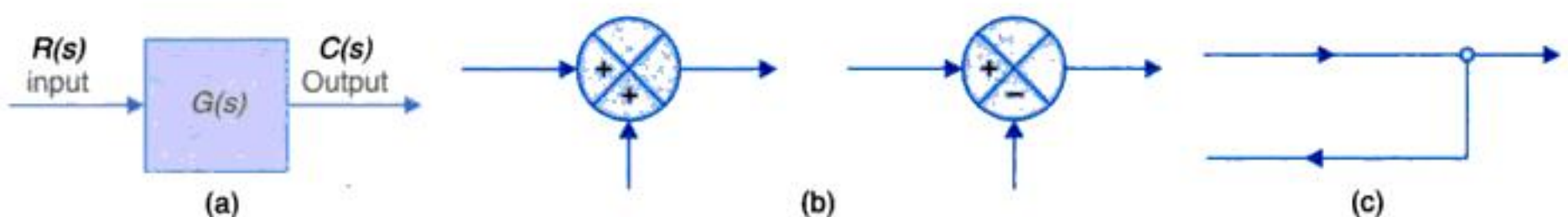


Fig. 2.25

Block diagrams of some of the control systems turn out to be very complex such that the evaluation of their performance requires simplification (or reduction) of block diagrams which

is carried out by block diagram rearrangements. Some of the important block diagram rearrangements are discussed in this section.

Block Diagram of a Closed-loop System

Fig. 2.26 (a) shows the block diagram of a negative feedback system. With reference to this figure, the terminology used in block diagrams of control systems is given below.

$R(s)$ = reference input.

$C(s)$ = output signal or controlled variable.

$B(s)$ = feedback signal.

$E(s)$ = actuating signal.

$G(s) = C(s)/E(s)$ = forward path transfer function.

$H(s)$ = transfer function of the feedback elements.

$G(s)H(s) = B(s)/E(s)$ = loop transfer function.

$T(s) = C(s)/R(s)$ = closed-loop transfer function.

From Fig. 2.26 (a) we have

$$C(s) = G(s)E(s) \quad \dots(2.64)$$

$$E(s) = R(s) - B(s) = R(s) - H(s)C(s) \quad \dots(2.65)$$

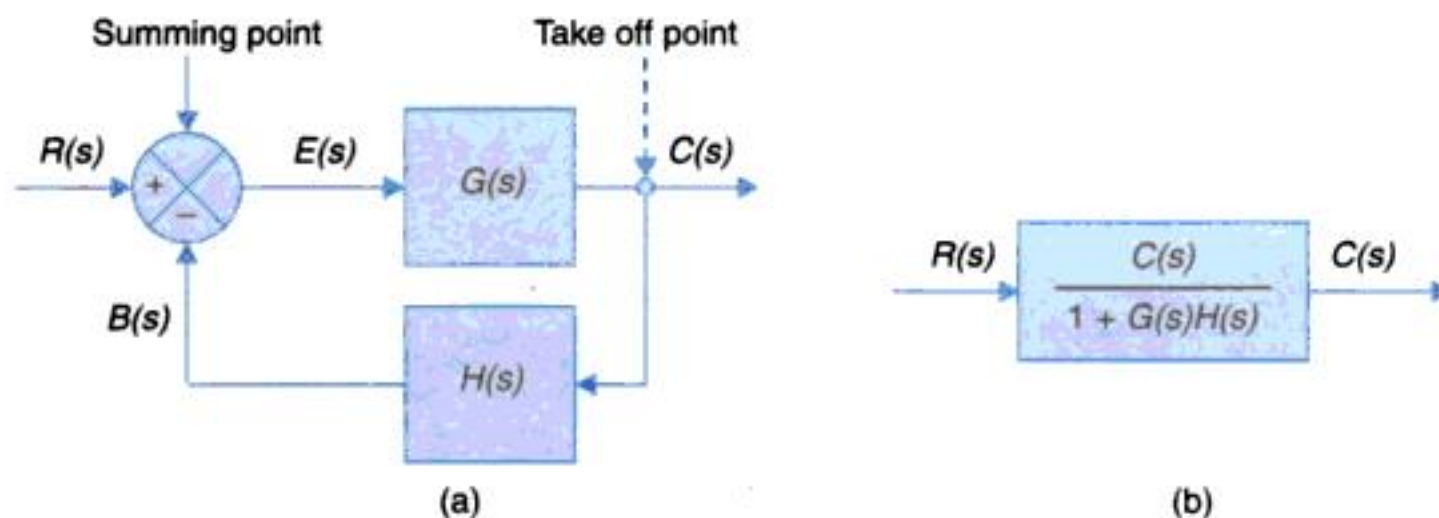


Fig. 2.26. (a) Block diagram of closed-loop system;
(b) Reduction of block diagram shown in Fig. 2.26 (a).

Eliminating $E(s)$ from eqns. (2.64) and (2.65) we have

$$C(s) = G(s)R(s) - G(s)H(s)C(s)$$

$$\text{or} \quad \frac{C(s)}{R(s)} = T(s) = \frac{G(s)}{1 + G(s)H(s)} \quad \dots(2.66)$$

Therefore the system shown in Fig. 2.26 (a) can be reduced to a single block shown in Fig. 2.26 (b).

Multiple-input-multiple-output Systems

When multiple inputs are present in a linear system, each input can be treated independently of the others. Complete output of the system can then be obtained by superposition, *i.e.*, outputs corresponding to each input along are added together.

Consider a two-input linear system shown in Fig. 2.27 (a). The response to the reference input can be obtained by assuming $U(s) = 0$. The corresponding block diagram shown in Fig. 2.27 (b) gives

$$\begin{aligned} C_R(s) &= \text{output due to } R(s) \text{ acting alone} \\ &= \frac{G_1(s)G_2(s)}{1 + G_1(s)G_2(s)H(s)} R(s) \end{aligned} \quad \dots(2.67)$$

Similarly the response to the input $U(s)$ is obtained by assuming $R(s) = 0$. The block diagram corresponding to this case is shown in Fig. 2.27 (c), which gives

$$\begin{aligned} C_U(s) &= \text{input due to } U(s) \text{ acting along} \\ &= \frac{G_2(s)}{1 + G_1(s)G_2(s)H(s)} U(s) \end{aligned} \quad \dots(2.68)$$

The response to the simultaneous application of $R(s)$ and $U(s)$ can be obtained by adding the two individual responses.

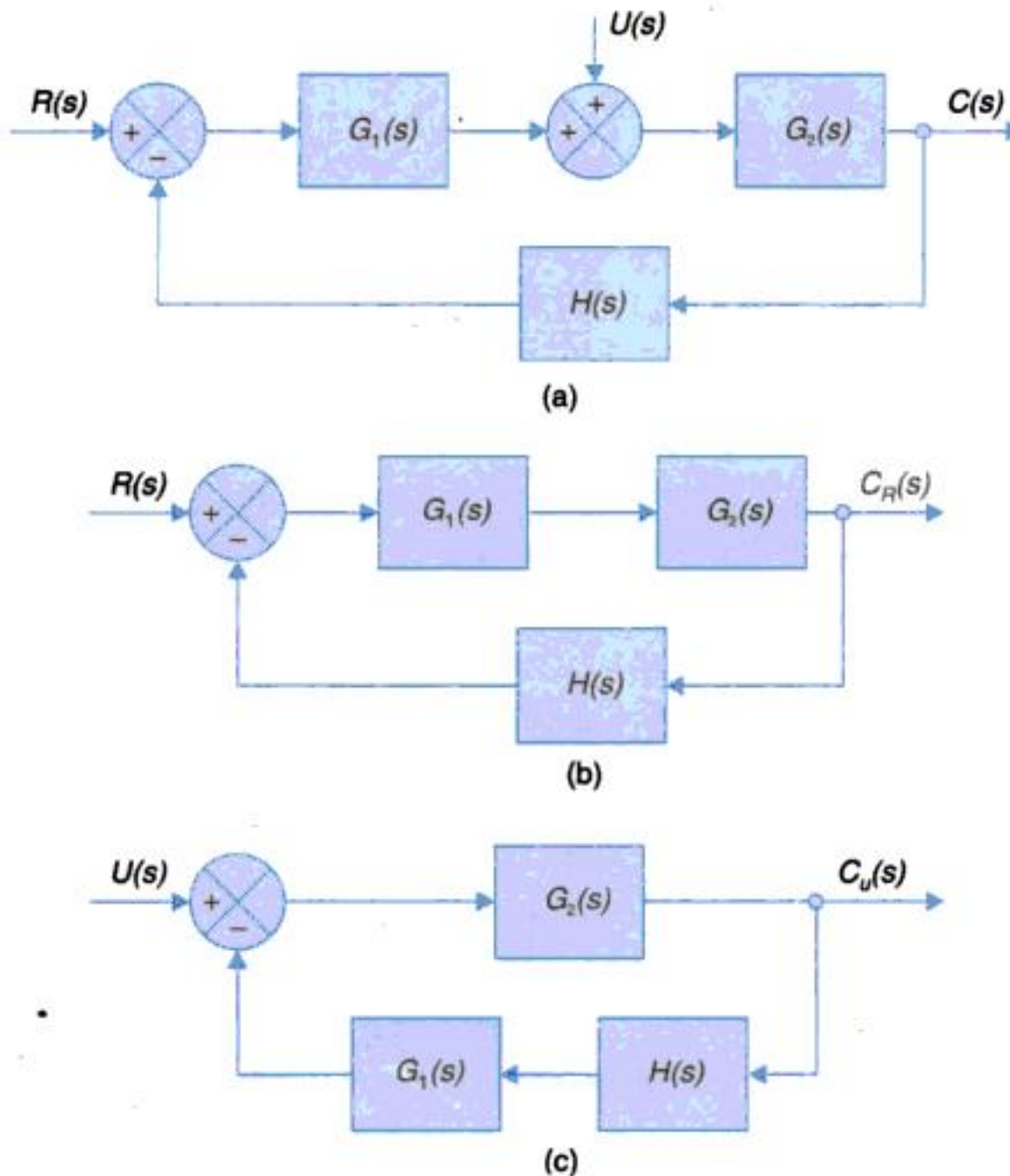


Fig. 2.27. Block diagram of two-input system.

Adding eqns. (2.67) and (2.68), we get

$$C(s) = C_R(s) + C_U(s) = \frac{G_2(s)}{1 + G_1(s)G_2(s)H(s)} [G_1(s)R(s) + U(s)] \quad \dots(2.69)$$

In case of multiple-input multiple-output system shown in Fig. 2.28 (r inputs and m outputs), the i -th output $C_i(s)$ is given by the principle of superposition as

$$C_i(s) = \sum_{j=1}^r G_{ij}(s)R_j(s); i = 1, 2, \dots, m \quad \dots(2.70)$$

where $R_j(s)$ is the j -th input and $G_{ij}(s)$ is the transfer function between the i -th output and j -th input with all other inputs reduced to zero.

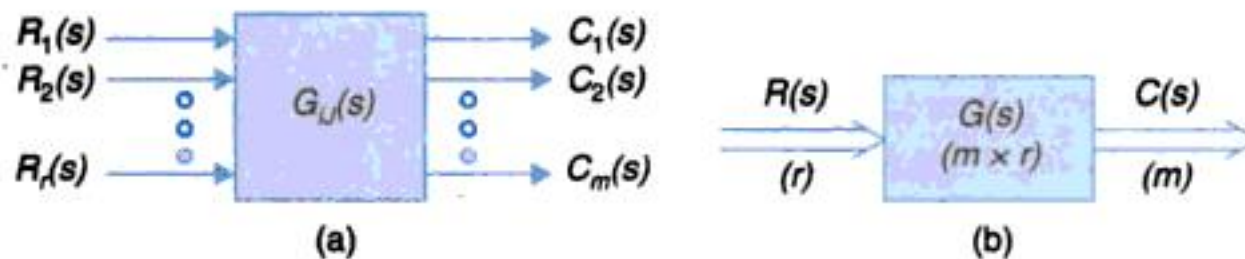


Fig. 2.28. Multiple-input-multiple-output systems.

Equation (2.69) can be expressed in matrix form as

$$\begin{bmatrix} C_1(s) \\ C_2(s) \\ \vdots \\ C_m(s) \end{bmatrix} = \begin{bmatrix} G_{11}(s) & G_{12}(s) & \dots & G_{1r}(s) \\ \vdots & \vdots & & \vdots \\ G_{m1}(s) & G_{m2}(s) & \dots & G_{mr}(s) \end{bmatrix} \begin{bmatrix} R_1(s) \\ R_2(s) \\ \vdots \\ R_r(s) \end{bmatrix} \quad \dots(2.71)$$

This can be expressed in compressed matrix notation as

$$\mathbf{C}(s) = \mathbf{G}(s)\mathbf{R}(s) \quad \dots(2.72)$$

where $\mathbf{R}(s)$ = vector of inputs (in Laplace transform), dimension r

$\mathbf{G}(s)$ = matrix transfer function ($m \times r$)

$\mathbf{C}(s)$ = vector of output (m)

The corresponding block diagram can be drawn as in Fig. 2.28(b) where thick arrows represent multi inputs and outputs.

When feedback loop is present each feedback signal is obtained by processing in general all the outputs. Thus for i th feedback signal we can write

$$B_i(s) = \sum_{j=1}^m H_{ij}(s)C_j(s) \quad \dots(2.73)$$

The i th error signal is then

$$E_i(s) = R_i(s) - B_i(s) \quad \dots(2.74)$$

Generalizing in matrix form we can write

$$\mathbf{C}(s) = \mathbf{G}(s) \mathbf{E}(s) \quad \dots(i)$$

$$\mathbf{E}(s) = \mathbf{R}(s) - \mathbf{B}(s) \quad \dots(ii)$$

$$\mathbf{B}(s) = \mathbf{H}(s) \mathbf{C}(s) \quad \dots(iii)$$

Substituting eqns. (ii) and (iii) in eqn. (i), we get

$$\mathbf{C}(s) = \mathbf{G}(s) [\mathbf{R}(s) - \mathbf{H}(s) \mathbf{C}(s)] = \mathbf{G}(s) \mathbf{R}(s) - \mathbf{G}(s) \mathbf{H}(s) \mathbf{C}(s) \quad \dots(iv)$$

This can be simplified as

$$\mathbf{C}(s) + \mathbf{G}(s) \mathbf{H}(s) \mathbf{C}(s) = \mathbf{G}(s) \mathbf{R}(s)$$

or $\mathbf{C}(s) [\mathbf{I} + \mathbf{G}(s) \mathbf{H}(s)] = \mathbf{G}(s) \mathbf{R}(s)$

or $\mathbf{C}(s) = [\mathbf{I} + \mathbf{G}(s) \mathbf{H}(s)]^{-1} \mathbf{G}(s) \mathbf{R}(s) \dots(2.75)$

wherein closed loop matrix transfer function as

$$\mathbf{T}(s) = \mathbf{G}(s) [\mathbf{I} + \mathbf{G}(s) \mathbf{H}(s)]^{-1} \dots(2.76)$$

The results are represented in thick arrow block diagram of Fig. 2.29. The reader may compare this block diagram and matrix equation (2.76) with the block diagram of Fig. 2.26 and eqn. (2.66) of the single-input-single-output case.

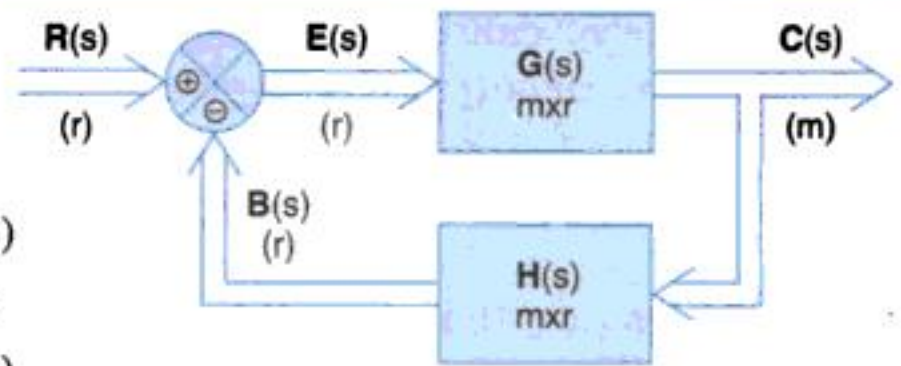


Fig. 2.29. Block diagram of multi-input multi-output closed-loop system.

Block Diagram Reduction

As indicated earlier, a complex block diagram configuration can be simplified by certain rearrangements of block diagram using the rules of block diagram algebra. Some of the important rules are given in Table 2.4. All these rules are derived by simple algebraic manipulations of the equations representing the blocks.

As an example, let us consider the liquid-level system shown in Fig. 2.30 (note that because of interaction of the tanks, the complete transfer function cannot be obtained by multiplying individual transfer functions of the tanks).

In this system, a tank having liquid capacitance C_1 is supplying liquid through a pipe of resistance R_1 to another tank of liquid capacitance C_2 , which delivers this liquid through a pipe of resistance R_2 . The steady-state outflow rates of tank 1 and that of tank 2 are Q_1 and Q_2 and heads are H_1 and H_2 respectively.

Let ΔQ be a small deviation in the inflow rate Q . This results in

ΔH_1 = small deviation of the head of tank 1 from its steady-state value.

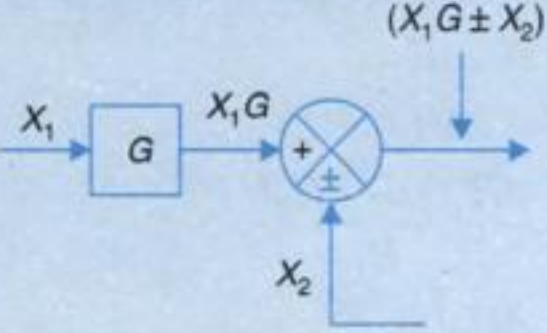
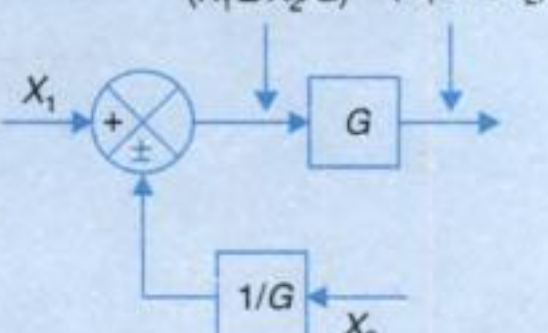
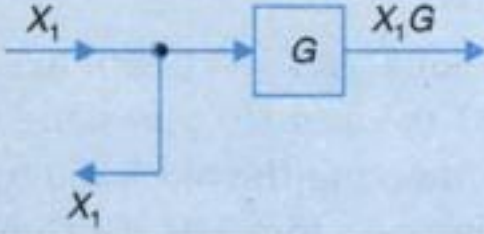
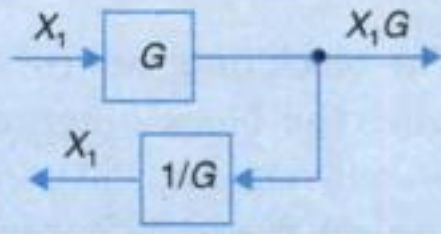
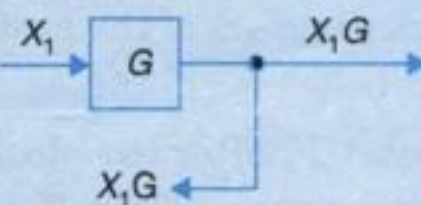
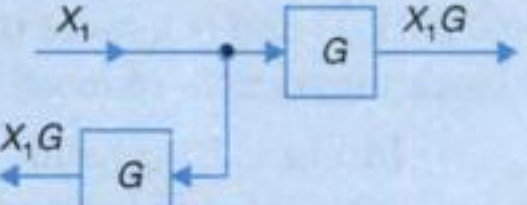
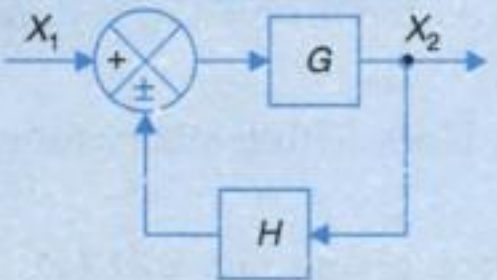
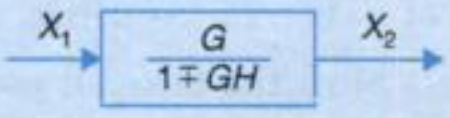
ΔH_2 = small deviation of the head of the tank 2 from its steady-state value.

ΔQ_1 = small deviation of the outflow rate of tank 1 from its steady-state value.

ΔQ_2 = small deviation of the outflow rate of tank 2 from its steady-state value.

Table 2.5. Rules of Block Diagram Algebra

| Rule | Original diagram | Equivalent diagram |
|-----------------------------------------|------------------|--------------------|
| 1. Combining blocks in cascade | | |
| 2. Moving a summing point after a block | | |

| | | |
|----------------------------------------------------|--------------------------------------------------------------------------------------|---------------------------------------------------------------------------------------|
| <p>3. Moving a summing point ahead of a block</p> |  |  |
| <p>4. Moving a take off point after a block</p> |  |  |
| <p>5. Moving a take off point ahead of a block</p> |  |  |
| <p>6. Eliminating a feedback loop</p> |  |  |

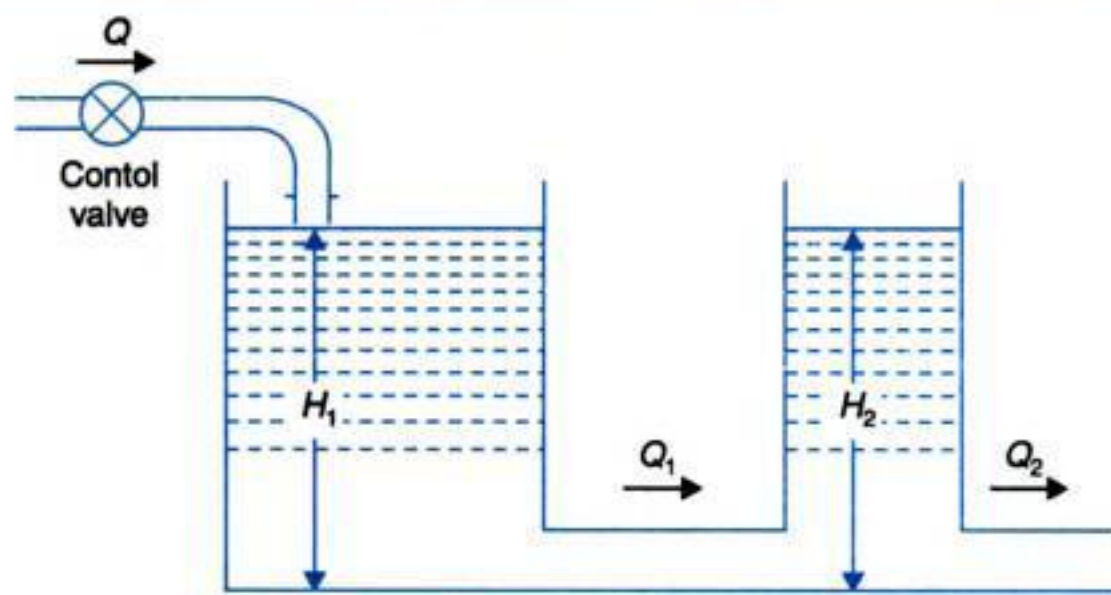


Fig. 2.30. Liquid-level system.

The flow balance equation for tank 1 is

$$\Delta Q = \Delta Q_1 + C_1 \frac{d}{dt} (\Delta H_1)$$

Similarly for tank 2

$$\Delta Q_1 = \Delta Q_2 + C_2 \frac{d}{dt} (\Delta H_2)$$

where

$$\Delta Q_1 = \frac{\Delta H_1 - \Delta H_2}{R_1} \quad \text{and} \quad \Delta Q_2 = \frac{\Delta H_2}{R_2}$$

Taking the Laplace transform of the above equations we get

$$\Delta Q(s) - \Delta Q_1(s) = sC_1\Delta H_1(s) \quad \dots(2.77)$$

$$\Delta Q_1(s) - \Delta Q_2(s) = sC_2\Delta H_2(s) \quad \dots(2.78)$$

$$\Delta Q_1(s) = \frac{\Delta H_1(s) - \Delta H_2(s)}{R_1} \quad \dots(2.79)$$

$$\Delta Q_2(s) = \frac{\Delta H_2(s)}{R_2} \quad \dots(2.80)$$

The block diagram corresponding to eqns. (2.77) – (2.80) are given in Figs. 2.31 (a)-(d). Connecting the block diagrams of Fig. 2.31 (a) and (b) gives the block diagram for tank 1, which is shown in Fig. 2.31 (e). Similarly connecting the block diagrams of Fig. 2.31 (c) and (d) gives the block diagram for tank 2 which is shown in Fig. 2.31 (f). Connecting the block diagrams of Figs. 2.31 (e) and (f), gives the overall block diagram of the system as shown in Fig. 2.31 (g). This block diagram is reduced in steps given below.

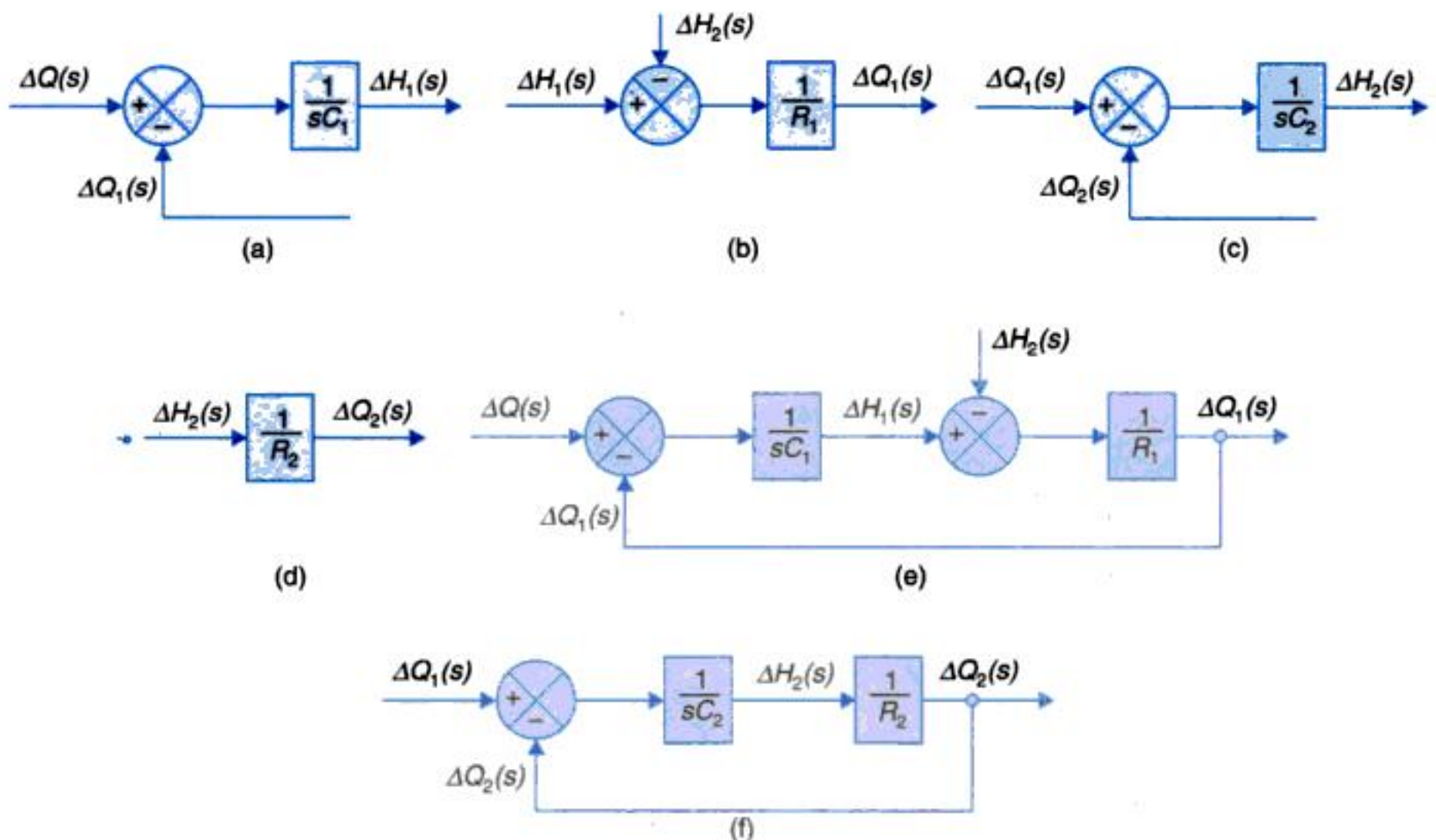
(i) In Fig. 2.31 (g) shift the take off point T_1 after the block with transfer function $1/R_2$ (rule 4 of Table 2.5). This results in the block diagram of Fig. 2.31.

(ii) Minor feedback loop enclosed in dotted line is now reduced to a single block by rules 1 and 6 of Table 2.5 resulting in Fig. 2.31.

(iii) Shift the take off point T_2 to the block with transfer function $1/(R_2C_2s + 1)$ resulting in Fig. 2.31.

(iv) Reduce the encircled feedback loop giving Fig. 2.31 (k).

(v) Reduce Fig. 2.31 (k) to the single block of Fig. 2.31, which gives the overall transfer function of the system.



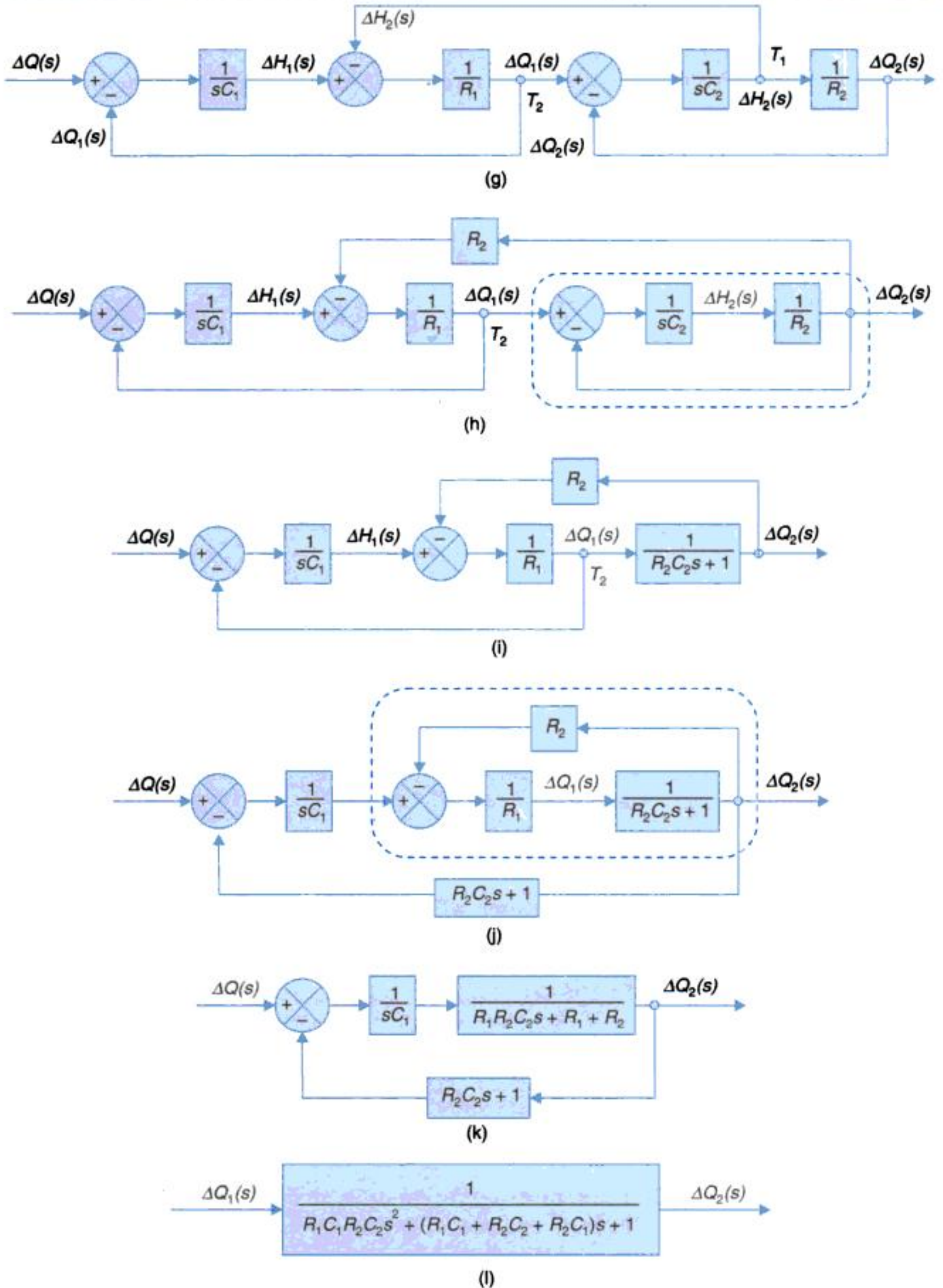


Fig. 2.31. Formation and reduction of block diagram of the system shown in Fig. 2.30.

Feedforward Compensation

Let us consider the example of Fig. 2.27 (a). The input $U(s)$ in this block diagram represents **Disturbance input** in control systems. Such an example will be considered later in this section 2.5 speed control system of Fig. 2.40. The effect of such an input is to introduce error into the system performance which needs to be kept low, within acceptable limits this is known as compensation. In several systems where the disturbance input can be predicted (or computed before hand), its effect can be eliminated by a feedforward compensation technique illustrated in the modified block diagram of Fig. 2.32.

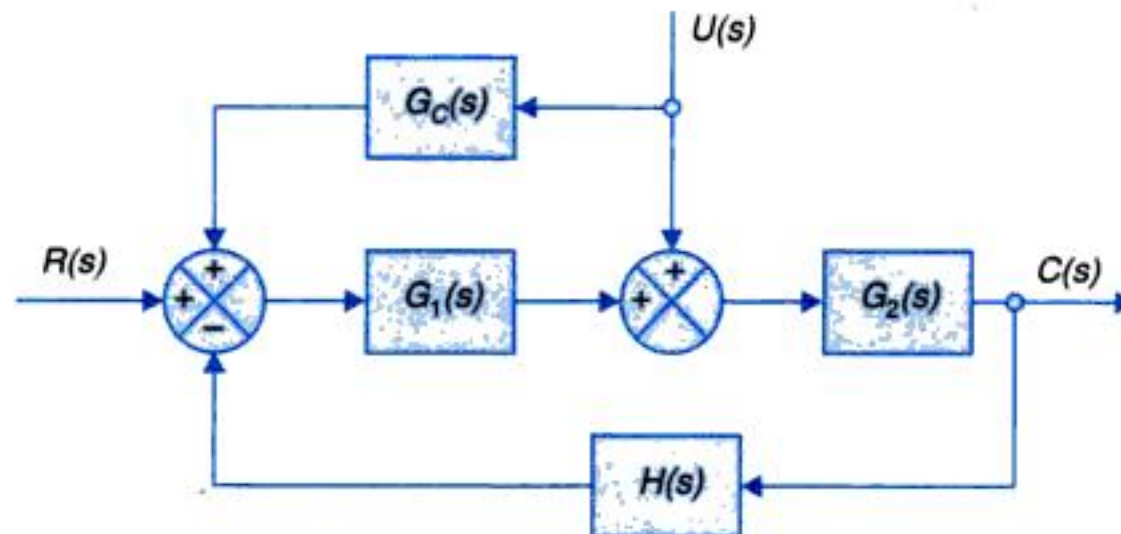


Fig. 2.32. Forward compensation.

The compensating block $G_c(s)$ causes additional input of $G_c(s)U(s)$ alongwith $U(s)$. It then follows from eqn. (2.67) that this would contribute to output a term

$$C_U(s) = \frac{G_2(s) + G_1(s)G_2(s)G_c(s)}{1 + G_1(s)G_2(s)H(s)} U(s) \quad \dots(2.81)$$

For this to cancel out the output component $C_U(s)$ due to disturbance input $U(s)$, the following condition has to be met.

$$G_2(s) + G_1(s)G_2(s)G_c(s) = 0 \quad \text{or} \quad G_c(s) = -\frac{1}{G_1(s)} \quad \dots(2.82)$$

The issues of this type of compensation will be considered further in chapter.

2.6 SIGNAL FLOW GRAPHS

Block diagrams are very successful for representing control systems, but for complicated systems, the block diagram reduction process is tedious and time consuming. An alternate approach is that of signal flow graphs developed by S.J. Mason, which does not require any reduction process because of availability of a flow graph gain formula which relates the input and output system variables.

A signal flow graph is a graphical representation of the relationships between the variables of a set of linear algebraic equations. It consists of a network in which nodes representing each of the system variables are connected by directed branches. The closed-loop system whose block diagram is shown in Fig. 2.26 (a) has the signal flow representation given

in Fig. 2.33 (a). The formulation of this signal flow graph is explained through the various signal flow terms defined below.

1. *Node*. It represents a system variable which is equal to the sum of all incoming signals at the node. Outgoing signals from the node do not affect the value of the node variable. For example, *R*, *E*, *B* and *C* are nodes in Fig. 2.33 (a). These symbols are also represent the corresponding node variables.

2. *Branch*. A signal travels along a branch from one node to another in the direction indicated by the branch arrow and in the process gets multiplied by the gain or transmittance of the branch. For example, the signal reaching the node *C* from the node *E* is given by GE where *G* is the branch transmittance and the brance is directed from the node *E* to the node *C* in Fig. 2.33 (a). Thus the value of the node variable $C = GE$.

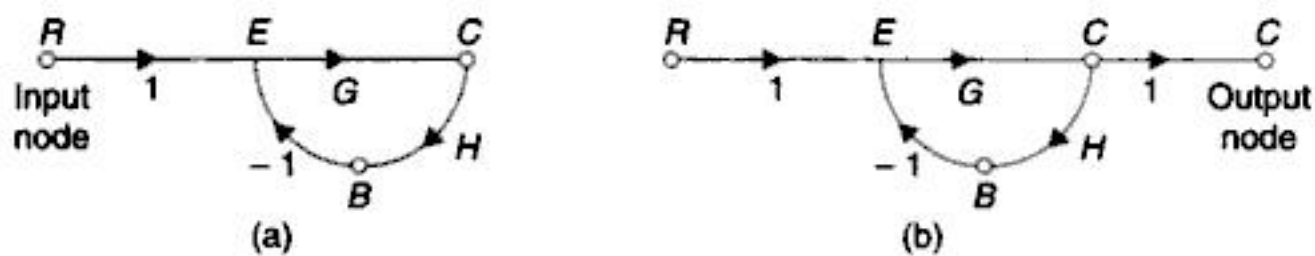


Fig. 2.33. Signal flow graph of a closed-loop system.

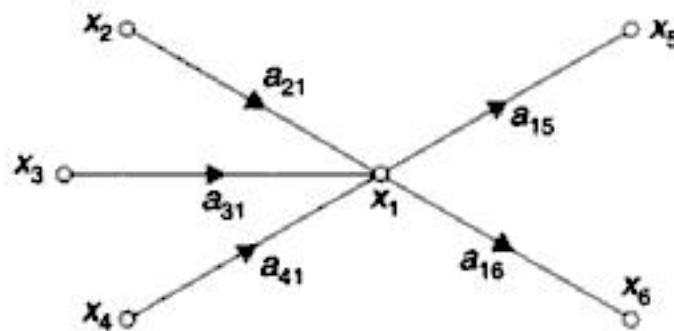


Fig. 2.34. Node as a summing point and as a transmitting point.

(a) *Node as a summing point*

With reference to the signal flow graph of Fig. 2.34, the node variable x_1 is expressed

$$x_1 = a_{21} x_2 + a_{31} x_3 + a_{41} x_4 = \text{sum of all incoming signals.}$$

(b) *Node as a transmitting point*

A node variable is transmitted through all branches outgoing from the node. Thus in the signal flow graph of Fig. 2.34.

$$x_5 = a_{15} x_1 \tag{2.83}$$

$$x_6 = a_{16} x_1$$

As already stated in (1) above the value of the node variable is not affected by the outgoing branches.

3. *Notation*. a_{ij} is the transmittance of the branch directed from node x_i to node x_j .

4. *Input node or source*. It is a node with only outgoing branches. For example, *R* is an input node in Fig. 2.33 (a).

5. *Output node or sink.* It is a node with only incoming branches. However, this condition is not always met. An additional branch with unit gain may be introduced in order to meet this specified condition. For example, the node *C* in Fig. 2.33 (a) has one outgoing branch but after introducing an additional branch with unit transmittance as shown in Fig. 2.33 (b) the node becomes an output node.

6. *Path.* It is the traversal of connected branches in the direction of the branch arrows such that no node is traversed more than once.

7. *Forward path.* It is a path from the input node to the output node. For example, *R-E-C* is a forward path in Fig. 2.33 (a).

8. *Loop.* It is a path which originates and terminates at the same node. For example, *E-C-B-E* is a loop in Fig. 2.33 (a).

9. *Non-touching loops.* Loops are said to be non-touching if they do not possess any common node.

10. *Forward path gain.* It is the product of the branch gains encountered in traversing a forward path. For example, forward path gain of the path *R-E-C* in Fig. 2.33 (a) is *G*.

11. *Loop gain.* It is the product of branch gains encountered in traversing the loop. For example, loop gain of the loop *E-C-B-E* in Fig. 2.33 (a) is *-GH*.

Construction of Signal Flow Graphs

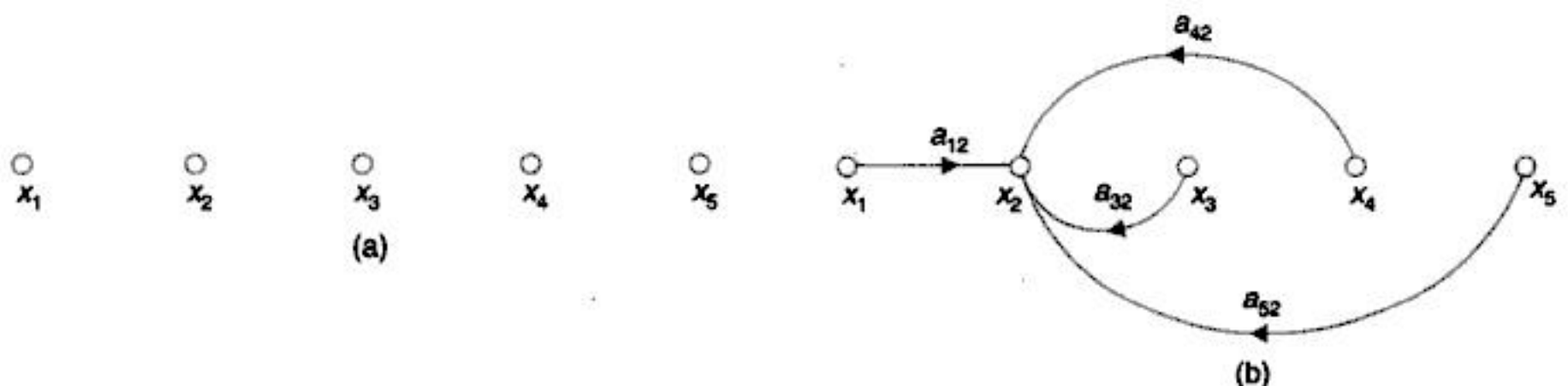
The signal flow graph of a system is constructed from its describing equations. To outline the procedure, let us consider a system described by the following set of equations:

$$\begin{aligned}x_2 &= a_{12}x_1 + a_{32}x_3 + a_{42}x_4 + a_{52}x_5 \\x_3 &= a_{23}x_2 \\x_4 &= a_{34}x_3 + a_{44}x_4 \\x_5 &= a_{35}x_3 + a_{45}x_4\end{aligned}\quad \dots(2.84)$$

where x_1 is the input variable and x_5 is the output variable.

The signal flow graph for this system is constructed as shown in Fig. 2.35. First the nodes are located as shown in Fig. 2.35 (a). The first equation in (2.84) states that x_2 is equal to sum of four signals and its signal flow graph is shown in Fig. 2.35 (b). Similarly, the signal flow graphs for the remaining three equations in (2.84) are constructed as shown in Figs. 2.35 (c), (d) and (e) respectively giving the complete signal flow graph of Figs. 2.35 (f).

The overall gain from input to output may be obtained by Mason's gain formula.



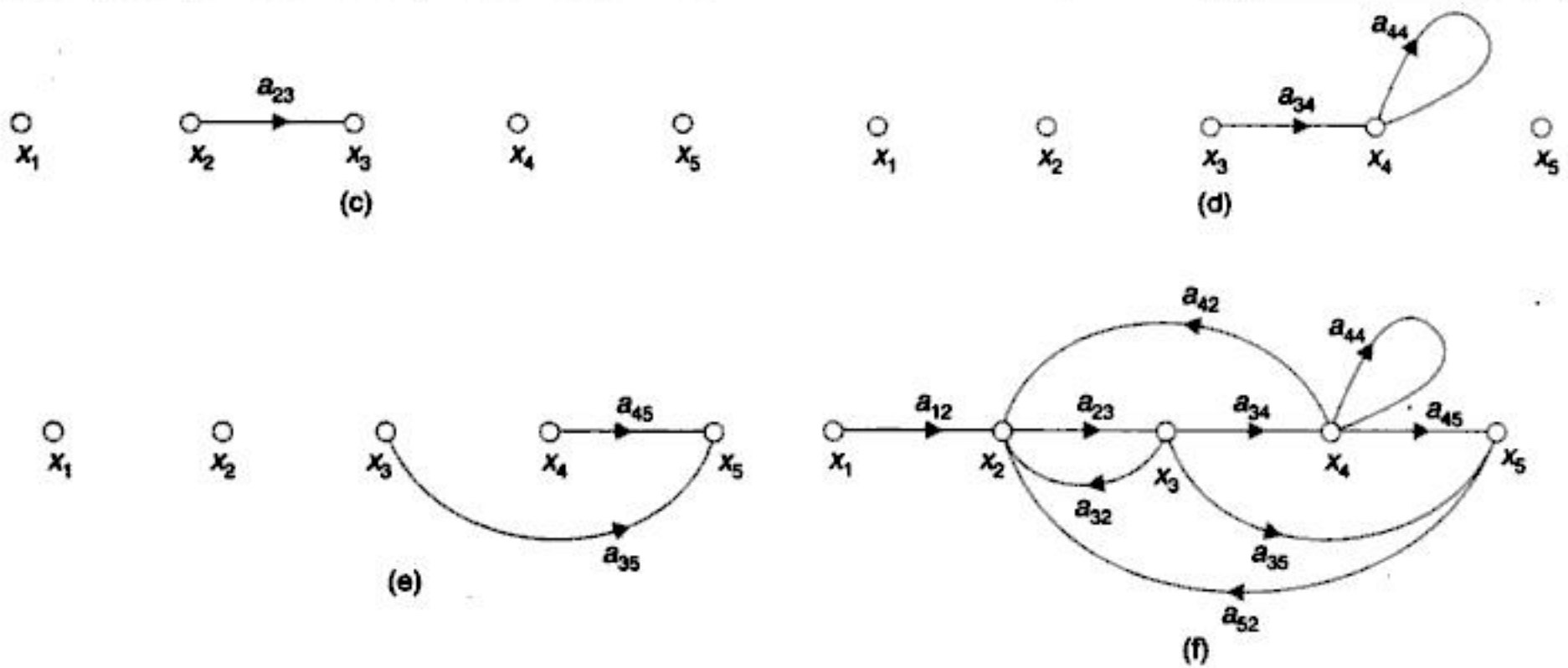


Fig. 2.35. Construction of signal flow graph for eqns. (2.84).

Mason's Gain Formula

The relationship between an input variable and an output variable of a signal flow graph is given by the net gain between the input and output nodes and is known as the overall gain of the system. Mason's gain formula for the determination of the overall system gain is given by:

$$T = \frac{1}{\Delta} \sum_K P_K \Delta_K \quad \dots(2.85)$$

where P_K = path gain of K -th forward path; Δ = determinant of the graph = 1 - (sum of loop gains of all individual loops) + (sum of gain products of all possible combinations of two non-touching loops) - (sum of gain products of all possible combinations of three non-touching loops) + ... , i.e.,

$$\Delta = 1 - \sum_m P_{m_1} + \sum_m P_{m_2} - \sum_m P_{m_3} + \dots \quad \dots(2.86)$$

where P_{mr} = gain product m -th possible combination of r non-touching* loops; Δ_K = the value of Δ for the part of the graph not touching the K -th forward path; and T = overall gain of the system.

Let us illustrate the use of Mason's formula by finding the overall gain of the signal flow graph shown in Fig. 2.35. The following conclusions are drawn by inspection of this signal flow graph.

1. There are two forward paths with path gains

$$P_1 = a_{12} a_{23} a_{34} a_{45} \quad \text{Fig. 2.36 (a)}$$

$$P_2 = a_{12} a_{23} a_{35} \quad \text{Fig. 2.36 (b)}$$

2. There are five individual loops with loop gains

$$P_{11} = a_{23} a_{32} \quad \text{Fig. 2.36 (c)}$$

*Non-touching implies that no node is common between the two.

$$P_{21} = a_{23}a_{34}a_{42} \quad \text{Fig. 2.36 (d)}$$

$$P_{31} = a_{44} \quad \text{Fig. 2.36 (e)}$$

$$P_{41} = a_{23}a_{34}a_{45}a_{52} \quad \text{Fig. 2.36 (f)}$$

$$P_{51} = a_{23}a_{35}a_{52} \quad \text{Fig. 2.36 (g)}$$

3. There are two possible combinations of two non-touching loops with loop gain products

$$P_{12} = a_{23}a_{32}a_{44} \quad \text{Fig. 2.36 (h)}$$

$$P_{22} = a_{23}a_{35}a_{52}a_{44} \quad \text{Fig. 2.36 (i)}$$

4. There are no combinations of three non-touching loops, four non-touching loops, etc.

Therefore

$$P_{m3} = P_{m4} = \dots = 0$$

Hence from eqn. (2.85)

$$\Delta = 1 - (a_{23}a_{32} + a_{23}a_{34}a_{42} + a_{44} + a_{23}a_{34}a_{45}a_{52} + a_{23}a_{35}a_{52}) + (a_{23}a_{32}a_{44} + a_{23}a_{35}a_{52}a_{44})$$

5. First forward path is in touch with all the loops. Therefore, $\Delta_1 = 1$. The second forward path is not in touch with one loop (Fig. 2.36 (j)). Therefore, $\Delta_2 = 1 - a_{44}$.

From eqn. (2.85), the

$$\begin{aligned} T &= \frac{x_5}{x_1} = \frac{P_1\Delta_1 + P_2\Delta_2}{\Delta} \\ &= \frac{a_{12}a_{23}a_{34}a_{45} + a_{12}a_{23}a_{35}(1 - a_{44})}{1 - a_{23}a_{32} - a_{23}a_{34}a_{42} - a_{44} - a_{23}a_{34}a_{45}a_{52} + a_{23}a_{32}a_{44} + a_{23}a_{35}a_{52}a_{44}} \quad \dots(2.87) \end{aligned}$$

State Variable Formulation

So far we have considered the transfer function approach (single/multi input, output) using both block diagram algebra and signal flow graph. Before we consider further examples of signal flow graphs in control systems, we will consider an alternate organization of a system's differential equations as a set of first-order differential equations. This is known as the state variable formulation and will be studied in detail in Chapter 12. Here we shall introduce the technique through a simple example by using the insight acquired into the physical systems considered so far.

Consider a simple system described by the first-order differential equation

$$\dot{x} = ax ; x(t = 0) = x(0) \quad \dots(2.88)$$

As x defines the system state for $t \geq 0$, it is called a *state variable* and eqn. (2.88) is the *state equation*.

Observe that the system has no input but has an initial condition (at $t = 0$). Integrating \dot{x} we have

$$x = \int \dot{x} dt + x(0) \quad \dots(2.89)$$

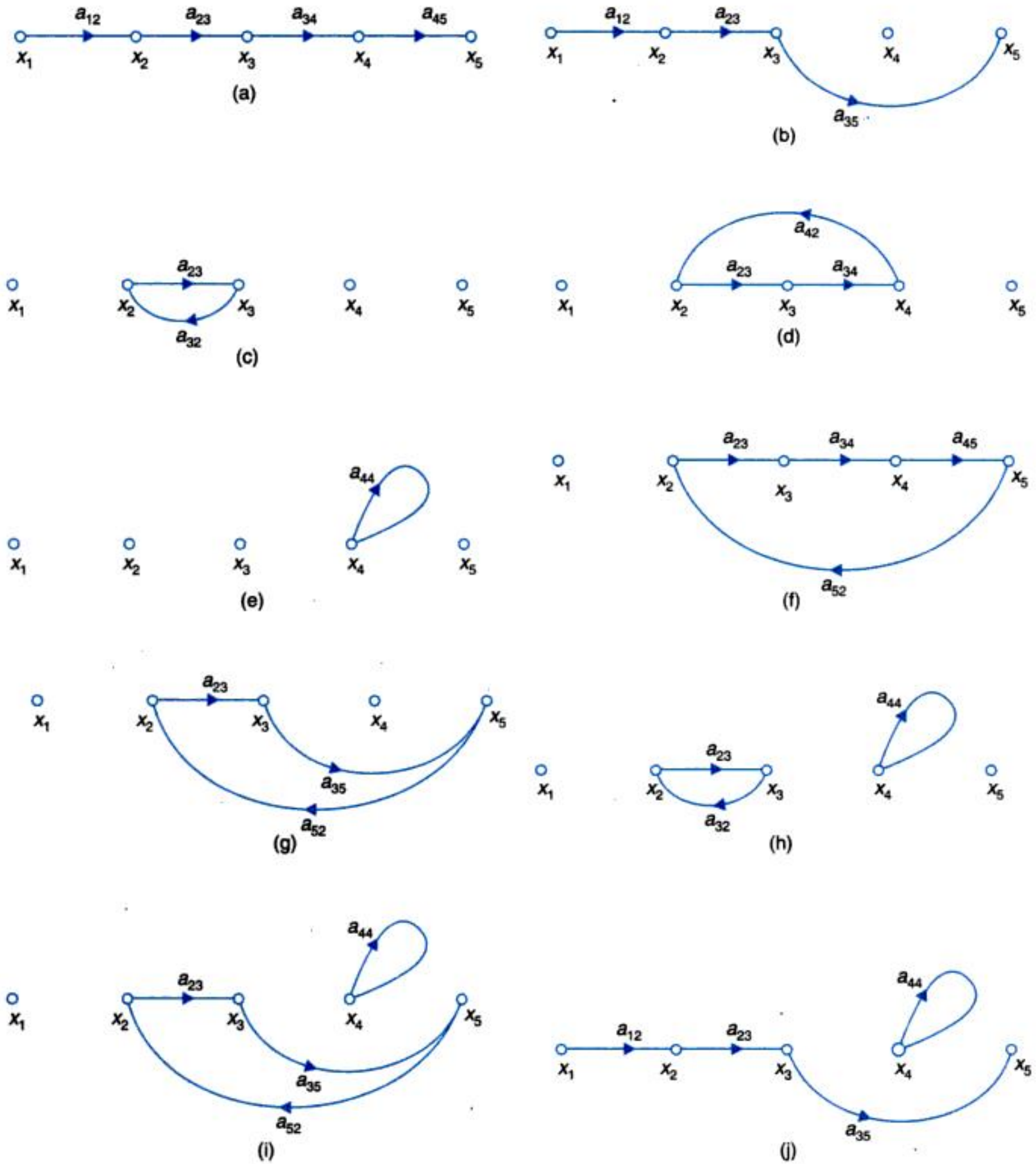


Fig. 2.36. Application of Mason's formula to the signal flow graph shown in Fig. 2.35.

The signal flow diagram for eqns. (2.88) and (2.89) can be drawn as in Fig. 2.37 (a) with integration symbol introduced as a transmittance of the branch from node \dot{x} to x . This is the time-domain representation.

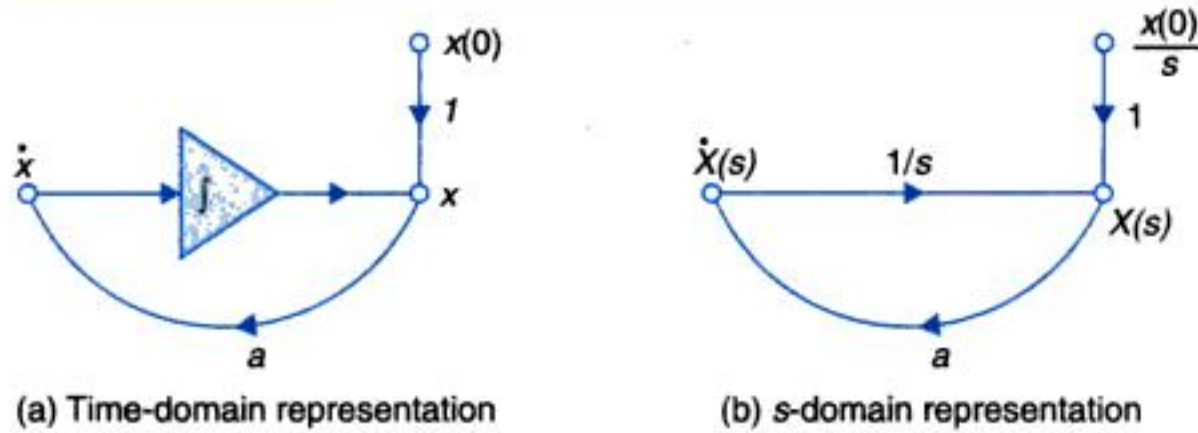


Fig. 2.37. Signal flow graph of first-order system.

Take now the Laplace transform of eqn. (2.88)

$$\dot{X}(s) = aX(s) \quad \dots(2.90a)$$

But

$$\dot{X}(s) = sX(s) - x(0) \quad \dots(2.90b)$$

or

$$X(s) = \frac{1}{s}\dot{X}(s) + \frac{1}{s}x(0) \quad \dots(2.91)$$

Equations (2.90a) and (2.91) would give the signal flow graph in s -domain, as in Fig. 2.37 (b).

Consider now a first-order system with input u

$$\dot{x} = ax + bu; x(t=0) = x(0) \quad \dots(2.92)$$

whose s -domain signal flow diagram is drawn in Fig. 2.38 (a).

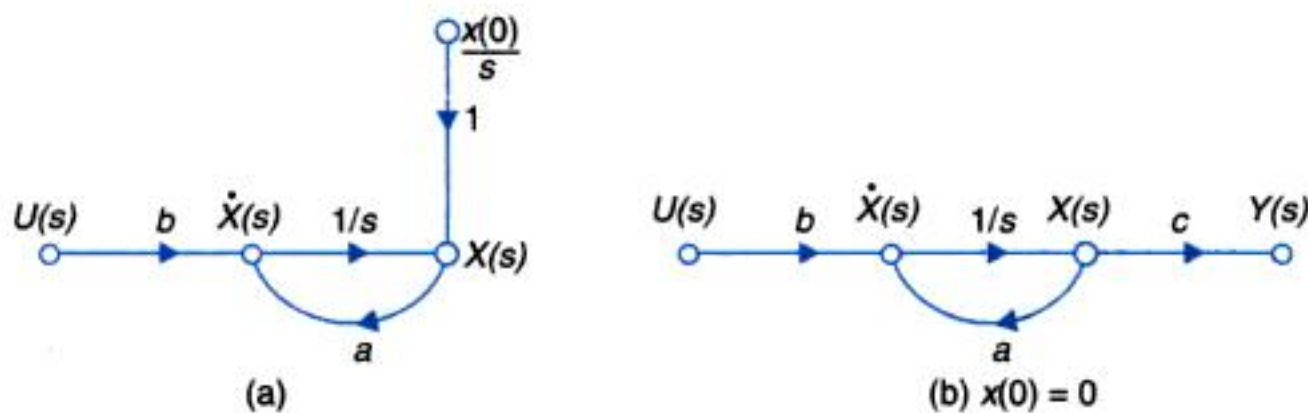


Fig. 2.38

Assume that the system output is given as

$$y = cx \quad \dots(2.93)$$

The modified signal flow graph is drawn in Fig. 2.38 (b) wherein it is assumed that $x(0) = 0$. Observing that there is one forward path and one loop and applying the Mason's gain formula, we have

$$\begin{aligned} P_1 &= bc/s \\ \Delta_1 &= 1 \\ \Delta &= 1 - \Delta_{11} = 1 - (a/s) = (s-a)/s \\ T(s) &= \frac{Y(s)}{U(s)} = \frac{P_1 \Delta_1}{\Delta} = \frac{(bc/s)}{(s-a)/s} = \frac{bc}{s-a} \quad \dots(2.94) \end{aligned}$$

In case of second-order system two first-order state variable equations would be needed and in general n equations for n -th-order system. Let us consider the example of armature-

controlled *dc* motor of Fig. 2.21 wherein we shall now regard the output of interest as motor speed $\omega = \dot{\theta}$. The block diagram of Fig. 2.22 is then redrawn as in Fig. 2.38 from which we can write

$$\begin{aligned} K_T I_a(s) &= Js\omega(s) + f_0 \omega(s) \\ E(s) - K_b \omega(s) &= L_a s I_a(s) + R_a I_a(s) \end{aligned}$$

Taking the inverse Laplace transform (initial condition being zero)

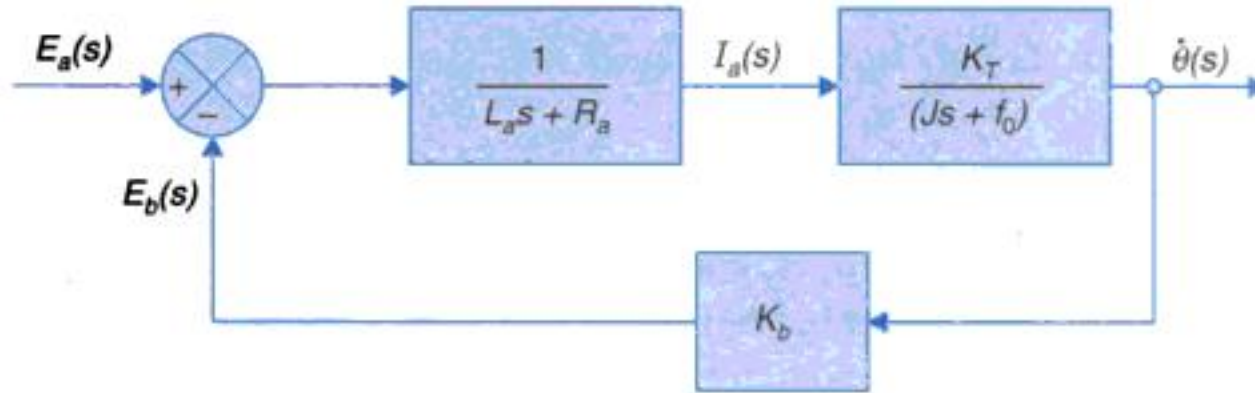


Fig. 2.38. Armature-controlled d.c. motor.

$$\begin{aligned} K_T i_a(t) &= J \frac{d\omega(t)}{dt} + f_0 \omega(t) \\ e_a(t) - K_b \omega(t) &= L_a \frac{di_a(t)}{dt} + R_a i_a(t) \end{aligned}$$

We can recognize these equations as first-order equations in ω and i_a which are then recognized as state variables, while $e(t)$ is the system input. We thus have

$$\frac{d\omega(t)}{dt} = (f_0/J)\omega(t) + (K_T/J)i_a(t) \quad \dots(2.95a)$$

$$\frac{di_a(t)}{dt} = -(K_b/L_a)\omega(t) - (R_a/L_a)i_a(t) + (1/L_a)e_a(t) \quad \dots(2.95b)$$

Dropping the bracketed variable t for convenience of writing we can then rewrite these state equations in vector-matrix form as

$$\begin{bmatrix} \frac{d\omega}{dt} \\ \frac{di_a}{dt} \end{bmatrix} = \begin{bmatrix} -(f_0/J) & (K_T/J) \\ -(K_b/L_a) & -(R_a/L_a) \end{bmatrix} \begin{bmatrix} \omega \\ i_a \end{bmatrix} + \begin{bmatrix} 0 \\ 1/L_a \end{bmatrix} e_a \quad \dots(2.96a)$$

We will reidentify the state variables as

$$x_1 = \omega, x_2 = i_a$$

and input as $u = e$ and output as

$$y = \omega = [1 \ 0] \begin{bmatrix} \omega \\ i_a \end{bmatrix} \quad \dots(2.96b)$$

We can now write eqns. (2.96a) and (b) in standard form as

$$\begin{bmatrix} \dot{x}_1 \\ \dot{x}_2 \end{bmatrix} = \begin{bmatrix} a_{11} & a_{12} \\ a_{21} & a_{22} \end{bmatrix} \begin{bmatrix} x_1 \\ x_2 \end{bmatrix} + \begin{bmatrix} b_1 \\ b_2 \end{bmatrix} u; u = e_a \quad \dots(2.97a)$$

$$y = [c_1 \ c_2] \begin{bmatrix} x_1 \\ x_2 \end{bmatrix} \quad \dots(2.97b)$$

In compact vector-matrix notation

$$\dot{\mathbf{x}} = \mathbf{Ax} + \mathbf{bu} \quad \dots(2.98a)$$

$$\mathbf{y} = \mathbf{Cx} \quad \dots(2.98b)$$

This is the state variable representation of a single-input-single-output (SISO) system. In multi-input multi-output (MIMO) system u and y will acquire the vector form.

The state variables identified in the above example are physical variables and are directly available for measurement. Indeed the state variables for a given system are not unique and these can be defined in a number of other ways. These and associated topics and will be discussed at length in Chapter 12.

Speed Control System

As an example let us consider a feedback speed control system whose objective is move the load at desired speed. This is easily achieved using the armature controlled dc motor of Fig. 2.21 by providing a feedback control loop as in Fig. 2.39 wherein the voltage signal e_t proportional to input speed (ω) generated by a dc tachometer coupled the motor armature is fed back negatively and is subtracted from the reference voltage e_r , creating the difference (error) signal e . This error signal e is then amplified to control the armature current i_a such that the motor acquires the desired speed, while driving the load (J, f and torque T_D).

A dc tachometer is just a conventional dc generator usually of permanent magnet kind, whose output voltage is a measure of speed. Thus

$$e_t = K_t \omega, \text{ excitation being constant} \quad \dots(2.99)$$

where K_t (V/rad/s) is the tachometer constant.

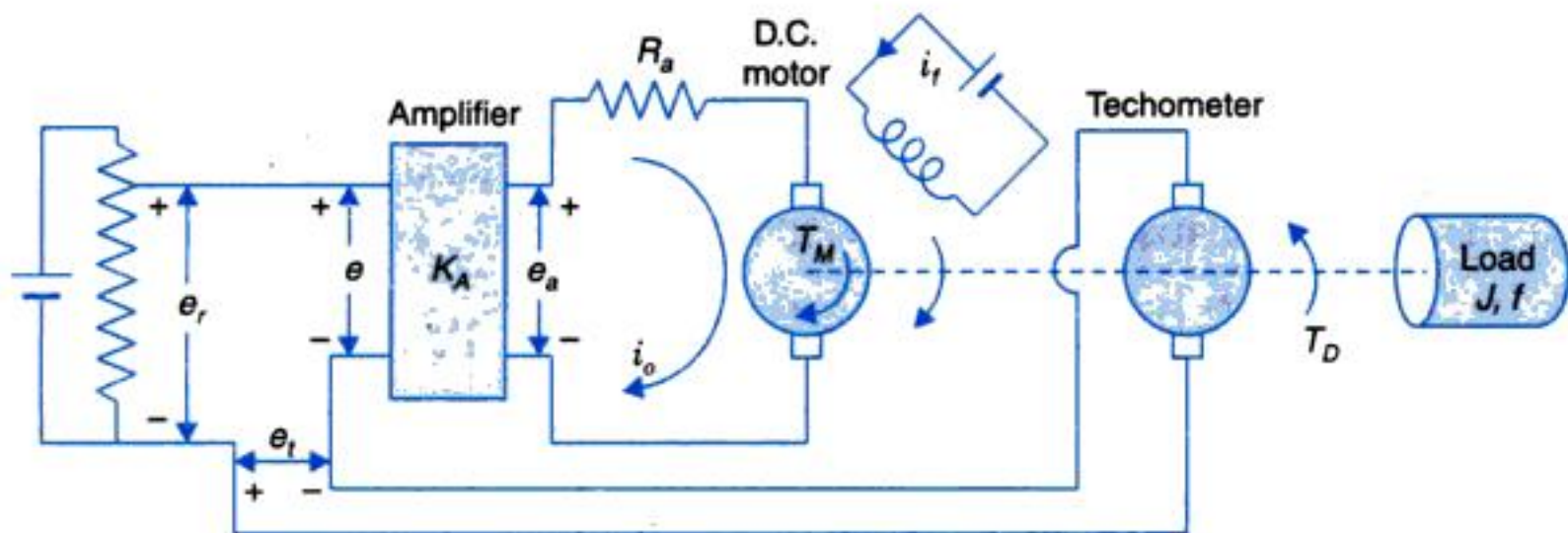
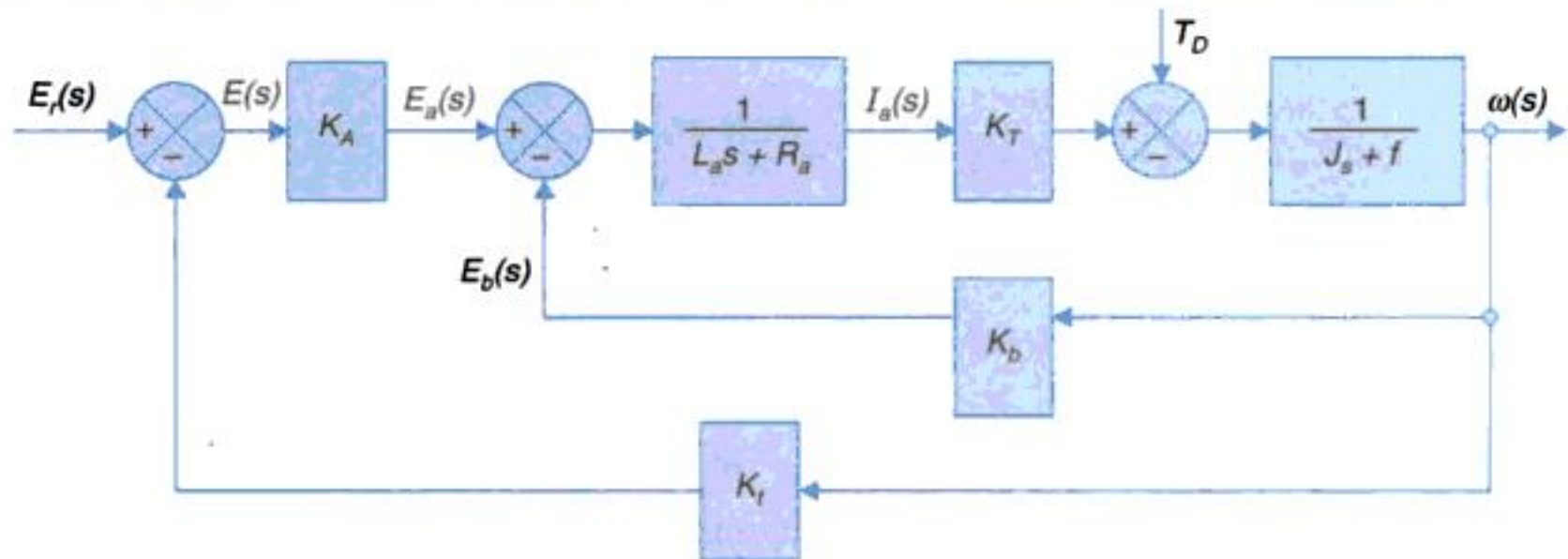


Fig. 2.39. A speed control system.

The block diagram of the speed control system of Fig. 2.39 can be easily drawn as in Fig. 2.40 (a) by modifying the block diagram of Fig. 2.23 of the armature-controlled dc motor. The outer feedback loop accounts for the speed feedback which is basic to the speed regulation action. The load torque T_D which opposes the motor torque enters negatively in the block diagram so that the torque applied to load (and motor) inertia and friction is $(T_M - T_D)$.

Let us convert this block diagram into a signal flow graph while making the simplifying assumption that $L_a \approx 0$. The signal flow graph is drawn in Fig 2.40 (b). Various system transfer functions are derived below using the Mason's gain formula.



(a) Block diagram

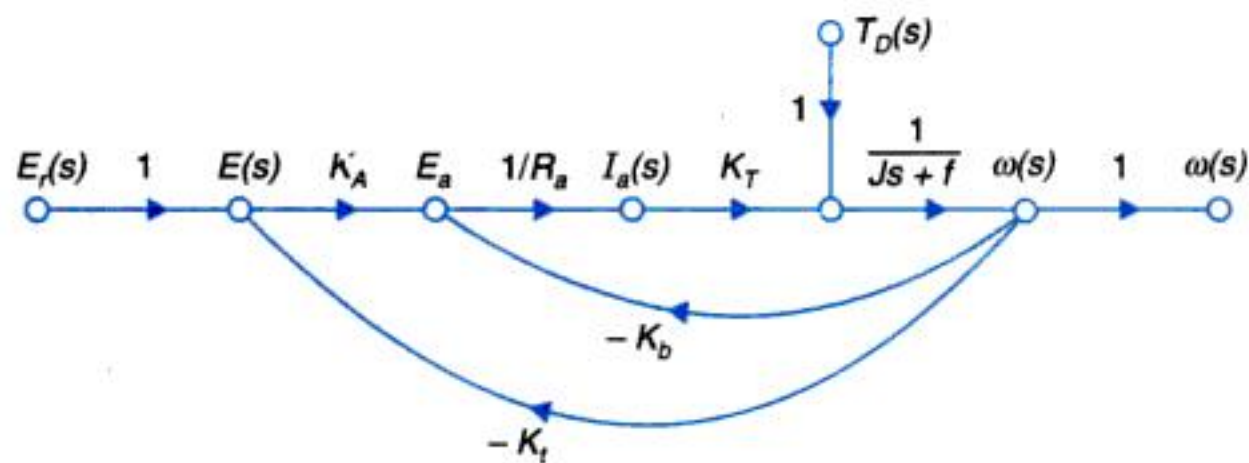

 (b) Signal flow graph ($L_a \approx 0$)

Fig. 2.40. Speed control system.

Consider first the case with zero disturbance torque. By inspection of the signal flow graph, with $T_D(s) = 0$, it is found that:

1. There is only one forward path with path gain

$$P_1 = \frac{K_A K_T}{R_a (J_s + f)}$$

2. There are two individual loops with loop gains

$$P_{11} = \frac{-K_T K_b}{R_a (J_s + f)}$$

$$P_{21} = \frac{K_A K_T K_t}{R_a (J_s + f)}$$

3. There are no combinations of two non-touching loops, three non-touching loops, etc. Therefore

$$P_{m2} = P_{m3} = \dots = 0$$

Hence from eqn. (2.86)

$$\Delta = 1 - \left[\frac{K_T K_b}{R_a (J_s + f)} + \frac{K_A K_T K_t}{R_a (J_s + f)} \right] = 1 + \frac{K_T K_b + K_A K_T K_t}{R_a (J_s + f)}$$

4. The forward path is in touch with both the loops. Therefore

$$\Delta_1 = 1$$

From the Mason's gain formula of eqn. (2.84), the overall gain is

$$T(s) = \frac{\omega(s)}{E_r(s)} = \frac{P_1 \Delta_1}{\Delta} = \frac{K_A K_T}{R_a (Js + f) + K_T K_b + K_A K_T K_t} \quad \dots(2.100)$$

With $K_t = 0$, the system is reduced to open-loop with the transfer function

$$G(s) = \frac{K_A K_T}{R_a (Js + f) + K_b K_T} = \frac{K}{(\tau s + 1)} \quad \dots(2.101)$$

where

$$K = \frac{K_A K_T}{R_a f + K_T K_b}; \tau = \frac{R_a J}{R_a f + K_T K_b}$$

From eqn. (2.100), the closed-loop transfer function of the system is given by

$$T(s) = \frac{K/\tau}{s + \left(\frac{1 + KK_t}{\tau} \right)} \quad \dots(2.102)$$

When the load (*disturbance*) torque $T_D(s)$ is present, the only change in the graph is the additional input $T_D(s)$.

Applying Mason's gain formula to the graph, the following transfer function is obtained between output speed and disturbance torque with zero reference voltage, i.e., $E_r(s) = 0$

$$\left. \frac{\omega(s)}{T_D(s)} \right|_{E_r(s)=0} = \frac{\omega_D(s)}{T_D(s)} = \frac{-1}{Js + f + \frac{K_T}{R_a} (K_A K_t + K_b)} \quad \dots(2.103)$$

When there is no feedback ($K_t = 0$), eqn. (2.102) modifies to

$$\left. \frac{\omega(s)}{T_D(s)} \right|_{E_r(s)=0} = \frac{\omega_D(s)}{T_D(s)} = \frac{-1}{Js + f + \frac{K_T K_b}{R_a}} \quad \dots(2.104)$$

The additional term $\left(\frac{K_T K_A}{R_a} \right) K_t$ in the denominator of eqn. (2.102) (compared to eqn.

(2.103)) arises on account of output (speed) feedback. As we shall see in Chapter 5 that this term reduces the effect of load (disturbance) torque on motor speed.

2.7 ILLUSTRATIVE EXAMPLES

Example 2.1 : Consider the mechanical system shown in Fig. 2.41 (a). A force $F(t)$ is applied to mass M_2 . The free-body diagrams for the two masses are shown in Fig. 2.41 (b). From this figure, we have the following differential equations describing the dynamics of the system.

Solution.

$$F(t) - f_2(\dot{y}_2 - \dot{y}_1) - K_2(y_2 - y_1) = M_2 \ddot{y}_2$$

$$f_2(\dot{y}_2 - \dot{y}_1) + K_2(y_2 - y_1) - f_1 \dot{y}_1 - K_1 y_1 = M_1 \ddot{y}_1$$

Rearranging we get

$$M_2 \ddot{y}_2 + f_2(\dot{y}_2 - \dot{y}_1) + K_2(y_2 - y_1) = F(t) \quad \dots(2.105)$$

$$M_1 \ddot{y}_1 + f_1 \dot{y}_1 - f_2(\dot{y}_2 - \dot{y}_1) + K_1 y_1 - K_2(y_2 - y_1) = 0 \quad \dots(2.106)$$

These are two simultaneous second-order linear differential equations. Manipulation of these equations will result in a single differential equation (fourth-order) relating the response y_2 (or y_1) to input $F(t)$.

A spring-mass-damper system may be schematically represented as a network by showing the inertial reference frame as the second terminal of every mass (or inertia) element. As an example, the mechanical system of Fig. 2.41 (a) is redrawn in Fig. 2.42 which may be referred to as the *mechanical network*. Analogous electrical circuit based on force-current analogy (Table 2.2) is shown in Fig. 2.43. A look at Fig. 2.43 (electrical analog of Fig. 2.41 (a)) and Fig. 2.42 reveals that they are alike topologically.

The dynamical equations of the system [eqns. (2.105)-(2.106)] could also be obtained by writing nodal equations for the electrical network of Fig. 2.43 or for the mechanical network of Fig. 2.42 (with force and velocity analogous to current and voltage respectively) since the two are alike topologically. The result is:

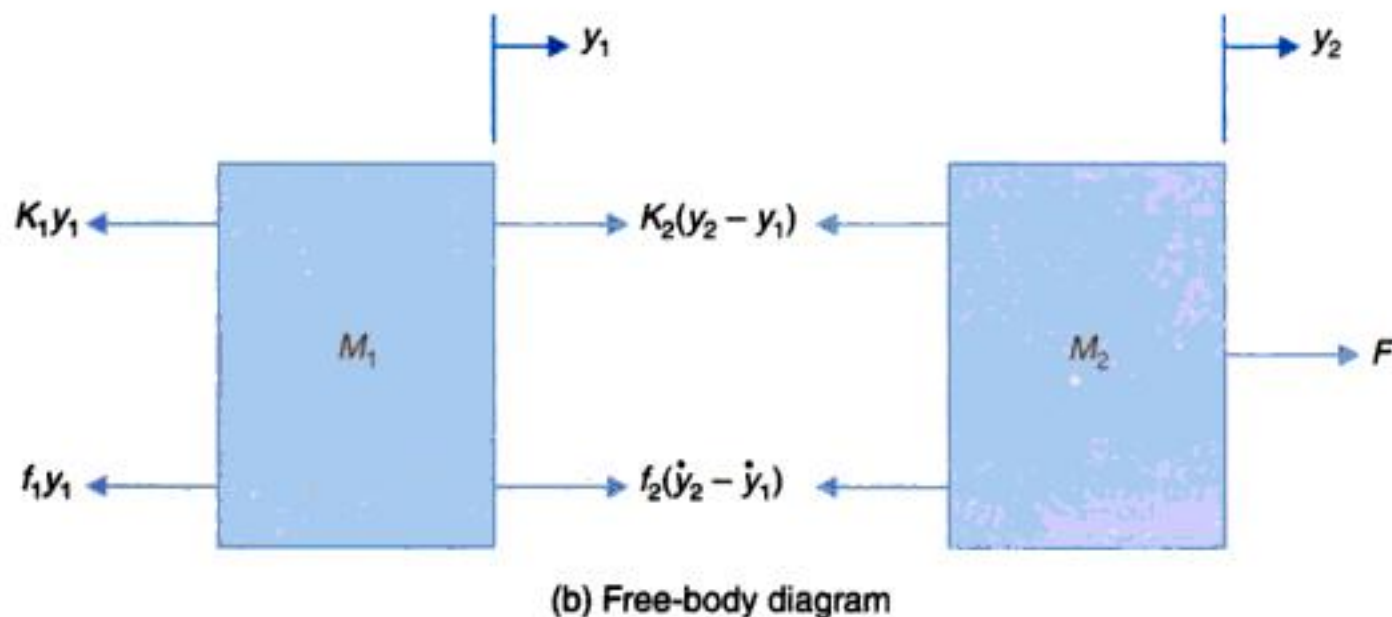
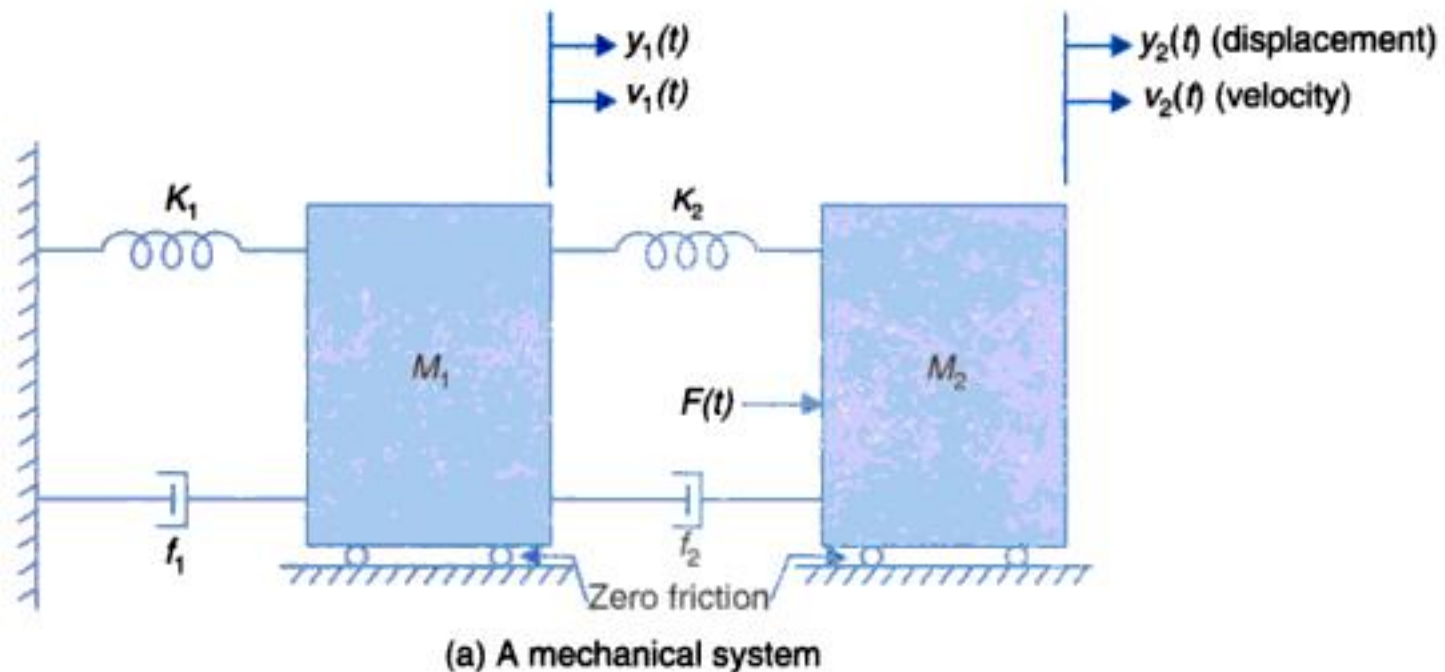


Fig. 2.41. (a) A mechanical system; (b) Free-body diagram.

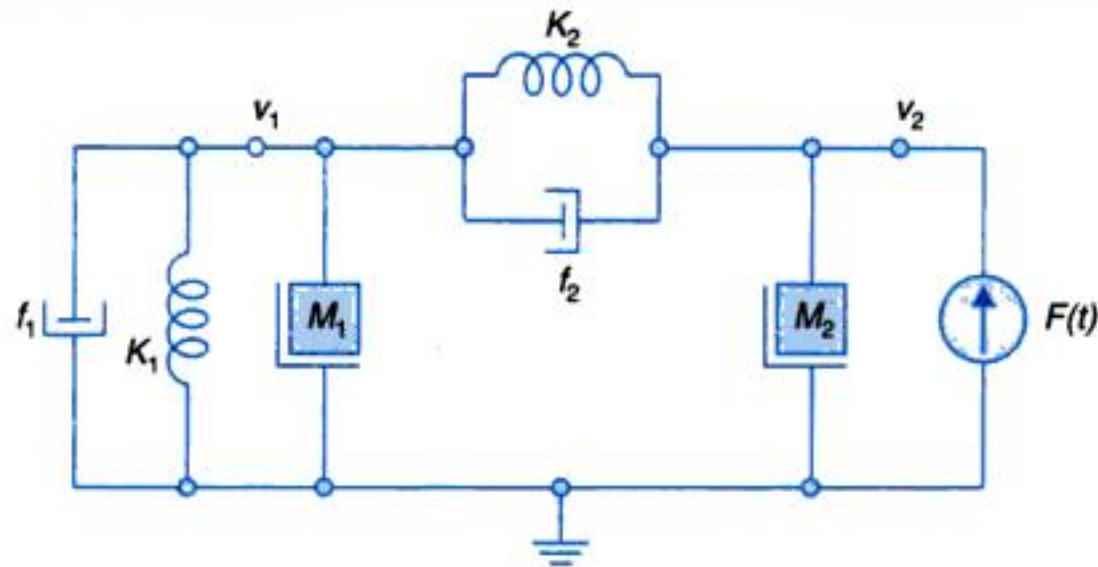


Fig. 2.42. Mechanical network for the system of Fig. 2.41.

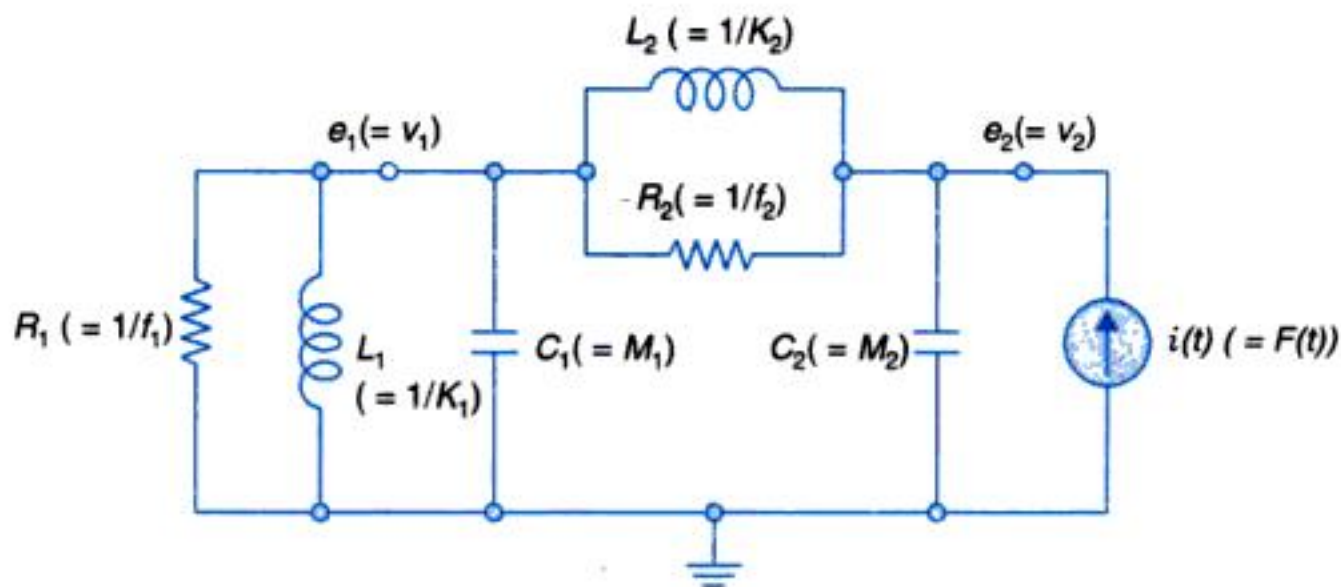


Fig. 2.43. Electrical analog for the system of Fig. 2.30 (a).

$$f_1 v_1 = K_1 \int_{-\infty}^t v_1 dt + M_1 \dot{v}_1 + K_2 \int_{-\infty}^t (v_1 + v_2) dt + f_2 (v_1 - v_2) = 0$$

$$M_2 \dot{v}_2 + K_2 \int_{-\infty}^t (v_2 - v_1) dt + f_2 (v_2 - v_1) = F(t)$$

The result is same as obtained earlier (with $y = \int_{-\infty}^t v dt$, $\dot{y} = v$ and $\ddot{y} = \dot{v}$) in eqns. (2.105) and (2.106) using the free-body diagram approach.

Signal Flow Graph

The mechanical system of Fig. 2.41(a) has four storage elements so it is a fourth order system and would be identified by four state variables. These can be defined as $x_1 = y_1$, $x_2 = \dot{y}_1$, $x_3 = y_2$, $x_4 = \dot{y}_2$. With reference to the free-body diagram of Fig. 2.41(b), the signal flow graph of Fig. 2.44 can be immediately drawn. The state variable equations can be written directly from the signal flow graph. The reader should write out these equations and organize them in matrix form. Here again the state variables are defined as physical variables, but this is not a unique choice.

Using Mason's gain formula the transfer function between any output and input $F(s)$ can be derived. It is identified here that there are seven loops but no combinations of two or more loops. Further there are two forward paths but there are no loops non-touching these paths. The reader should find the transfer function $y_1(s)/F(s)$.

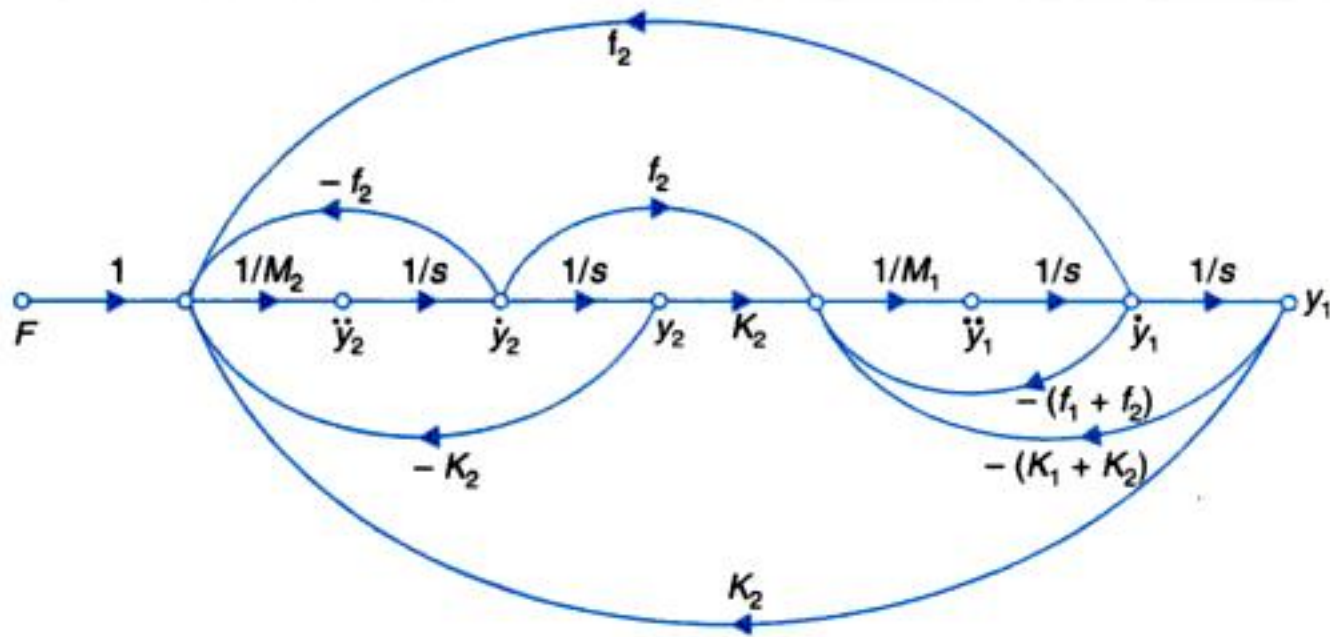


Fig. 2.44. Signal flow graph of the mechanical system of Fig. 2.41 (a).

Example 2.2 : Consider the circuit (electrical) of Fig. 2.45.

- (a) Identify a set of state variables (physical variables).
- (b) Draw the signal flow graph of the circuit in terms of the state variables identified in part (a).
- (c) From the signal flow graph, write the state variable equations of the circuit.
- (d) From the signal flow graph, determine the transfer function $E_C(s)/E(s)$.

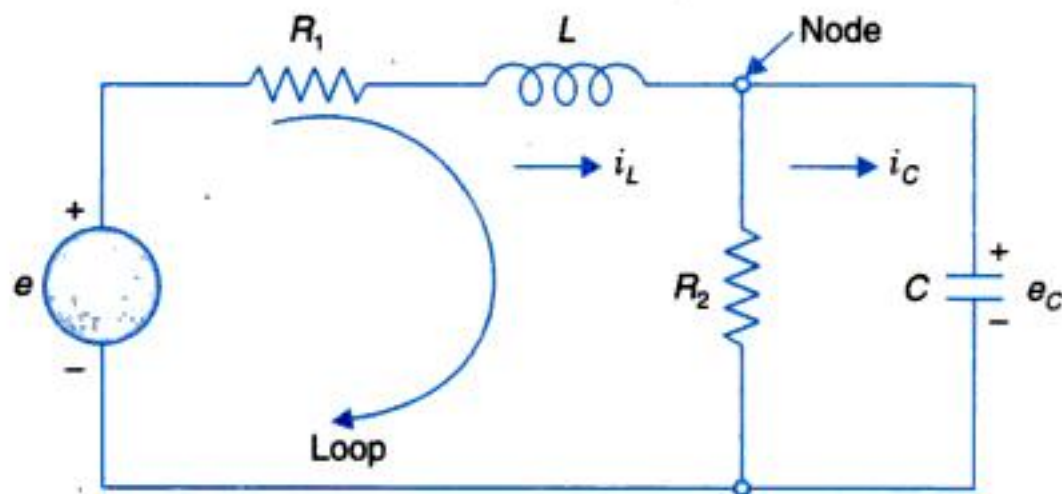


Fig. 2.45

Solution.

(a) This circuit has two storage elements, so these shall be two state variables. We shall identify these as the inductor current i_L and capacitor voltage e_C ; both these are associated with energy storage. Remember that the state variables do not form a unique set.

From the elemental laws of inductor and capacitor we can draw the signal flow graph as in Fig. 2.46(a). The complete signal flow graph is then constructed by the KCL equation at the node and the KVL equation round the loop. These equations are:

$$i_L = \frac{e_C}{R_2} + i_C \quad \text{or} \quad i_C = i_L - \frac{e_C}{R_2} \quad \dots(i)$$

and

$$e = R_1 i_L + e_L + e_C \quad \text{or} \quad e_L = e - R_1 i_L - e_C \quad \dots(ii)$$

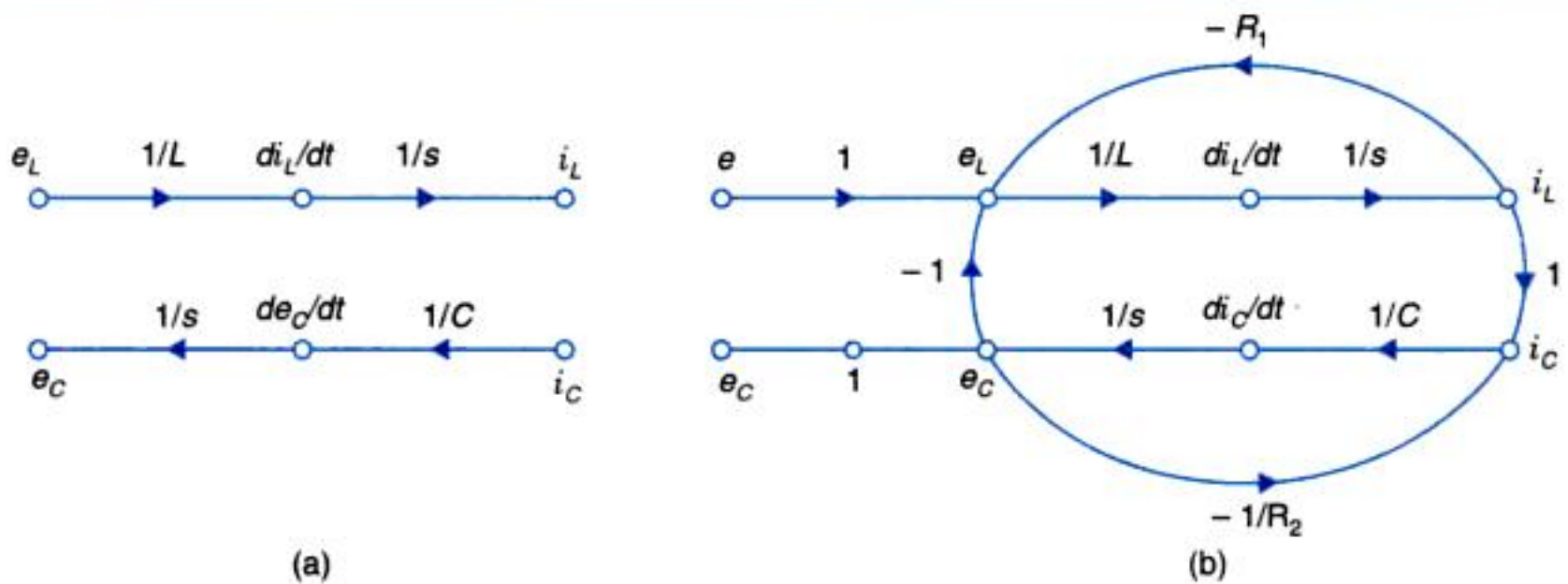


Fig. 2.46

The complete signal flow graph is drawn in Fig. 2.47(b).

(c) From the signal flow graph the two state variable equations can be written as below.

$$\frac{di_L}{dt} = \frac{1}{L} e_L = \frac{1}{L} (-e_C - R_1 i_L + e) = -\frac{R_1}{L} i_L - \frac{1}{L} e_C + \frac{1}{L} e \quad \dots(iii)$$

and

$$\frac{de_C}{dt} = \frac{1}{C} i_C = \frac{1}{C} \left(i_L + \frac{e_C}{R_2} \right) = \frac{1}{C} i_L - \frac{1}{R_2 C} e_C \quad \dots(iv)$$

Equations (iii) and (iv) can be written in matrix form

$$\begin{bmatrix} di_L/dt \\ di_C/dt \end{bmatrix} = \begin{bmatrix} -R_1/L & -1/L \\ 1/C & 1/R_2 C \end{bmatrix} \begin{bmatrix} i_L \\ e_C \end{bmatrix} + \begin{bmatrix} 1/L \\ 0 \end{bmatrix} e$$

These are also known as **state space** equations.

(d) Input $E(s)$, output $E_C(s)$. From the signal flow graph we have,

Forward path $P_1 = \frac{1}{sL} \times \frac{1}{sC} = \frac{1}{s^2 LC}; \Delta_1 = 1$

Single loops $P_{11} = -\frac{R_1}{sL}, P_{21} = -\frac{1}{sR_2 C}, P_{31} = -\frac{1}{s^2 LC}$

$$\Delta = 1 + \frac{R_1}{sL} + \frac{1}{sR_2 C} + \frac{1}{s^2 LC}$$

Hence
$$\frac{E_C(s)}{E(s)} = \frac{P_1 \Delta_1}{\Delta} = \frac{\frac{1}{s^2 LC}}{1 + \frac{R_1}{sL} + \frac{1}{sR_2 C} + \frac{1}{s^2 LC}} = \frac{1}{1 + s \left(R_1 C + \frac{L}{R_2} \right) + s^2 LC}$$

Example 2.3 : Consider a salt mixing tank shown in Fig. 2.48. A solution of salt in water at a concentration C_f (moles* of salt/m³ of solution) is mixed with pure water to obtain an outflow

*A mole of a substance is defined as the amount of substance whose mass numerically equals its molecular weight. For example, a gram-mole of helium would have a mass of 4.003 g (molecular weight of helium = 4.003).

stream with salt concentration C_o . The water flow rate is assumed fixed at Q_w and the solution flow rate may be varied to achieve the desired concentration C_o (also see Problem 2.6). Volumetric hold-up of the tank is V , which is held constant. Let us assume that stirring causes perfect mixing so that composition of the liquid in the tank is uniform throughout.

Solution. For this system,

$$Q_f = K_v x_v; K_v \text{ is valve coefficient}$$

$$Q_o = Q_w + Q_f$$

The rate of salt inflow in the tank

$$m_i = Q_f C_f; \left(\frac{\text{m}^3}{\text{s}} \cdot \frac{\text{moles}}{\text{m}^3} = \text{moles/s} \right)$$

The rate of salt outflow from the tank

$$m_o = Q_o C_o; (\text{moles/s})$$

The rate of salt accumulation in the tank

$$m_a = \frac{d}{dt} [VC_o(t)] = V \frac{dC_o}{dt}$$

where $VC_o(t)$ the salt hold-up of the tank at time t .

From the law of conservation of mass, we have

$$m_i = m_a + m_o \quad \text{or} \quad Q_f C_f = V \frac{dC_o}{dt} + Q_o C_o$$

or
$$\tau \frac{dC_o}{dt} + C_o = K x_v$$

where $K = (C_f K_v)/Q_o$ and $\tau = V/Q_o$ is the tank hold-up time.

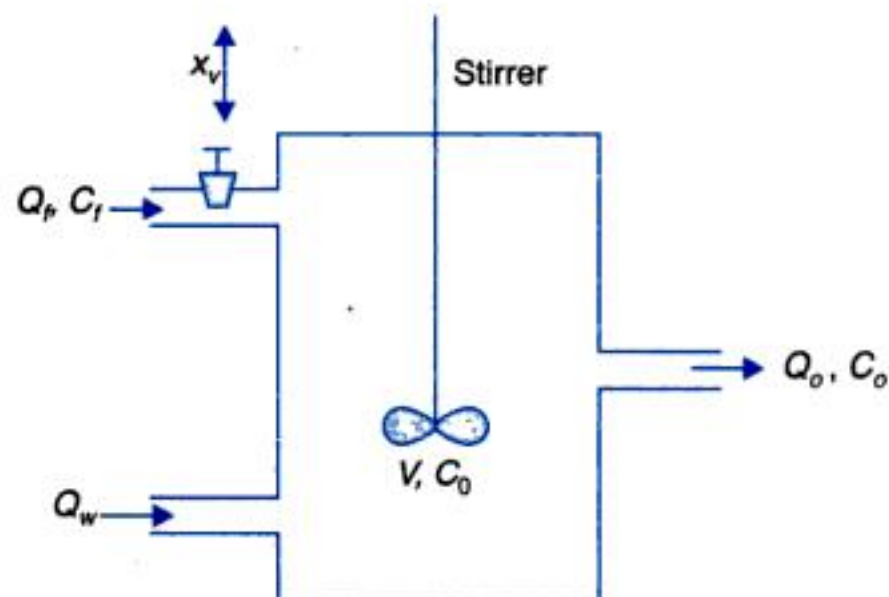


Fig. 2.48. A salt mixing tank.

The transfer function of the system is

$$\frac{C_o(s)}{X_v(s)} = \frac{K}{s\tau + 1}$$

Example 2.4 : The manipulator shown in Fig. 2.49 has a rotating joint followed by a linear (prismatic) joint. The whole mass of links is concentrated at the centre of mass. Derive the dynamic equations for the manipulator.

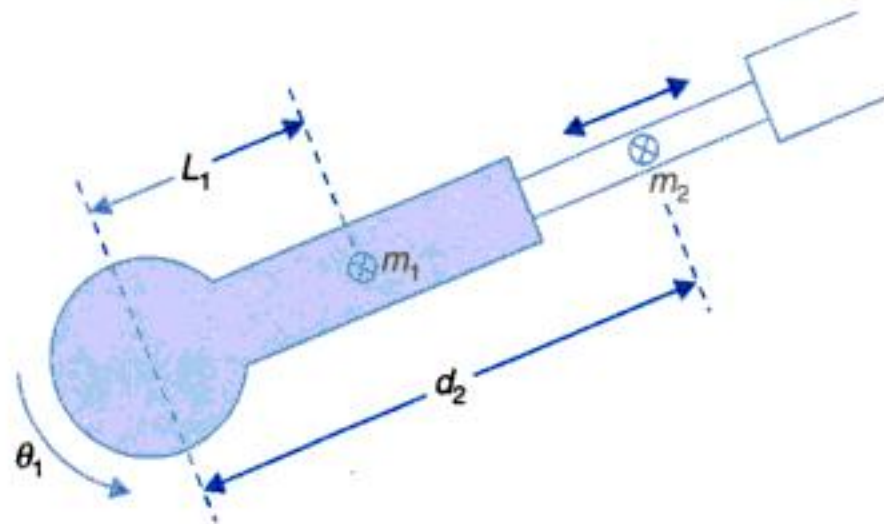


Fig. 2.49

Solution. Linear velocity of first centre of mass, $v_{c1} = l_1 \dot{\theta}_1$... (i)

Kinetic energy of link 1 is

$$K_1 = (1/2)m_1 l_1^2 \dot{\theta}_1^2 \quad \dots (ii)$$

Linear velocity of second centre of mass is

$$v_{c2} = \sqrt{(d_2^2 \dot{\theta}_1^2 + \dot{d}_2^2)} \quad \dots (iii)$$

Kinetic energy of link 2 is

$$K_2 = \frac{1}{2} m_2 (d_2^2 \dot{\theta}_1^2 + \dot{d}_2^2) \quad \dots (iv)$$

Hence the total kinetic energy of manipulator is

$$K = K_1 + K_2 \quad \dots (v)$$

or $K(\theta_1, \dot{\theta}_1, d_2, \dot{d}_2) = (1/2)(m_1 l_1^2 + m_2 d_2^2) \dot{\theta}_1^2 + \frac{1}{2} m_2 \dot{d}_2^2$... (vi)

Potential energy of link 1 is

$$u_1 = m_1 l_1 g \sin \theta_1 \quad \dots (vii)$$

Potential energy of link 2 is

$$u_2 = m_2 d_2 g \sin \theta_1 \quad \dots (viii)$$

Hence total potential energy of manipulator is

$$U(\theta_1, d_2) = u_1 + u_2 = g(m_1 l_1 + m_2 d_2) \sin \theta_1 \quad \dots (ix)$$

Taking partial derivatives, we have

$$\begin{bmatrix} \frac{\partial K}{\partial \dot{\theta}_1} \\ \frac{\partial K}{\partial \dot{d}_2} \end{bmatrix} = \begin{bmatrix} (m_1 l_1^2 + m_2 d_2^2) \dot{\theta}_1 \\ m_2 \dot{d}_2 \end{bmatrix} \quad \dots (x)$$

$$\begin{bmatrix} \frac{\partial K}{\partial \theta_1} \\ \frac{\partial K}{\partial d_2} \end{bmatrix} = \begin{bmatrix} 0 \\ m_2 d_2 \dot{\theta}_1^2 \end{bmatrix} \quad \dots(xi)$$

$$\begin{bmatrix} \frac{\partial U}{\partial \theta_1} \\ \frac{\partial U}{\partial d_2} \end{bmatrix} = \begin{bmatrix} g(m_1 l_1 + m_2 d_2) \cos \theta_1 \\ gm_2 \sin \theta_1 \end{bmatrix} \quad \dots(xii)$$

From Lagrangian mechanics we know that

$$\begin{bmatrix} \tau_1 \\ \tau_2 \end{bmatrix} = \begin{bmatrix} \frac{d}{dt} \left(\frac{\partial K}{\partial \dot{\theta}_1} \right) \\ \frac{d}{dt} \left(\frac{\partial K}{\partial \dot{d}_2} \right) \end{bmatrix} - \begin{bmatrix} \frac{\partial K}{\partial \theta_1} \\ \frac{\partial K}{\partial d_2} \end{bmatrix} + \begin{bmatrix} \frac{\partial U}{\partial \theta_1} \\ \frac{\partial U}{\partial d_2} \end{bmatrix} \quad \dots(xiii)$$

Thus from (x), (xi), (xii), and (xiii) we have

$$\tau_1 = (m_1 l_1^2 + m_2 d_2^2) \ddot{\theta}_1 + 2m_2 d_2 \dot{\theta}_1 \dot{d}_2 + (m_1 l_1 + m_2 d_2) g \cos \theta_1 \quad \dots(xiv)$$

$$\tau_2 = m_2 \dot{d}_2 - m_2 d_2 \dot{\theta}_1^2 + m_2 g \sin \theta_1 \quad \dots(xv)$$

Equations (xiv) and (xv) are the dynamic equations of the manipulator.

Example 2.5 : The schematic diagram of a position control system is drawn in Fig. 2.50.

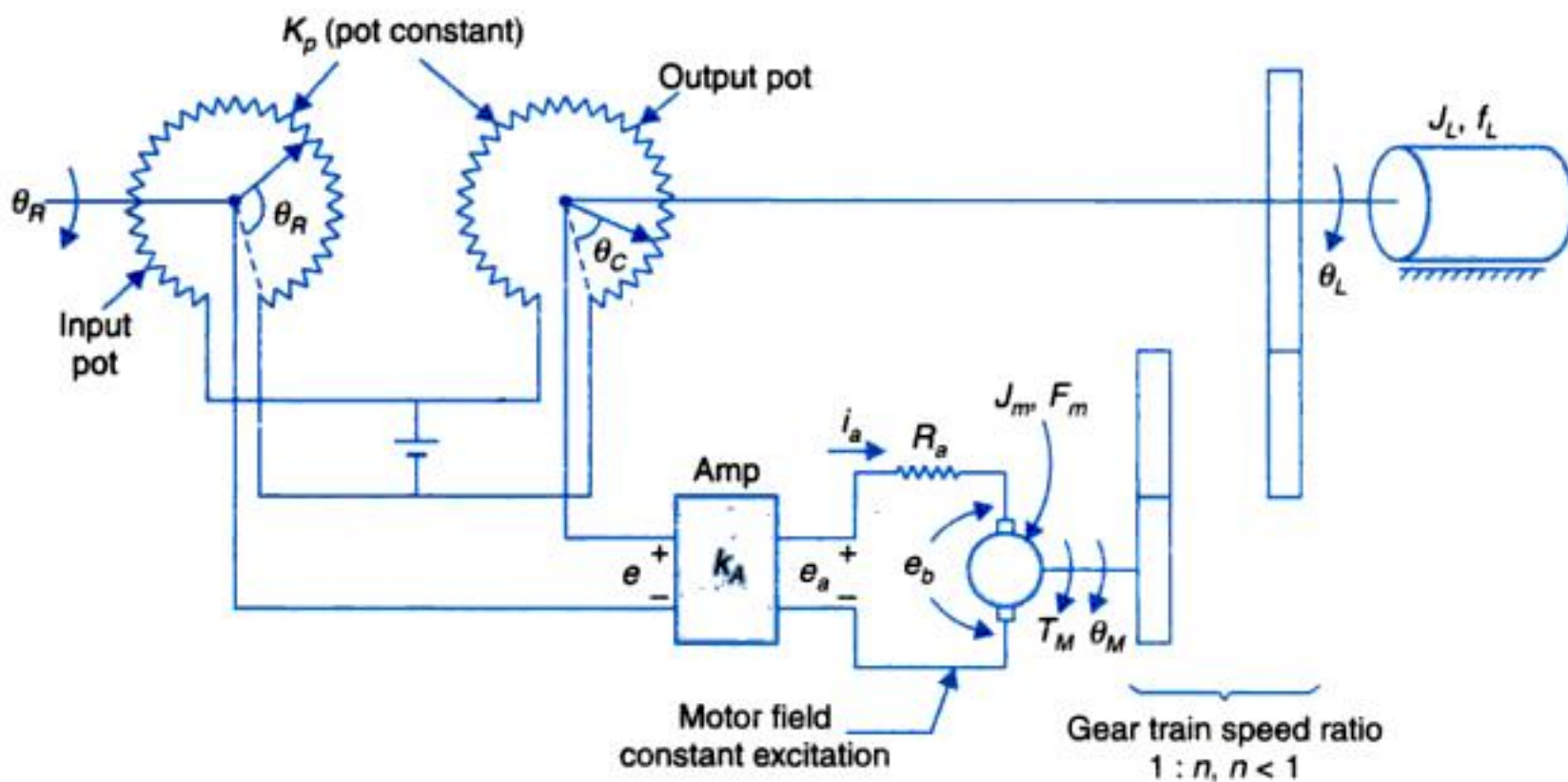


Fig. 2.50

— Various constituents of the system are:

- Drive motor-dc armature controlled.
- Load is driven through a reduction gearing, to amplify torque for moving the load.

- Load angular position is sensed by a circular potentiometer.
- Angle reference input is sensed by an identical potentiometer.
- Position error (in form of voltage e) is fed to amplifier with a power stage to feed the motor armature at voltage e_a .

From physical reasoning it is easily seen that at steady position of load, voltage e should be zero so the motor armature is stationary. It means $\theta_C = \theta_R$ i.e. steady-state error is zero. Any change in command θ_R introduces error e and the motor drives the load till $\theta_C = \theta_R$ once again. The nature of this moment is an important performance measure.

Various parameters and variables are indicated in Fig. 2.50. Motor parameters are:

Torque constant $= K_T$ kg-m/Amp. (armature)

Back emf $= K_b$ V/rad/sec

It is reminded here that numerically $K_T = K_b$.

Motor armature inductance L_a is negligible.

(a) Draw the block diagram of the motor and reduce it to the form $\omega_M(s)/E_a(s)$; ω_M = motor speed.

(b) Draw the complete system block diagram.

(c) Determine the overall transfer function $T(s) = \theta_C(s)/\theta_R(s)$.

(d) Briefly discuss the nature of $T(s)$.

(e) For numerical data given within the solution determine $T(s)$; K_A is variable gain.

Solution. From the control system knowledge acquired so far the block of the position control system (Fig. 2.50) can be drawn directly. For this purpose the load is reflected to the motor shaft giving the effective inertia and friction at motor shaft as

$$J = J_M + n^2 J_L \quad \dots(i)$$

$$f = f_M + n^2 f_L \quad \dots(ii)$$

(a) To begin with let us first draw the motor block diagram linking ω_M , motor speed, to armature voltage e_a . It is given in Fig. 2.51 (a) (this has been presented earlier and is repeated here for the reader to become fully conversant with it).

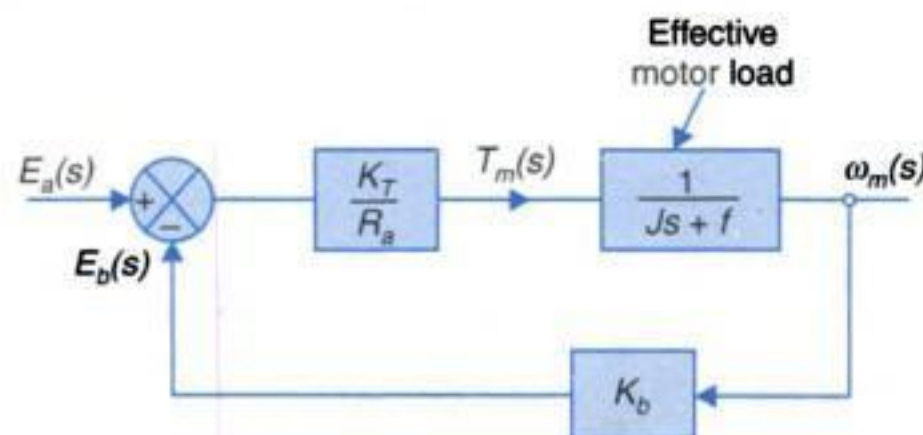


Fig. 2.51

Reducing the block diagram of Fig. 2.51, we get

$$\frac{\omega_M(s)}{E_a(s)} = \frac{K_m}{\tau' s + 1} \quad \dots(iii)$$

$$\text{where } K_m = \frac{K_T}{R_a f + K_T K_b} \quad \dots(iv)$$

$$\tau' = \frac{J}{f + (K_T K_b)/R_a} \quad \dots(v)$$

This is represented in Fig. 2.52

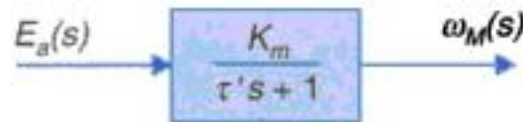


Fig. 2.52. Motor and load.

Note. τ' is the effective motor time constant including friction f and equivalent frictional effect caused by motor back emf $(K_b K_T)/R_a$. Symbol τ is reserved for motor's mechanical time constant i.e. $\tau = J/f$.

(b) The complete block diagram of the speed control system is now drawn in Fig. 2.53.

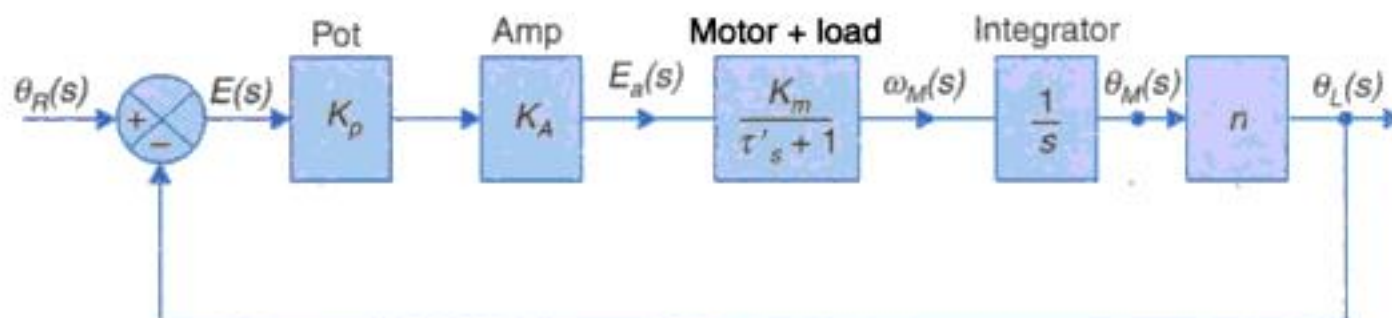


Fig. 2.53

(c) Forward path transfer function

$$G(s) = \frac{K_p K_A K_m n}{s(\tau' s + 1)} \quad \dots(vi)$$

Overall transfer function

$$T(s) = \frac{\theta_L(s)}{\theta_R(s)} = \frac{G(s)}{1 + G(s)}$$

Substituting $G(s)$, we get

$$\frac{\theta_L(s)}{\theta_R(s)} = \frac{K_p K_A K_m n}{\tau' s^2 + s + K_p K_A K_m n} \quad \dots(vii)$$

It is to be noticed that it is a second-order system compared to the first-order speed control system of Fig. 2.39. Increase in order has been caused by the integrator to get angle θ_M from speed $\dot{\theta}_M$.

(d) Data of system components

DC Motor

$$K_T = 60 \times 10^{-3} \text{ kg-m/A}$$

$$J_M = 1 \times 10^{-3} \text{ kg-m}^2$$

$$f_M = 10 \times 10^{-3} \text{ kg-m/rad/sec}$$

$$R_a = 1 \Omega$$

Potentiometer

$$K_p = 1 \text{ V/rad}$$

Gear Train

$$n = 1/10 = 0.1$$

Load

$$J_L = 900 \times 10^{-3} = \text{kg-m}^2$$

$$f_L = 9,000 \times 10^{-3} \text{ kg-m/rad/sec.}$$

Effective load at motor shaft

$$J = 1 \times 10^{-3} + 900 \times 10^{-3} \times (0.1)^2$$

$$= 10 \times 10^{-3} \text{ kg-m}^2$$

$$f = 10 \times 10^{-3} + 9,000 \times 10^{-3} \times (0.1)^2$$

$$= 100 \times 10^{-3} \text{ kg-m/rad/sec.}$$

From Eqs. (iv) and (v)

$$K_m = \frac{60 \times 10^{-3}}{1 \times 100 \times 10^{-3} + (60 \times 10^{-3})^2} ; K_b = K_T$$

$$= \frac{60}{10 + 3.6} = 4.41$$

$$\tau' = \frac{10 \times 10^{-3}}{100 \times 10^{-3} + (60 \times 10^{-3})^2/1} = \frac{10}{100 + 3.6} = 0.097 \text{ sec.}$$

Substituting (values in Eq. (vii))

$$\frac{\theta_L(s)}{\theta_R(s)} = \frac{1 \times K_A \times 4.41 \times 0.1}{0.097s^2 + s + 1 \times K_A \times 4.41 \times 0.1}$$

or

$$\frac{\theta_L(s)}{\theta_R(s)} = \frac{4.55 K_A}{s^2 + 10.31s + 4.55 K_A} \quad \dots(viii)$$

Choice of gain K_A in this transfer function depends on the system dynamics desired. The issues involved will be discussed in Chapter 5.

Example 2.6 : The block diagram of a speed control system is drawn in Fig. 2.54. Define the state variables and write the state and output equations of the system in vector-matrix form.

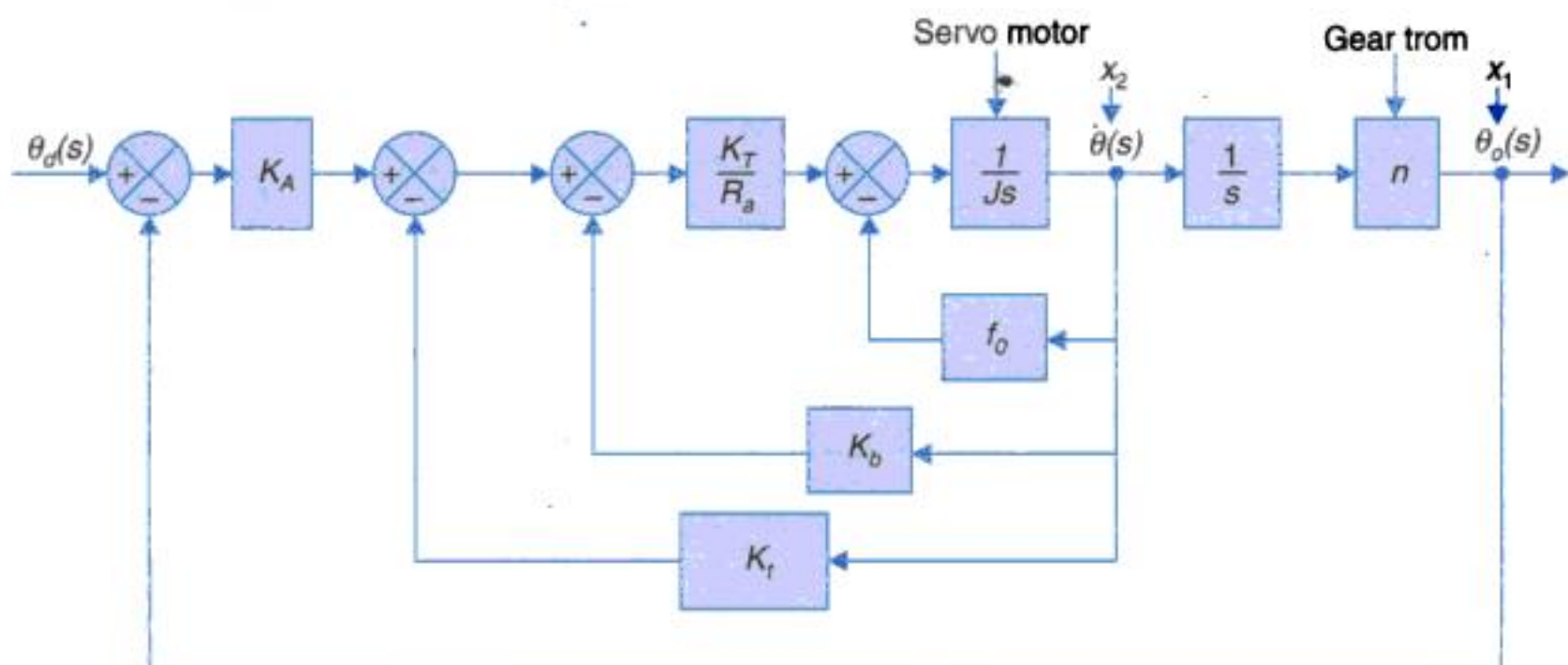


Fig. 2.54

Solution. There will be two state variables as this is a second-order system. We define the state variables as:

$$x_1 = \theta_o, \quad x_2 = \dot{\theta}$$

State equations written from the block diagram. For each block with one denominator s , input-output relations are written. In this block diagram there are two such blocks (2nd order system)

- Block $\left(\frac{n}{s}\right)$

$$x_1 = \left(\frac{n}{s}\right) x_2$$

In time domain $\dot{x}_1 = nx_2$

- Block $\left(\frac{1}{Js}\right)$

$$\left\{ (x_d - x_1)K_A - \left[(K_t + K_b) \frac{K_T}{R_a} + f_0 \right] x_2 \right\} \frac{1}{Js} = x_2$$

In time domain it can be expressed as

$$\dot{x}_2 = -\left(\frac{K_A}{J}\right) x_1 - \frac{f_0 + (K_t + K_b) \left(\frac{K_T}{R_a}\right)}{J} x_2 + \left(\frac{K_A}{J}\right) \theta_d$$

These two equations are written below as state equations

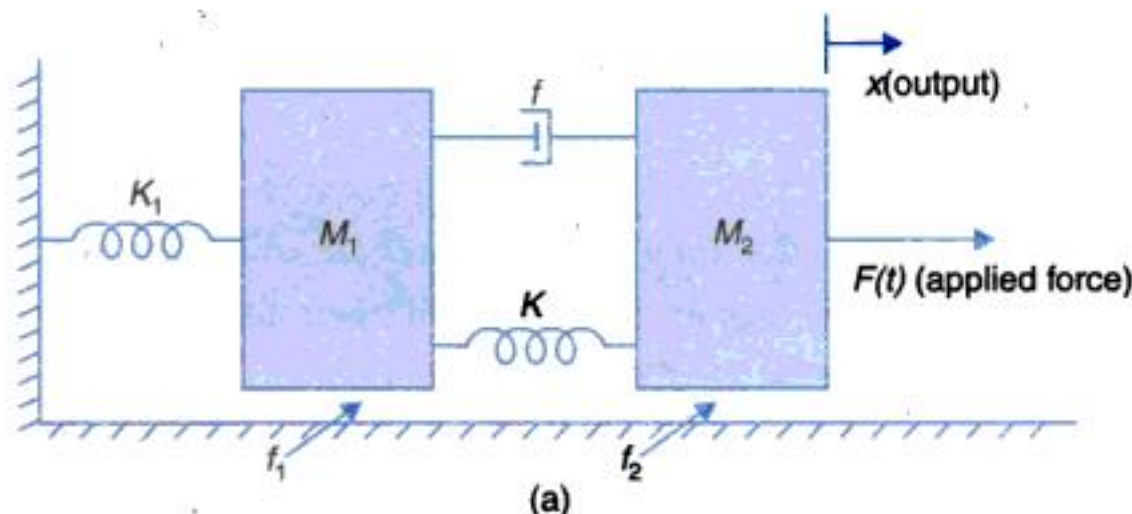
$$\begin{bmatrix} \dot{x}_1 \\ \dot{x}_2 \end{bmatrix} = \begin{bmatrix} 0 & n \\ -\left(\frac{K_A}{J}\right) & -\frac{f_0 + (K_t + K_b) \left(\frac{K_T}{R_a}\right)}{J} \end{bmatrix} \begin{bmatrix} x_1 \\ x_2 \end{bmatrix} + \begin{bmatrix} 0 \\ \frac{K_A}{J} \end{bmatrix} \theta_d \quad \dots(iii)$$

Output equation

$$y = \theta_o = x_1 \quad \text{or} \quad y = [1 \quad 0] \begin{bmatrix} x_1 \\ x_2 \end{bmatrix}. \quad \dots(iv)$$

PROBLEMS

2.1. Obtain the transfer functions of the mechanical systems shown in Figs. P-2.1(a) and (b).



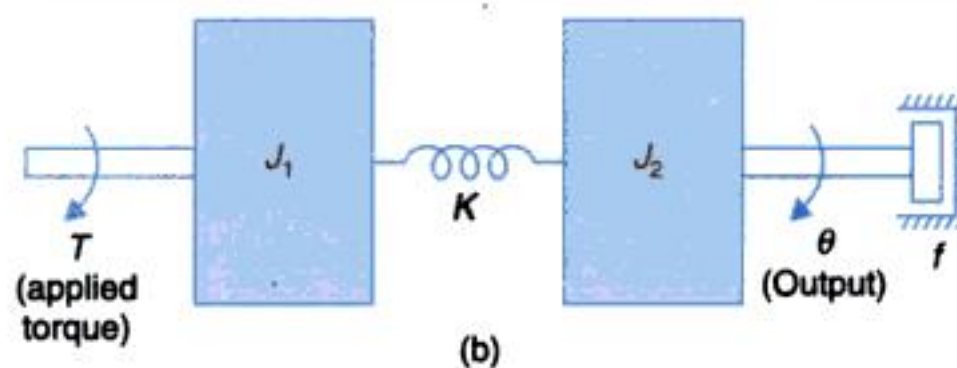


Fig. P-2.1.

- 2.2. Write the differential equations governing the behaviour of the mechanical system shown in Fig. P-2.2. Also obtain an analogous electrical circuit based on force-current analogy.

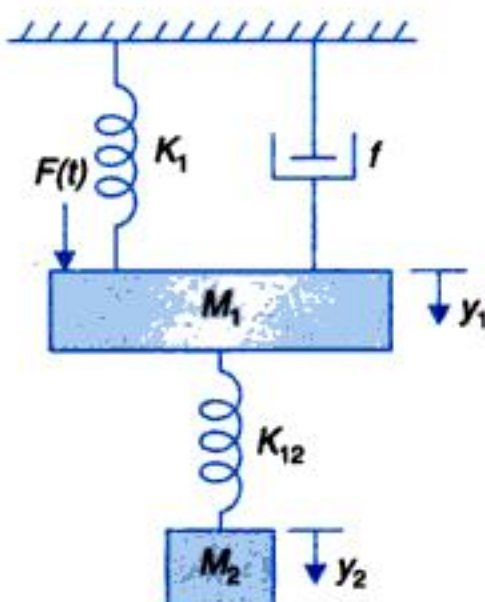


Fig. P-2.2.

- 2.3. Write the differential equations for the mechanical system shown in Fig. P-2.3. Also obtain an analogous electrical circuit based on force-current analogy.

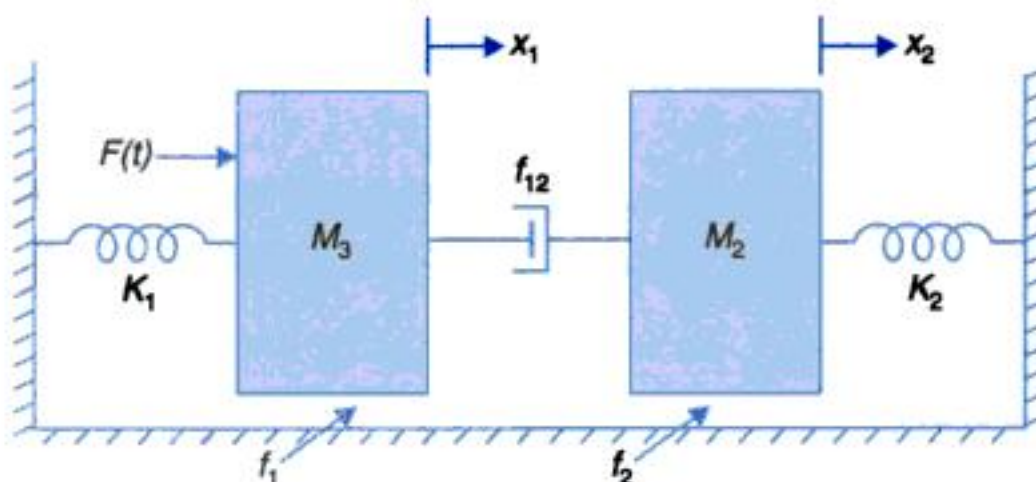


Fig. P-2.3.

- 2.4. Find the transfer function $X(s)/E(s)$ for the electromechanical system shown in Fig. P-2.4. [Hint: for a simplified analysis, assume that the coil has a back emf $e_b = k_1 dx/dt$ and the coil current i produces a force $F_C = k_2 i$ on the mass M]

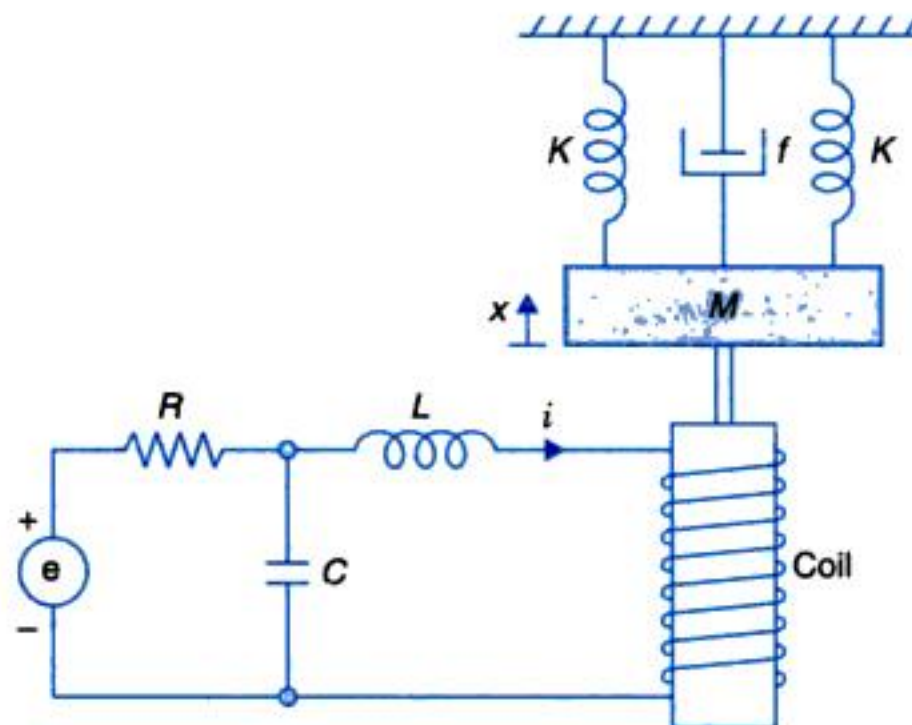


Fig. P-2.4.

- 2.5. Fig. P-2.5 shows a thermometer plugged into a bath of temperature θ_i . Obtain the transfer function $\theta(s)/\theta_i(s)$ of the thermometer and its electrical analogue. (The thermometer may be considered to have a thermal capacitance C which stores heat and a thermal resistance R which limits the heat flow). How the temperature indication of the thermometer will vary with time after the thermometer is suddenly plugged in ?

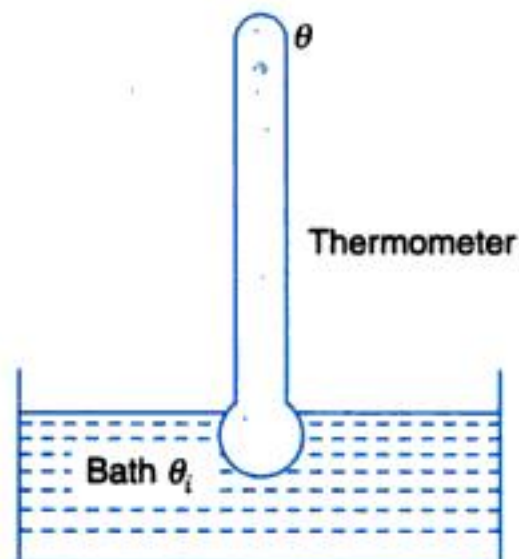


Fig. P-2.5.

- 2.6. The scheme of Fig. P-2.6 produces a steady stream flow of dilute salt solution with controlled concentration C_0 . A concentrated solution of salt with concentration C_i is continuously mixed with pure water in a mixing valve. The valve characteristic is such that the total flow rate Q_0 through it is maintained constant but the inflow Q_i of concentrated salt solution may be linearly varied by controlling valve stem position x . The outflow rate from the salt mixing tank is the same as the flow rate into it from the mixing valve, such that the level of the dilute salt solution in the tank is maintained constant. Obtain the transfer function $C_0(s)/X(s)$. If from fully closed position, the valve stem is suddenly opened by x_0 , determine the outstream salt concentration C_0 as a function of time.

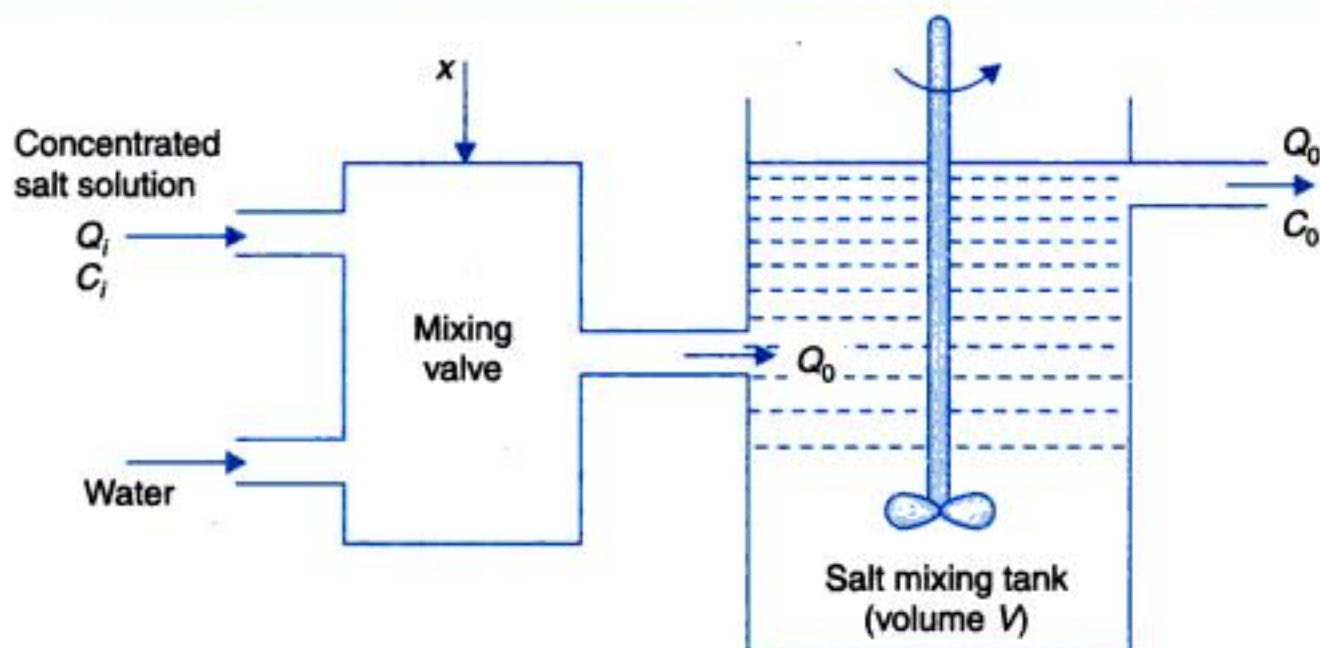


Fig. P-2.6.

- 2.7. In the speed control system shown in Fig. P-2.7, the generator field time constant is negligible. It is driven at constant speed giving a generated voltage of K_g volts/field amp. The motor is separately excited so as to have a counter emf of K_b volts per rad/sec. It produces a torque of K_T newton-m/amp. The motor and its load have a combined moment of inertia J kg-m² and negligible friction. The tachometer has K_t volts per rad/sec and the amplifier gain is K_A amps/volt. Draw the block diagram of this system and determine therefrom the transfer function $\omega(s)/E_i(s)$, where ω is the load speed.

With the system originally at rest, a control voltage $e_i = 100$ volts is suddenly applied. Determine how the load speed will change with time.

Given:

$$J = 6 \text{ kg-m}^2$$

$$K_A = 4 \text{ amp/volt}$$

$$K_T = 1.5 \text{ newton-m/amp}$$

$$K_g = 50 \text{ volts/amp}$$

$$R_a = 1 \text{ ohm}$$

$$K_t = 0.2 \text{ volts per rad/sec}$$

[Hint: $K_b = K_T$ in MKS units]

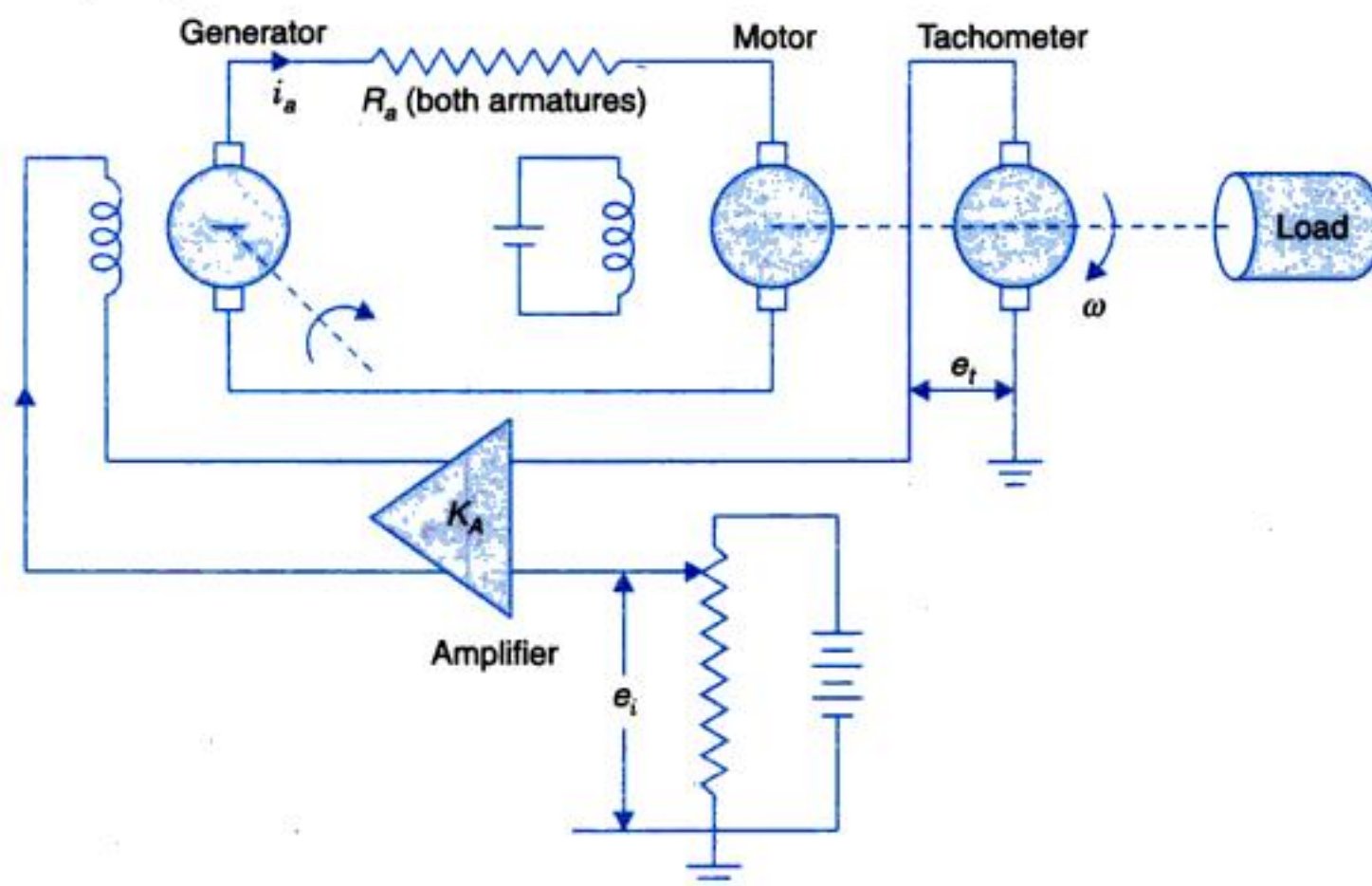


Fig. P-2.7.

- 2.8. Consider the positional servomechanism shown in Fig. P-2.8. Assume that the input to the system is the reference shaft position θ_R and the system output is the load shaft position θ_L . Draw the block diagram of the system indicating the transfer function of each block. Simplify the block diagram to obtain $\theta_L(s)/\theta_R(s)$ for the closed-loop system and also when the loop is open (in opening the loop, the lead from the output potentiometer driven by θ_C is disconnected and grounded). The parameters of the system are given below:

| | |
|--------------------------------------------|------------------------------------------|
| Sensitivity of error detector, | $K_p = 10$ volt/rad |
| Gain of d.c. amplifier, | $K_A = 50$ volts/volt |
| Motor field resistance, | $R_f = 100$ ohms |
| Motor field inductance, | $L_f = 20$ henrys |
| Motor torque constant, | $K_T = 10$ newton-m/amp |
| Moment of inertia of load, | $J_L = 250$ kg-m ² |
| Coefficient of viscous friction of load, | $f_L = 2,500$ newton-m per rad/sec |
| Motor to load gear ratio, | $(\dot{\theta}_L/\dot{\theta}_M) = 1/50$ |
| Load to potentiometer gear ratio, | $(\dot{\theta}_C/\dot{\theta}_L) = 1$ |
| Motor inertia and friction are negligible. | |

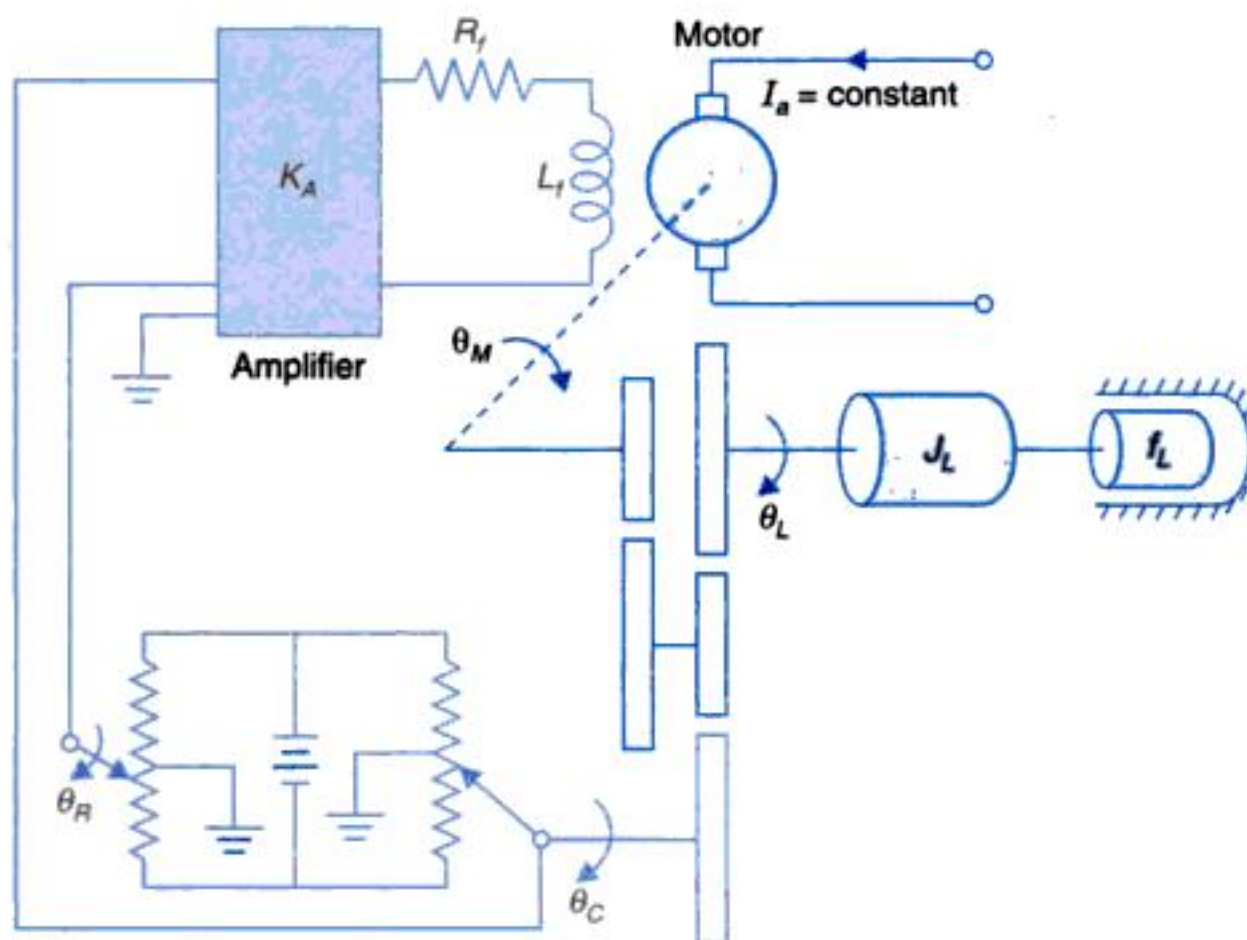


Fig. P-2.8.

- 2.9. Using block diagram reduction techniques, find the closed-loop transfer functions of the systems whose block diagrams are given in Figs. P-2.9(a) and (b).
- 2.10. For the system represented by the block diagram shown in Fig. P-2.10, evaluate the closed-loop transfer function, when the input R is (i) at station I, (ii) at station II.
- 2.11. From the block diagrams shown in Fig. P-2.11, determine C_1/R_1 and C_2/R_1 (assuming $R_2 = 0$).
- 2.12. Fig. P-2.12 shows a schematic diagram of liquid-level system. The flow of liquid Q_i into the tank is controlled by the pressure P of the incoming liquid and valve opening V_x (note that this is a more realistic model than the one shown in Fig. 2.15) through a nonlinear relationship.

$$Q_i = f(P, V_x)$$

Linearized liquid-level model and about the operating point $(P_0, Q_i = Q_0 H_0)$ is given as $\Delta Q_i = K_1 \Delta P + K_2 \Delta V_x$. Draw the signal flow graph and obtain therefrom the transfer function $\left. \frac{\Delta Q_0(s)}{\Delta V_x(s)} \right|_{\Delta Q_D = 0}$

with pressure remaining constant.

(The tank and output pipe may be considered to have liquid capacitance C and flow resistance R respectively).

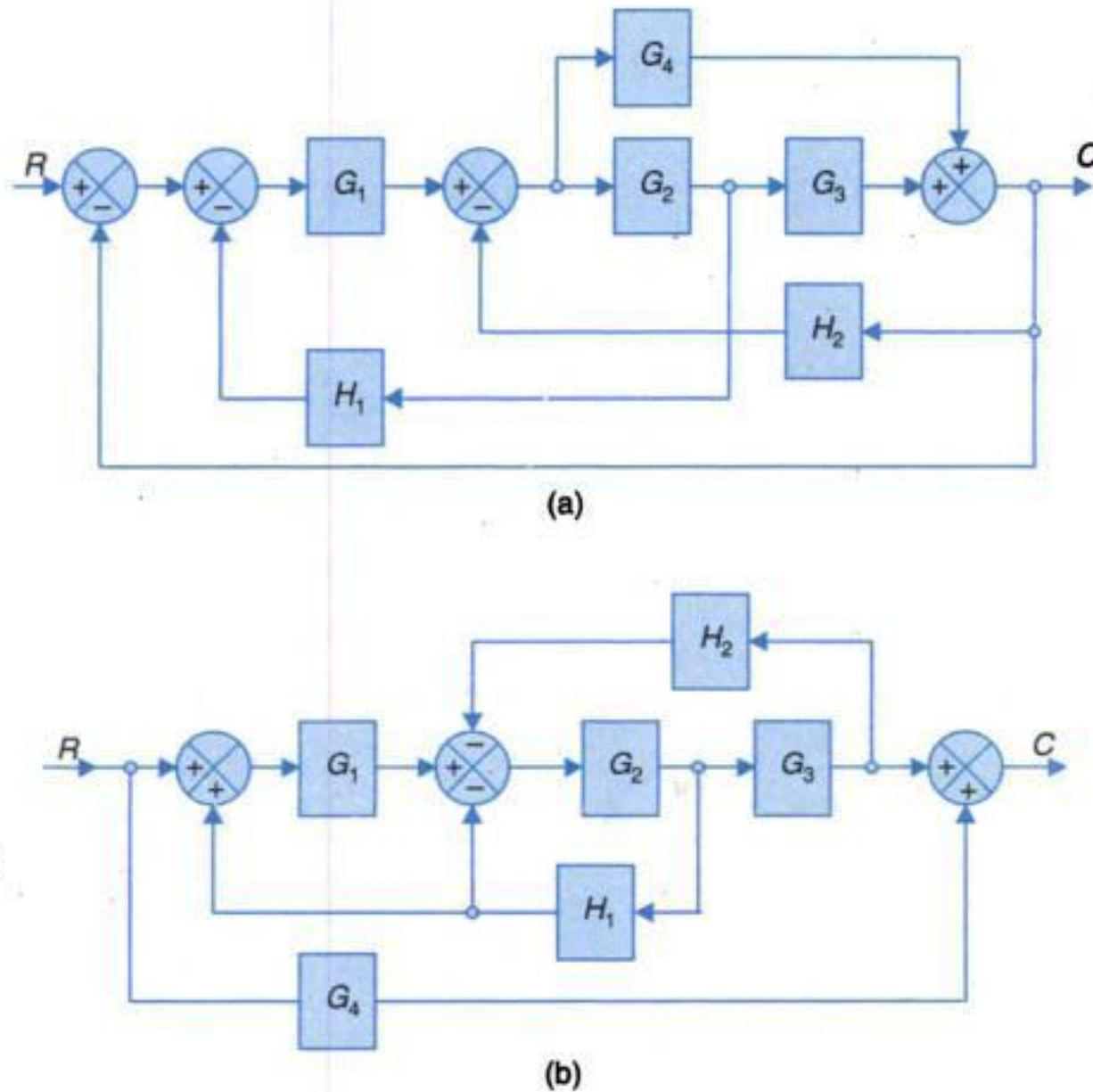


Fig. P-2.9.

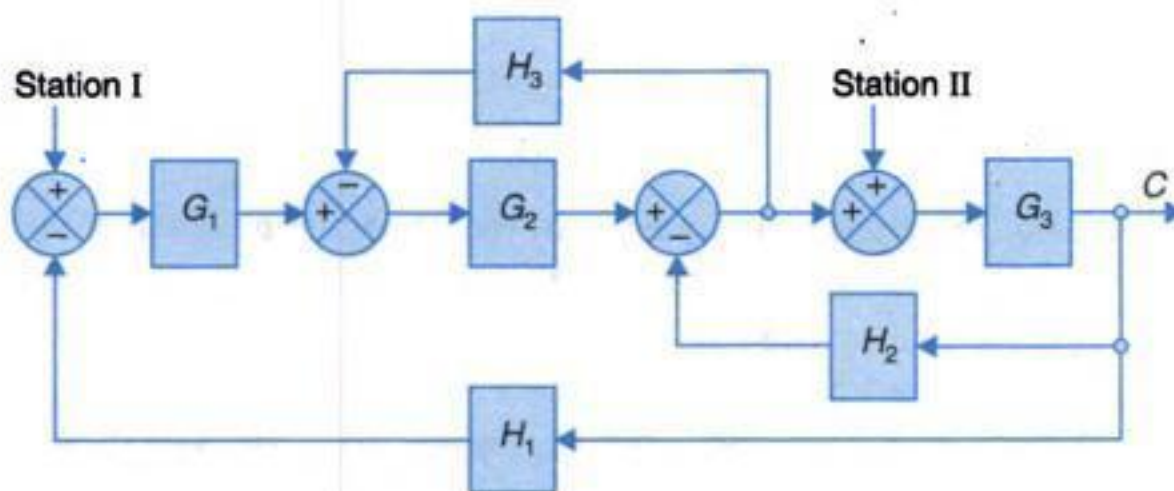


Fig. P-2.10.

2.14. Obtain the overall transfer function C/R from the signal flow graph shown in Fig. P-2.14.

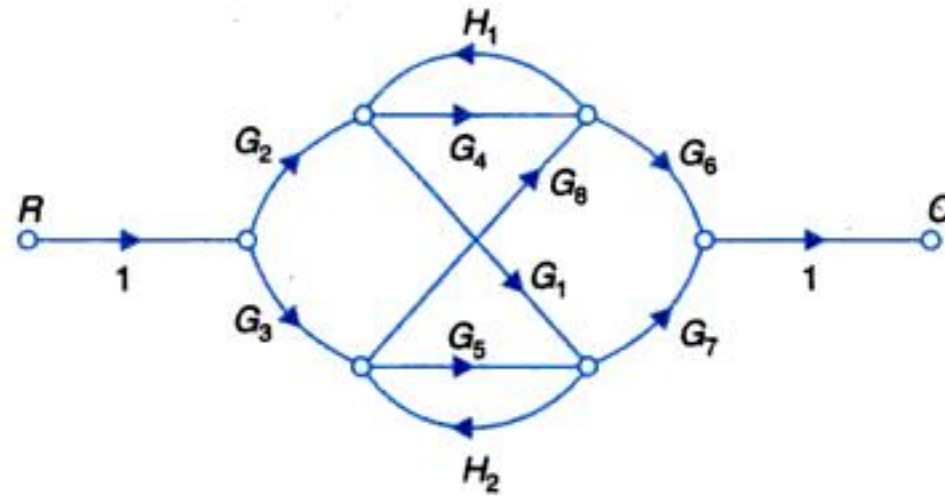


Fig. P-2.14.

2.15. Fig. P-2.15 gives the signal flow graph of a system with two inputs and two outputs. Find expressions for the outputs C_1 and C_2 . Also determine the condition that makes C_1 independent of R_2 and C_2 independent of R_1 .

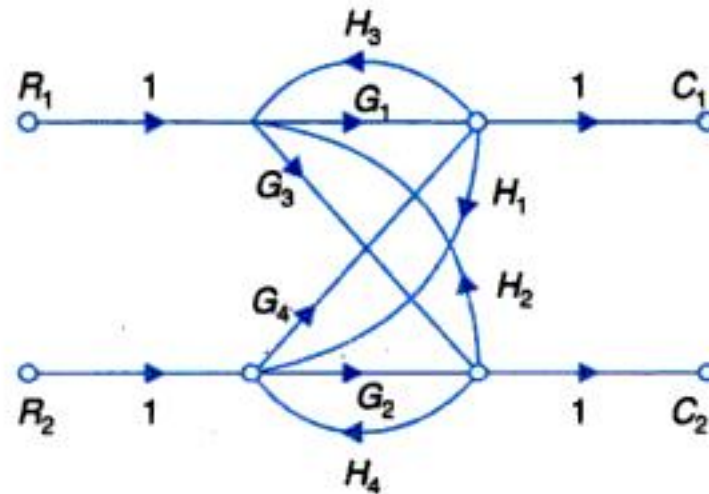


Fig. P-2.15.

2.16. For the system represented by the following equations, find the transfer function $X(s)U(s)$ by signal flow graph technique.

$$x = x_1 + \beta_3 u$$

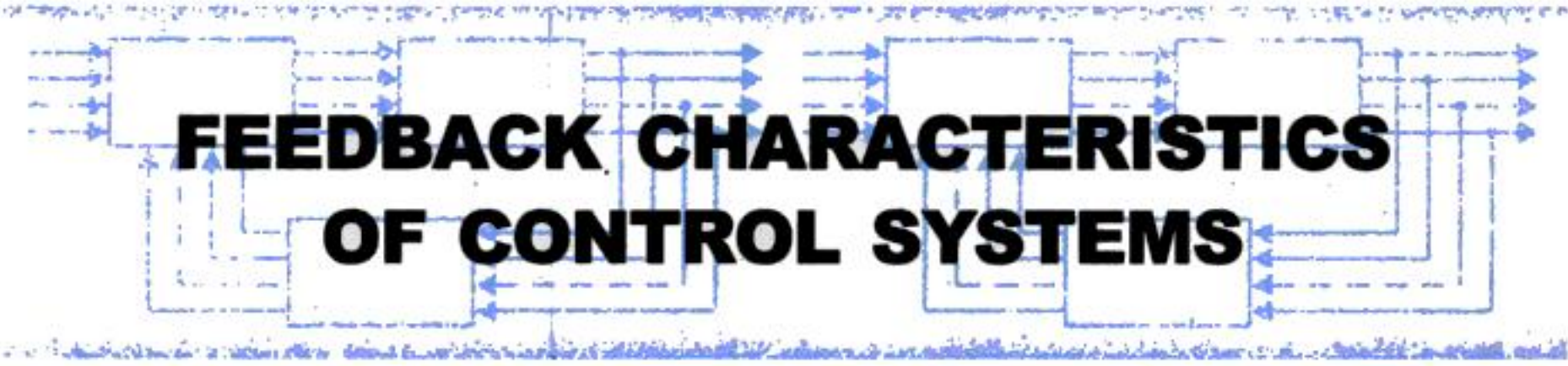
$$\dot{x}_1 = -a_1 x_1 + x_2 + \beta_2 u$$

$$\dot{x}_2 = -a_2 x_1 + \beta_1 u.$$

3

FEEDBACK CHARACTERISTICS OF CONTROL SYSTEMS

3



FEEDBACK CHARACTERISTICS OF CONTROL SYSTEMS

3.1 FEEDBACK AND NON-FEEDBACK SYSTEMS

Feedback systems play an important role in modern engineering practice because they have the possibility for being adopted to perform their assigned tasks automatically. A *non-feedback (open-loop) system* represented by the block diagram and signal flow graph in Fig. 3.1 (a), is activated by a single signal at the input (for single-input systems). There is no provision within this system for supervision of the output and no mechanism is provided correct (or compensate) the system behaviour for any lack of proper performance of system components, changing environment, loading or ignorance of the exact value of process parameters. On the other hand, a *feedback (closed-loop) system* represented by the block diagram and signal flow graph in Fig. 3.1 (b) is driven by two signals (more signals could be employed), one the input signal and the other, a signal called the feedback signal derived from the output of the system. The feedback signal gives this system the capability to act as self-correcting mechanism as explained below.

The output signal c is measured by a sensor $H(s)$, which produces a feedback signal b . The comparator compares the feedback signal b with the input (command) signal r generating the actuating signal e , which is as measure of discrepancy between r and b . The actuating signal is applied to the process $G(s)$ so as to influence the output c in a manner which tends to reduce the errors.

Feedback as a means of automatic regulation and control is, in fact, inherent in nature and can be noticed in many physical, biological and soft systems. For example, the body temperature of any living being is automatically regulated through a process which is essentially a feedback process, only it is far more complex than the diagram of Fig. 3.1 (b).

The beneficial effects of feedback in feedback systems with high loop gain, which will be elaborated in this Chapter, are enumerated below (discussion will not follow this order).

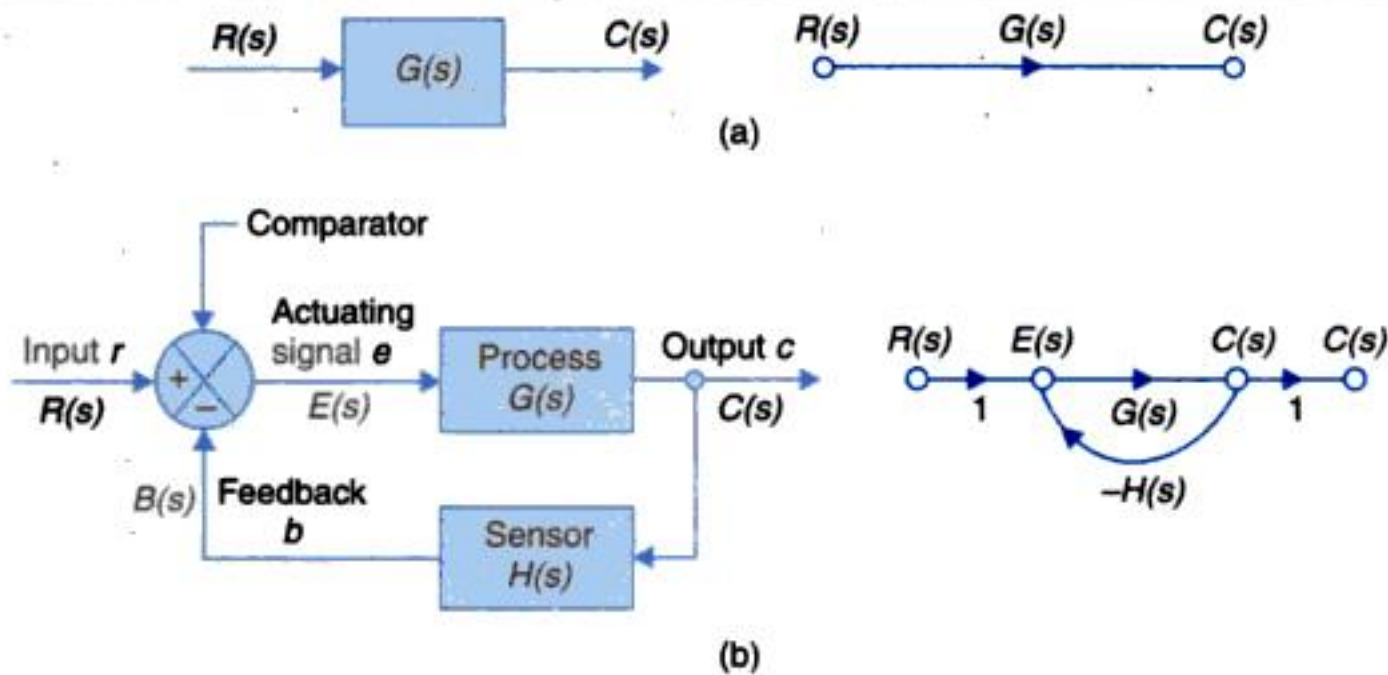


Fig. 3.1. (a) A non-feedback (open-loop) system
(b) A feedback (closed-loop) system

1. The controlled variable accurately follows the desired value.
2. Effect on the controlled variable of external disturbances other than those associated with the feedback sensor are greatly reduced.
3. Effect of variation in controller and process parameters (the forward path) on system performance is reduced to acceptable levels. These variations occur due to wear, aging, environmental changes etc.

Feedback in the control loop allows accurate control of the output (by means of the input signal) even when process or controlled plant parameters are not known accurately.

4. Feedback in a control system greatly improves the speed of its response compared to the response speed capability of the plant/components composing the system (forward path).

The cost of achieving these improvements in system's performance through feedback will be discussed alongwith. These are: greater system complexity, need for much larger forward path gain and possibility of system instability (it means undesired/persistent oscillations of the output variable).

3.2 REDUCTION OF PARAMETER VARIATIONS BY USE OF FEEDBACK

One of the primary purpose of using feedback in control systems is to reduce the sensitivity of the system to parameter variations. The parameters of a system may vary with age, with changing environment (e.g., ambient temperature), etc. Conceptually, *sensitivity* is a measure of the effectiveness of feedback in reducing the influence of these variations on system performance.

Let us define sensitivity on a quantitative basis. In the open-loop case

$$C(s) = G(s) R(s)$$

Suppose due to parameter variations $G(s)$ changes to $[G(s) + \Delta G(s)]$ where $|G(s)| \gg |\Delta G(s)|$. The output of the open-loop system then changes to

$$C(s) + \Delta C(s) = [G(s) + \Delta G(s)] R(s)$$

or

$$\Delta C(s) = \Delta G(s) R(s) \quad \dots(3.1)$$

Similarly, in the closed-loop case, the output

$$C(s) = \frac{G(s)}{1 + G(s)H(s)} R(s)$$

changes to

$$C(s) + \Delta C(s) = \frac{G(s) + \Delta G(s)}{1 + G(s)H(s) + \Delta G(s)H(s)} R(s)$$

due to the variation $\Delta G(s)$ in $G(s)$, the forward path transfer function. Since $|G(s)| \gg |\Delta G(s)|$ we have from the above, the variation in the output as

$$\Delta C(s) = \frac{\Delta(s)}{1 + G(s)H(s)} R(s) \quad \dots(3.2)$$

From eqns. (3.1) and (3.2) it is seen that in comparison to the open-loop system, the change in the output of the closed-loop system due to variation $G(s)$ is reduced by a factor of $[1 + G(s)H(s)]$ which is much greater than unity in most practical cases over the frequency ($s = j\omega$) of interest.

The term *system sensitivity* is used to describe the relative variation in the overall transfer function $T(s) = C(s)/R(s)$ due to variation in $G(s)$ and is defined below:

$$\text{Sensitivity} = \frac{\text{percentage change in } T(s)}{\text{percentage change in } G(s)}$$

For small incremental variation in $G(s)$, the sensitivity is written in the quantitative form as

$$S_G^T = \frac{\partial T / T}{\partial G / G} = \frac{\partial \ln T}{\partial \ln G} \quad \dots(3.3)$$

where S_G^T denotes the sensitivity of T with respect to G .

In accordance with the above definition, the sensitivity of the closed-loop system is

$$S_G^T = \frac{\partial T}{\partial G} \times \frac{G}{T} = \frac{(1 + GH) - GH}{(1 + GH)^2} \times \frac{G}{G / (1 + GH)} = \frac{1}{1 + GH} \quad \dots(3.4)$$

Similarly, the sensitivity of the open-loop system is

$$S_G^T = \frac{\partial T}{\partial G} \times \frac{G}{T} = 1 \quad (\text{in this case } T = G) \quad \dots(3.5)$$

Thus, the sensitivity of a closed-loop system with respect to variation in G is reduced by a factor $(1 + GH)$ as compared to that of an open-loop system.

The sensitivity of T with respect to H , the feedback sensor, is given as

$$S_H^T = \frac{\partial T}{\partial H} \times \frac{H}{T} = G \left[\frac{-G}{(1 + GH)^2} \right] \frac{H}{G / (1 + GH)} = \frac{-GH}{1 + GH} \quad \dots(3.6)$$

The above equation shows that for large values of GH , sensitivity of the feedback system with respect to H approaches unity. Thus, we see that the changes in H directly affect the system output. Therefore, it is important to use feedback elements which do not vary with environmental changes or can be maintained constant.

Very often the system's sensitivity is to be determined with a particular parameter (or parameters), with the transfer function expressed in ratio of polynomial form *i.e.*,

$$T(s) = \frac{N(s, \alpha)}{D(s, \alpha)}; \alpha = \text{parameter under consideration}$$

From eqn.(3.3)

$$S_{\alpha}^T = \left. \frac{\partial \ln N}{\partial \ln \alpha} \right|_{\alpha_0} - \left. \frac{\partial \ln D}{\partial \ln \alpha} \right|_{\alpha_0} \quad \dots(3.7a)$$

$$= S_{\alpha}^N - S_{\alpha}^D \quad \dots(3.7b)$$

where α_0 is the nominal value of the parameter around which the variation occurs.

The use of feedback in reducing sensitivity to parameter variations is an important advantage of feedback control systems. To have a highly accurate open-loop system, the components of $G(s)$ must be selected to meet the specifications rigidly in order to fulfil the overall goals of the system. On the other hand, in a closed-loop system $G(s)$ may be less rigidly specified, since the effects of parameter variations are mitigated by the use of feedback. However, a closed-loop system requires careful selection of the components of the feedback sensor $H(s)$. Since $G(s)$ is made up of power elements and $H(s)$ is made up of measuring elements which operate at low power levels, the selection of accurate $H(s)$ is far less costly than that of $G(s)$ to meet the exact specifications.

The price for improvement in sensitivity by use of feedback is paid in terms of *loss of system gain*. The open-loop system has a gain $G(s)$, while the gain of the closed-loop system is $G(s)/[1 + G(s)H(s)]$. Hence by use of feedback, the system gain is reduced by the same factor as by which the sensitivity of the system to parameter variations is reduced. Sufficient open-loop gain can, however, be easily built into a system so that we can afford to lose some gain to achieve improvement in sensitivity.

As a first example of feedback in reducing the system's sensitivity to parameter variations consider the feedback amplifier of Fig. 3.2(a) with negative feedback provided through a potential divider (feedback gain less than unity). Assuming the input impedance of the amplifier

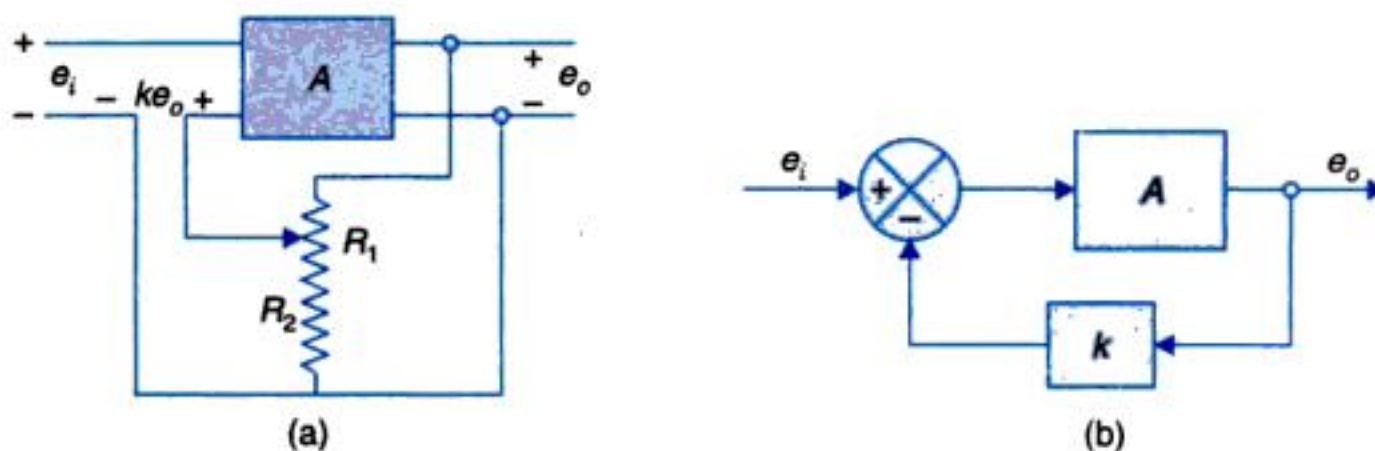


Fig. 3.2. Feedback amplifier.

to be infinite and its output impedance as zero, the equivalent block diagram of the system is drawn in Fig. 3.2 (b). Observe that both the forward gain A and feedback gain $k (< 1)$ are independent of frequency (in the range of frequencies of interest here).

It easily follows from the block diagram of Fig. 3.2 (b) that the overall gain of the amplifier circuit is

$$\frac{e_0}{e_i} = T = \frac{A}{1 + kA}; \quad k = \frac{R_2}{R_1} \leq 1 \quad \dots(3.8a)$$

$$S_A^T = \frac{dT}{dA} \cdot \frac{A}{T} = \frac{1}{1 + kA}; \quad \text{see eqn. (3.4)} \quad \dots(3.8b)$$

For $A = 10^4$, $k = 0.1$

$$S_A^T = \frac{1}{1 + 10^3} = 0.001$$

While the feedback reduces the sensitivity to variation in forward gain to a very low figure (0.001), it also reduces the overall gain to

$$T = \frac{10^4}{1 + 10^3} = 10; \quad \text{compare with forward gain of } 10^4$$

Now sensitivity to feedback gain is given by

$$\begin{aligned} S_k^T &= \frac{dT}{dk} \cdot \frac{k}{T} = \frac{-kA}{1 + kA}; \quad \text{eqn. (3.6)} \quad \dots(3.8c) \\ &= \frac{-10^3}{1 + 10^3} = -1 \end{aligned}$$

S_k^T being equal to unity, the feedback constant $k = R_2/R_1$ must not vary *i.e.*, the resistor ratio R_2/R_1 must be accurate and stable.

In fact for such large $A (= 10^4)$, $kA \gg 1$ and so from eqn. (3.8a)

$$T = \frac{1}{k} = \frac{R_1}{R_2} = 10; \quad \text{independent of } A$$

As an example of control of system sensitivity, let us consider the speed control system of Fig. 2.39 which may be operated in open-or-closed-loop mode. The signal flow graph of this system is given in Fig. 2.40(b). The reduced signal flow graph of this system with $T_D = 0$, is drawn in Fig. 3.3

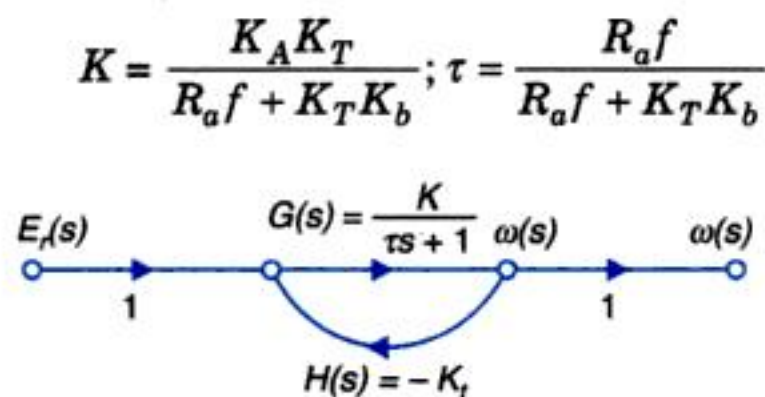


Fig. 3.3. Reduced signal flow graph ($T_D = 0$) obtained from Fig. 2.29.

The sensitivity of the open-loop mode of operation to variation-in the constant K is unity, while the corresponding sensitivity of the closed-loop mode is evaluated below.

From the signal flow graph of Fig. 3.3

$$T(s) = \frac{K}{\tau s + (1 + KK_t)} \quad (3.9a)$$

$$S_K^T = \frac{\partial T}{\partial K} \times \frac{K}{T} = \frac{s + \frac{1}{\tau}}{s + \left(\frac{1 + KK_t}{\tau}\right)} \quad (3.9b)$$

The expression (3.9b) can also be obtained by substituting $G(s) = K/(\tau s + 1)$ and $H(s) = K_t$ in eqn. (3.4).

For a typical application of this system, we might have $1/\tau = 0.1$ and $(1 + KK_t)\tau = 10$. Therefore from eqn. (3.4) we obtain

$$S_K^T = \frac{s + 0.1}{s + 10}$$

It follows from above that the sensitivity is a function of s and must be evaluated over the complete frequency band within which input has significant components. Our interest is to determine the upper limit for the sensitivity function $|S_K^T|$ over the frequency band and the frequency at which the maximum value occurs.

At a particular frequency, e.g., $s = j\omega = j1$, the magnitude of the sensitivity is approximately:

$$|S_K^T| = 0.1$$

Thus the sensitivity of the closed-loop speed control system at this frequency is reduced by a factor of ten compared to that of the open-loop case.

Sensitivity studies in the frequency domain will be taken up in Chapter 9.

3.3 CONTROL OVER SYSTEM DYNAMICS BY USE OF FEEDBACK

Let us consider the elementary single-loop feedback system of Fig. 3.4. The open-loop transfer function of this system is

$$\frac{C(s)}{R(s)} = G(s) = \frac{K'}{s + \alpha} \quad \dots(3.10 (a))$$

$$= \frac{K}{\tau s + 1}; K = K'/\alpha, \tau = 1/\alpha \quad \dots(3.10 (b))$$

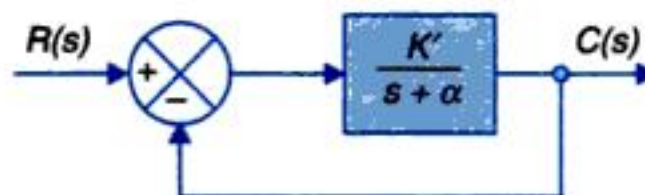


Fig. 3.4. A simple feedback system.

These are two alternative forms of expressing a transfer function. At $s = -\alpha$, $G(s)$ tends to infinity so is known as the **pole** of the system, while $\tau = 1/\alpha$ is known as its **time constant**. The *dc* gain of the system is

$$G(0) = K = K'/\alpha$$

With the feedback loop closed the closed-loop transfer function is

$$\frac{C(s)}{R(s)} = \frac{K}{\tau s + (1+K)} = \frac{K'}{s + (\alpha + K')} \quad \dots(3.11 (a))$$

$$= \frac{K/(1+K)}{\tau_c s + 1} ; \tau_c = \tau(1+K) \quad \dots(3.11 (b))$$

We find from eqns (3.11 (a)) and (3.11 (b)) that the effect of closing the loop (that is introduction of negative feedback) is to shift the system's pole from $-\alpha$ to $-(\alpha + K')$ or $-\alpha(1 + K)$; alternatively to reduce the system time constant from τ to $\tau/(1 + K)$. Of course in the mean time the *dc* gain has reduced to $K/(1 + K)$.

We shall now examine the effect of these changes in system transfer function on its dynamic response.

For this purpose we shall assume that the system is excited (disturbed) by an impulse input $r(t) = \delta(t)$ (infinitely large input lasting for infinity short time). The Laplace transform of an impulse excitation is $R(s) = 1$ (this will be further discussed in Chapter 5). Taking the inverse Laplace transform of eqn. (3.10 (a)) and (3.11 (a)) with $R(s) = 1$, we have

$$\begin{aligned} c(t) &= \mathcal{L}^{-1} \frac{K'}{s + \alpha} = K' e^{-\alpha t} \\ &= K' e^{-t/\tau} \text{ (for non-feedback (open-loop) system)} \quad \dots(3.12) \end{aligned}$$

and

$$\begin{aligned} c(t) &= \mathcal{L}^{-1} \frac{K'}{s + \alpha(1+K)} = K' e^{-\alpha(1+K)t} \\ &= K' e^{-t/\tau_c} \text{ (for feedback (closed-loop) system)} \quad \dots(3.13) \end{aligned}$$

The location of pole and the dynamic response of non-feedback (open-loop) and feedback (closed-loop) system are shown in Fig. 3.5. These responses decay in accordance with respective

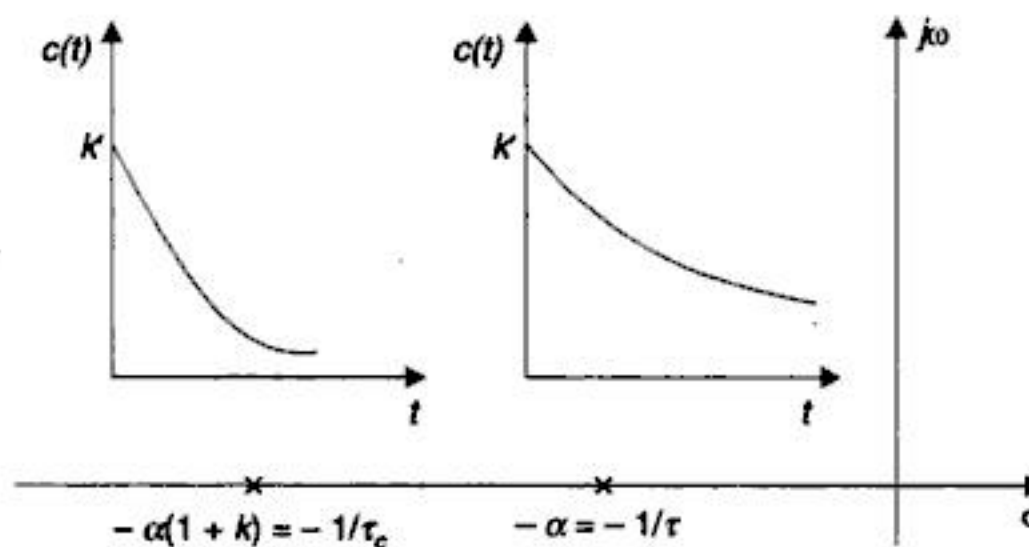


Fig. 3.5. Impulse response of open and closed-loop system (Fig. 3.4).

time constants. As the closed-loop time constant $\tau_c = \tau/(1 + K)$, its response decays much faster* which means that the speed of system's response with loop closed is faster by a factor of $(1 + K)$ compared to the open-loop system.

From this example, it is concluded that feedback controls the dynamics of the system by adjusting the location of its poles. It is, however, important to note here that feedback introduces the possibility of instability, that is, a closed-loop system may be unstable even though the open-loop is stable. The question of stability of control systems is treated in details in Chapter 6.

Consider once again the speed control system of Fig. 2.40 (a). Let the system be subjected to a suddenly applied constant input called step** input for which $E_r(s) = A/s$, where A is a constant. The output response of the system obtained by reference to the signal flow graph of Fig. 3.3 or directly from eqn. (2.101) is given by

$$\begin{aligned} \omega(s) &= \frac{K/\tau}{s\left(s + \frac{1}{\tau}\right)} && \text{(for open-loop operation, i.e., } K_t = 0) \\ &= \frac{K/\tau}{s\left(s + \frac{1 + KK_t}{\tau}\right)} && \text{(for closed-loop operation)} \end{aligned}$$

Taking the inverse Laplace transform of the above equations, we get

$$\omega(t) = K(1 - e^{-t/\tau}) \text{ (for open-loop operation)} \quad \dots(3.14)$$

$$= \frac{K}{1 + KK_t} (1 - e^{-t/\tau_c}) \text{ (for closed-loop operation)} \quad \dots(3.15)$$

where τ_c (closed-loop time constant) = $\tau/(1 + KK_t)$.

It is seen from above that if the open-loop time constant τ is large, the transient response is poor and one choice is to replace the motor by another one with a lower time constant. Such a motor will obviously be more expensive and further due to physical limitations it is not possible to design and manufacture motor of a given size with time constant lower than a certain minimum value. Under such circumstances the closed-loop mode provides a lower time constant τ_c which can be conveniently adjusted by a suitable choice of KK_t . Unlimited reduction in τ_c is of course not practicable.

It is seen from eqn (2.102) and also eqn. (3.15) that the dc gain $T(0)$ of the closed-loop system is reduced by a factor of $(1 + KK_t)$ on account of the feedback loop. However, this only needs a scaling of $r(t)$ to obtain the desired $c(t)$.

From the above illustration we conclude that feedback is a powerful technique for control of system dynamics.

Effect of feedback on bandwidth

A control system is a low-pass filter—it responds to frequencies from *dc* up to a certain value ω_b at which the gain drops to $1/\sqrt{2}$ of its *dc* value. This frequency ω_b is the bandwidth of the

*In time 5τ the response decay to $e^{-5} = 0.0067$ or 0.67% of the value immediately after application of impulse.

**Discussed in detail in Chapter 5.



You have either reached a page that is unavailable for viewing or reached your viewing limit for this book.



You have either reached a page that is unavailable for viewing or reached your viewing limit for this book.

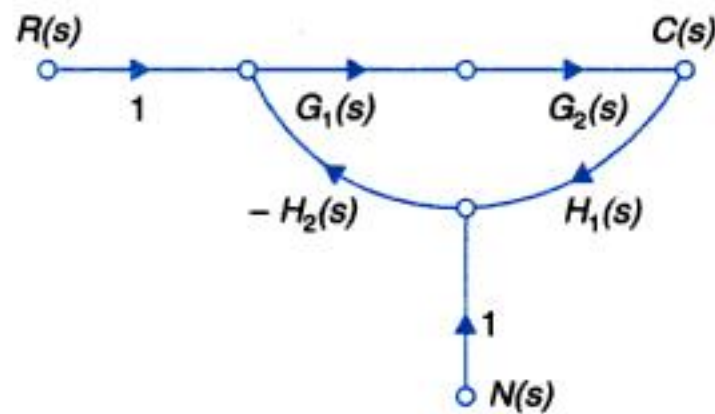


Fig. 3.7. Closed-loop system with measurement noise.

For large values of loop gain ($|G_1 G_2 H_1 H_2(s)| \gg 1$), the above equation reduces to

$$\frac{C_n(s)}{N(s)} \approx -\frac{1}{H_1(s)}$$

Therefore, the effect of noise on output is

$$C_n(s) = -\frac{N(s)}{H_1(s)} \quad \dots(3.24)$$

Thus, for optimum performance of the system, the measurement sensor should be designed such that $H_1(s)$ is maximum, which is equivalent to maximizing the signal-to-noise ratio of the sensor.

The design specifications of the feedback sensor are far more stringent than those of the forward path transfer function. The feedback sensor must have low parameter variations as these are directly reflected in system response (the sensitivity $S_H^T \approx -1$). Further the signal-to-noise ratio for the sensor must be high as explained above. Usually it is possible to design and construct the sensor with such stringent specifications and at reasonable cost because the feedback elements operate at low power level.

To conclude, the use of feedback has the advantages of reducing sensitivity, improving transient response and minimizing the effects of disturbance signals in control systems. On the other hand, the use of feedback increases the number of components of the system, thereby increasing its complexity. Further it reduces the gain of the system and also introduces the possibility of instability. However, in most cases the advantages outweigh the disadvantages and therefore the feedback systems are commonly employed in practice.

3.5 LINEARIZING EFFECT OF FEEDBACK

Yet another property of feedback is its linearizing effect which is illustrated by means of the simple single-loop static system of Fig. 3.8 (a). In a static system various gains (transmittances) are independent of time. We shall assume that the forward block function is nonlinear expresses as

$$e = f(e) = e^2; \text{ square law function}$$

When the feedback loop is open

$$e = r \Rightarrow c = r^2$$



You have either reached a page that is unavailable for viewing or reached your viewing limit for this book.



You have either reached a page that is unavailable for viewing or reached your viewing limit for this book.



You have either reached a page that is unavailable for viewing or reached your viewing limit for this book.

Subtracting eqn. (3.28) from eqn. (3.27), we have the describing equation in terms of the incremental values about the operating point as

$$2K_s^2 e_o R \Delta e = C(d\Delta\theta/dt) + (\Delta\theta - \Delta\theta_i)/R_t \quad \dots(3.29)$$

The incremental error is given by

$$\Delta e = \Delta e_r - \Delta e \quad \dots(3.30)$$

Now

$$\Delta e = K_t \Delta\theta \quad \dots(3.31)$$

K_t being the constant of the temperature sensor.

Taking the Laplace transform of eqns. (3.29), (3.30) and (3.31) and reorganizing we get

$$\Delta\theta(s) = \frac{K\Delta E(s)}{\tau s + 1} + \frac{\Delta\theta_i(s)}{\tau s + 1} \quad \dots(3.32)$$

$$\Delta E(s) = \Delta E_r(s) - \Delta E_i(s) \quad \dots(3.33)$$

$$\Delta E_i(s) = K_t \Delta\theta(s) \quad \dots(3.34)$$

where

$$K = 2K_s^2 e_o R R_t ; \tau = R_t C$$

From eqns. (3.32), (3.33) and (3.34) we can draw the block diagram of the system as shown in Fig. 3.12 where the open-loop transfer function is

$$G(s) = \frac{K}{\tau s + 1}$$

and $\Delta\theta_i(s)$ is the change in the temperature of the inflowing liquid which can be regarded as a disturbance input entering the system through $1/(\tau s + 1)$.

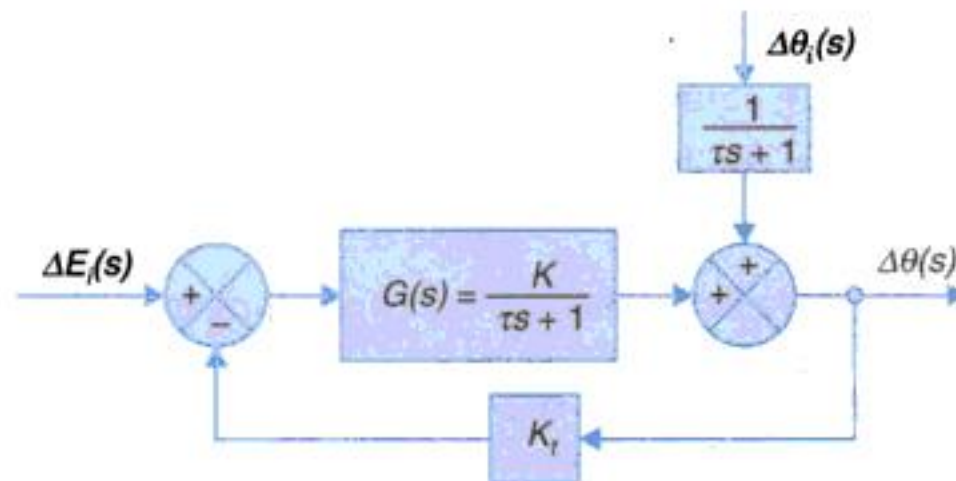


Fig. 3.12. Block diagram of the system shown in Fig. 3.9.

Assuming the disturbance signal $\Delta\theta_i$ to be zero, the steady change in the temperature of the outflowing liquid caused by an unwanted step change ΔE_r in the reference voltage is given by

$$\Delta\theta(t) = \lim_{s \rightarrow 0} s \left(\frac{\Delta E_r}{s} \right) \frac{K}{\tau s + 1 + KK_t} = \frac{\Delta E_r K}{1 + KK_t} \quad (\text{for closed-loop}) \quad \dots(3.35)$$

$$= \Delta E_r K \quad (\text{for open-loop ; } K_t = 0) \quad \dots(3.36)$$

It is easily observed from above that the steady change in the temperature of the outflowing liquid caused by an unwanted change in reference voltage is reduced by the factor $1/(1 + KK_t)$ in the closed-loop compared to the open-loop case.



You have either reached a page that is unavailable for viewing or reached your viewing limit for this book.



You have either reached a page that is unavailable for viewing or reached your viewing limit for this book.



You have either reached a page that is unavailable for viewing or reached your viewing limit for this book.

(c) Under vehicle stalled conditions:

Vehicle speed, tachometer output (feedback signal), input to engine-vehicle block are all = 0

$$\text{Hence} \quad AK_1 = K_g D \quad \text{or} \quad D = \frac{AK_1}{K_g} = \frac{60.8 \times 50}{100} = 30.4\%$$

(d) Steady vehicle speed on level road = 10 km/h

$$\text{Then} \quad A = 60.8 \times \frac{10}{60} = 10.133 \text{ km/h}$$

$$[(10.133 - 10) K_1 - (-D) K_g] K = 100$$

$$(6.65 + 100 D) \times 1.5 = 100 \quad \text{or} \quad D = 0.6\% \text{ (down)}$$

$$(e) \text{ As in part (c)} \quad AK_1 = K_g D \quad \text{or} \quad K_g/K_1 = A/D = \frac{60.4}{50} = 1.21$$

$$(f) \text{ Open-loop system} \quad R \times K_1 \times K = 60 \quad \text{or} \quad R = \frac{60}{50 \times 15} = 0.8 \text{ km/h}$$

$$\text{Closed-loop system} \quad R \times \frac{K_1 K}{1 + K_1 K} = 60 \quad \text{or} \quad R = 60.8 \text{ km/h}$$

$$(g) \text{ Open-loop system} \quad V(s) = \frac{K_1 K}{\tau s + 1} \cdot \frac{0.8}{s}$$

Taking inverse Laplace transform

$$v(f) = 0.8 K_1 K (1 - e^{-t/\tau}); \tau = 20s \text{ (given)} \\ = 60 (1 - e^{-t/20})$$

If 90% speed, $t = t_1$

$$0.9 = 1 - e^{-t_1/20} \quad \text{or} \quad t_1 = 46 \text{ s}$$

Closed-loop system

$$V(s) = \frac{K_1 K}{\tau s + 1 + K_1 K} \cdot \frac{60.8}{s} = \frac{60.8 K'}{s(\tau' s + 1)}$$

Taking the inverse Laplace transform

$$v(t) = 0.8 k' (1 - e^{-t/\tau'})$$

$$K' = \frac{K_1 K}{1 + K_1 K} = \frac{50 \times 15}{1 + 50 \times 15} = \frac{75}{76}$$

$$\tau' = \frac{\tau}{1 + K_1 K} = \frac{20}{76} = 0.263 \text{ s}$$

$$\text{Substituting value} \quad v(t) = 60 (1 - e^{-t/0.263})$$

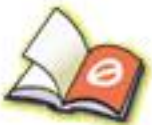
From which we get time at 90% speed as

$$t_1 = 0.6 \text{ s}$$

Remarks : Observe that the closed-loop system reaches 90% of steady state speed in 0.6s compared to the corresponding time 46s for the open-loop system *i.e.*, speeding up of dynamic response by a factor of $46/0.6 \approx 77$ times.



You have either reached a page that is unavailable for viewing or reached your viewing limit for this book.



You have either reached a page that is unavailable for viewing or reached your viewing limit for this book.



You have either reached a page that is unavailable for viewing or reached your viewing limit for this book.

Example 3.5 : Consider the speed control system of Fig. 3.17 wherein the inner loop corresponds to motor back emf. The controller is an integrator with gain k observe that the load is inertia only.

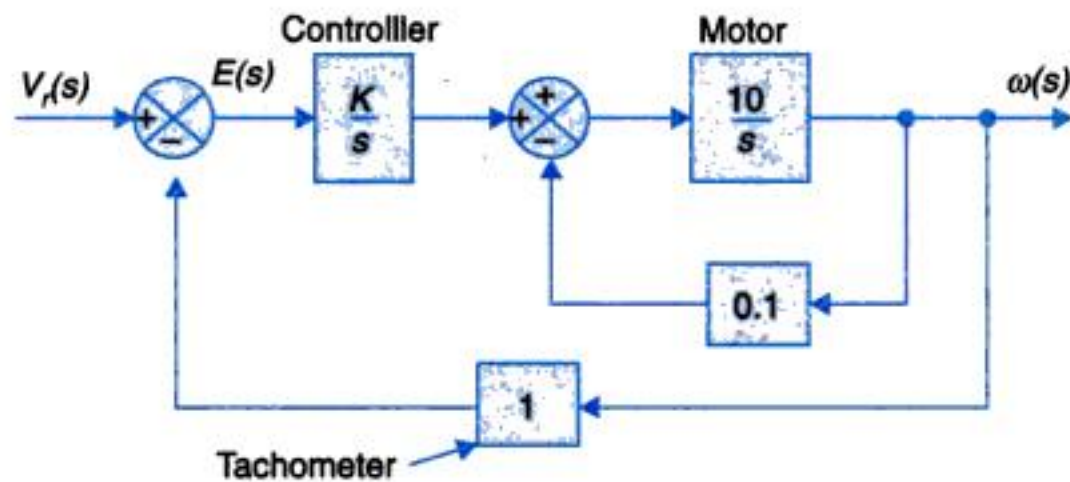


Fig. 3.17

- (a) Determine the value of K for which steady-state error to unit ramp input ($V_r(s) = 1/s^2$) is less than 0.01 rad/sec.
- (b) For the value of K found in part (a) determine, the sensitivity S_K^T , $T(s) = \omega(s)/V_r(s)$. What will be the limiting value of S_K^T at low frequencies ?

Solution. (a) Reducing the inner loop

$$G_{\text{mot}}(s) = \frac{10/s}{1 + 0.1 \times 10/s} = \frac{10}{s+1} \quad \dots(i)$$

From the forward path

$$\omega(s) = \left[\frac{10K}{s(s+1)} \right] E(s) \quad \dots(ii)$$

$$E(s) = V_r(s) - \omega(s) \quad \dots(iii)$$

$$E(s) = V_r(s) - \left[\frac{10K}{s(s+1)} \right] E(s)$$

or
$$E(s) = \left[\frac{s(s+1)}{s(s+1) + 10K} \right] V_r(s) \quad \dots(iv)$$

Input unit ramp, $V_r(s) = 1/s^2$. Then

$$E(s) = \frac{s(s+1)}{s(s+1) + 10K} \cdot \frac{1}{s^2} \quad \dots(v)$$

Steady-state error
$$e(ss) = \lim_{s \rightarrow 0} sE(s) = \lim_{s \rightarrow 0} \frac{(s+1)}{s(s+1) + 10K}$$

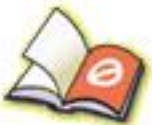
or
$$e(ss) = \frac{1}{10K} = 0.01$$

which gives $K = 10$

(b)
$$T(s) = \frac{\omega(s)}{V_r(s)} = \frac{\frac{10K}{s(s+1)}}{1 + \frac{10K}{s(s+1)}}$$



You have either reached a page that is unavailable for viewing or reached your viewing limit for this book.



You have either reached a page that is unavailable for viewing or reached your viewing limit for this book.



You have either reached a page that is unavailable for viewing or reached your viewing limit for this book.

Laplace transforming yields

$$Q_i(s) + Q_d(s) = \frac{(RCs + 1)}{R} H(s) \quad \dots(iv)$$

or
$$H(s) = \frac{R}{(RCs + 1)} [Q_i(s) + Q_d(s)] \quad \dots(v)$$

According to level sensing feedback controller

$$Q_i(s) = -G_c(s) H(s) ; \text{negative feedback} \quad \dots(vi)$$

From Eqs. (v) and (vi) the block diagram of Fig. 3.20 can be drawn.

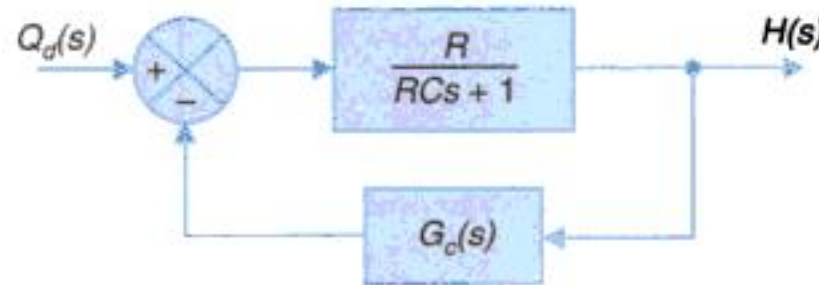


Fig. 3.21

(i) $G_c(s) = K$

From Fig. 3.20

$$\frac{H(s)}{Q_d(s)} = \frac{\frac{R}{RCs + 1}}{1 + \frac{KR}{RCs + 1}}$$

or
$$\frac{H(s)}{Q_d(s)} = \frac{R}{RCs + (1 + KR)} \quad \dots(vii)$$

For unit step $Q_d(s) = \frac{1}{s}$. Then

$$h_{ss} = \lim_{s \rightarrow 0} sH(s) = \lim_{s \rightarrow 0} \frac{sR}{s[RCs + (1 + KR)]}$$

or
$$h_{ss} = \frac{R}{1 + KR} \quad \dots(viii)$$

(ii) $G_c(s) = \frac{K}{s}$

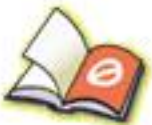
From Fig. 3.20

$$\frac{H(s)}{Q_d(s)} = \frac{Rs}{RCs + (1 + KR)}$$

For unit step disturbance $\theta_d(s) = \frac{1}{s}$ (ix)

$$h_{ss} = \lim_{s \rightarrow 0} sH(s) = \lim_{s \rightarrow 0} \frac{s \times sR}{s[RCs + (1 + KR)]}$$

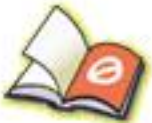
or
$$h_{ss} = 0 \quad \dots(x)$$



You have either reached a page that is unavailable for viewing or reached your viewing limit for this book.



You have either reached a page that is unavailable for viewing or reached your viewing limit for this book.



You have either reached a page that is unavailable for viewing or reached your viewing limit for this book.

- 3.7. The field of a d.c. servomotor is separately excited by means of a d.c. amplifier of gain $K_A = 90$ (see Fig. P-3.7). The field has an inductance of 2 henrys and a resistance of 50 ohms. Calculate the effective field time constant.

A voltage proportional to the field current is now fed back negatively to the amplifier input. Determine the value of the feedback constant K to reduce the field time constant to 4 milliseconds.

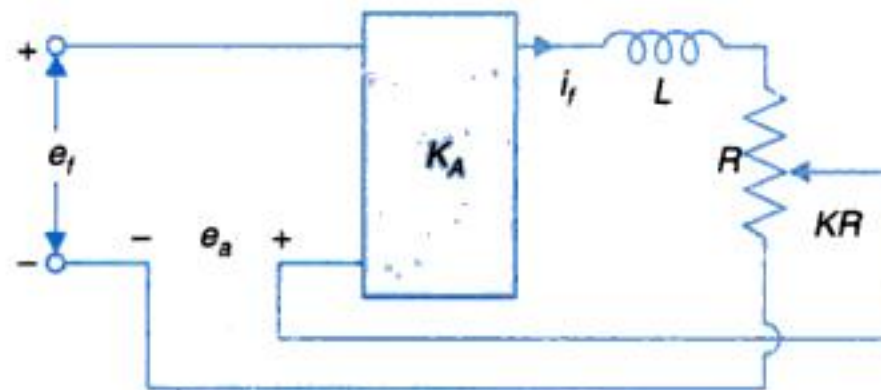


Fig. P-3.7

- 3.8. For the speed control system shown in Fig. P-3.8 assume that
- the reference and feedback tachometer are identical;
 - generator field time constant is negligible and its generated voltage is K_g^g volts/amp;
 - friction of motor and mechanical load is negligible.
- Find the time variation of output speed (ω_o) for a sudden reference input of 10 rad/sec. Find also the steady-state output speed.
 - If the feedback loop is opened and gain K_A adjusted to give the same steady-state speed as in the case of the closed-loop, determine how the output speed varies with time and compare the speed of response in the two cases (closed- and open-loop).
 - Compare the sensitivity of ω_o to changes in amplifier gain K_A and generator speed ω_g , with and without feedback.

[Hint : The generator gain constant K_g changes in direct proportion to generator speed *i.e.*, $K_g = K_g' \omega_g$ where K_g' is constant.]

The system constants are given below:

Moment of inertia of motor and load

$$J = 5 \text{ kg-m}^2$$

Motor back emf constant

$$K_t = 5 \text{ volts per rad/sec}$$

Total armature resistance of motor and generator

$$R_a = 1 \text{ ohm}$$

Generator gain constant

$$K_g = 50 \text{ volts/amp}$$

Amplifier gain

$$K_A = 5 \text{ amps/volt}$$

Tachometer constant

$$K_t = 0.5 \text{ volts per rad/sec}$$

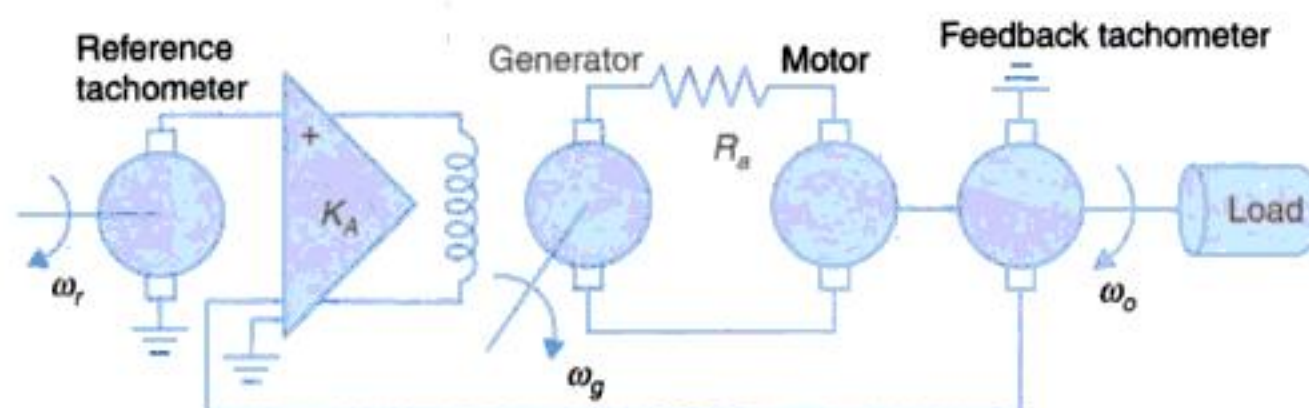
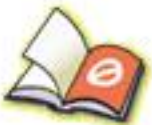


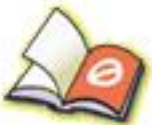
Fig. P-3.8



You have either reached a page that is unavailable for viewing or reached your viewing limit for this book.



You have either reached a page that is unavailable for viewing or reached your viewing limit for this book.



You have either reached a page that is unavailable for viewing or reached your viewing limit for this book.

3.13. For the system whose signal flow graph is drawn in Fig. P-3.13

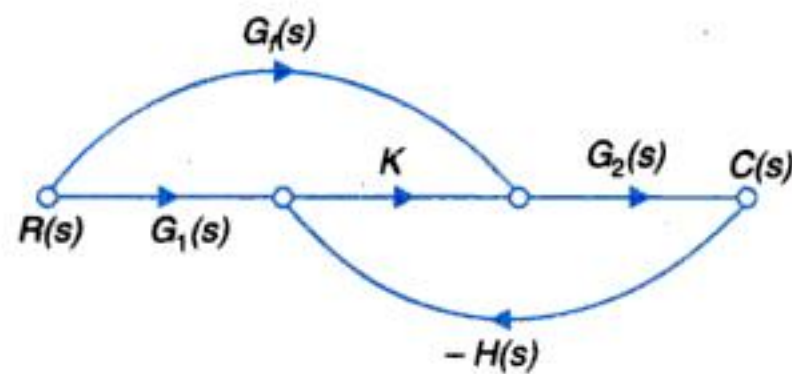


Fig. P-3.13

Find the transfer function $T(s) = C(s)/R(s)$

Find the system sensitivity S_K^T using eqn. (3.7a)

3.14 Fig. P-3.14 shows the block diagram of a speed control system with an integrator (K/s) in the forward path for a desired speed of 100 rad/s, show that steady output speed will be 100 rad/s (indicative of zero steady state error).

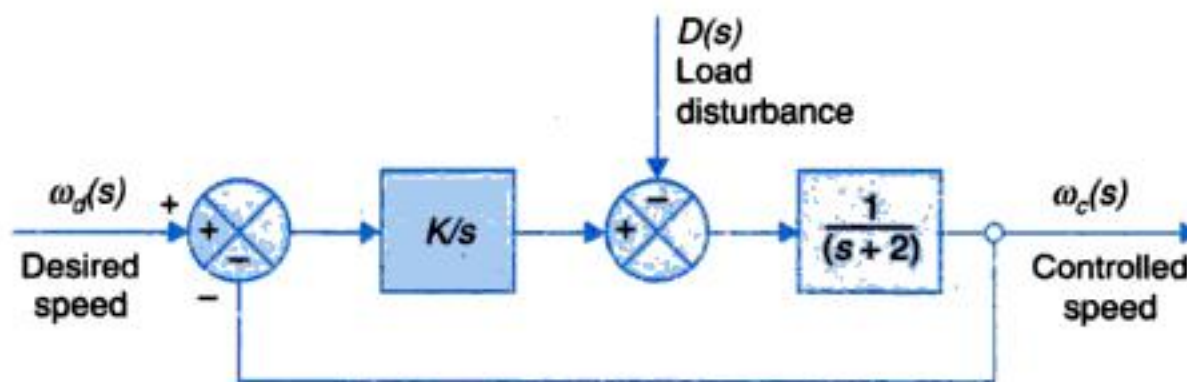


Fig. P-3.14

For a unit load disturbance $D(s) = 1/s$ find the s -domain expression for change in controlled speed, $\omega_c^D(s)$. Find the change in speed, caused by the disturbance at $t = 0$ and $t = \infty$ (steady state change).

Find the expression for $\omega_c^D(t)$ for $K = 0.5, 1, 2$ and 4 . Sketch the nature of response. Which value of K should be preferred and why? You may use Table 1.3 (Appendix 1) for finding Laplace inverse.

3.15 In a radar system, an electromagnetic pulse is radiated from an antenna into space. An echo pulse is received back if a conducting surface such as an airplane appears in the path of the signal. When the radar is in search of target, the antenna is continuously rotated. When target is located, the antenna is stopped and pointed towards the target by varying its angular direction until a maximum echo is heard. If energy is radiated in a narrow directional beam, accurate information about target location can be obtained. Narrow beam can be realised if the antenna size is large (e.g., 20 m diameter). To drive this size of antenna, hydraulic or electric motors are used. One of the schemes utilizing electric motor is depicted in Fig. P-3.15. Determine:

(a) Sensitivity to changes in SCR gain, K_s for $\omega = 0.1$.

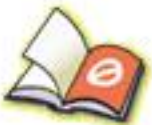
(b) The steady-state error of motor shaft, i.e., $(\theta_R - \theta_M)$ when antenna is subjected to a constant wind gust torque of 100 newton-m.



You have either reached a page that is unavailable for viewing or reached your viewing limit for this book.



You have either reached a page that is unavailable for viewing or reached your viewing limit for this book.



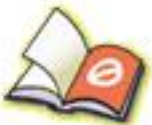
You have either reached a page that is unavailable for viewing or reached your viewing limit for this book.

4

CONTROL SYSTEMS AND COMPONENTS



You have either reached a page that is unavailable for viewing or reached your viewing limit for this book.



You have either reached a page that is unavailable for viewing or reached your viewing limit for this book.



You have either reached a page that is unavailable for viewing or reached your viewing limit for this book.

process (plant), turn a robot link w.r.t. to its neighbouring link, move a transformer tap (up or down), move up/down the control rods of a nuclear reactor etc.

Because of the flexibility inherent in transmitting electrical power (through cables) and desirable speed-torque characteristics which are linear, electric actuators (motors) are now widely adopted in control systems except in low speed but high torque applications where hydraulic actuators are still in use. Pneumatic actuators are not as messy as hydraulic ones but suffer from leakages and inherent inaccuracies.

4. *Electric system.* DC and ac motors are the two kinds of electric actuators; in low power ratings these are known as servomotors. DC motors are costlier than ac motors because of the additional cost of commutation gear. These have, however, the important advantages of linearity of characteristics and higher **stalled torque/inertia** ratio; this being an important figure of merit for a servomotor. Stalled torque is the torque developed by motor when stationary with full applied voltage (and full field in case of a DC motor). It may be pointed out here that high torque/inertia ratio means lower motor time constant and so faster dynamic response.

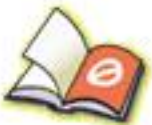
With advanced manufacturing techniques, low brush commutator friction and still higher torque/inertia ratios have been achieved in dc servomotors, such that these have practically taken over from ac servomotors in most control applications.

Electric actuators for stepped motion are known as stepper motors which will be dealt in details in section 4.

DC Servomotors

Modelling of dc motors, armature controlled and field controlled, has been considered at length in Chapter 2. Here we shall consider some of the constructional features of dc servomotors. With recent development in rare earth permanent magnets (PM) which have high residual flux density and a very high coercivity, dc servomotors are now constructed with PMs resulting in much higher torque/inertia ratio and also higher operating efficiency as these motor have no field losses. The speed of a permanent magnet dc (PMDC) motor is nearly directly proportional to armature voltage at a given load torque. Also the speed-torque characteristic at a given voltage is more flat than in a wound field motor as the effect of armature reaction is less pronounced in a PM motor.

Three types of constructions employed in PMDC servomotors are illustrated in Fig. 4.3 (a), (b) and (c). In Fig. 4.3 (a) the armature is slotted with dc winding placed inside these slots (as in a normal dc motor). Though quite reliable and rugged this type of construction has high inertia to reduce which the construction of Fig. 4.3 (b) is adopted where the winding is placed on the armature surface. Because of the larger air gap, stronger PMs are needed in this construction. A much lower inertia is achieved by placing the winding on a nonmagnetic cylinder which rotates in annular space between the PM stator and stationary rotor as illustrated in Fig. 4.3 (c). The air gap has to be still larger with consequent need of much stronger PMs. The constructional details of this low inertia motor are further brought out in Fig. 4.3 (d).



You have either reached a page that is unavailable for viewing or reached your viewing limit for this book.



You have either reached a page that is unavailable for viewing or reached your viewing limit for this book.



You have either reached a page that is unavailable for viewing or reached your viewing limit for this book.

1. The rotor of the servomotor is built with high resistance so that its X/R ratio is small and the torque-speed characteristic, as shown by the curve b of Fig. 4.7, is nearly linear in contrast to the highly nonlinear characteristic when large X/R ratio is used for servo applications, then because of the positive slope for part of the characteristic, the system using such a motor becomes unstable.

The rotor construction is usually squirrel cage or drag-cup type. The diameter of the rotor is kept small in order to reduce inertia and thus to obtain good accelerating characteristics. Drag-cup construction is used for very low inertia applications.

2. In servo applications, the voltages applied to the two stator windings are seldom balanced. As shown in Fig. 4.8, one of the phases known as the *reference phase* is excited by a constant voltage and the other phase, known as the *control phase* is energized by a voltage which is 90° out of phase with respect to the voltage of the reference phase. The control phase voltage is supplied from a servo amplifier and it has a variable magnitude and polarity ($\pm 90^\circ$ phase angle with respect to the reference phase). The direction of rotation of the motor reverses as the polarity of the control phase signal changes sign.

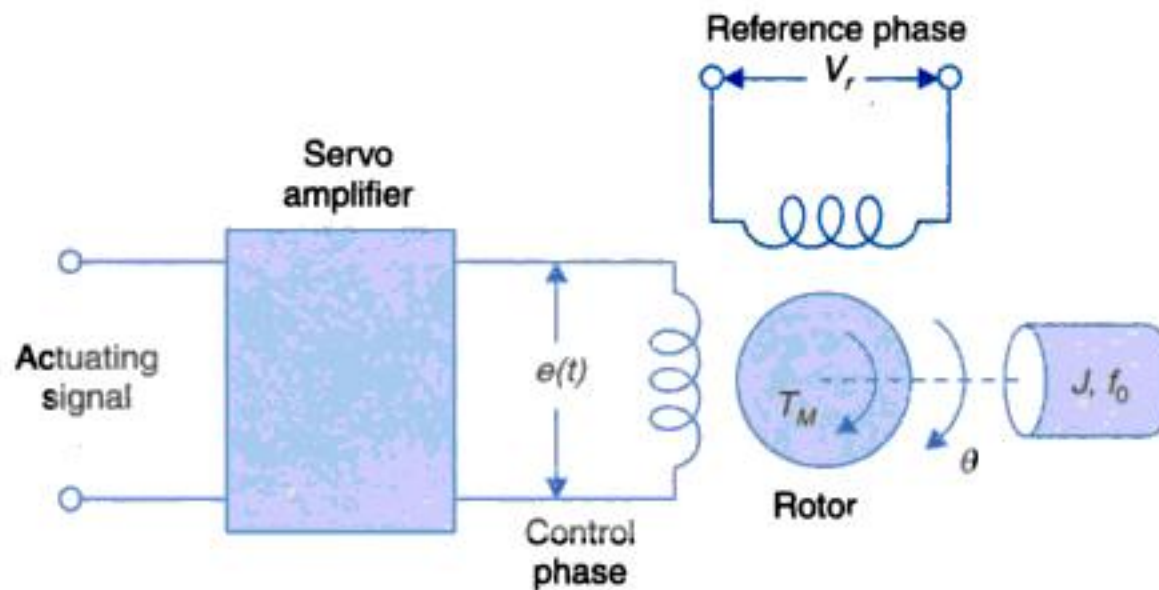


Fig. 4.8. Schematic diagram of a two-phase servomotor.

It can be proved using symmetrical components that starting torque of servomotor under unbalanced operation, is proportional to E , the rms value of the sinusoidal control voltage $e(t)$. A family of torque-speed curves with variable rms control voltage is shown in Fig. 4.9 (a). All these curves have negative slope. Note that the curve for zero control voltage goes through the origin and the motor develops a decelerating torque.

As seen from Fig. 4.9 (a), the torque-speed curves are still somewhat nonlinear. However, in the low-speed region, the curves are nearly linear and equidistant, *i.e.*, the torque varies linearly with speed as well as with control voltage. Since a servomotor seldom operates at high speeds, these curves can be linearized about the operating point.

The torque generated by the motor is a function of both the speed $\dot{\theta}$ and rms control voltage E , *i.e.*, $T_M = f(\dot{\theta}, E)$. Expanding this equation into Taylor's series about the normal operating point $(T_{M_0}, E_0, \dot{\theta}_0)$ and dropping off the terms of second- and higher-order derivatives, we get



You have either reached a page that is unavailable for viewing or reached your viewing limit for this book.



You have either reached a page that is unavailable for viewing or reached your viewing limit for this book.



You have either reached a page that is unavailable for viewing or reached your viewing limit for this book.

terminal (w.r.t. one of the fixed terminals (the ground)) is proportional to displacement. This linear relationship is affected by the magnitude of the load resistance. The load resistance in fact is the input resistance of the device (usually amplifier) to which the potentiometer output is connected.

With reference to Fig. 4.11

R_p = total potentiometer resistance

x_t = total displacement of the potential over which R_p is spread out (uniformly)

x_i = displacement of the jockey from the ground terminal G (input)

R_L = load resistance

V_{REF} = reference voltage

V_o = output voltage (V_{MG})

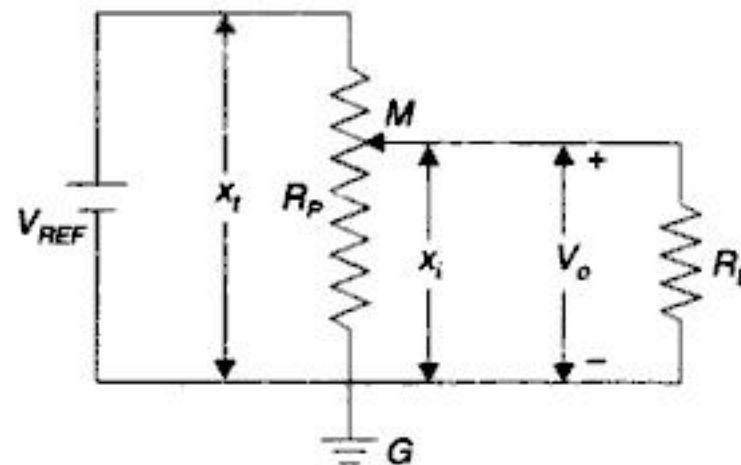


Fig. 4.11. A potentiometer with load.

As the resistance is spread out uniformly

$$R_i = (x_i/x_t)R_p$$

$$R_{eq} = R_i \parallel R_L = \frac{1}{\left[\frac{1}{R_L} + \left(\frac{x_t}{x_i} \right) \frac{1}{R_p} \right]}$$

Then by voltage dividing action

$$V_o = V_{REF} \frac{R_{eq}}{R_{eq} + (R_p - R_i)}$$

Substituting values and manipulating it is easily established that

$$V_o = \frac{V_{REF}}{(x_t/x_i) + (R_p/R_L)[1 - (x_i/x_t)]} \quad \dots(4.10)$$

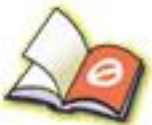
If $R_L =$ (jockey open *i.e.*, no load)

$$V_o = V_{REF} (x_i/x_t); \text{ a linear relationship} \quad \dots(4.11)$$

Finite value of R_L causes the output voltage to be nonlinear function of (x_i/x_t) (Eq. (4.10)). This relationship is plotted as V_o/V_{REF} vs x_i/x_t in Fig. 4.12. The figure also shows the actual relationship without loading which can vary above or below the ideal case because of manufacturing tolerances. Potentiometer linearity is defined later with reference to this.



You have either reached a page that is unavailable for viewing or reached your viewing limit for this book.



You have either reached a page that is unavailable for viewing or reached your viewing limit for this book.



You have either reached a page that is unavailable for viewing or reached your viewing limit for this book.

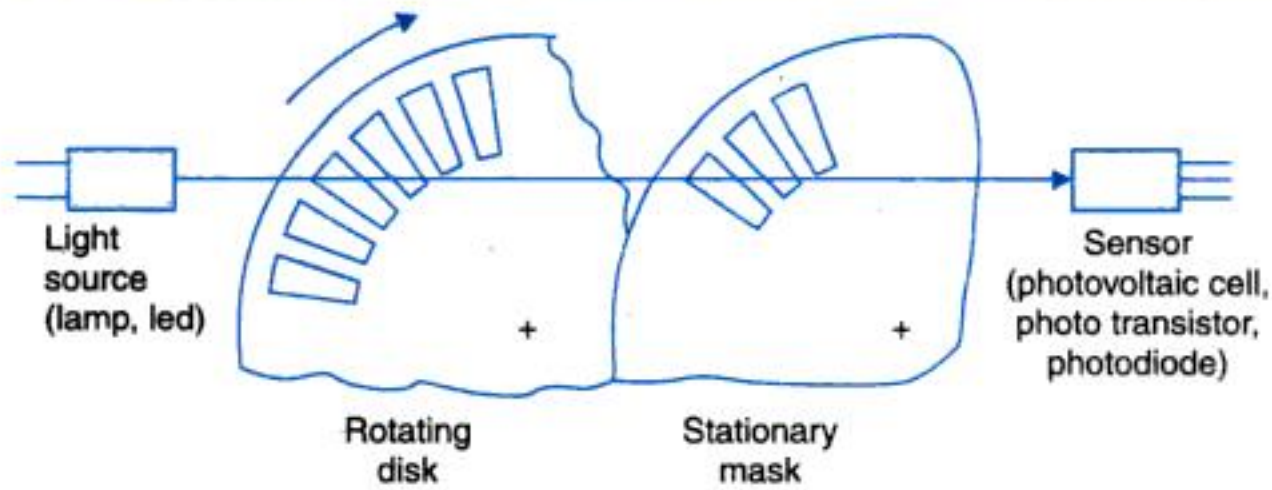


Fig. 4.14. Typical incremental optomechanics.

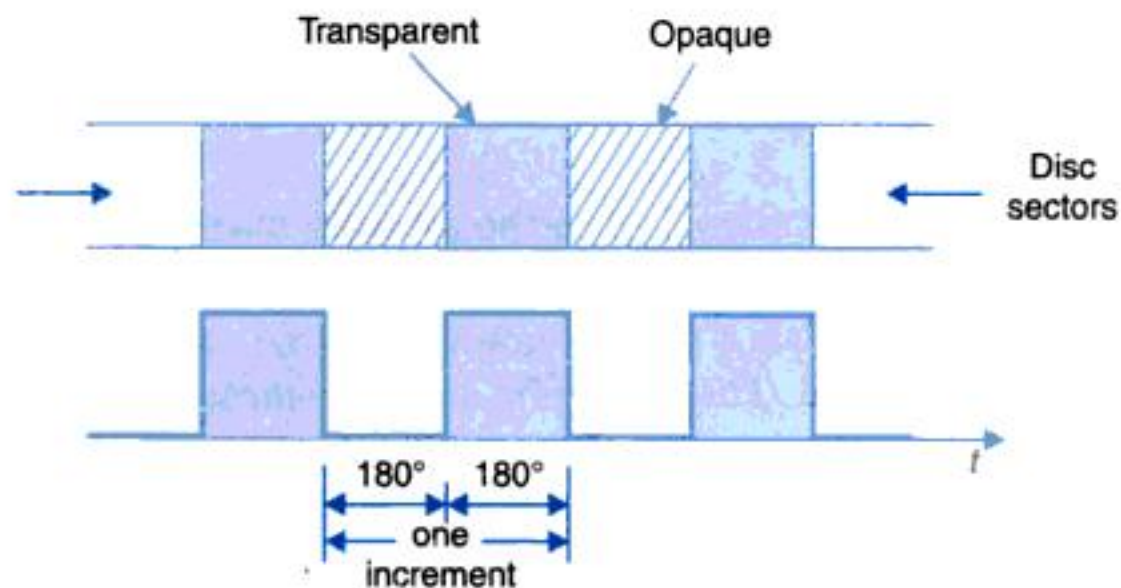
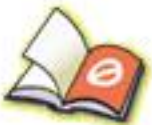


Fig. 4.15

In a dual channel encoder two optoelectronic channels are employed. These are installed on the same rotating disc and the mask but displaced at 90° to each other such that the two pulse output signals have a relative time phase displacement of 90° as shown in Fig. 4.16. The output of channel 2 is called the quadrature output. A circuit that senses the relative time phase of the outputs of the two channels determines the direction of rotation of the disc or the encoder shaft.

Considerable improvement in resolution of the encoder with two channels is achieved by processing these outputs by means of a digital circuit which generates a short duration pulse (impulse) at each change of state. Reader can easily imagine that this can be done by differentiating the signals and reversing the polarity of the negative impulses. The processed output is also shown in Fig. 4.16. It is easy to observe that there are now four impulses/disc increment so that the basic resolution becomes $(360^\circ/4N)$ *i.e.*, an improvement by a factor 4.

The output of the encoder is fed to a counter which counts the number of pulses; the count being a measure of angle (or translation) through which the encoder shaft has rotated. By sampling the counter at regular intervals by means of clock pulses it is possible to compute the speed of the encoder shaft.



You have either reached a page that is unavailable for viewing or reached your viewing limit for this book.



You have either reached a page that is unavailable for viewing or reached your viewing limit for this book.



You have either reached a page that is unavailable for viewing or reached your viewing limit for this book.

angular separation of $\phi = (90^\circ - \theta + \alpha)$ between the two rotors. From eqn. (4.18), the voltage at the rotor terminals of the control transformer is then

$$e(t) = K V_r \sin(\theta - \alpha) \sin \omega_c t \quad \dots(4.19)$$

For small angular displacement between the two rotor positions,

$$e(t) = K V_r (\theta - \alpha) \sin \omega_c t \quad \dots(4.20)$$

The synchro transmitter-control transformer pair thus acts as an error detector giving a voltage signal at the rotor terminals of the control transformer proportional to the angular difference between the transmitter and control transformer shaft positions. Equation (4.20), though derived for constant $(\theta - \alpha)$, is valid for varying conditions as well, so long as the rate of angle change is small enough for the speed voltages induced in the device to be negligible.

Equation (4.20) is represented graphically in Fig. (4.20) for an arbitrary time variation of $(\theta - \alpha)$.

We see from this diagram that the output of synchro error detector is a modulated signal, the modulating wave has the information regarding the lack of correspondence between the two rotor positions and the carrier wave is the ac input to the rotor of the synchro transmitter. This type of modulation is known as *suppressed-carrier modulation*. From eqn. (4.20) the modulating signal representing the discrepancy between the two shaft positions is

$$e_m(t) = K_s (\theta - \alpha) \quad \dots(4.21)$$

where K_s is known as *sensitivity* of error detector and has the units of volts (rms)/rad angular difference of the shafts of the synchro pair.

As pointed out earlier the rotor of the control transformer is made cylindrical in shape so that the air gap is practically uniform. This is essential for a control transformer, since its rotor terminals are usually connected to an amplifier, therefore the change in the rotor output impedance with rotation of the shaft must be minimized. Another distinguishing feature is that the stator winding of the control transformer has a higher impedance per phase. This feature permits several control transformers to be fed from a single transmitter.

A.C. Position Control System

Consider the system shown in Fig. 4.21 in which the position of the mechanical load is controlled in accordance with the position of the reference shaft. This system employs ac components and all the signals other than the input and output shaft positions are suppressed-carrier modulated signals. Such systems are known as *carrier control systems* and are designed so that the signal cut-off frequency is much less than the carrier frequency. It is then sufficiently accurate to analyze these systems on the basis of modulating signals only.

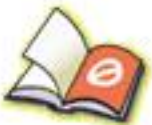
The components used in this system are: synchro transmitter-control transformer pair as error detector; ac amplifier for signals amplification; ac servomotor to drive the load shaft through a gearing; ac tachometer for providing rate feedback. The servomotor for proper operation has to be provided with carrier voltages on the two phases 90° out of phase with respect to each other. This is achieved easily by exciting the reference motor phase and the synchro transmitter rotor coil directly from the carrier supply, while the carrier voltage driving



You have either reached a page that is unavailable for viewing or reached your viewing limit for this book.



You have either reached a page that is unavailable for viewing or reached your viewing limit for this book.



You have either reached a page that is unavailable for viewing or reached your viewing limit for this book.

There are two advantages in using stepper motors. One is their compatibility with digital systems and secondly no sensors are needed for position and speed sensing as these are directly obtained by counting input pulses and periodic counting if speed information is needed. Stepper motors have a wide range of applications: paper feed motors in typewriters and printer, positioning of print heads, pens in XY-plotters, recording heads in computer disk drives and in positioning of work tables and tools in numerically controlled machining equipment. The range of applications of these motors is increasing as these motors are becoming available in larger power ratings and with reducing cost.

Elementary operation of a four phase stepper motor with a two-pole PM rotor can be illustrated through the diagram of Fig. 4.23. Let us assume that the rotor is permanent magnet excited. Such a rotor aligns with the axis of the stator field with torque being proportion to the $\sin \theta$, θ being the angle of displacement between the rotor axis and stator field axis. The torque-angle characteristics is drawn in Fig. 4.24 (a) which phase 'a' excited and also with phase b excited. The rotor thus assumes positions $\theta = 0^\circ, 45^\circ, 90^\circ$ as phases a, a + b, b, are excited. It is easily observed that the stable position of the rotor corresponds to that angle at which the torque is zero and is positive for smaller angles and negative for larger angles. Thus with phase 'a' excited the stable (or locked) position is $\theta = 0^\circ$ but not $\theta = 180^\circ$ (unstable) and the torque has a maximum value at $\theta = 90^\circ$. It is therefore easily concluded that each excitation pattern of phases corresponds to a unique position of the rotor. Patterns for phase windings excitations can be easily visualized for steps of $22.5^\circ, 11.25^\circ$. Another feature of a PM stepper motor is that when excited it seeks a preferred position offers advantage in certain application.

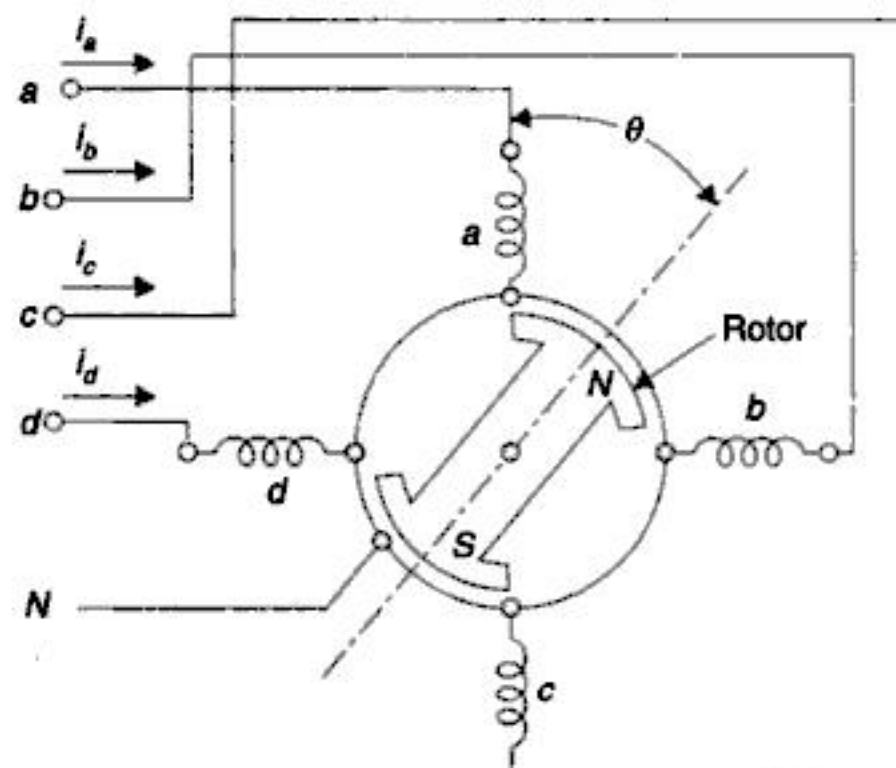
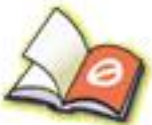


Fig. 4.23. A 4-phase 2-pole stepper motor-elementary diagram.

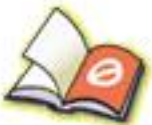
Consider now that the rotor (projecting pole) is made of just ferromagnetic material (no permanent magnets). The device now behaves as a variable-reluctance motor. The ferromagnetic rotor seeks the position in which it presents minimum reluctance to the stator field *i.e.*, the rotor axis aligns itself to the stator field axis. In Fig. 4.24 with phase 'a' excited this happens at $\theta = 0^\circ$ as well as $\theta = 180^\circ$ in which positions the torque on the rotor is zero. At $\theta = 90^\circ$ the rotor



You have either reached a page that is unavailable for viewing or reached your viewing limit for this book.



You have either reached a page that is unavailable for viewing or reached your viewing limit for this book.



You have either reached a page that is unavailable for viewing or reached your viewing limit for this book.

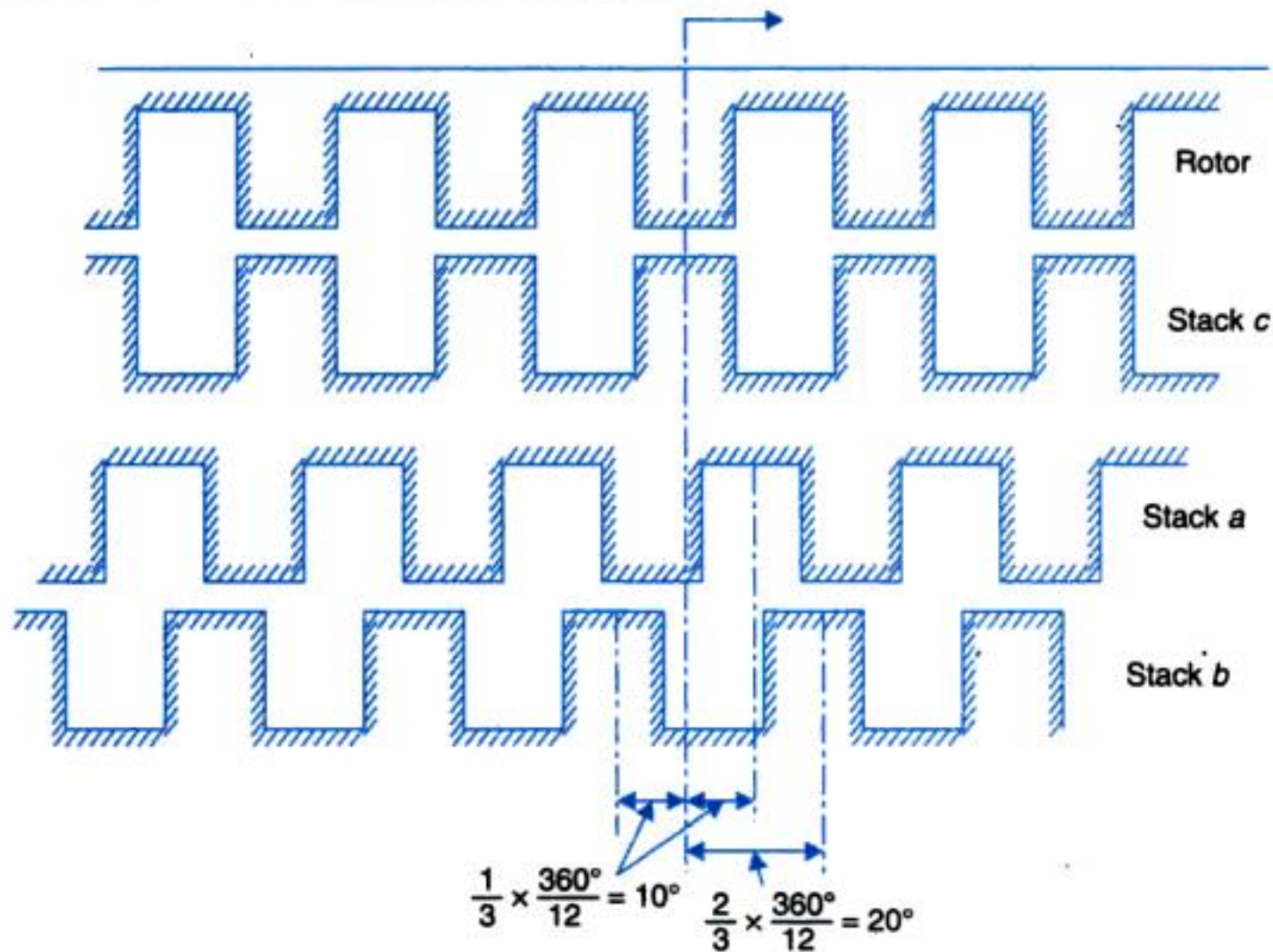


Fig. 4.29. Developed view of rotor and stator stacks of a 3-stack stepper motor.

Permanent-magnet Motor

Figure 4.30 shows the phases (stacks) of a 2 phase, 4-pole permanent-magnet stepper motor. The rotor is made of ferrite or rare earth material which is permanently magnetized. The stator

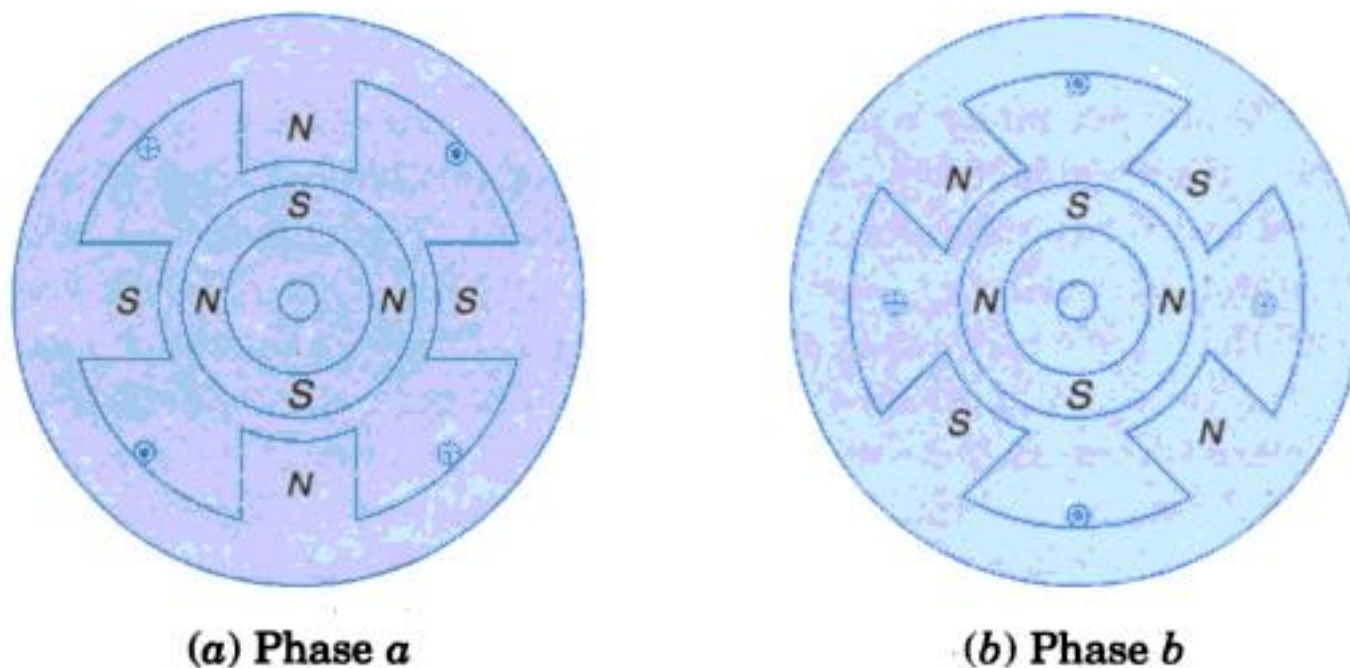
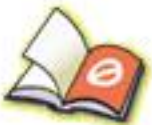


Fig. 4.30. Permanent-magnet stepper motor.

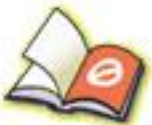
stack of phase *b* is staggered from that of phase *a* by an angle of 90° . When the phase *a* is excited, the rotor is aligned as shown in Fig. 4.30 (a). If now the phase *b* is also excited, the effective stator poles shift counter-clockwise by $22\frac{1}{2}^\circ$ [Fig. 4.30 (b)] causing the rotor to move accordingly. If the phase *a* is now de-energized (with *b* still energized), the rotor will move



You have either reached a page that is unavailable for viewing or reached your viewing limit for this book.



You have either reached a page that is unavailable for viewing or reached your viewing limit for this book.



You have either reached a page that is unavailable for viewing or reached your viewing limit for this book.

Since stepper motors are essentially digital actuators, there is no need to use digital-to-analog and analog-to-digital converters in constructing digital control systems (refer Chapter 11).

4.5 HYDRAULIC SYSTEMS

Hydraulically operated components are frequently used in hydraulic feedback systems and in combined electromechanical-hydraulic systems. In these elements, power is transmitted through the action of fluid flow under pressure. The fluid used is relatively incompressible such as petroleum-base oils or certain non-inflammable synthetic fluids.

The main advantage of the hydraulic systems lies in the hydraulic motor which can be made much smaller in physical size than an electric motor for the same power output. In addition to this, hydraulic components are rapid acting and more rugged compared to the corresponding electrical components. On the other hand, hydraulic systems have the inherent problems of leak and of sealing them against foreign particles, operating noise and the tendency to become sluggish at low temperatures because of increase viscosity of the fluid. Furthermore, hydraulic lines are not as flexible as electric cables.

Common hydraulic control applications are power steering and brakes in automobiles, the steering mechanisms of large ships, the control of large machine tools, etc.

The hydraulic output devices used in control systems are generally of two types—those intended to produce rotatory motion and those whose output is translational. The first type of devices are known as hydraulic motors and the second ones are known as hydraulic linear actuators.

Some of the important hydraulic components are discussed in this section.

Hydraulic Pumps and Motors

A device frequently used in control systems giving large output torque and short response time is the *hydraulic transmission* shown in Fig. 4.36. It consists of a variable stroke hydraulic

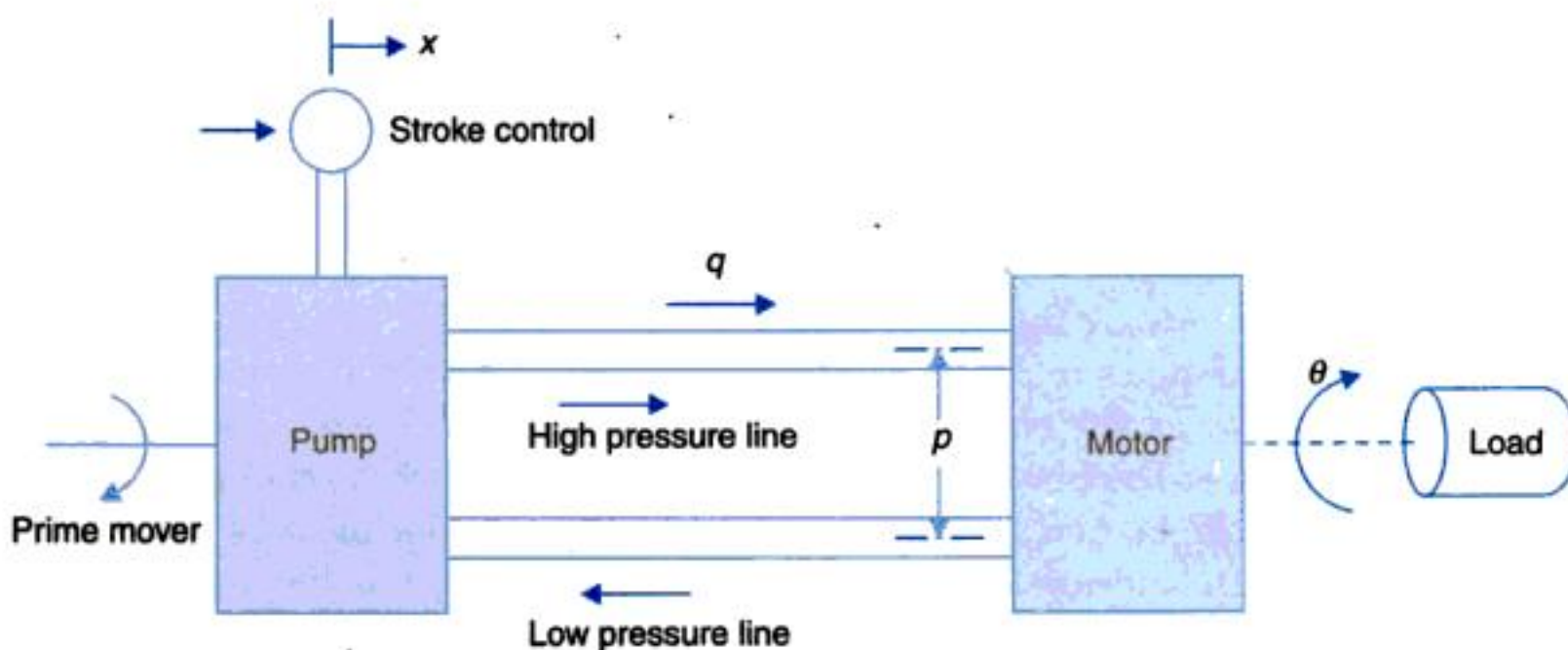


Fig. 4.36. Hydraulic transmission.



You have either reached a page that is unavailable for viewing or reached your viewing limit for this book.



You have either reached a page that is unavailable for viewing or reached your viewing limit for this book.



You have either reached a page that is unavailable for viewing or reached your viewing limit for this book.

Hydraulic Valves

In place of the variable displacement pump, one frequently used device is a constant pressure source and a valve to control the flow of oil to the hydraulic motor. This system has the advantage that the movable parts of the valve can be made much lighter than those of the stroke control mechanism in the pump, as a result of which, the time constants are reduced and the system becomes fast acting. The disadvantage of this system is that the valve has nonlinear characteristics and introduces problems of its own.

Figure 4.38 shows a three-way spool valve controlling the oil flow to the hydraulic motor. When the spool is in the neutral position ($x = 0$), the oil flow is blocked completely. As the spool is moved downwards (x positive), the upper pipe line to the motor gets connected to the high pressure source and the lower pipe line to the sump causing the motor to rotate in a particular direction. If the spool is moved upward (x negative) the lower pipe line to the motor gets connected to the high pressure source and the upper pipe line to the sump. The direction of oil flow in the motor and hence direction of its rotation is reversed.

Because turbulent flow exists at a sharp-edged orifice such as a valve, the flow equation is (refer section 2.2)

$$q_1 = Kx\sqrt{P_0 - P_1}; x > 0$$

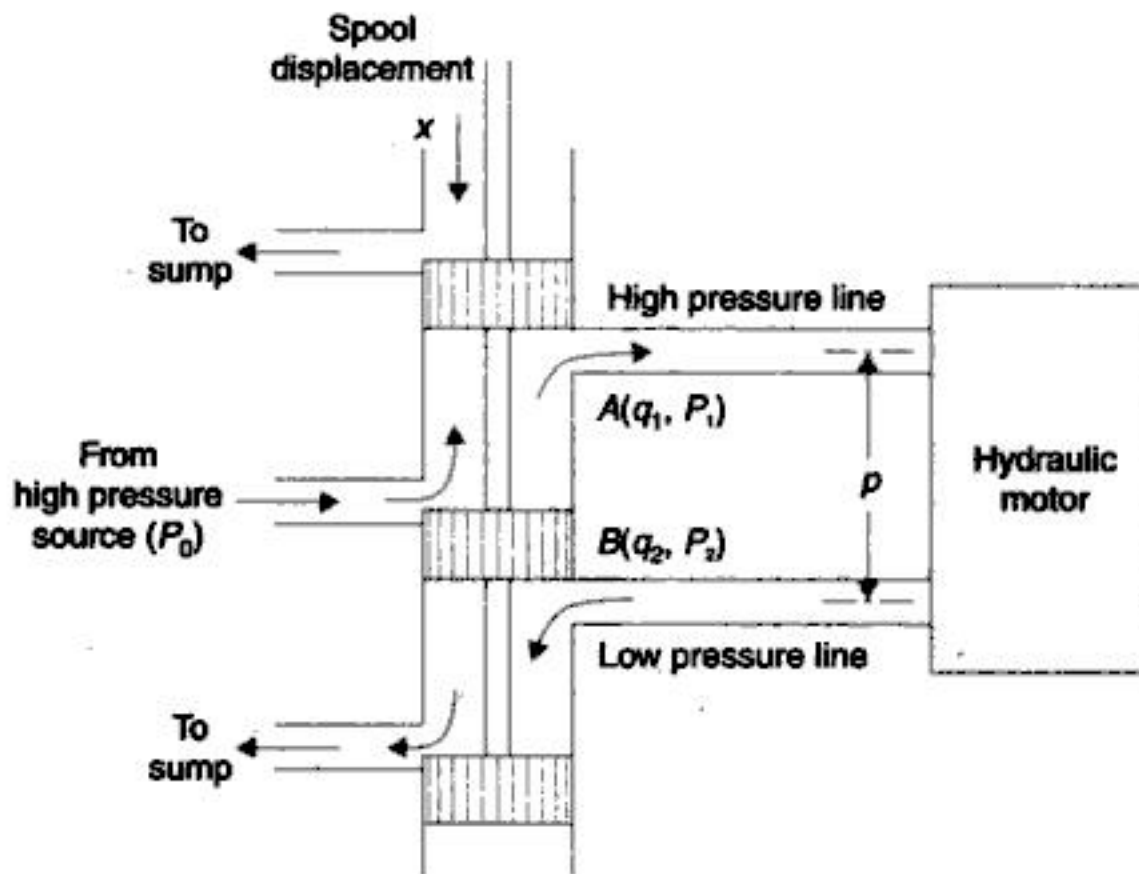


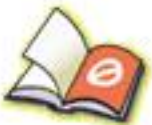
Fig. 4.38. Hydraulic valve.

where q_1 is the rate of flow through port A and K is flow coefficient which is a function of valve and fluid properties.

In addition, it follows that

$$q_2 = Kx\sqrt{P_2}; x > 0$$

where q_2 is the flow rate at port B.



You have either reached a page that is unavailable for viewing or reached your viewing limit for this book.



You have either reached a page that is unavailable for viewing or reached your viewing limit for this book.



You have either reached a page that is unavailable for viewing or reached your viewing limit for this book.

Substituting the various flow rates in eqn. (4.45) we have

$$q = K_1x - K_2p = K_p \frac{dy}{dt} + K_l p + K_c \frac{dp}{dt}$$

or
$$K_p \frac{dy}{dt} + K_c \frac{dp}{dt} + (K_l + K_2)p = K_1x \quad \dots(4.49)$$

The differential equation governing the load remains the same as in eqn. (4.43). Substituting for p from eqn. (4.43) in (4.49), we obtain

$$\frac{KM}{A} \ddot{y} + \left[\frac{K_c f}{A} + (K_l + K_2) \frac{M}{A} \right] \dot{y} + \left[K_p + (K_l + K_2) \frac{f}{A} \right] y = K_1 x$$

From the above equation, the transfer function of the system is

$$\frac{Y(s)}{X(s)} = \frac{K_l}{s \left[\frac{K_c M}{A} s^2 + \left\{ \frac{K_c f}{A} + (K_l + K_2) \frac{M}{A} \right\} s + \left\{ K_p + (K_l + K_2) \frac{f}{A} \right\} \right]}$$

As previously stated, K_c is very small, therefore $K_c M/A$ and $K_c f/A$ can be neglected. The transfer function then reduces to

$$\frac{Y(s)}{X(s)} = \frac{K}{s(\tau s + 1)} \quad \dots(4.50)$$

where
$$K = \frac{K_l}{K_p + (K_l + K_2) f / A}; \quad \tau = \frac{(K_l + K_2) M / A}{K_p + (K_l + K_2) f / A}$$

With $K_l = 0$ and $K_p = A$, this transfer function reduces to the simplified case transfer function given in eqn. (4.44)

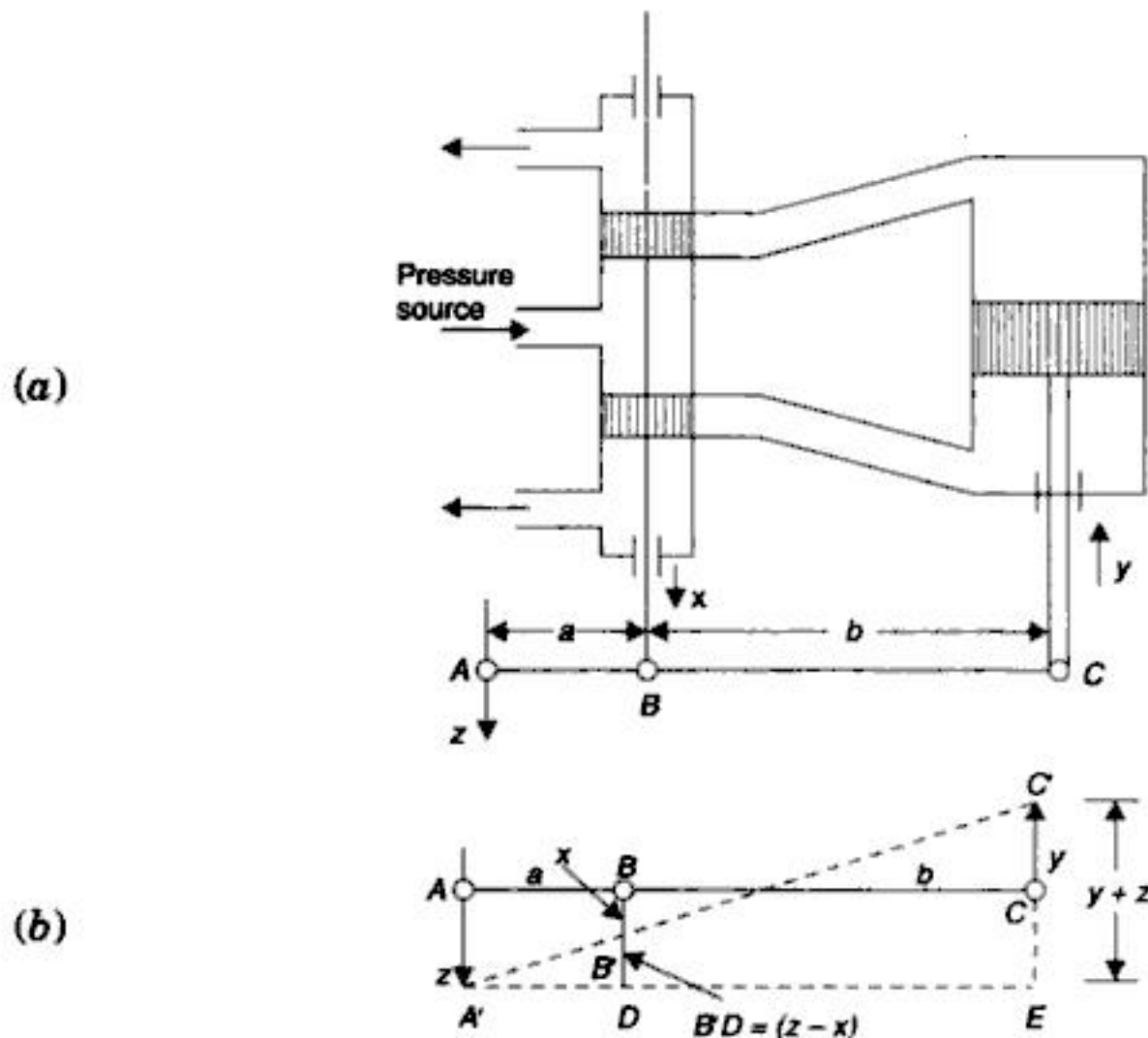


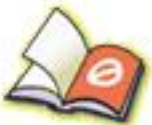
Fig. 4.42. Hydraulic actuator with negative feedback.



You have either reached a page that is unavailable for viewing or reached your viewing limit for this book.



You have either reached a page that is unavailable for viewing or reached your viewing limit for this book.



You have either reached a page that is unavailable for viewing or reached your viewing limit for this book.

Solution. It can be easily shown that

$$x = \left(\frac{a_2}{a_1 + a_2} \right) e - \left(\frac{a_1}{a_1 + a_2} \right) z \quad \dots(i)$$

and

$$w = \left(\frac{a_3}{a_2 + a_3} \right) e + \left(\frac{a_1 + a_2 + a_3}{a_2 + a_3} \right) z \quad \dots(ii)$$

For the actuator $z = K \int x dt \quad \dots(iii)$

The block diagram with transfer functions indicated therein is drawn in Fig. 4.48.

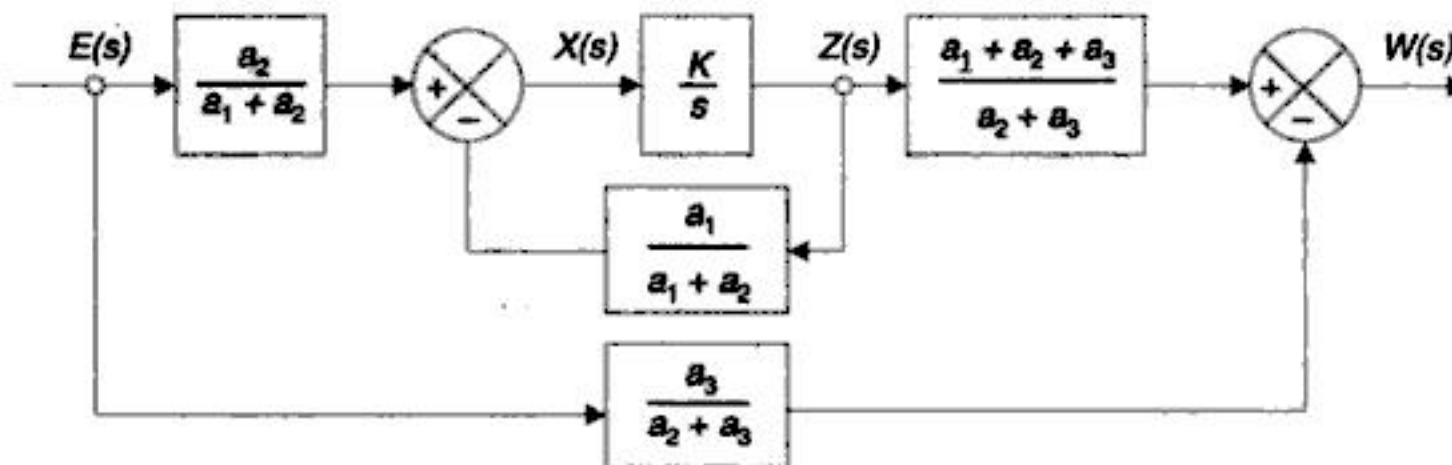


Fig. 4.48

Example 4.2 : Consider the fly-ball speed governing system of Fig. 4.48. Explain the operation of the system. Find the transfer function of each component and draw the overall block diagram and the transfer function $Y(s)/E(s)$. Show that under high gain condition the speed controller has proportional plus-integral action.

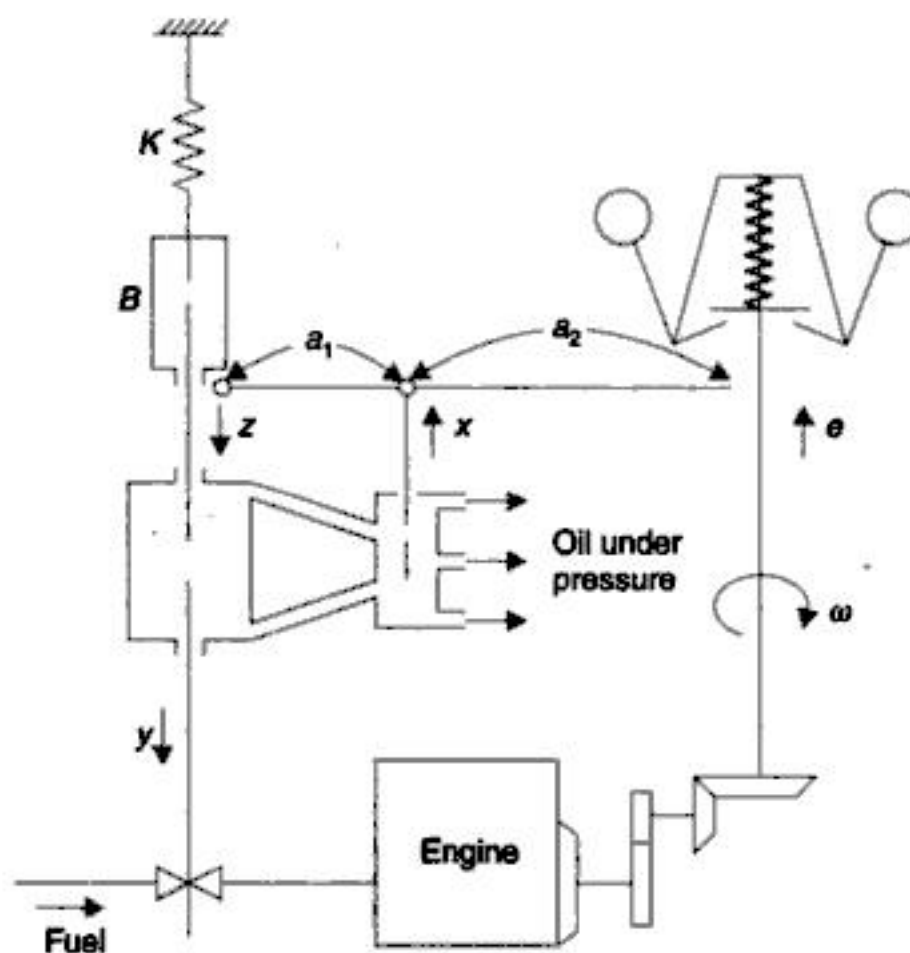


Fig. 4.49. Engine speed governing system.



You have either reached a page that is unavailable for viewing or reached your viewing limit for this book.



You have either reached a page that is unavailable for viewing or reached your viewing limit for this book.



You have either reached a page that is unavailable for viewing or reached your viewing limit for this book.

this, the change in the output pressure is very small and therefore the need of a pneumatic amplifier in cascade with this device arises. This pneumatic amplifier is commonly known as pneumatic relay. A typical combination of flapper valve and relay is shown in Fig. 4.54. A ball is attached to the lower bellows surface. When the ball rests on its upper seat, the atmospheric opening is closed and the output pressure P becomes equal to the supply pressure P_s . When the ball rests on its lower seat, it shuts off the air supply and output pressure drops to ambient pressure. The output pressure can thus be made to vary from ambient to full supply pressure.

The movement of the flapper away from the nozzle causes the nozzle back pressure P_b to decrease, thus the bellows contracts, moving the ball upwards. The atmospheric opening is partially closed and the output pressure increases. When the flapper moves towards the nozzle, the opposite action takes place.

It is thus seen that an increase in separation between nozzle and flapper results in a decrease in output pressure in the case of the flapper valve and an increase in output pressure when the flapper valve is used with the pneumatic relay. The transfer function of the combination is therefore

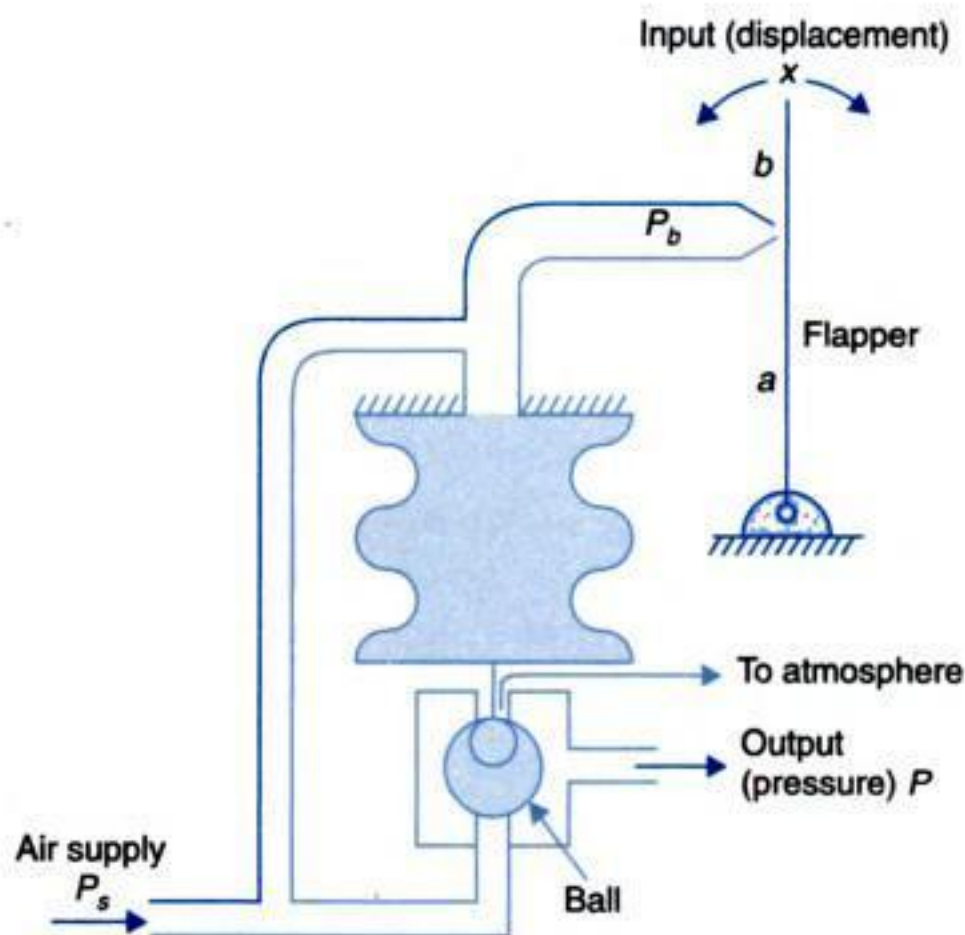


Fig. 4.54. A flapper valve with relay.

$$\frac{\Delta P(s)}{\Delta X(s)} = \frac{a}{a+b} K \quad \dots(4.63)$$

where $K > 0$.

Pneumatic Actuator

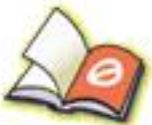
The majority of the modern pneumatic control systems require translatory output motion. This motion is achieved by pneumatic actuators responding to changes in input air pressure. A schematic diagram of the pneumatic actuator is shown in Fig. 4.55. Assume that the actuator is used to position a load consisting of a spring with stiffness K , viscous friction with coefficient



You have either reached a page that is unavailable for viewing or reached your viewing limit for this book.



You have either reached a page that is unavailable for viewing or reached your viewing limit for this book.



You have either reached a page that is unavailable for viewing or reached your viewing limit for this book.

At the operating point the relay nozzle combination is characterized by the relationship

$$p_c = Kx ; K > 0$$

What kind of controller results if

(i) $R_i = 0$

(ii) $R_d = 0$

Low resistance values are achieved by making the respective pipes wide enough.

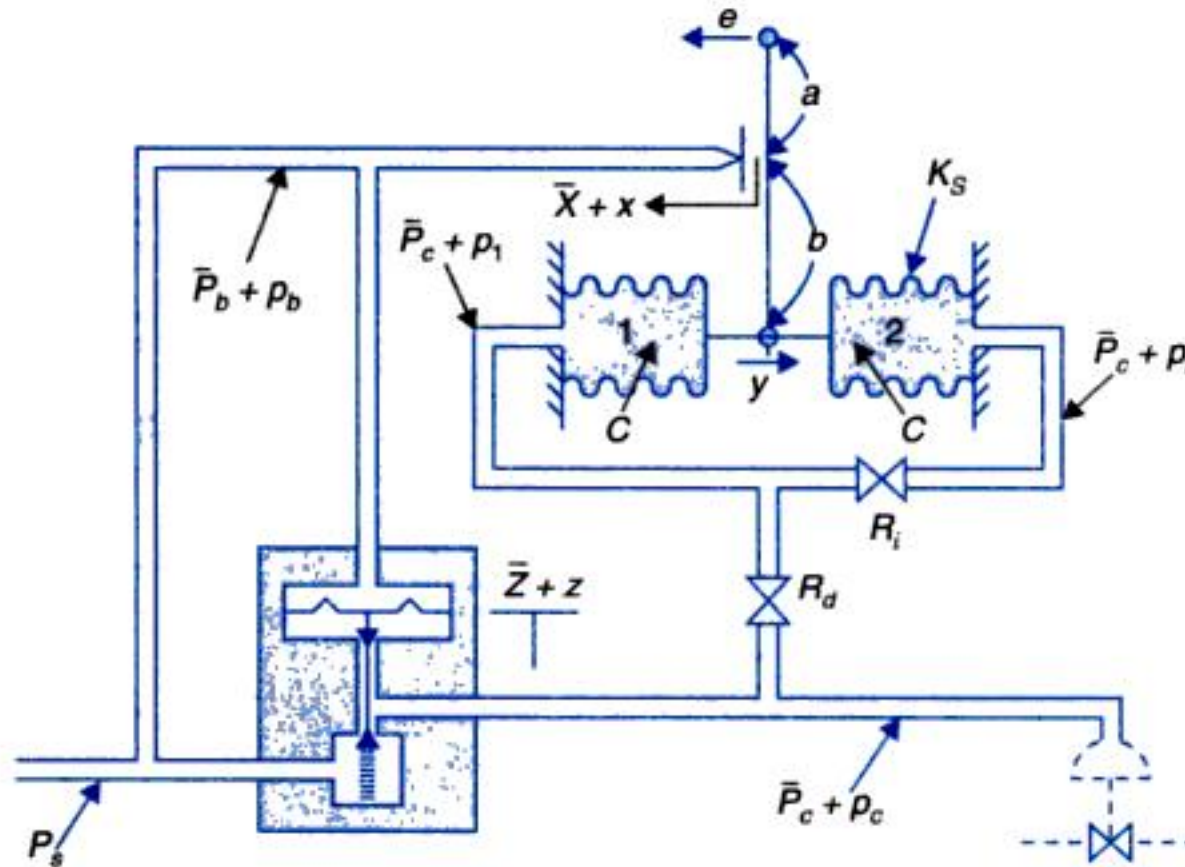


Fig. 4.60. Pneumatic controller—variables indicated are incremental changes about the operating point.

Solution. The electric analog of the bellows and pneumatic flow into these is drawn in Fig. 4.61. Assuming $R_i \gg R_d$, it can be written that

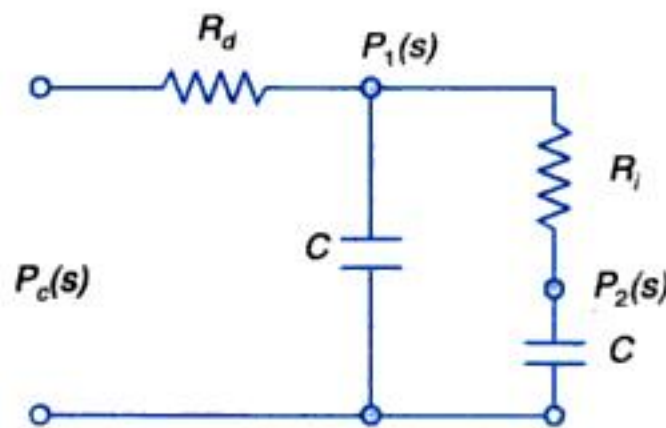


Fig. 4.61

$$\frac{P_1(s)}{P_c(s)} = \frac{1}{R_d C s + 1} = \frac{1}{\tau_d s + 1} \quad \dots(i)$$

and

$$\frac{P_2(s)}{P_c(s)} = \frac{1}{R_i C s + 1} = \frac{1}{\tau_i s + 1} ; \text{ assuming } R_i \gg R_d \quad \dots(ii)$$

The force-balance equation for the two bellows gives

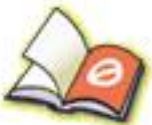
$$(P_1 - P_2)A = K_s y \quad \dots(iii)$$



You have either reached a page that is unavailable for viewing or reached your viewing limit for this book.



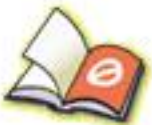
You have either reached a page that is unavailable for viewing or reached your viewing limit for this book.



You have either reached a page that is unavailable for viewing or reached your viewing limit for this book.



You have either reached a page that is unavailable for viewing or reached your viewing limit for this book.



You have either reached a page that is unavailable for viewing or reached your viewing limit for this book.



You have either reached a page that is unavailable for viewing or reached your viewing limit for this book.



You have either reached a page that is unavailable for viewing or reached your viewing limit for this book.

- (a) Suggest a suitable hardware for the autopilot system.
- (b) Draw block diagram of the autopilot system with each block having the transfer function of the corresponding component in the pitch circuit.

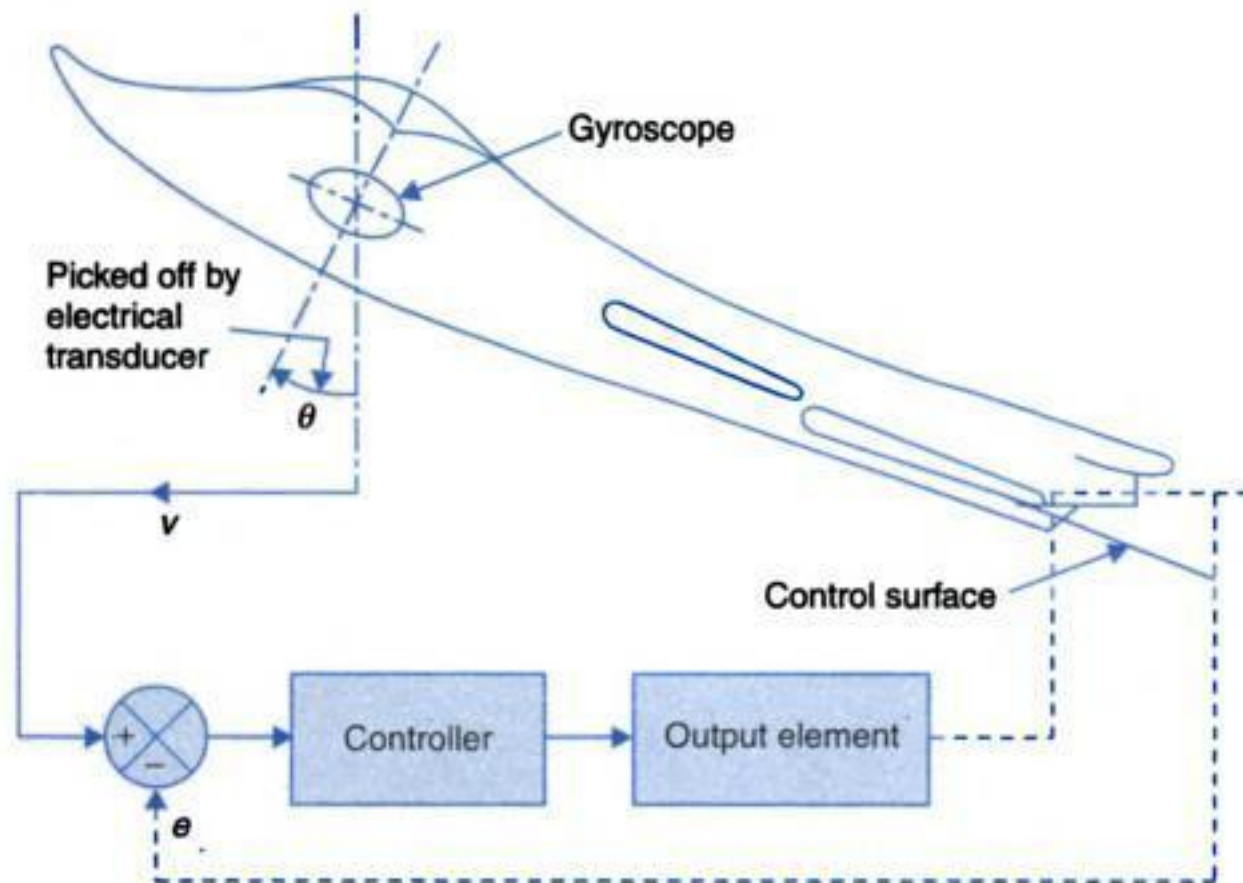


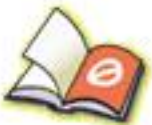
Fig. P-4.12



You have either reached a page that is unavailable for viewing or reached your viewing limit for this book.



You have either reached a page that is unavailable for viewing or reached your viewing limit for this book.



You have either reached a page that is unavailable for viewing or reached your viewing limit for this book.

In the Laplace transform form,

$$R(s) = A/s^2$$

The graphical representation of a ramp signal is shown in Fig. 5.1(b). From eqns. (5.1) and (5.2), it is seen that a ramp signal is integral of a step signal.

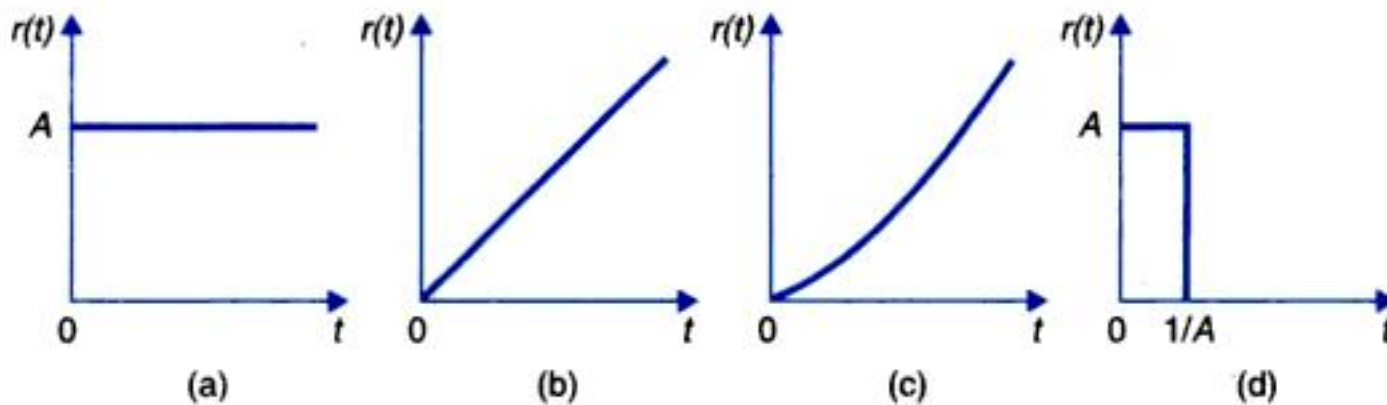


Fig. 5.1. Standard test signals.

Parabolic Signal

The mathematical representation of this signal is

$$\begin{aligned} r(t) &= At^2/2 ; t > 0 \\ &= 0 ; t < 0 \end{aligned} \quad \dots(5.3)$$

In the Laplace transform form,

$$R(s) = A/s^3$$

The graphical representation of a parabolic signal is shown in Fig. 5.1(c). From eqns. (5.2) and (5.3), it is seen that a parabolic signal is integral of a ramp signal.

Impulse Signal

A unit-impulse is defined as a signal which has zero value everywhere except at $t = 0$, where its magnitude is infinite. It is generally called the δ -function and has the following property:

$$\delta(t) = 0 ; t \neq 0$$

$$\int_{-\varepsilon}^{+\varepsilon} \delta(t) dt = 1$$

where ε tends to zero.

Since a perfect impulse cannot be achieved in practice, it is usually approximated by a pulse of small width but unit area as shown in Fig. 5.1(d).

Mathematically, an impulse function is the derivative of a step function *i.e.*,

$$\delta(t) = \dot{u}(t)$$

The Laplace transform of a unit-impulse is

$$\mathcal{L}\delta(t) = 1 = R(s)$$

The impulse response of a system with transfer function $C(s)/R(s) = G(s)$, is given by

$$C(s) = G(s) R(s) = G(s)$$

or

$$c(t) = \mathcal{L}^{-1}G(s) = g(t) \quad \dots(5.4)$$

Thus the impulse response of a system, indicated by $g(t)$, is the inverse Laplace transform of its transfer function. This is sometimes referred to as *weighting function* of the system.



You have either reached a page that is unavailable for viewing or reached your viewing limit for this book.



You have either reached a page that is unavailable for viewing or reached your viewing limit for this book.



You have either reached a page that is unavailable for viewing or reached your viewing limit for this book.

be a PM dc motor. If any error exists, the motor develops a torque which is transmitted to the output shaft through a gear train of ratio n ($n = \text{load shaft speed } \dot{c} / \text{motor shaft speed } \dot{\theta}$). The transmitted torque rotates the output shaft in such a direction so as to reduce the error to zero.

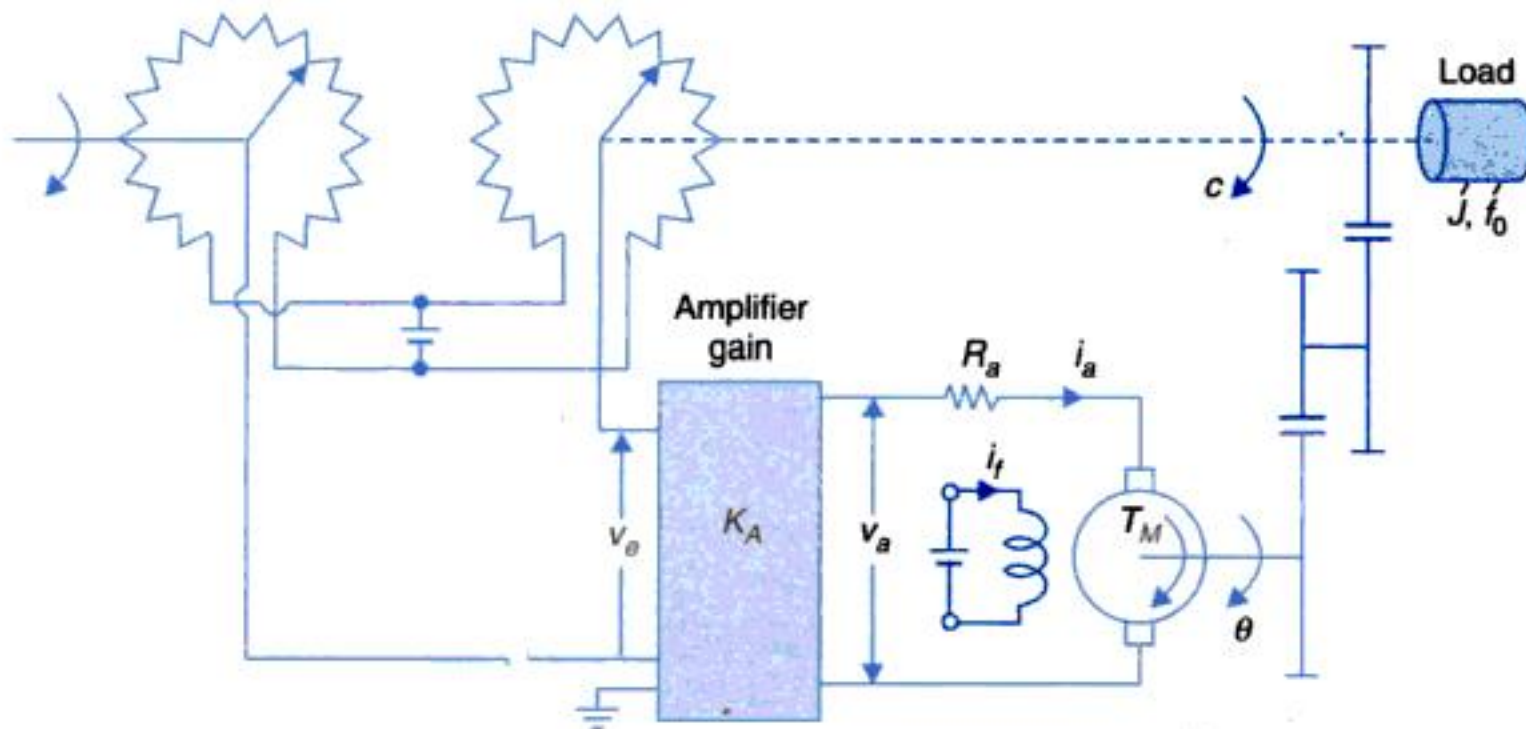
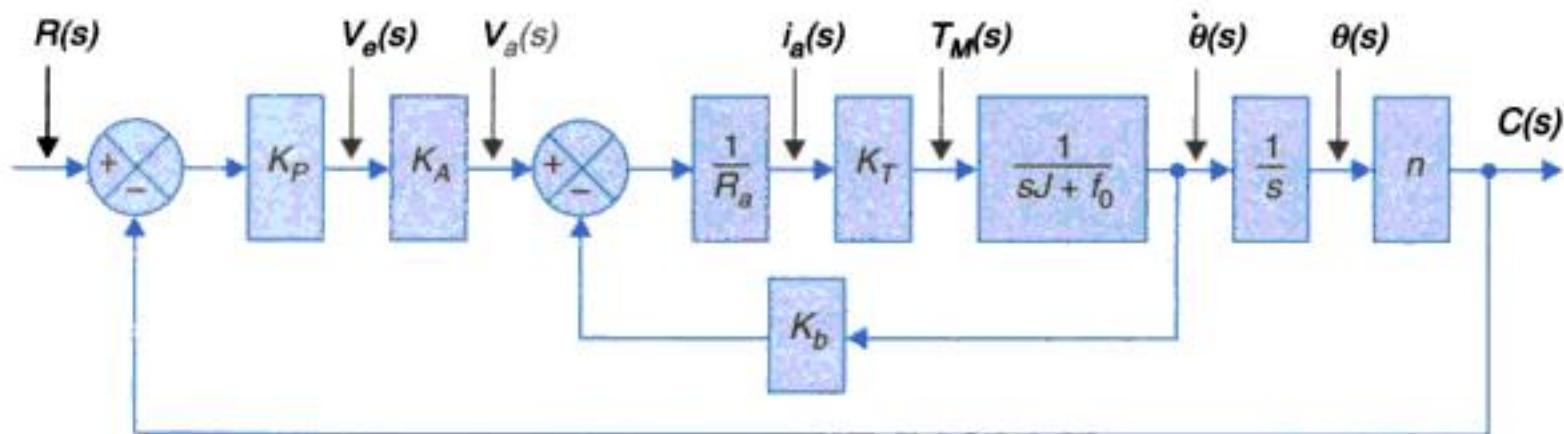
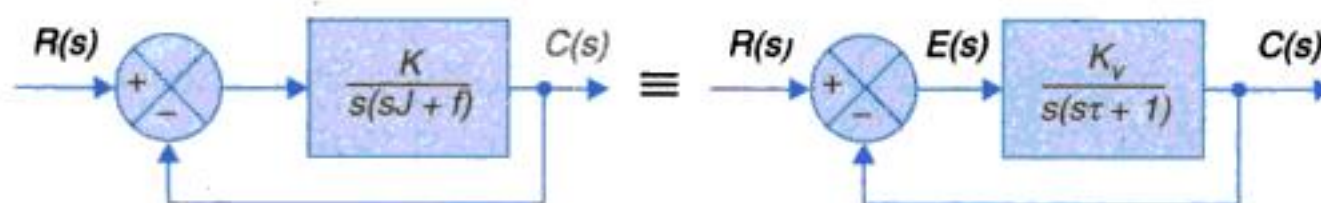


Fig. 5.6. Schematic diagram of position servomechanism.

The block diagram of the system is shown in Fig. 5.7(a). Here J and f_0 are the equivalent inertia and friction at the motor shaft.



(a)



(b)

Fig. 5.7. (a) Block diagram of the system shown in Fig. 5.6;
(b) Simplified block diagram of the system.

The inner loop can be reduced to give the motor transfer function as

$$\frac{\theta(s)}{V_a(s)} = \frac{K_T/R_a}{s(sJ + f)}$$



You have either reached a page that is unavailable for viewing or reached your viewing limit for this book.



You have either reached a page that is unavailable for viewing or reached your viewing limit for this book.



You have either reached a page that is unavailable for viewing or reached your viewing limit for this book.

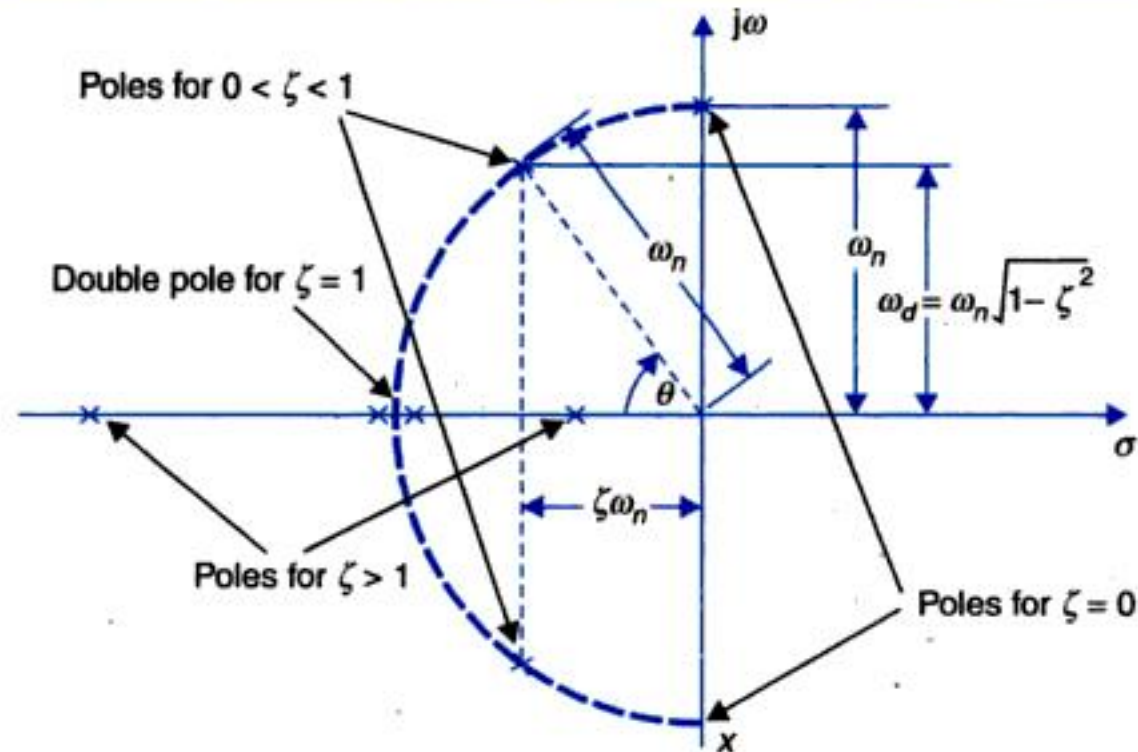


Fig. 5.10. Pole locations for a second-order system.

Time Response Specifications

As pointed out earlier, control systems are generally designed with damping less than one, *i.e.*, oscillatory step response. High-order control systems usually have a pair of complex conjugate poles with damping less than one which dominate over other poles. Therefore the time response of second- and higher-order control systems to a step input is generally of damped oscillatory nature as shown in Fig. 5.11. It is observed from this figure that the step response has a number of overshoots and undershoots with respect to the final steady value. Since the overshoots and undershoots decay exponentially, the peak overshoot is the first overshoot and is the same as the peak of the complete time response. This type of step response is characterized by the following performance indices. The indices are qualitatively related to:

- (i) How fast the system moves to follow the input ?
- (ii) How oscillatory it is (indicative of damping) ?
- (iii) How long does it take to practically reach the final value ?

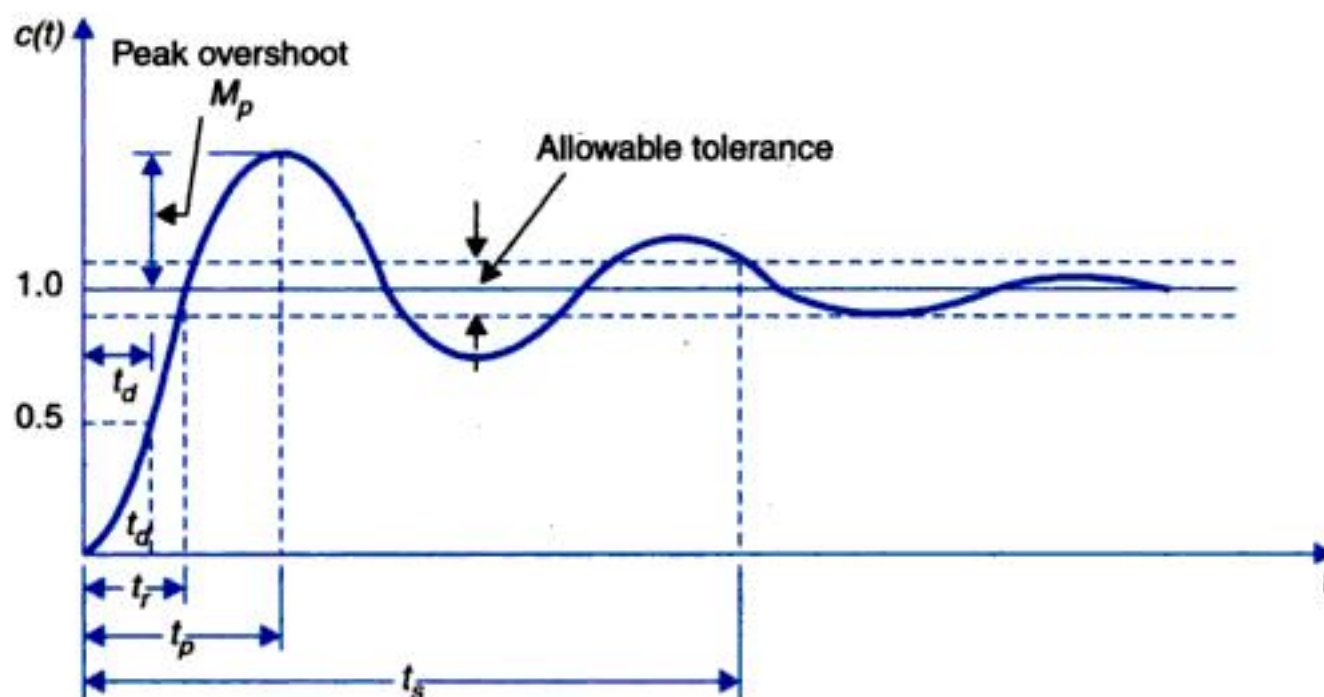


Fig. 5.11. Time response specifications.



You have either reached a page that is unavailable for viewing or reached your viewing limit for this book.



You have either reached a page that is unavailable for viewing or reached your viewing limit for this book.



You have either reached a page that is unavailable for viewing or reached your viewing limit for this book.

Fig. 5.14 shows the unit-step response versus normalized time $\omega_n t$ for various values of ζ as well as the tolerance band. It is observed from this figure that as the damping ζ is reduced from the value of unity (corresponding to the critical damping case), the normalized settling time decreases monotonically till the first overshoot just touches the upper limit of the tolerance band. As the damping is decreased further, $\omega_n t_s$ suddenly jumps up (i.e., it has a discontinuity and then increases slightly with further decrease in damping. The plot of $\omega_n t_s$ versus ζ is shown in Fig. 5.15. The plot has another discontinuity corresponding to the first undershoot touching the lower limit of the tolerance band and similar discontinuities occur corresponding to each overshoot and undershoot, respectively touching the upper and lower limits of the tolerance band.

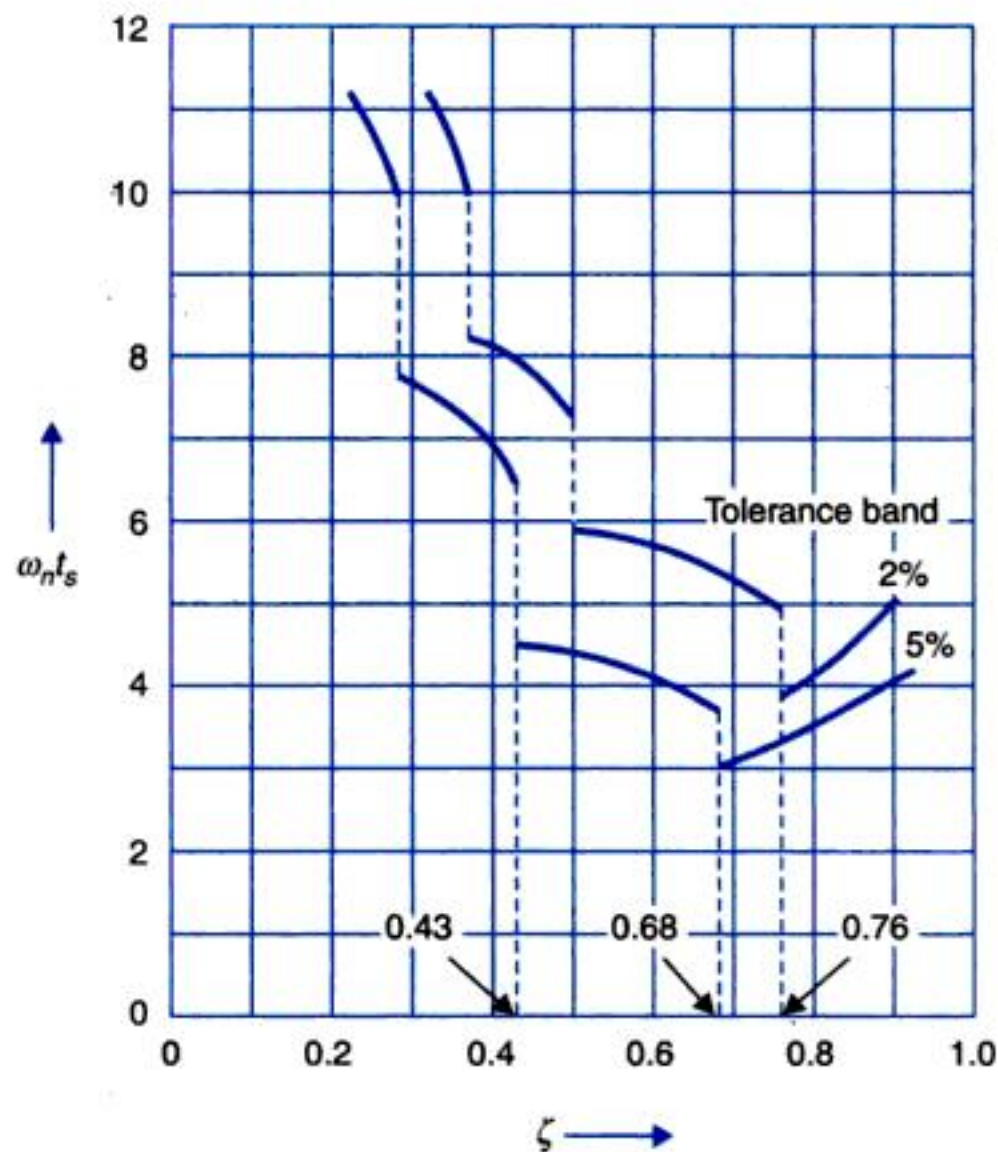


Fig. 5.15. Normalized settling time versus ζ .

The normalized settling time $\omega_n t_s$ is the least at the first discontinuity ($\zeta = 0.76$ for 2% tolerance band and $\zeta = 0.68$ for 5% tolerance band). This fact justifies why the control systems are normally designed to be underdamped. This argument is further strengthened by the observation that rise time reduces monotonically as the damping is decreased.

In fact many control systems are designed to have even lower damping. Justification of this lies in the fact that almost all practical systems possess some coulomb friction and other nonlinearities (backlash, binding in gears and linkages, etc.). The presence of these nonlinearities tends to introduce steady-state error. As these nonlinearities do not appear in the linear mathematical model, therefore in order to compensate for error introduced by them, the linear system is designed with somewhat higher gain and hence lower damping since

$$\zeta = (1/2) \sqrt{(K_v \tau)}$$



You have either reached a page that is unavailable for viewing or reached your viewing limit for this book.



You have either reached a page that is unavailable for viewing or reached your viewing limit for this book.



You have either reached a page that is unavailable for viewing or reached your viewing limit for this book.

$$G(s) = \frac{K(T_{z1}s + 1)(T_{z2}s + 1) \dots}{s^n (T_{p1}s + 1)(T_{p2}s + 1) \dots} \quad \text{(time-constant form)} \quad \dots(5.28)$$

$$= \frac{K'(s + z_1)(s + z_2) \dots}{s^n (s + p_1)(s + p_2) \dots} \quad \text{(pole-zero form)} \quad \dots(5.29)$$

The gains in the two forms are related by

$$K = K' \frac{\prod_i z_i}{\prod_j p_j} \quad \dots(5.30)$$

With the gain relation of eqn. (5.30) for the two forms of $G(s)$, it is sufficient to obtain steady-state errors in terms of the gains of any one of the forms. We shall use the time constant form in the discussions below.

Equation (5.28) involves the term s^n in the denominator which corresponds to number of integrations in the system. As s tends to zero, this term dominates in determining the steady-state error. Control systems are therefore classified in accordance with the number of integrations in the open-loop transfer function $G(s)$ as described below:

1. Type-0 System

If $n = 0$, the steady-state errors to various standard inputs, obtained from eqns. (5.25), (5.26), (5.27), and (5.28) are

$$e_{ss}(\text{position}) = \frac{1}{1 + G(0)} = \frac{1}{1 + K} = \frac{1}{1 + K_p} \quad \dots(5.31)$$

$$e_{ss}(\text{velocity}) = \lim_{s \rightarrow 0} \frac{1}{sG(s)} = \infty$$

$$e_{ss}(\text{acceleration}) = \lim_{s \rightarrow 0} \frac{1}{s^2 G(s)} = \infty$$

Thus a system with $n = 0$ or no integration in $G(s)$ has a constant position error, infinite velocity and acceleration errors. The position error constant is given by the open-loop gain of the transfer function in the time-constant form.

2. Type-1 System

If $n = 1$, the steady-state errors to various standard inputs are

$$e_{ss}(\text{position}) = \frac{1}{1 + G(0)} = \frac{1}{1 + \infty} = 0$$

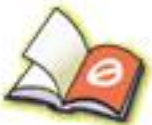
$$e_{ss}(\text{velocity}) = \lim_{s \rightarrow 0} \frac{1}{sG(s)} = \frac{1}{K} = \frac{1}{K_v} \quad \dots(5.32)$$

$$e_{ss}(\text{acceleration}) = \lim_{s \rightarrow 0} \frac{1}{s^2 G(s)} = \infty$$

Thus a system $n = 1$ or with one integration in $G(s)$ has zero position error, a constant velocity error and an infinite acceleration error at steady-state.

3. Type-2 System

If $n = 2$, the steady-state errors to various standard inputs are



You have either reached a page that is unavailable for viewing or reached your viewing limit for this book.



You have either reached a page that is unavailable for viewing or reached your viewing limit for this book.



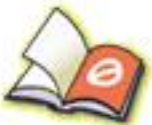
You have either reached a page that is unavailable for viewing or reached your viewing limit for this book.



You have either reached a page that is unavailable for viewing or reached your viewing limit for this book.



You have either reached a page that is unavailable for viewing or reached your viewing limit for this book.



You have either reached a page that is unavailable for viewing or reached your viewing limit for this book.

$$\tau' = \frac{JR_a}{R_a f + K_A K_T K_t} \quad \dots(5.42)$$

The natural frequency and damping of the closed-loop can then be expressed as

$$\omega_n' = \sqrt{(K_v' / \tau')} = \sqrt{(K_P K_A K_T n / JR_a)} \quad \dots(5.43)$$

$$\zeta' = (1/2) / \sqrt{(K_v' \tau')} = (R_a f + K_A K_T K_t) / 2 \sqrt{(K_P K_A K_T n JR_a)} \quad \dots(5.44)$$

For a specified K_v' , and ζ' , we can write from eqns. (5.41) and (5.44)

$$\zeta' K_v' = \frac{1}{2} \sqrt{(K_P K_A K_T n / JR_a)}$$

from which K_A is determined as

$$K_A = 4(\zeta' K_v')^2 (JR_a / K_P K_T n)$$

Using this value of K_A , K_t the tachometer constant is obtained from eqn. (5.41) as

$$K_t = \left(\frac{K_P n}{K_v'} - \frac{R_a f}{K_A K_T} \right)$$

Thus, we notice that by a suitable choice of K_A , K_P we can simultaneously meet the specification of K_v' and ζ' . On account of the negative derivative feedback, K_A required may sometimes be excessively large. Under such circumstances additional gain outside the derivative loop is very helpful.

Further, it is to be noticed that for the same value of velocity error constant, the system with compensation requires a higher value of K_A and hence it will have a higher natural frequency (eqn. 5.43). Compensation thus increases both the system damping and natural frequency resulting in reduced settling time.

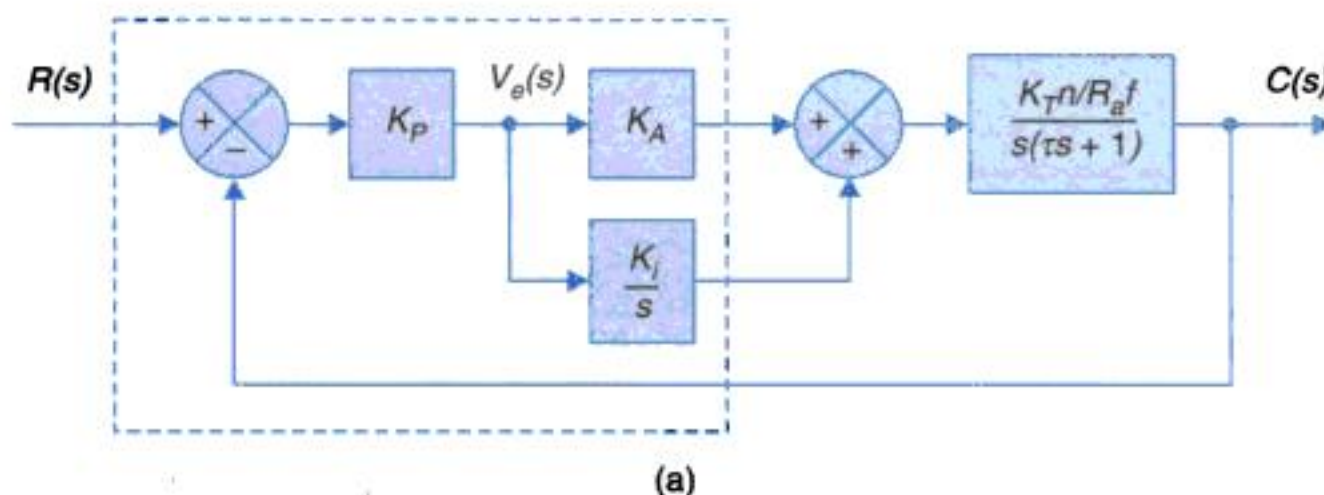
Integral Error Compensation

In an integral error compensation scheme, the output response depends in some manner upon the integral of the actuating signal. This type of compensation is introduced by using a controller which produces an output signal consisting of two terms, one proportional to the actuating signal and the other proportional to its integral. Such a controller is called *proportional plus integral controller* or *PI controller*.

The block diagram of the system of Fig. 5.6 with proportional plus integral compensation is shown in Fig. 5.23(a), while its simplified block diagram is given in Fig. 5.23(b) where

$$K_v' = K_P K_i K_T n / R_a f$$

$$K_A' = K_A / K_i$$





You have either reached a page that is unavailable for viewing or reached your viewing limit for this book.



You have either reached a page that is unavailable for viewing or reached your viewing limit for this book.



You have either reached a page that is unavailable for viewing or reached your viewing limit for this book.

5.9 PERFORMANCE INDICES

As discussed already, the design of a control system is an attempt to meet a set of specifications which define the overall performance of the system in terms of certain measurable quantities. A number of performance measures have been introduced so far in respect of dynamic response to step input (ζ , M_p , t_r , t_p , t_s etc.) and the steady-state error, e_{ss} , to both step and higher-order inputs. These measures have to be satisfied simultaneously in design and hence the design necessarily becomes a trial and error procedure. If, however, a single performance index could be established on the basis of which one may describe the goodness of the system response, then the design procedure will become logical and straightforward.

Furthermore, in many of the modern control schemes, the system parameters are automatically adjusted to keep the system at an optimum level of performance under varying inputs and varying conditions of operation. Such class of systems is called *adaptive control systems*. These systems require a performance index which is a function of the variable system parameters. Extremum (minimum or maximum) value of this index then corresponds to the optimum set of parameter values. Other desirable features of a performance index are its selectivity, *i.e.*, its power to clearly distinguish between an optimum and non-optimum system, its sensitivity to parameter variations and the ease of its analytical computation or its online analogic or digital determination.

A number of such performance indices are used in practice, the most common being the *integral square error* (ISE), given by

$$\text{ISE} = \int_0^{\infty} e^2(t) dt \quad \dots(5.51)$$

Apart from the ease of implementation, this index has the advantage that it is mathematically convenient both for analysis and computation. Fig. 5.27(a) and (b) show the system response $c(t)$ and error $e(t)$ respectively to unit-step input. The square error is shown in Fig. 5.27(c) and its integral in Fig. 5.27(d). It is obvious that ISE converges to a limit as $t \rightarrow \infty$. Minimization of ISE by adjusting system parameters is a good compromise between reduction of rise time to limit the effect of large initial error, reduction of peak overshoot and reduction of settling time to limit the effect of small error lasting for a long time.

Consider now the second-order system discussed previously in this chapter from eqn. (5.12), the error response to unit-step is given by

$$e(t) = \frac{e^{-\zeta\omega_n t}}{\sqrt{1-\zeta^2}} \sin \left[\omega_n \sqrt{1-\zeta^2} t + \tan^{-1} \frac{\sqrt{1-\zeta^2}}{\zeta} \right]$$

Therefore

$$\text{ISE} = \int_0^{\infty} e^2(t) dt = \frac{1}{\omega_n} \int_0^{\infty} e^2(t_n) dt_n$$

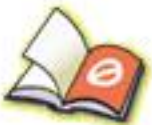
where $t_n = \omega_n t$, *i.e.*, the normalized time.



You have either reached a page that is unavailable for viewing or reached your viewing limit for this book.



You have either reached a page that is unavailable for viewing or reached your viewing limit for this book.



You have either reached a page that is unavailable for viewing or reached your viewing limit for this book.



You have either reached a page that is unavailable for viewing or reached your viewing limit for this book.

Example 5.1 : Reconsider the servomechanism shown in Fig. 5.6. The parameters of the system are given as follows:

| | |
|-----------------------------------------|-------------------------------------------|
| Sensitivity of error detector, | $K_p = 1\text{V/rad}$ |
| Gain of dc amplifier, | K_A (variable) |
| Resistance of armature of motor, | $R_a = 5\Omega$ |
| Equivalent inertia at the motor shaft, | $J = 4 \times 10^{-3} \text{ kg-m}^2$ |
| Equivalent friction at the motor shaft, | $f_0 = 2 \times 10^{-3} \text{ Nm/rad/s}$ |
| Torque constant of motor, | $K_T = 1 \text{ Nm/A}$ |
| Gear ratio, | $n = 1/10$ |

Solution. The value of the back emf constant K_b is not given in the above list of parameters. However, a definite relationship exists between K_b and K_T (refer Section 2.3). In MKS units $K_b = K_T$

The open-loop transfer function of the system in the pole-zero form is (refer Fig. 5.7(a))

$$G(s) = \frac{K}{s(sJ + f)}$$

where $f = f_0 + \frac{K_T K_b}{R_a} = 202 \times 10^{-3}$

$$J = 4 \times 10^{-3}$$

$$K = K_p K_A K_T \frac{n}{R_a} = \frac{K_A}{50}$$

The open-loop transfer function of the system in the time-constant form is (refer Fig. 5.7(b))

$$G(s) = \frac{K_v}{s(s\tau + 1)}$$

where $K_v = K/f = \frac{10^3 K_A}{50 \times 202}$

$$\tau = J/f = 4/202$$

The closed-loop transfer function of the system is

$$\frac{C(s)}{R(s)} = \frac{5K_A}{s^2 + 50.5s + 5K_A}$$

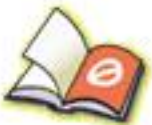
The natural undamped frequency of the system is

$$\omega_n = \sqrt{5K_A} \quad \dots(5.55)$$

The damping ratio is $\zeta = 25.25/\omega_n \quad \dots(5.56)$

The system under consideration is a type-1 system. Therefore, from Table 5.1 we find that the steady-state error to unit step input is zero and steady-state error to unit-ramp input is

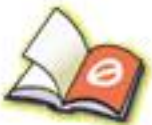
$$e_{ss} = \frac{1}{K_v} = \frac{50 \times 202}{10^3 K_A} = \frac{101}{K_A} \quad \dots(5.57)$$



You have either reached a page that is unavailable for viewing or reached your viewing limit for this book.



You have either reached a page that is unavailable for viewing or reached your viewing limit for this book.



You have either reached a page that is unavailable for viewing or reached your viewing limit for this book.

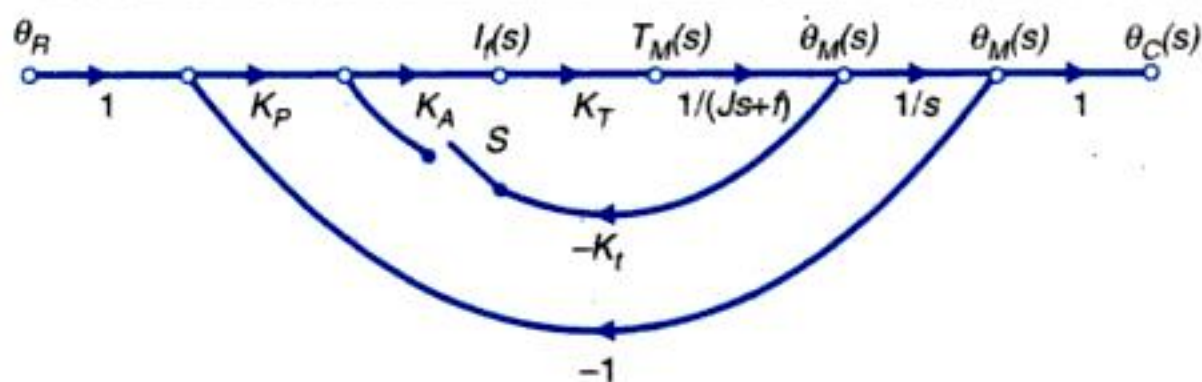


Fig. 5.31

The governing differential equation can be written from the transfer function as

$$J\ddot{\theta}_M(t) + f\dot{\theta}_M(t) + K_P K_A K_T \theta_M(t) = K_P K_A K_T \theta_R(t)$$

The system characteristic equation is

$$s^2 + (f/J)s + K_P K_A K_T / J = 0$$

$$\therefore \omega_n^2 = \frac{K_P K_A K_T}{J}$$

$$\text{or } 10^2 = \frac{0.6 \times K_A \times 2}{0.4} \quad \text{or } K_A = 33.3 \text{ amp/volt}$$

(c) With tachogenerator (switch 'S' closed)

$$\frac{\theta_M(s)}{\theta_R(s)} = \frac{K_P K_A K_T}{Js^2 + (f + K_A K_t K_T)s + K_P K_A K_T}$$

$$2\zeta\omega_n = (f + K_A K_t K_T) / J ; \omega_n = \sqrt{(K_P K_A K_T / J)}$$

$$\therefore \zeta = \frac{1}{2} \frac{f + K_A K_t K_T}{\sqrt{(JK_P K_A K_T)}}$$

$$\text{or } 1 = \frac{1}{2} \frac{2 + 5 \times 2 \times K_t}{\sqrt{(0.4 \times 0.6 \times 5 \times 2)}} \quad \text{or } K_t = 0.11 \text{ V/rad/sec.}$$

Example 5.4 : The system illustrated in Fig. 5.32 is a unity feedback control system with a minor feedback loop (output derivative feedback).

(a) In the absence of derivative feedback ($a = 0$), determine the damping factor and natural frequency. Also determine the steady-state error resulting from a unit-ramp input.

(b) Determine the derivative feedback constant of which will increase the damping factor the system to 0.7. What is the steady-state error to unit-ramp input with this setting of the derivative feedback constant?

(c) Illustrate how the steady-state error of the system with derivative feedback to unit-ramp input can be reduced to the same value as in part (a), while the damping factor is maintained at 0.7.

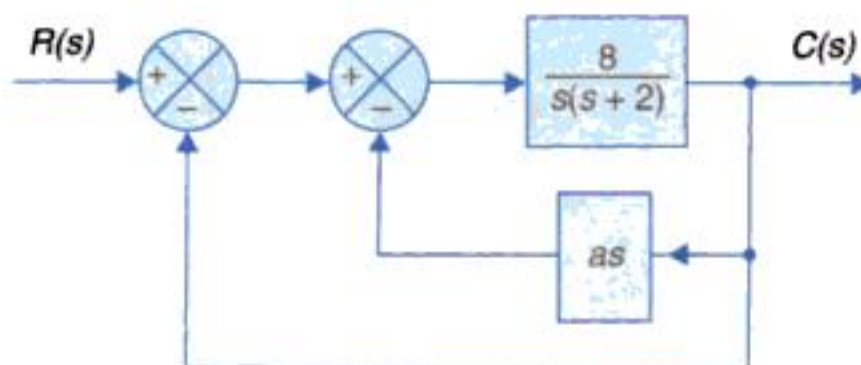
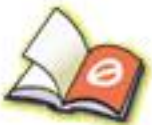


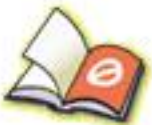
Fig. 5.32



You have either reached a page that is unavailable for viewing or reached your viewing limit for this book.



You have either reached a page that is unavailable for viewing or reached your viewing limit for this book.



You have either reached a page that is unavailable for viewing or reached your viewing limit for this book.

Hence

$$J_e(\min) = \frac{1}{2K} = \frac{1}{2\sqrt{3N}} \quad \dots(5.67)$$

Example 5.6 : A unity feedback position control system has a forward path transfer function

$$G(s) = K/s$$

For unit-step input, compute the value of K that minimizes ISE.

Solution.

For the system under consideration

$$\frac{E(s)}{R(s)} = \frac{1}{1+G(s)} = \frac{s}{s+K}$$

For unit-step input

$$E(s) = \frac{1}{s+K}$$

Therefore,

$$e(t) = e^{-Kt} \quad \dots(5.68)$$

$$\text{ISE} = \int_0^{\infty} e^2(t) dt = \frac{1}{2K} \quad \dots(5.69)$$

Obviously, the minimum value of ISE is obtained as $K \rightarrow \infty$. This is an impractical solution resulting in excessive strain on physical components of the system. A more practical solution results by limiting the second derivative of the output which amounts to limiting the maximum torque of the system.

Let the constraint be

$$|\ddot{c}| \leq M \quad \dots(5.70)$$

where c is the output and M is a constant.

For the system considered here, the output is

$$C(s) = \frac{K}{s(s+K)}$$

$$c(t) = 1 - e^{-Kt}$$

Therefore,

$$\ddot{c}(t) = K^2 e^{-Kt}$$

$$|\ddot{c}(t)|_{\max} = K^2 \leq M \quad \dots(5.71)$$

The maximum value of K satisfying the constraint (5.71) will give the minimum value of ISE. Thus the optimum value of K obtained from eqn. (5.67) is

$$K = \sqrt{M}$$

Therefore, minimum ISE = $1/2 \sqrt{M}$

Example 5.7 : For the system of Example 5.6, compute the value of K that minimizes the following performance index.

$$J = \int_0^{\infty} (e^2 + \lambda \ddot{e}) dt ; \lambda \text{ is a positive constant}$$

What is the minimum value of J ?



You have either reached a page that is unavailable for viewing or reached your viewing limit for this book.



You have either reached a page that is unavailable for viewing or reached your viewing limit for this book.



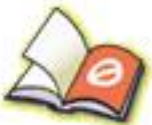
You have either reached a page that is unavailable for viewing or reached your viewing limit for this book.



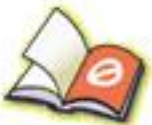
You have either reached a page that is unavailable for viewing or reached your viewing limit for this book.



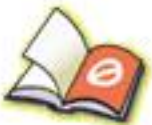
You have either reached a page that is unavailable for viewing or reached your viewing limit for this book.



You have either reached a page that is unavailable for viewing or reached your viewing limit for this book.



You have either reached a page that is unavailable for viewing or reached your viewing limit for this book.



You have either reached a page that is unavailable for viewing or reached your viewing limit for this book.



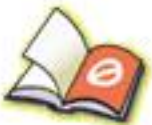
You have either reached a page that is unavailable for viewing or reached your viewing limit for this book.



You have either reached a page that is unavailable for viewing or reached your viewing limit for this book.



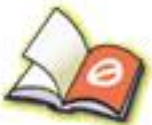
You have either reached a page that is unavailable for viewing or reached your viewing limit for this book.



You have either reached a page that is unavailable for viewing or reached your viewing limit for this book.



You have either reached a page that is unavailable for viewing or reached your viewing limit for this book.



You have either reached a page that is unavailable for viewing or reached your viewing limit for this book.

The area on s plane where the complex dominant roots should be in Fig. 5.45

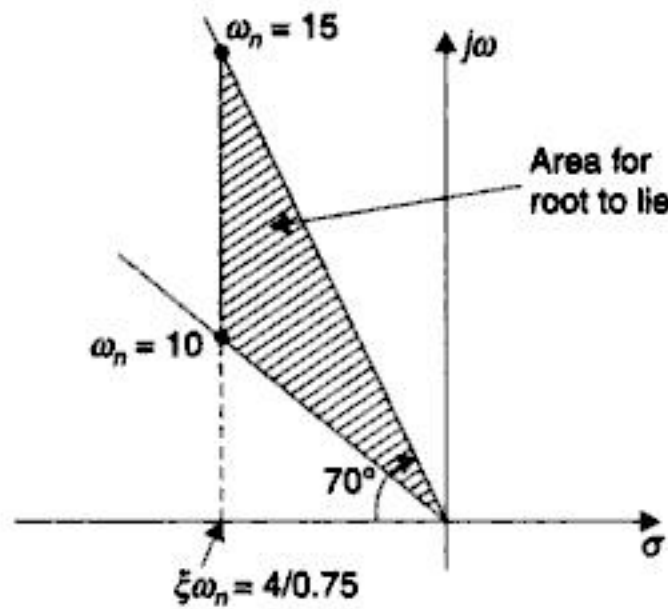


Fig. 5.45

(b) From Eq. (i) $\xi\omega_n = \frac{4}{0.75}$

We choose the third root to be at least 6-time further on negative real axis than the real part of the complex conjugate roots. Thus

$$s = -6 \times (\xi\omega_n) = \frac{6 \times 4}{0.75}$$

or $s = -32$

(c) $t_s = 0.75, M_p = 30\% \Rightarrow \xi = 0.35, \xi\omega_n = \frac{4}{0.75} = 5.33, \omega_n = 15$

Complex conjugate roots term is

$$(s^2 + 2\xi\omega_n s + \omega_n^2) = (s^2 + 10.66s + 225)$$

Third root $s = -32$

The closed-loop transfer function can then be written as

$$T(s) = \frac{C(s)}{R(s)} = \frac{32 \times 225}{(s + 32)(s^2 + 10.66s + 225)}$$

The numerator (32×225) assures that $T(s = 0) = 1$, which mean $C(0) = R(0)$ or steady state error is zero, system type-1.

Now $T(s) = \frac{G(s)}{1 + G(s)} = \frac{32 \times 225}{(s + 32)(s^2 + 10.66s + 225)}$

From which we can write

$$G(s) = \frac{T(s)}{1 - T(s)}$$

Solving yield $G(s) = \frac{32 \times 225}{s(s^2 + 43s + 566)}$

Example 5.11. The open-loop transfer function of a unity feedback system is

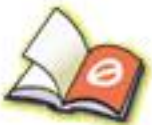
$$G(s) = \frac{K}{s(s + 2)}$$



You have either reached a page that is unavailable for viewing or reached your viewing limit for this book.



You have either reached a page that is unavailable for viewing or reached your viewing limit for this book.



You have either reached a page that is unavailable for viewing or reached your viewing limit for this book.

Let us now take into account the effect of zero. For this we will consult the curves of Fig. 5.19 (b)

$$\text{Zero, } z = 6, \quad \xi\omega_n = 0.6\sqrt{20}$$

$$\frac{z}{\xi\omega_n} = \frac{6}{0.6\sqrt{20}} = 2.24, \quad \xi = 0.6$$

We obtain from this figure

$$M_p \approx 16\%$$

We find that the effect of zero is to increase M_p from 9.4% to 16%.

Example 5.13. A certain system is described by the differential equation

$$\ddot{y} + b\dot{y} + 4 = r$$

Determine the value of b to satisfy the following specifications.

1. M_p to be as small as possible but no greater than 15%.
2. Rise time t_r to be as small as possible but no greater than 1.2 sec.

If both specifications can not be met simultaneously at least (1) should be met and (2) to be met as closely as possible.

Solution. Since specification (1) must be met, we choose $M_p = 15\%$

$$M_p = e^{-\pi\xi/\sqrt{1-\xi^2}} = 0.15$$

Take log natural on both sides

$$-\pi\xi/\sqrt{1-\xi^2} = -1.9$$

$$\pi\xi = 1.9\sqrt{1-\xi^2}$$

Squaring we get $\pi^2\xi^2 = (1.9)^2(1-\xi^2)$

$$9.87\xi^2 = 3.61(1-\xi^2) \quad \text{or} \quad \xi = 0.52$$

From the given differential equation

$$\omega_n = \sqrt{4} = 2 \text{ rad/s}$$

Rise time $t_r = \frac{\pi - \phi}{\omega_n \sqrt{1-\xi^2}}, \quad \phi = \tan^{-1} \frac{\sqrt{1-\xi^2}}{\xi}, \quad \xi = 0.51$

or $t_r = 1.22 \text{ sec.} \quad \phi = 1.036 \text{ rad}$

We find that t_r condition is met.

In this example the two specifications are such that both are met with one parameter ξ (corresponding to b). This is usually not the case.

Example 3.14. The block diagram of a robot joint control is drawn in Fig. 5.47.

Various system parameters are :

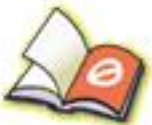
$$J = 10 \text{ kg/m}^2, \quad f = 20 \text{ Nm/rad/sec.}$$

$$K_m \text{ (motor torque constant)} = 2 \text{ Nm/V}$$

$$K_v \text{ (velocity feedback constant)} = 1 \text{ V/rad/sec}$$

$$K_e \text{ (error amplification) in V/degree, to be determined.}$$

(a) Calculate the value of K_e for the closed-loop system to have $\xi = 1$.



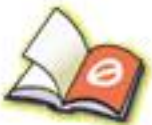
You have either reached a page that is unavailable for viewing or reached your viewing limit for this book.



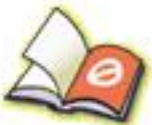
You have either reached a page that is unavailable for viewing or reached your viewing limit for this book.



You have either reached a page that is unavailable for viewing or reached your viewing limit for this book.



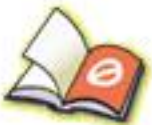
You have either reached a page that is unavailable for viewing or reached your viewing limit for this book.



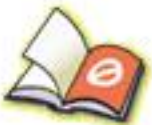
You have either reached a page that is unavailable for viewing or reached your viewing limit for this book.



You have either reached a page that is unavailable for viewing or reached your viewing limit for this book.



You have either reached a page that is unavailable for viewing or reached your viewing limit for this book.



You have either reached a page that is unavailable for viewing or reached your viewing limit for this book.

- (1) Unit-step response is recorded and M_p measured therefrom has a value of 25%.
- (2) A constant velocity input of 1 rad/sec produces a steady-state error of 0.04 rad.
- (3) With the reference potentiometer shaft held fixed, a torque of 10 newton-m applied to the output shaft produces a steady-state error of 0.01 rad.

From the above data, determine:

- (a) The natural frequency ω_n .
- (b) The moment of inertia J referred to the motor shaft.
- (c) The coefficient of viscous friction f referred to the motor shaft.

- 5.7 Measurements conducted on a servomechanism show the system response to be

$$c(t) = 1 + 0.2 e^{-60t} - 1.2 e^{-10t}$$

when subjected to a unit-step input.

- (a) Obtain the expression for the closed-loop transfer function.
- (b) Determine the undamped natural frequency and damping ratio of the system.

- 5.8 A unity feedback system is characterized by an open-loop transfer function

$$G(s) = K/s(s + 10)$$

Determine the gain K so that the system will have a damping ratio of 0.5. For this value of K determine settling time, peak overshoot and time to peak overshoot for a unit-step input.

- 5.9 Figure P-5.9 shows a system employing proportional plus error-rate control. Determine the value of the error-rate factor K_e so that the damping ratio is 0.5. Determine the values of settling time, maximum overshoot and steady-state error (for unit-ramp input) with and without error-rate control. Comment upon the effect of error-rate control on system dynamics.

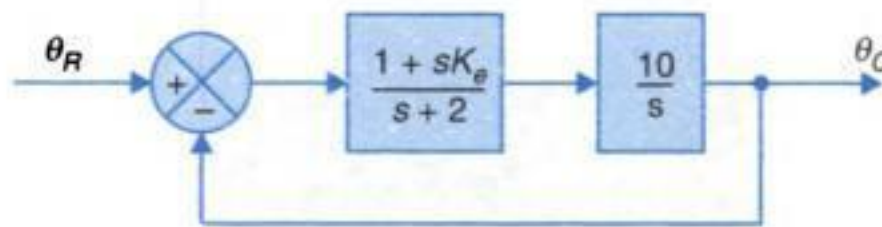


Fig. P-5.9

- 5.10 A feedback system employing output-rate damping is shown in Fig. P-5.10.

- (a) In the absence of derivative feedback ($K_0 = 0$), determine the damping factor and natural frequency of the system. What is the steady-state error resulting from unit-ramp input?

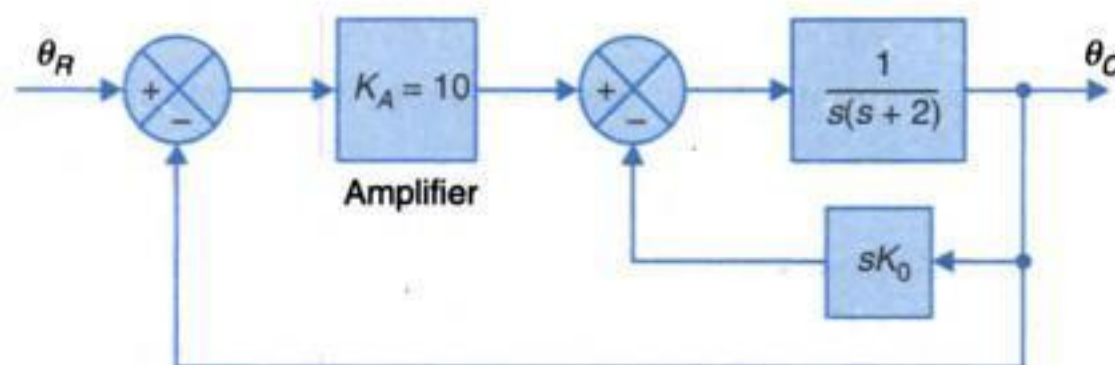


Fig. P-5.10

- (b) Determine the derivative feedback constant K_0 , which will increase the damping factor of the system to 0.6. What is the steady-state error resulting from unit-ramp input with this setting of the derivative feedback constant?



You have either reached a page that is unavailable for viewing or reached your viewing limit for this book.



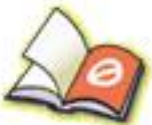
You have either reached a page that is unavailable for viewing or reached your viewing limit for this book.



You have either reached a page that is unavailable for viewing or reached your viewing limit for this book.

6

CONCEPTS OF STABILITY AND ALGEBRAIC CRITERIA



You have either reached a page that is unavailable for viewing or reached your viewing limit for this book.



You have either reached a page that is unavailable for viewing or reached your viewing limit for this book.



You have either reached a page that is unavailable for viewing or reached your viewing limit for this book.

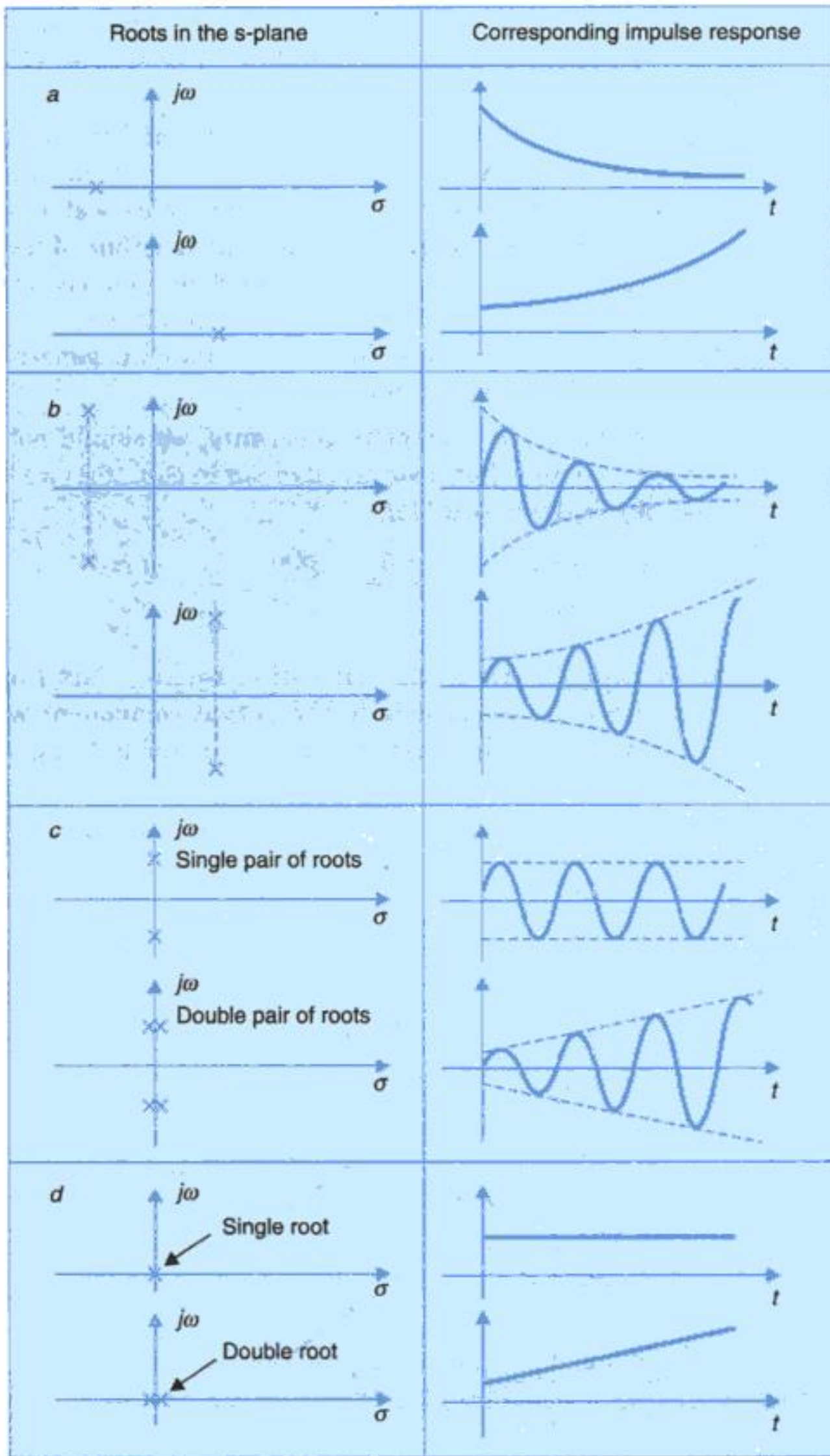
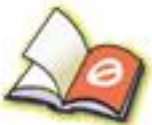


Fig. 6.1. Response terms contributed by various types of roots.

The response to initial conditions is not evident from the model of eqn. (6.1) since the transfer function of a system is derived with the assumption of zero initial conditions. However,



You have either reached a page that is unavailable for viewing or reached your viewing limit for this book.



You have either reached a page that is unavailable for viewing or reached your viewing limit for this book.



You have either reached a page that is unavailable for viewing or reached your viewing limit for this book.

which has the roots

$$s_1, s_2 = [-a_1 \pm \sqrt{(a_1^2 - 4a_0a_2)}] / 2a_0 \quad \dots(6.6)$$

From eqn. (6.6) it is seen that positiveness of a_0, a_1 and a_2 ensures that the roots lie in left half of the s -plane (either both the roots are negative or they have negative real parts) which implies the stability of the system.

2. The positiveness of the coefficients of the characteristic equation ensures the negativeness of real roots but does not ensure the negativeness of the real parts of the complex roots for third-and higher-order systems. Therefore it cannot be a sufficient condition for stability of third-and higher-order systems.

Consider a third-order system with characteristic equation

$$s^3 + s^2 + 2s + 8 = 0 \quad \dots(6.7)$$

Equation (6.7) may be put in the factored form as

$$(s + 2) \left(s - 0.5 + j \frac{\sqrt{15}}{2} \right) \left(s - 0.5 + j \frac{\sqrt{15}}{2} \right) = 0$$

We see that the real part of the complex roots is positive indicating instability of the system even though all the coefficients of the characteristic equation (6.7) are positive.

Therefore, if the characteristic equation of a system is of degree higher than second, the possibility of its instability cannot be excluded even when all the coefficients of its characteristic equation are positive. The first step in analyzing the stability of the system is to examine its characteristic equation. If some of the coefficients are zero or negative it can be concluded that the system is not stable. On the other hand, if all the coefficients of the characteristic equation are positive (or negative), the possibility of stability of system exists and one should proceed further to examine the sufficient conditions of stability.

A. Hurwitz and E.J. Routh independently published the method of investigating the sufficient conditions of stability of a system. The Hurwitz Criterion is in terms of determinants and the Routh Criterion is in terms of array formulation, which is more convenient to handle. We first discuss the Hurwitz Criterion. The Routh Criterion which is derivable from that of Hurwitz, is then presented.

6.3 HURWITZ STABILITY CRITERION

The characteristic equation of an n th order system is

$$q(s) = a_0s^n + a_1s^{n-1} + \dots + a_{n-1}s + a_n = 0$$

For the stability of this system, it is necessary and sufficient that the n determinants formed from the coefficients a_0, a_1, \dots, a_n of the characteristic equation be positive, where these determinants are taken as the principal minors of the following arrangement (called the Hurwitz determinant):



You have either reached a page that is unavailable for viewing or reached your viewing limit for this book.



You have either reached a page that is unavailable for viewing or reached your viewing limit for this book.



You have either reached a page that is unavailable for viewing or reached your viewing limit for this book.

Applying Routh criterion

$$\begin{array}{rcc} s^3 & 1 & K_V K_P \\ s^2 & (1 + K_V K_D) & K_P K_I \\ s^1 & b_3 & 0 \\ s^0 & K_P K_I & 0 \end{array}$$

Assuming all parameters and variables to be positive the condition of stability is given as

$$b_3 = K_V K_P (1 + K_V K_D) - (K_P K_I) > 0$$

This corroborates the statement made earlier in Section 5.7 that PI and PID controllers, while improving the system's dynamic response and reducing its steady-state error, cause it become conditionally stable. A second-order system with a proportional controller is otherwise absolutely stable.

Example 6.5 : A unity negative feedback control system has an open-loop transfer function consisting of two poles, two zeros and a variable gain K . The zeros are located at -2 and -1 ; and the poles at 0.1 and $+1$.

Using Routh stability criterion, determine the range of values of K for which the closed-loop system has 0, 1 or 2 poles in the right-half s -plane.

Solution.
$$G(s) = \frac{K(s + 1)(s + 2)}{(s + 0.1)(s - 1)}$$

The characteristic equation of the system is given as

$$1 + G(s) = 0$$

or
$$(s + 0.1)(s - 1) + K(s + 1)(s + 2) = 0$$

or
$$(1 + K)s^2 + (3K - 0.9)s + (2K - 0.1) = 0 \quad \dots(i)$$

Applying Routh criteria

$$\begin{array}{rcc} s^2 & (1 + K) & (2K - 0.1) \\ s^1 & (3K - 0.9) & 0 \\ s^0 & (2K - 0.1) & 0 \end{array}$$

(i) No poles in right half s -plane (system stable)

$$K + 1 > 0 \quad \text{or} \quad K > -1$$

$$3K - 0.9 > 0 \quad \text{or} \quad K > 0.3$$

$$2K - 0.1 > 0 \quad \text{or} \quad K > 0.05$$

Hence, $K > 0.3$

(ii) 1 pole in right half s -plane (= one change of sign in first column terms)

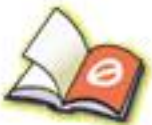
$$-1 < K < 0.05$$

(iii) 2 poles in right half s -plane (= two changes in sign in first column terms)

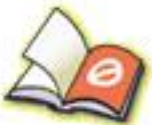
$$0.05 < K < 0.3$$



You have either reached a page that is unavailable for viewing or reached your viewing limit for this book.



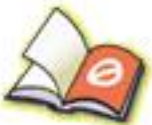
You have either reached a page that is unavailable for viewing or reached your viewing limit for this book.



You have either reached a page that is unavailable for viewing or reached your viewing limit for this book.



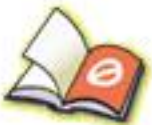
You have either reached a page that is unavailable for viewing or reached your viewing limit for this book.



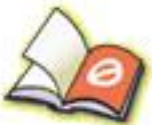
You have either reached a page that is unavailable for viewing or reached your viewing limit for this book.



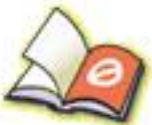
You have either reached a page that is unavailable for viewing or reached your viewing limit for this book.



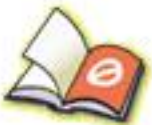
You have either reached a page that is unavailable for viewing or reached your viewing limit for this book.



You have either reached a page that is unavailable for viewing or reached your viewing limit for this book.



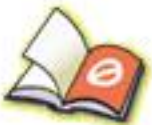
You have either reached a page that is unavailable for viewing or reached your viewing limit for this book.



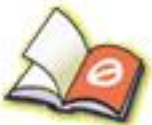
You have either reached a page that is unavailable for viewing or reached your viewing limit for this book.



You have either reached a page that is unavailable for viewing or reached your viewing limit for this book.



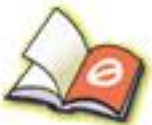
You have either reached a page that is unavailable for viewing or reached your viewing limit for this book.



You have either reached a page that is unavailable for viewing or reached your viewing limit for this book.



You have either reached a page that is unavailable for viewing or reached your viewing limit for this book.



You have either reached a page that is unavailable for viewing or reached your viewing limit for this book.



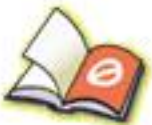
You have either reached a page that is unavailable for viewing or reached your viewing limit for this book.



You have either reached a page that is unavailable for viewing or reached your viewing limit for this book.



You have either reached a page that is unavailable for viewing or reached your viewing limit for this book.



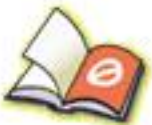
You have either reached a page that is unavailable for viewing or reached your viewing limit for this book.



You have either reached a page that is unavailable for viewing or reached your viewing limit for this book.



You have either reached a page that is unavailable for viewing or reached your viewing limit for this book.



You have either reached a page that is unavailable for viewing or reached your viewing limit for this book.

In case $m < n$, the open-loop transfer function has $(n - m)$ zeros at infinity. Examining the magnitude condition (7.15) in the form

$$\frac{\prod_{i=1}^m |(s + z_i)|}{\prod_{j=1}^n |(s + p_j)|} = \frac{1}{K}$$

we find that this is satisfied by $s \rightarrow \infty e^{j\phi}$ as $K \rightarrow \infty$. Therefore, $(n - m)$ branches of the root locus terminate on infinity.

Rule 3 : A point on the real axis lies on the locus if the number of open-loop poles plus zeros on the real axis to the right of this point is odd.

Consider the open-loop pole-zero configuration shown in Fig. 7.6. Let us examine any point s_0 on the real axis. As this point is joined by phasors to all the open-loop poles and zeros, it is easily seen that (i) the poles and zeros on the real axis to the right of this point contribute an angle of 180° each, (ii) the poles and zeros to the left of this point contribute an angle of 0° each, and (iii) the net angle contribution of a complex conjugate pole or zero pair is always zero. Therefore

$$\angle[G(s)H(s)] = (m_r - n_r)180^\circ = \pm (2q + 1) 180^\circ ; q = 0, 1, 2, \dots$$

where m_r = number of zeros on the right of s_0 ; and n_r = number of poles on the right of s_0 .

We therefore see that for a point on the real axis, the angle criterion is only met if $(n_r - m_r)$ or $(n_r + m_r)$ is odd and hence the rule. If this rule is satisfied at any point on the real axis, it continues to be satisfied as the point is moved on either side unless the point crosses a real axis pole or zero. By use of this additional fact, the real axis can be divided into segments on-locus and not-on-locus, the dividing points being the real open-loop poles and zeros. The on-locus segments of the real axis must alternate.

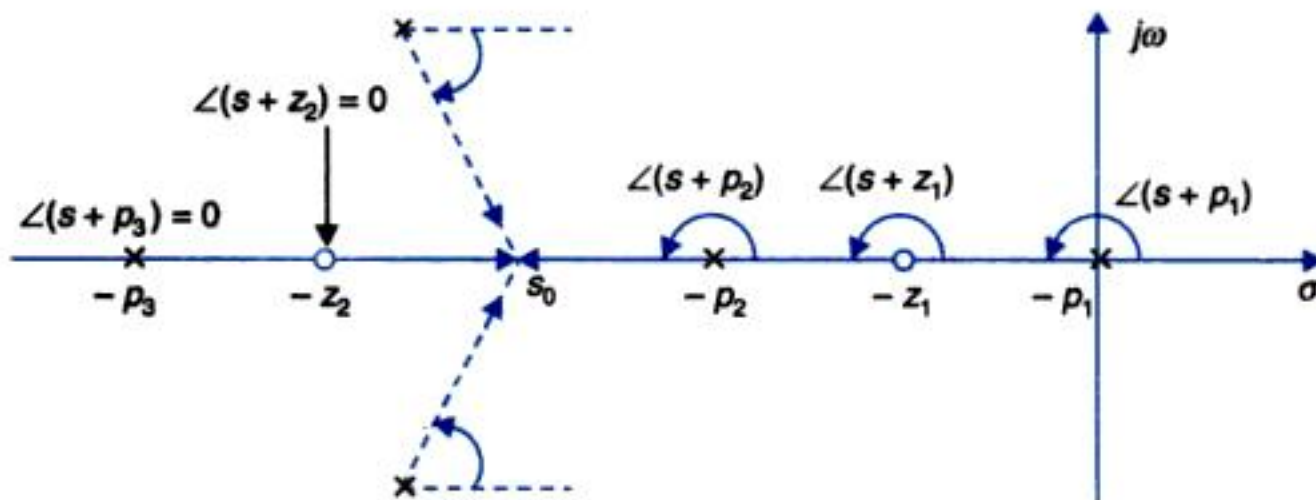


Fig. 7.6. Angle contributions for a point on the real axis.

Example 7.1 : Consider the system shown in Fig. 7.7 with the open-loop transfer function:

The open-loop pole-zero-configuration is shown in Fig. 7.8.

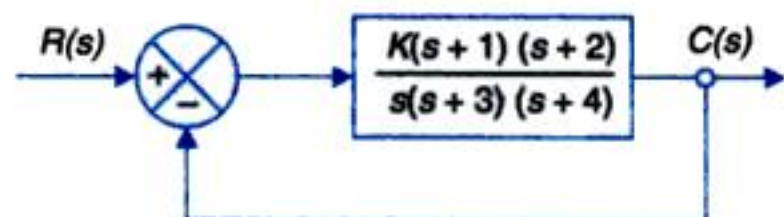


Fig. 7.7



You have either reached a page that is unavailable for viewing or reached your viewing limit for this book.



You have either reached a page that is unavailable for viewing or reached your viewing limit for this book.



You have either reached a page that is unavailable for viewing or reached your viewing limit for this book.



You have either reached a page that is unavailable for viewing or reached your viewing limit for this book.



You have either reached a page that is unavailable for viewing or reached your viewing limit for this book.

Breakaway Points on the Real Axis

We discuss below different methods of evaluating breakaway points on the real axis.

Method 1 : An analytical approach. This method requires the determination of the roots of the equation $dK/ds = 0$ to evaluate the breakaway points. The practical efficacy of the method is limited to third-order systems as in higher-order cases the determination of the roots of $dK/ds = 0$ in itself is a time-consuming job. The method is illustrated through the example below.

Example 7.3 : In the root locus plot of equation $1 + K/[s(s + 1)(s + 2)] = 0$ shown in Fig. 7.9 we found that there is a breakaway point on the real axis between 0 and -1 as the two real-root branches are oppositely directed on this segment.

From the characteristic equation, the gain K is given by

$$\begin{aligned} K &= -s(s + 1)(s + 2) \\ &= -(s^3 + 3s^2 + 2s) \end{aligned} \quad \dots(7.31)$$

Differentiating eqn. (7.31), we get

$$\frac{dK}{ds} = -(3s^2 + 6s + 2)$$

The roots of the equation $dK/ds = 0$ are

$$s_{1,2} = \frac{-6 \pm \sqrt{(36 - 24)}}{6} = -0.423, -1.577$$

Since the breakaway point must lie between 0 and -1 , it is clear that $s = -0.423$ corresponds to the actual breakaway point.

Method 2 : A graphical approach. It is a more practical method for determining the breakaway points. Along the real axis, the condition $dK/ds = 0$ implies that the gain K is extremized with respect to the real variable $s = \sigma$. A breakaway on the real axis may occur in two ways. First, a breakaway point may result from two real-root branches moving towards each other as K is increased. After the breakaway point these branches become complex-root branches. In this case K is increasing along the real axis from either side to the breakaway point. The condition $dK/ds = 0$, therefore results in maximization of K at the breakaway point. Secondly, a real axis breakaway point may occur with complex-root branches moving towards the real axis and meeting at the breakaway point. These branches then become real-root branches and move in opposite direction along the real axis as K is further increased. In this case K decreases as breakaway point is approached from either side of the real axis. Therefore, the condition $dK/ds = 0$ results in minimization of K at the breakaway point.

As an example of the first case consider the third-order system whose root locus plot is drawn in Fig. 7.9. Fig. 7.10 shows plot of K for this system for various values of s between 0 and -1 . The maximum value of K is 0.385 at $s = -0.423$. Thus the breakaway point occurs at $s = -0.423$ with $K = 0.385$.

An example of the second case is shown in the root locus plot of $1 + K(s + 2)/(s^2 + 2s + 2) = 0$ in Fig. 7.11.

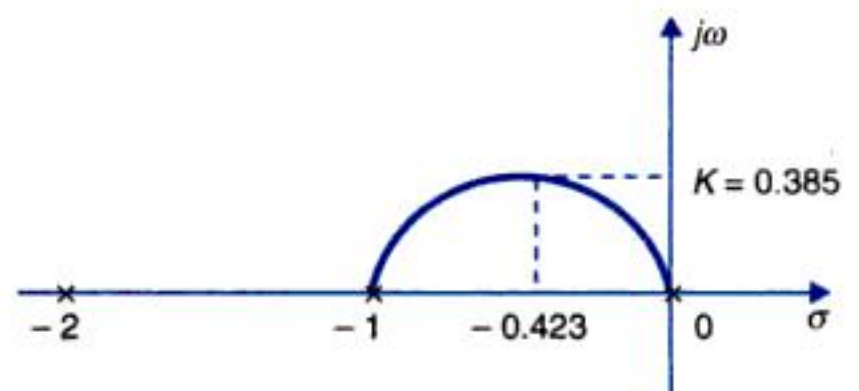


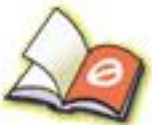
Fig. 7.10. Graphical evaluation of a real axis breakaway point.



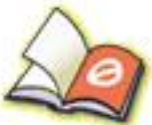
You have either reached a page that is unavailable for viewing or reached your viewing limit for this book.



You have either reached a page that is unavailable for viewing or reached your viewing limit for this book.



You have either reached a page that is unavailable for viewing or reached your viewing limit for this book.



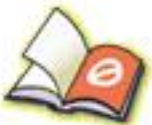
You have either reached a page that is unavailable for viewing or reached your viewing limit for this book.



You have either reached a page that is unavailable for viewing or reached your viewing limit for this book.



You have either reached a page that is unavailable for viewing or reached your viewing limit for this book.



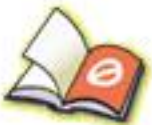
You have either reached a page that is unavailable for viewing or reached your viewing limit for this book.



You have either reached a page that is unavailable for viewing or reached your viewing limit for this book.



You have either reached a page that is unavailable for viewing or reached your viewing limit for this book.



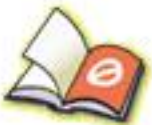
You have either reached a page that is unavailable for viewing or reached your viewing limit for this book.



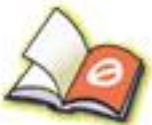
You have either reached a page that is unavailable for viewing or reached your viewing limit for this book.



You have either reached a page that is unavailable for viewing or reached your viewing limit for this book.



You have either reached a page that is unavailable for viewing or reached your viewing limit for this book.



You have either reached a page that is unavailable for viewing or reached your viewing limit for this book.

The root locus is plotted in Fig. 7.20.

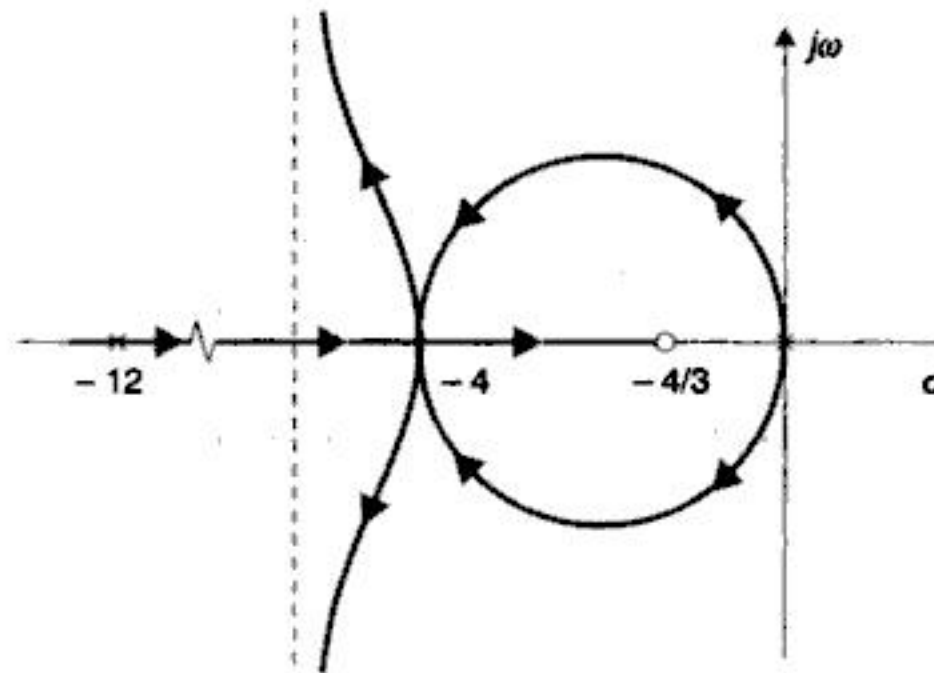


Fig. 7.20

Example 7.10 : In order to overcome the inherent instability of a helicopter (let us say w.r.t. pitch attitude), a stabilizing feedback loop is introduced in its autopilot system as shown in Fig. 7.21. The forward transfer function of the helicopter is estimated to be

$$G(s) = \frac{10(s + 0.04)}{(s + 0.5)(s^2 - 0.4s + 0.2)}$$

The feedback path transfer function is shown in the figure where the gain of the transfer function (K_h) is adjustable.

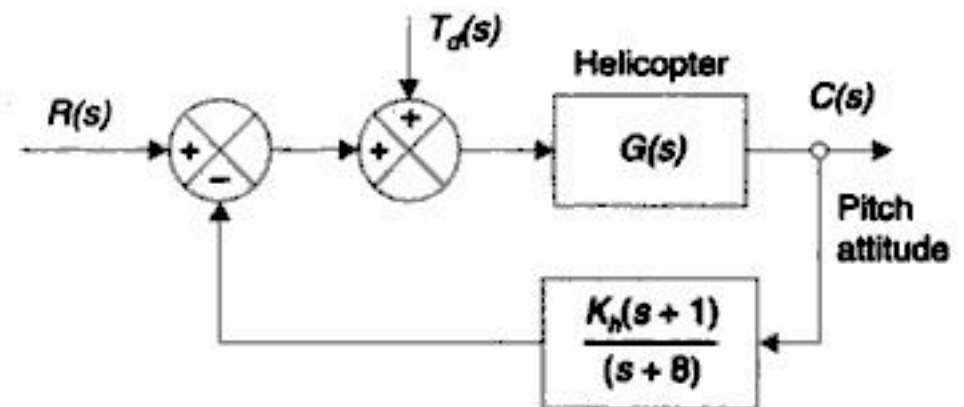


Fig. 7.21

Plot the root locus of the system with variable K_h and find its value for the closed-loop system to have a dominant pole damping of $1/\sqrt{2}$.

With this value of K_h , find the steady state error ($e = r - c$) caused by a wind gust disturbance of $T_d(s) = 1/s$ as shown in the block diagram.

Solution.

$$GH(s) = \frac{10K_h(s + 0.04)(s + 1)}{(s + 0.5)(s^2 - 0.4s + 0.2)(s + 8)}$$

Open-loop poles : $-0.5, 0.2 \pm j0.2, -8$

Open-loop zeros : $-0.04, -1$

Centroid of asymptotes is given by

$$-\sigma_A = \frac{(-8 - 0.5 + 0.2 + 0.2) - (-1 - 0.04)}{4 - 2} = -3.53$$

The root locus plot is drawn in Fig. 7.22 with $K = 10K_h$ as variable. We can now find the value of K at which the root locus crosses over to negative half of the s -plane. The system's characteristic equation is



You have either reached a page that is unavailable for viewing or reached your viewing limit for this book.



You have either reached a page that is unavailable for viewing or reached your viewing limit for this book.



You have either reached a page that is unavailable for viewing or reached your viewing limit for this book.

$$s^2(s + 1) + \alpha s(s + 1) + K = 0 \quad \text{or} \quad s^3 + (\alpha + 1)s^2 + \alpha s + K = 0$$

The Routh array is

| | | |
|-------|-----------------------------------------------|----------|
| s^3 | 1 | α |
| s^2 | $(\alpha + 1)$ | K |
| s^1 | $\frac{\alpha(\alpha + 1) - K}{(\alpha + 1)}$ | 0 |
| s^0 | K | |

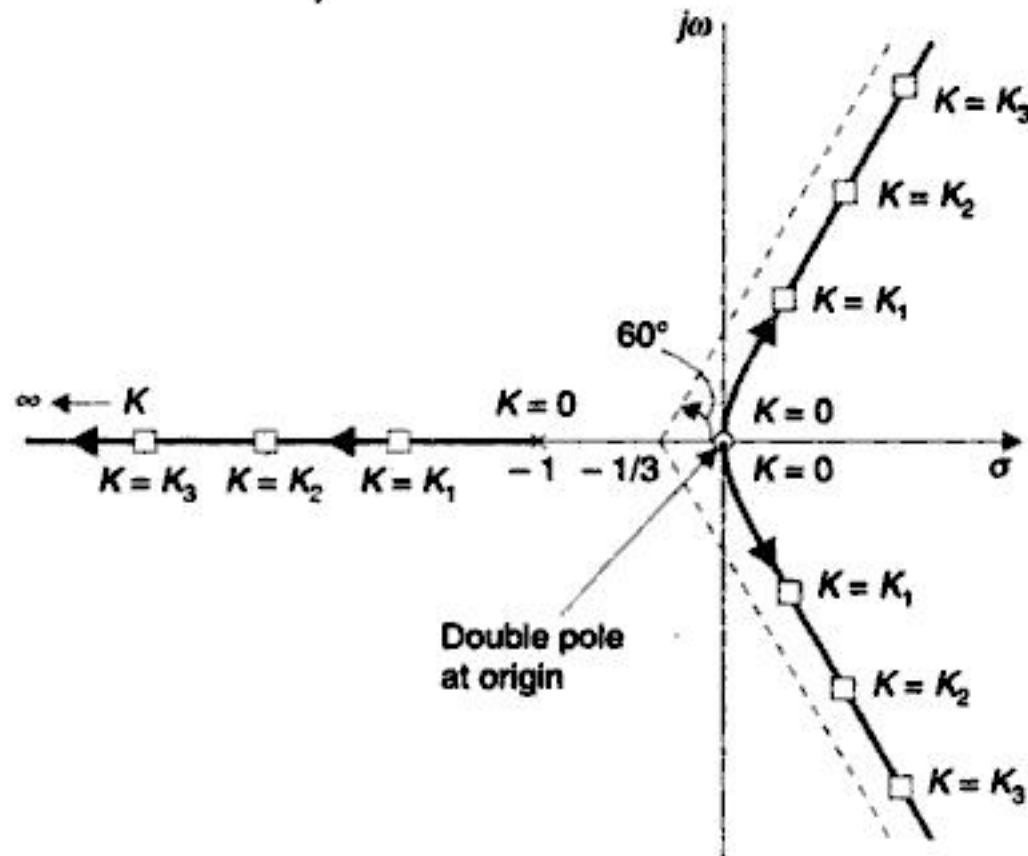


Fig. 7.24. (a) Root locus plot of the auxiliary characteristic equation $s^2(s + 1) + K = 0$.

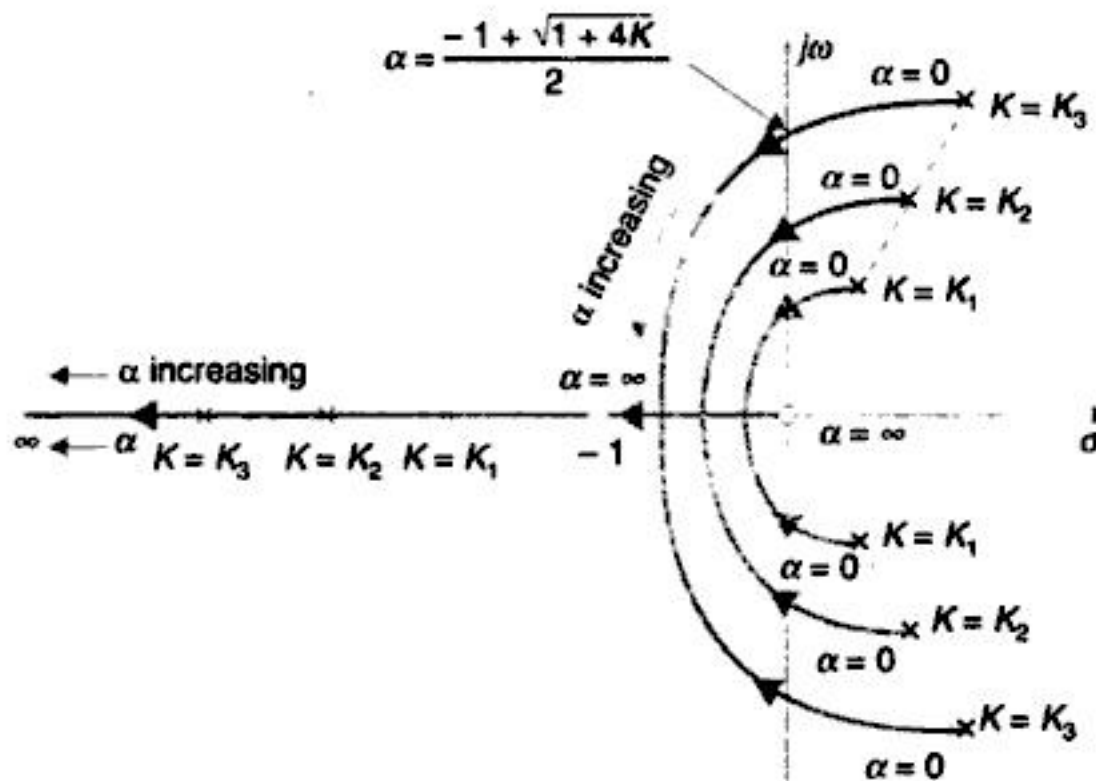


Fig. 7.24. (b) Root contours of $1 + K/s(s + 1)(s + \alpha) = 0$.

Therefore, the root contours cross the $j\omega$ -axis for

$$\alpha(\alpha + 1) - K = 0$$



You have either reached a page that is unavailable for viewing or reached your viewing limit for this book.



You have either reached a page that is unavailable for viewing or reached your viewing limit for this book.



You have either reached a page that is unavailable for viewing or reached your viewing limit for this book.

Comparing the above equation* with eqn. (7.5), we observe that the angle criterion given by eqn. (7.8) is now modified as

$$\angle P(s) = \pm 180^\circ (2q) ; q = 0, 1, 2, \dots$$

This leads to following modification in Rules 3, 4 and 7 of Table 7.1.

- (i) Replace 'odd number' by 'even number'.
- (ii) Replace ' $180^\circ (2q + 1)$ ' by ' $180^\circ (2q)$ '

The root locus plot for eqn. (7.45) with $\alpha = 2$ and $T = 1$ sec is shown in Fig. 7.27. This plot generally agrees with the exact plot in the region of small values of s where the dominant roots are located.

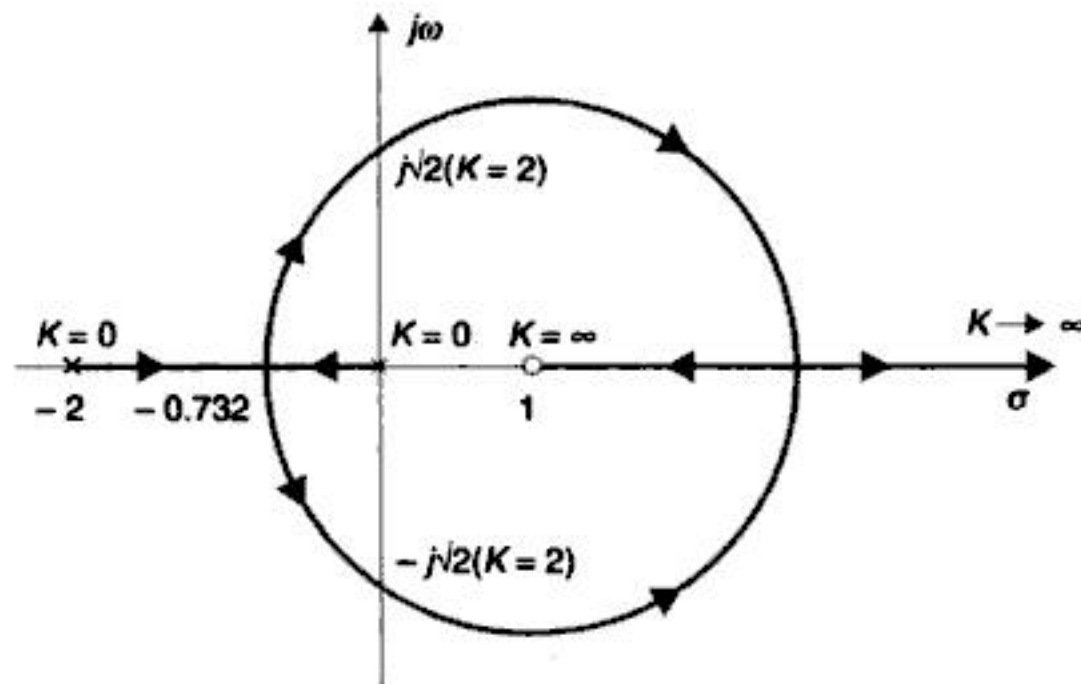


Fig. 7.27. Root locus plot of $1 + Ke^{-s}/[s(s+2)] = 0$ where e^{-s} is approximated as $(1-s)$.

7.6 SENSITIVITY OF THE ROOTS OF THE CHARACTERISTIC EQUATION

Earlier in Chapter 3 the sensitivity of the system transfer function $T(s)$ to variation of a parameter has been defined as

$$S_K^T = \frac{d(\ln T)}{d(\ln K)} = \frac{\partial T / T}{\partial K / K}$$

where K is the parameter of interest. Because of the importance of root locus as a design technique, it is useful to define the sensitivity of the roots of the characteristic equation (*i.e.*, the closed-loop poles of the system) to variation of a parameter K . This is defined as

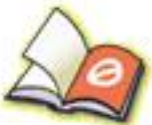
$$S_K^{-r_k} = \frac{\partial(-r_k)}{\partial(\ln K)} = \frac{\partial(-r_k)}{\partial K / K} \quad \dots(7.49)$$

where $-r_k$ is a root of the characteristic equation. In order that the system dynamic response be relatively unaffected by parameter changes, the system must be so designed that the roots of the characteristic equation and in particular the dominant roots are made insensitive to parameter changes, *i.e.*, the root sensitivity $S_K^{-r_k}$ is made less than a specified value.

*Such cases also occur in positive feedback systems.



You have either reached a page that is unavailable for viewing or reached your viewing limit for this book.



You have either reached a page that is unavailable for viewing or reached your viewing limit for this book.



You have either reached a page that is unavailable for viewing or reached your viewing limit for this book.



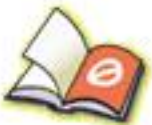
You have either reached a page that is unavailable for viewing or reached your viewing limit for this book.



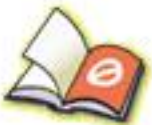
You have either reached a page that is unavailable for viewing or reached your viewing limit for this book.



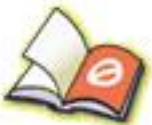
You have either reached a page that is unavailable for viewing or reached your viewing limit for this book.



You have either reached a page that is unavailable for viewing or reached your viewing limit for this book.



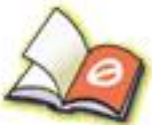
You have either reached a page that is unavailable for viewing or reached your viewing limit for this book.



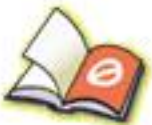
You have either reached a page that is unavailable for viewing or reached your viewing limit for this book.



You have either reached a page that is unavailable for viewing or reached your viewing limit for this book.



You have either reached a page that is unavailable for viewing or reached your viewing limit for this book.



You have either reached a page that is unavailable for viewing or reached your viewing limit for this book.



You have either reached a page that is unavailable for viewing or reached your viewing limit for this book.



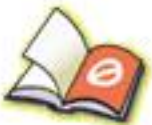
You have either reached a page that is unavailable for viewing or reached your viewing limit for this book.



You have either reached a page that is unavailable for viewing or reached your viewing limit for this book.



You have either reached a page that is unavailable for viewing or reached your viewing limit for this book.



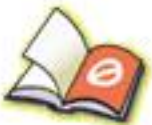
You have either reached a page that is unavailable for viewing or reached your viewing limit for this book.



You have either reached a page that is unavailable for viewing or reached your viewing limit for this book.



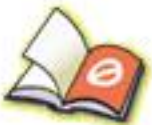
You have either reached a page that is unavailable for viewing or reached your viewing limit for this book.



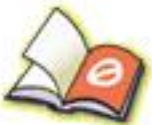
You have either reached a page that is unavailable for viewing or reached your viewing limit for this book.



You have either reached a page that is unavailable for viewing or reached your viewing limit for this book.



You have either reached a page that is unavailable for viewing or reached your viewing limit for this book.



You have either reached a page that is unavailable for viewing or reached your viewing limit for this book.

where r is the number of poles of $G(j\omega)$ at the origin, i.e., r is the system type number. For type-0, type-1 and type-2 systems, $K = K_p, K_v$ and K_a respectively.

From eqn. (8.20) the log-magnitude is given by

$$\begin{aligned}
 20 \log |G(j\omega)| &= 20 \log K + 20 \log |1 + j\omega T_a| + 20 \log |1 + j\omega T_b| + \dots \\
 &- 20r \log (\omega) - 20 \log |1 + j\omega T_1| - 20 \log |1 + j\omega T_2| \dots \\
 &- 20 \log |1 + j2\zeta(\omega/\omega_n) - (\omega/\omega_n)^2| \dots \quad \dots(8.21)
 \end{aligned}$$

and the phase angle is given by

$$\begin{aligned}
 \angle G(j\omega) &= \tan^{-1} \omega T_a + \tan^{-1} \omega T_b + \dots - r(90^\circ) - \tan^{-1} \omega T_1 \\
 &- \tan^{-1} \omega T_2 - \dots - \tan^{-1} \left(\frac{2\zeta\omega\omega_n}{\omega_n^2 - \omega^2} \right) \dots \quad \dots(8.22)
 \end{aligned}$$

From eqns. (8.21) and (8.22) it is seen that the Bode plots of $G(j\omega)$ may be obtained by adding the Bode plots of the factor of $G(j\omega)$, these factors are found to be of the forms given below:

1. Constant gain K
2. Poles at the origin $1/(j\omega)^r$
3. Pole on real axis $1/(1 + j\omega T)$
4. Zero on real axis $(1 + j\omega T)$
5. Complex conjugate poles $1/[1 + j2\zeta(\omega/\omega_n) - (\omega/\omega_n)^2]$
6. Complex conjugate zeros may also be present.

Let us now consider the plotting of each of these factors and the construction of the Bode plot for a given $G(j\omega)$ as sum of the plots of its individual factors.

Factors of the Form $K/(j\omega)^r$

The log-magnitude of this factors is

$$20 \log \left| \frac{K}{(j\omega)^r} \right| = - 20r \log \omega + 20 \log K \quad \dots(8.23)$$

and the phase is

$$\phi(\omega) = - 90^\circ r$$

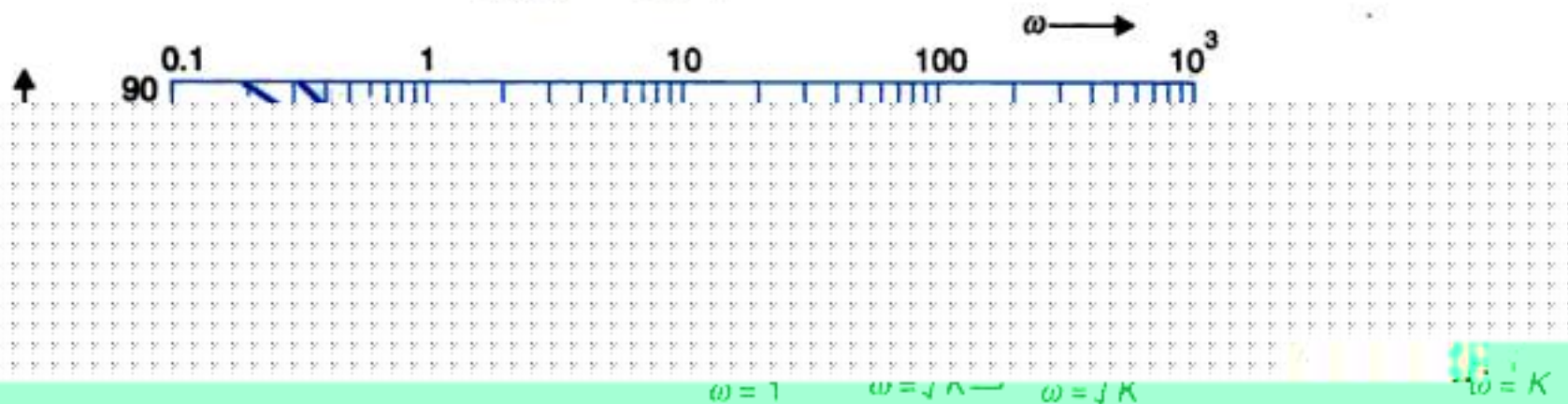
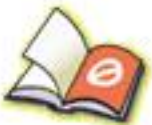
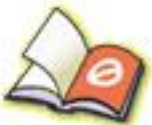


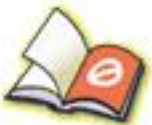
Fig. 8.12. Log-magnitude plot of $K/(j\omega)^r$.



You have either reached a page that is unavailable for viewing or reached your viewing limit for this book.



You have either reached a page that is unavailable for viewing or reached your viewing limit for this book.



You have either reached a page that is unavailable for viewing or reached your viewing limit for this book.

3. Knowing the corner frequencies, draw the asymptotic magnitude plot. This plot consists of straight line segments with line slope changing at each corner frequency by + 20 db/decade for a zero and - 20 db/decade for a pole ($\pm 20 m$ db/decade for a zero or pole multiplicity m). For a complex conjugate zero or pole the slope changes by ± 40 db/decade ($\pm 40 m$ db/decade for complex conjugate zero or pole of multiplicity m).

4. From the error graphs of Figs. 8.11 and 8.15, determine the corrections to be applied to the asymptotic plot.

5. Draw a smooth curve through the corrected points such that it is asymptotic to the line segments. This gives the actual log-magnitude plot.

6. Draw phase angle curve for each factor and add them algebraically to get the phase plot.

To illustrate the technique, let us draw the Bode plot for the transfer function

$$G(s) = \frac{64(s + 2)}{s(s + 0.5)(s^2 + 3.2s + 64)}$$

The rearrangement of the transfer function in the time-constant form gives

$$G(s) = \frac{4(1 + s/2)}{s(1 + 2s)(1 + 0.05s + s^2/64)}$$

Therefore, the sinusoidal transfer function in the time-constant form is given by

$$G(j\omega) = \frac{4(1 + j\omega/2)}{j\omega(1 + 2j\omega)[1 + j0.4(\omega/8) - (\omega/8)^2]} \quad \dots(8.25)$$

The factors of this transfer function in order of their occurrence as frequency increases, are

1. Constant gain, $K = 4$
2. Pole at origin, $1/j\omega$
3. Pole at $s = -0.5$; corner frequency $\omega_1 = 0.5$
4. Zero at $s = -2$; corner frequency $\omega_2 = 2$
5. Pair of complex conjugate poles with $\zeta = 0.2$, $\omega_n = 8$; corner frequency $\omega_3 = 8$.

The pertinent characteristics of each factor of the transfer function are given in Table 8.2.

Table 8.2 Asymptotic Approximation Table for Construction of Bode Plot of

$$\frac{4(1 + j\omega/2)}{j\omega(1 + j2\omega)[1 + j0.4(\omega/8) - (\omega/8)^2]}$$

| Factor | Corner frequency | Asymptotic log-magnitude characteristic | Phase angle characteristic |
|--------------------|------------------|------------------------------------------------------------------------------------------------------------------|-----------------------------------------------------------------------------|
| $4/j\omega$ | None | Straight line of constant slope -20 db/decade, passing through $20 \log 4 = 12$ db point at $\omega = 1$ | Constant -90° |
| $1/(1 + j2\omega)$ | $\omega_1 = 0.5$ | Straight line of the 0 db for $\omega < \omega_1$, straight line of slope -20 db/decade for $\omega > \omega_1$ | Phase angle varies, from 0 to -90° , angle at $\omega_1 = -45^\circ$ |

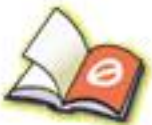
(Contd.)...



You have either reached a page that is unavailable for viewing or reached your viewing limit for this book.



You have either reached a page that is unavailable for viewing or reached your viewing limit for this book.



You have either reached a page that is unavailable for viewing or reached your viewing limit for this book.



You have either reached a page that is unavailable for viewing or reached your viewing limit for this book.



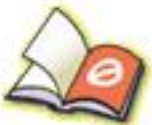
You have either reached a page that is unavailable for viewing or reached your viewing limit for this book.



You have either reached a page that is unavailable for viewing or reached your viewing limit for this book.



You have either reached a page that is unavailable for viewing or reached your viewing limit for this book.



You have either reached a page that is unavailable for viewing or reached your viewing limit for this book.



You have either reached a page that is unavailable for viewing or reached your viewing limit for this book.



You have either reached a page that is unavailable for viewing or reached your viewing limit for this book.



You have either reached a page that is unavailable for viewing or reached your viewing limit for this book.



You have either reached a page that is unavailable for viewing or reached your viewing limit for this book.



You have either reached a page that is unavailable for viewing or reached your viewing limit for this book.



You have either reached a page that is unavailable for viewing or reached your viewing limit for this book.



You have either reached a page that is unavailable for viewing or reached your viewing limit for this book.



You have either reached a page that is unavailable for viewing or reached your viewing limit for this book.

From Fig. 9.2(a) it is found that as the point s follows the prescribed path (i.e., clockwise direction) on the s -plane contour, eventually returning to the starting point, the phasor $(s - \alpha_1)$ generates a net angle of -2π , while all other phasors generate zero net angles. Therefore the $q(s)$ -phasor undergoes a net phase change of -2π . This implies that the tip of the $q(s)$ -phasor must describe a closed contour about the origin of the $q(s)$ -plane in the clockwise direction as shown in Fig. 9.2(b). As said earlier, the exact shape of the closed contour in the $q(s)$ -plane is not of interest to us, but it is sufficient for us to observe that this contour encircles the origin once. If the contour in the s -plane is so chosen that it does not enclose any zero or pole, the corresponding contour in the $q(s)$ -plane then will not encircle the origin. If the s -plane contour encloses two zeros, say at $s = \alpha_1$ and $s = \alpha_2$, the $q(s)$ -plane contour encircles the origin twice in the clockwise direction as shown in Fig. 9.3. Generalizing, we can say that for each zero of $q(s)$ enclosed by the s -plane contour, the corresponding $q(s)$ -plane contour encircles the origin once in the clockwise direction.

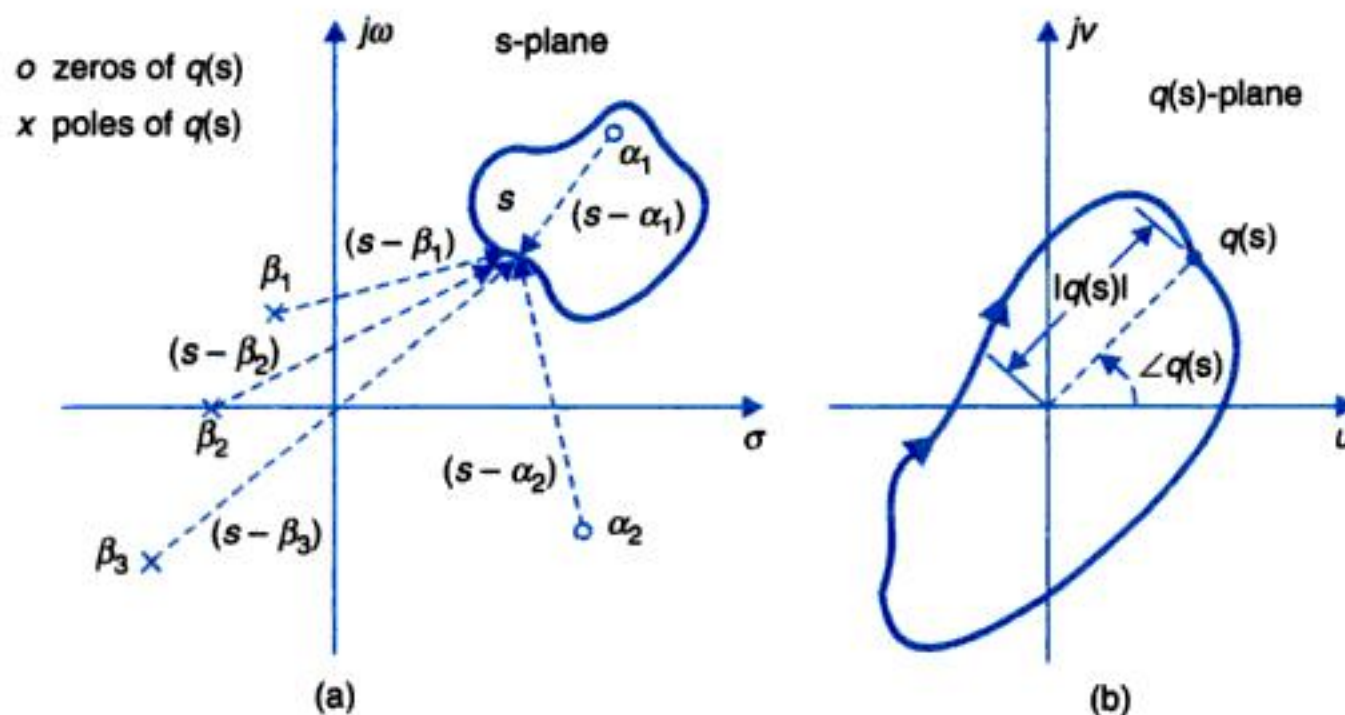


Fig. 9.2. An s -plane contour enclosing a zero of $q(s)$ and the corresponding $q(s)$ -plane contour.

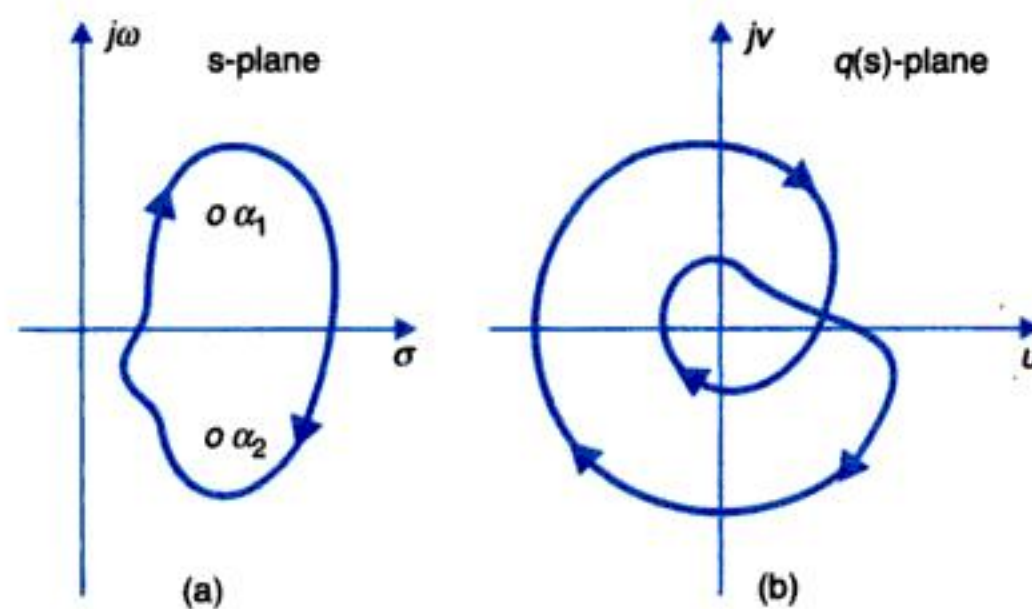
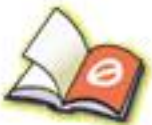


Fig. 9.3. An s -plane contour enclosing two zeros of $q(s)$ and the corresponding $q(s)$ -plane contour.



You have either reached a page that is unavailable for viewing or reached your viewing limit for this book.



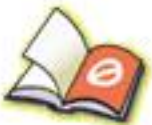
You have either reached a page that is unavailable for viewing or reached your viewing limit for this book.



You have either reached a page that is unavailable for viewing or reached your viewing limit for this book.



You have either reached a page that is unavailable for viewing or reached your viewing limit for this book.



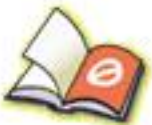
You have either reached a page that is unavailable for viewing or reached your viewing limit for this book.



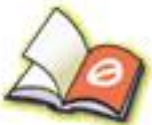
You have either reached a page that is unavailable for viewing or reached your viewing limit for this book.



You have either reached a page that is unavailable for viewing or reached your viewing limit for this book.



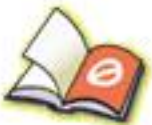
You have either reached a page that is unavailable for viewing or reached your viewing limit for this book.



You have either reached a page that is unavailable for viewing or reached your viewing limit for this book.



You have either reached a page that is unavailable for viewing or reached your viewing limit for this book.



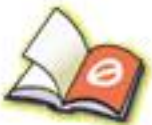
You have either reached a page that is unavailable for viewing or reached your viewing limit for this book.



You have either reached a page that is unavailable for viewing or reached your viewing limit for this book.



You have either reached a page that is unavailable for viewing or reached your viewing limit for this book.



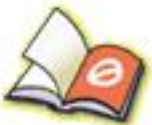
You have either reached a page that is unavailable for viewing or reached your viewing limit for this book.



You have either reached a page that is unavailable for viewing or reached your viewing limit for this book.



You have either reached a page that is unavailable for viewing or reached your viewing limit for this book.



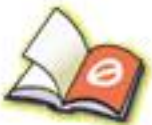
You have either reached a page that is unavailable for viewing or reached your viewing limit for this book.



You have either reached a page that is unavailable for viewing or reached your viewing limit for this book.



You have either reached a page that is unavailable for viewing or reached your viewing limit for this book.



You have either reached a page that is unavailable for viewing or reached your viewing limit for this book.

The Nyquist plot intersects the real axis at a point where

$$G(j\omega) = \frac{K}{j\omega(j0.2\omega + 1)(j0.05\omega + 1)} = \frac{K}{-0.25\omega^2 + j\omega(1 - 0.01\omega^2)} \quad \dots(9.21)$$

is real. Setting the imaginary part of eqn. (9.21) equal to zero, we have

$$\omega = \omega_2 = 10 \text{ rad/sec}$$

Now $|G(j\omega)|_{\omega=\omega_2} = \frac{K}{0.25(10)^2} = a = 0.1$

which gives $K = 2.5$

(ii) Let $\omega = \omega_1$ be the gain cross-over frequency. Then for a PM of 40°

$$-90^\circ - \tan^{-1} 0.2\omega_1 - \tan^{-1} 0.05\omega_1 + 180^\circ = 40^\circ$$

or $\tan^{-1} 0.2\omega_1 + \tan^{-1} 0.05\omega_1 = 50^\circ$

$$\frac{0.25\omega_1}{1 - 0.01\omega_1^2} = \tan 50^\circ = 1.2$$

or $0.012\omega_1^2 + 0.25\omega_1 - 1.2 = 0$

Solving for positive value of ω_1 , we get

$$\omega_1 = 4 \text{ rad/sec}$$

Hence $|G(j\omega)|_{\omega=\omega_1} = \frac{K}{\omega_1 \sqrt{[1 + (0.2\omega_1)^2]} \sqrt{[1 + (0.05\omega_1)^2]}} = 1$

which gives $K = 5.2$.

Example 9.11 : Let us determine the gain margin and phase margin of a unity feedback system having an open-loop transfer function

$$G(j\omega) = \frac{10}{j\omega(j0.1\omega + 1)(j0.05\omega + 1)}$$

by use of Bode plot.

The Bode plot of $G(j\omega)$ is shown in Fig. 9.27. From this figure, it is seen that GM = 9.5 db and PM 33° .

Let us now use the Bode plot for adjustment of the system gain for a specified GM or PM. Suppose it is desired to find the open-loop gain for (i) a GM of 20 db; and (ii) a PM of 24° .

(i) A GM of 20 db will be obtained if the log-magnitude plot in Fig. 9.27 is shifted downwards by $(20 - 9.5) = 10.5$ db. The system gain must therefore be reduced by 10.5 db or by a factor of 3.3. The corresponding open-loop gain is $10/3.3 \approx 3$.

(ii) From Fig. 9.27, it is observed that if the gain cross-over frequency is changed to 9.3 rad/sec, a PM of 24° is obtained. To change the gain cross-over frequency to 9.3 rad/sec, the log-magnitude curve should be raised upwards by 3.5 db or system gain should be raised upwards by 3.5 db or system gain should be increased by a factor of 1.5. Hence the open-loop gain for a PM of 24° is $10 \times 1.5 = 15$.



You have either reached a page that is unavailable for viewing or reached your viewing limit for this book.



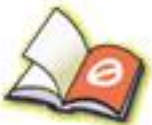
You have either reached a page that is unavailable for viewing or reached your viewing limit for this book.



You have either reached a page that is unavailable for viewing or reached your viewing limit for this book.



You have either reached a page that is unavailable for viewing or reached your viewing limit for this book.



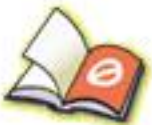
You have either reached a page that is unavailable for viewing or reached your viewing limit for this book.



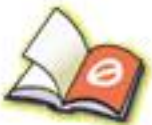
You have either reached a page that is unavailable for viewing or reached your viewing limit for this book.



You have either reached a page that is unavailable for viewing or reached your viewing limit for this book.



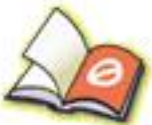
You have either reached a page that is unavailable for viewing or reached your viewing limit for this book.



You have either reached a page that is unavailable for viewing or reached your viewing limit for this book.



You have either reached a page that is unavailable for viewing or reached your viewing limit for this book.



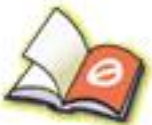
You have either reached a page that is unavailable for viewing or reached your viewing limit for this book.



You have either reached a page that is unavailable for viewing or reached your viewing limit for this book.



You have either reached a page that is unavailable for viewing or reached your viewing limit for this book.



You have either reached a page that is unavailable for viewing or reached your viewing limit for this book.



You have either reached a page that is unavailable for viewing or reached your viewing limit for this book.



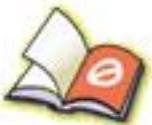
You have either reached a page that is unavailable for viewing or reached your viewing limit for this book.



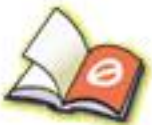
You have either reached a page that is unavailable for viewing or reached your viewing limit for this book.



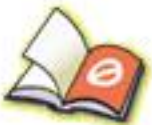
You have either reached a page that is unavailable for viewing or reached your viewing limit for this book.



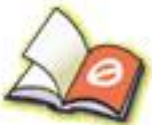
You have either reached a page that is unavailable for viewing or reached your viewing limit for this book.



You have either reached a page that is unavailable for viewing or reached your viewing limit for this book.



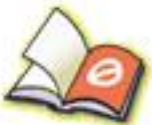
You have either reached a page that is unavailable for viewing or reached your viewing limit for this book.



You have either reached a page that is unavailable for viewing or reached your viewing limit for this book.



You have either reached a page that is unavailable for viewing or reached your viewing limit for this book.



You have either reached a page that is unavailable for viewing or reached your viewing limit for this book.



You have either reached a page that is unavailable for viewing or reached your viewing limit for this book.



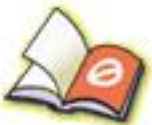
You have either reached a page that is unavailable for viewing or reached your viewing limit for this book.



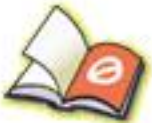
You have either reached a page that is unavailable for viewing or reached your viewing limit for this book.



You have either reached a page that is unavailable for viewing or reached your viewing limit for this book.



You have either reached a page that is unavailable for viewing or reached your viewing limit for this book.



You have either reached a page that is unavailable for viewing or reached your viewing limit for this book.

$$G_c(s) = \frac{(s + z_c)}{(s + p_c)} = \frac{(s + 1/\tau)}{(s + 1/\beta\tau)}; \beta = \frac{z_c}{p_c} \quad \dots(10.16)$$

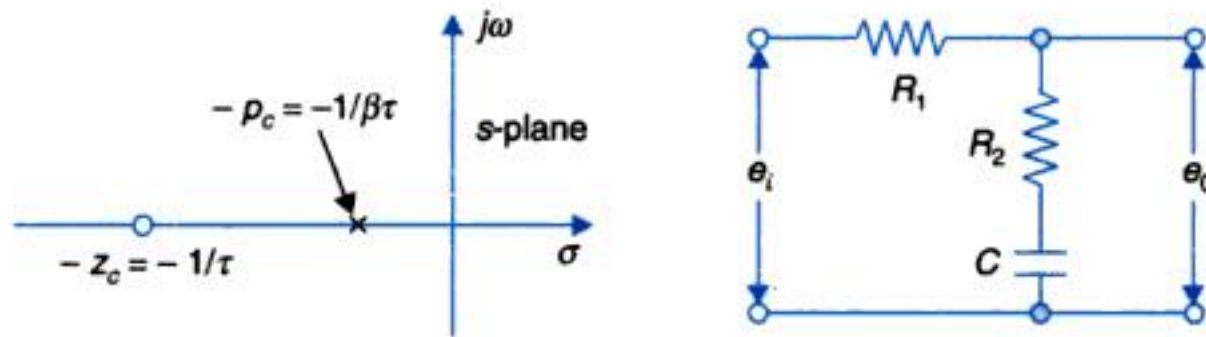


Fig. 10.13. (a) The s -plane representation of lag compensator; and (b) electric lag network.

The realization of the transfer function of eqn. (10.16) is achieved with an electric lag network shown in Fig. 10.13 (b) from which we can write

$$\frac{E_0(s)}{E_i(s)} = \frac{R_2 + \frac{1}{sC}}{R_1 + R_2 + \frac{1}{sC}} = \frac{1}{R_1 + R_2} \left[\frac{s + (1/R_2C)}{s + \frac{1}{\left(\frac{R_1 + R_2}{R_2}\right)R_2C}} \right] \quad \dots(10.17)$$

Comparing eqns. (10.16) and (10.17), we get

$$\tau = R_2C, \beta = (R_1 + R_2)/R_2 > 1$$

Therefore, the transfer function of the network becomes

$$G_c(s) = \frac{1}{\beta} \left(\frac{s + 1/\tau}{s + 1/\beta\tau} \right) = \frac{1}{\beta} \left(\frac{s + z_c}{s + p_c} \right); \beta = z_c/p_c > 1 \quad \dots(10.18)$$

$$= \frac{\tau s + 1}{\beta\tau s + 1} \quad \dots(10.19)$$

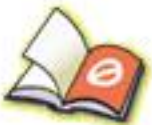
It is to be noted that compared to the form of transfer function (10.16) $G_c(s)$ realized by the network has a multiplicative factor of $1/\beta$. As in the case of lead network realization, we have an additional degree of freedom in the lag network realization also, which is used for impedance matching.

The sinusoidal transfer function of the lag network is given by

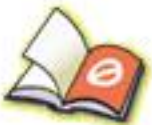
$$G_c(j\omega) = \frac{(1 + j\omega\tau)}{(1 + j\beta\omega\tau)} \quad \dots(10.20)$$

Since $\beta > 1$, the steady-state output has a lagging phase angle with respect to the sinusoidal input and hence the name lag network. The Bode diagram of the lag network is drawn in Fig. 10.14. The maximum phase lag ϕ_m and the corresponding frequency ω_m are obtained from eqns. (10.14) and (10.13) respectively by replacing α with β .

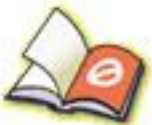
From Fig. 10.14 it is observed that the lag network has a d.c. gain of unity while it offers a high frequency gain of $1/\beta$. Since $\beta > 1$, it means that the high frequency noise is attenuated



You have either reached a page that is unavailable for viewing or reached your viewing limit for this book.



You have either reached a page that is unavailable for viewing or reached your viewing limit for this book.



You have either reached a page that is unavailable for viewing or reached your viewing limit for this book.



You have either reached a page that is unavailable for viewing or reached your viewing limit for this book.



You have either reached a page that is unavailable for viewing or reached your viewing limit for this book.

The system is to be compensated to meet the following specifications:

Damping ratio $\zeta = 0.5$

Undamped natural frequency $\omega_n = 2$

Using the transient response specifications the desired dominant closed-loop poles are found to lie at

$$s_d = -1 \pm j1.73$$

From Fig. 10.23, the angle contribution required from the lead compensator pole-zero pair is

$$\phi = -180^\circ - \angle G_f(s_d) = -180^\circ - (-120^\circ - 90^\circ - 30^\circ) = 60^\circ$$

Further it is observed that the open-loop pole at $s = -1$ lies directly below the desired closed-loop pole location. Place the compensator zero close to this pole to its left, say at $s = -1.2$. Such a choice of compensator zero generally ensures the dominance condition.

Join the compensator zero to s_d and locate the compensator pole by making an angle of $\phi = 60^\circ$ as shown in Fig. 10.23. The location of the pole is found to be at -4.95 .

Open-loop and closed-loop transfer function gains in pole-zero form are equal for unity feedback system. The value of this gain has to such that $C(s)/R(s)|_{s=0} = 1$, as this system is type-1. We then find from the closed-loop poles and zeros that

$$\text{Gain } K = \frac{4 \times 1.35 \times 6.65}{12} \approx 30$$

The open-loop transfer function of the compensated system becomes

$$G(s) = \frac{30(s + 1.2)}{s(s + 1)(s + 4)(s + 4.95)}$$

The velocity error constant is

$$K_v = \lim_{s \rightarrow 0} sG(s) = \frac{30 \times 1.2}{1 \times 4 \times 4.95} = 1.82$$

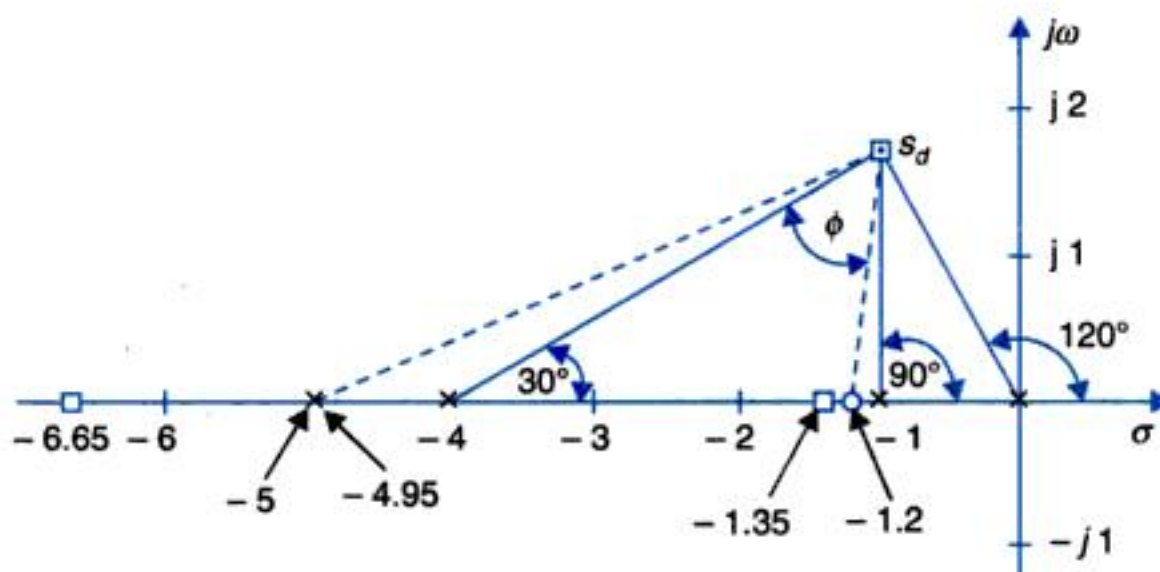
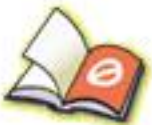


Fig. 10.23. Design of lead compensator for Example 10.3.

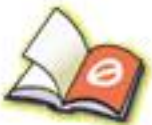
It must be understood here that only a marginal increase in K_v above this value can be achieved by a slight readjustment of the compensating zero. Any large shift in the compensating zero would result in violation of the dominance condition.



You have either reached a page that is unavailable for viewing or reached your viewing limit for this book.



You have either reached a page that is unavailable for viewing or reached your viewing limit for this book.



You have either reached a page that is unavailable for viewing or reached your viewing limit for this book.

Its characteristic equation is

$$1 + G_c(s)G(s) = 0 \quad \text{or} \quad s(s+4) + K(s+\alpha) = 0$$

$$\text{or} \quad s^2 + (4+k)s + K\alpha = 0 \quad \dots(ii)$$

Required :

$$M_p = e^{-\pi\xi/\sqrt{4-\xi^2}} = 0.2$$

which yields

$$\xi = 0.456$$

Settling time

$$t_s = \frac{4}{\xi\omega_n} = 1$$

which gives $\omega_n = \frac{4}{0.456} = 8.77$ rad/sec.

From the characteristic equation

$$K\alpha = \omega_n^2 = (8.77)^2 = 76.9$$

$$K + 4 = 2\xi\omega_n = 8$$

Solving we get

$$K = 4, \quad \alpha = 19.23$$

Transfer function of prefilter

$$G_p(s) = \frac{1}{s+19.23}$$

(b)

$$R(s) = \frac{1}{s^2}, \text{ unit ramp}$$

$$e_{ss} = \lim_{s \rightarrow 0} \frac{1}{sG_c(s)G(s)} = \lim_{s \rightarrow 0} \frac{(s+4)}{K(s+\alpha)} = \frac{4}{K\alpha}$$

or

$$e_{ss} = \frac{4}{4 \times 19.23} = 0.05$$

The reader may verify that the compensated system has zero steady-state error to unit step input.

Example 10.6: A unity feedback control system has open-loop transfer function

$$G(s) = \frac{K}{s(s+50)}$$

Design a *PI* controller

$$G_c(s) = \frac{s+\alpha}{s}$$

to meet the following specifications

$$(i) M_p = 20\% \text{ and} \quad (ii) t_s = 2 \text{ sec.}$$

Solution. Forward path transfer function of the compensated system

$$G_c(s)G(s) = \frac{K(s+\alpha)}{s^2(s+50)}$$

Poles 0, 0, -50; Zero - α (to be found). Converting specifications to desired root location (complex conjugate)

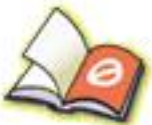
$$M_p = 20\% \quad \Rightarrow \quad \xi = 0.456, \text{ angle } \xi - \text{line} = 63^\circ$$



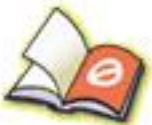
You have either reached a page that is unavailable for viewing or reached your viewing limit for this book.



You have either reached a page that is unavailable for viewing or reached your viewing limit for this book.



You have either reached a page that is unavailable for viewing or reached your viewing limit for this book.



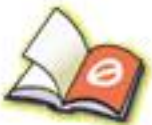
You have either reached a page that is unavailable for viewing or reached your viewing limit for this book.



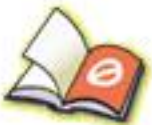
You have either reached a page that is unavailable for viewing or reached your viewing limit for this book.



You have either reached a page that is unavailable for viewing or reached your viewing limit for this book.



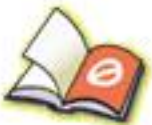
You have either reached a page that is unavailable for viewing or reached your viewing limit for this book.



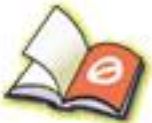
You have either reached a page that is unavailable for viewing or reached your viewing limit for this book.



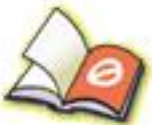
You have either reached a page that is unavailable for viewing or reached your viewing limit for this book.



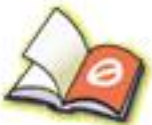
You have either reached a page that is unavailable for viewing or reached your viewing limit for this book.



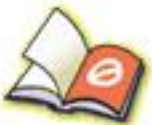
You have either reached a page that is unavailable for viewing or reached your viewing limit for this book.



You have either reached a page that is unavailable for viewing or reached your viewing limit for this book.



You have either reached a page that is unavailable for viewing or reached your viewing limit for this book.



You have either reached a page that is unavailable for viewing or reached your viewing limit for this book.



You have either reached a page that is unavailable for viewing or reached your viewing limit for this book.



You have either reached a page that is unavailable for viewing or reached your viewing limit for this book.



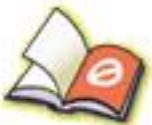
You have either reached a page that is unavailable for viewing or reached your viewing limit for this book.



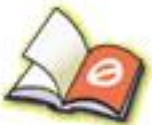
You have either reached a page that is unavailable for viewing or reached your viewing limit for this book.



You have either reached a page that is unavailable for viewing or reached your viewing limit for this book.



You have either reached a page that is unavailable for viewing or reached your viewing limit for this book.



You have either reached a page that is unavailable for viewing or reached your viewing limit for this book.



You have either reached a page that is unavailable for viewing or reached your viewing limit for this book.



You have either reached a page that is unavailable for viewing or reached your viewing limit for this book.



You have either reached a page that is unavailable for viewing or reached your viewing limit for this book.



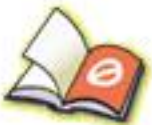
You have either reached a page that is unavailable for viewing or reached your viewing limit for this book.



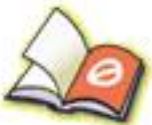
You have either reached a page that is unavailable for viewing or reached your viewing limit for this book.



You have either reached a page that is unavailable for viewing or reached your viewing limit for this book.



You have either reached a page that is unavailable for viewing or reached your viewing limit for this book.



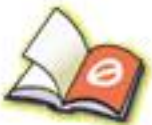
You have either reached a page that is unavailable for viewing or reached your viewing limit for this book.



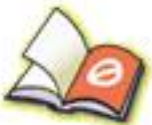
You have either reached a page that is unavailable for viewing or reached your viewing limit for this book.



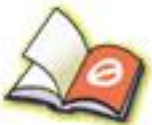
You have either reached a page that is unavailable for viewing or reached your viewing limit for this book.



You have either reached a page that is unavailable for viewing or reached your viewing limit for this book.



You have either reached a page that is unavailable for viewing or reached your viewing limit for this book.



You have either reached a page that is unavailable for viewing or reached your viewing limit for this book.

- 10.2.** A servomechanism has an open-loop transfer function of

$$G(s) = \frac{10}{s(1 + 0.5s)(1 + 0.1s)}$$

Draw the Bode plot and determine the phase and gain margins. A network having the transfer function $(1 + 0.23s)/(1 + 0.23s)$ is now introduced in tandem. Determine the new gain and phase margins. Comment upon the improvement in system response caused by the network.

- 10.3.** A unity feedback control system has an open-loop transfer function of

$$G(s) = 1/s^2$$

Design a suitable compensating network such that a phase margin of 45° is achieved without sacrificing system velocity error constant. Sketch the Bode plot of the uncompensated and compensated systems.

- 10.4.** A unity feedback system has an open-loop transfer function of

$$G(s) = \frac{4}{s(2s + 1)}$$

It is desired to obtain a phase margin of 40° without sacrificing the K_v of the system. Design a suitable lag-network and compute the value of network components assuming any suitable impedance level.

- 10.5.** A unity feedback system is characterized by the open-loop transfer function

$$G(s) = \frac{K}{s(s + 3)(s + 9)}$$

- (a) Determine the value of K if 20% overshoot to a step input is desired.
 (b) For the above value of K determine the settling time and K_v (velocity error constant).
 (c) Design a cascade compensator that will give approximately 15% overshoot to a unit step input, while the settling time is decreased by a factor of 2.5 and $K_v \geq 20$.

- 10.6.** Consider the system shown in Fig. P-10.6. Design a lead compensator for this system to meet the following specifications:

Damping ratio $\zeta = 0.7$

Settling time $t_s = 1.4$ sec

Velocity error constant $K_v = 2 \text{ sec}^{-1}$.

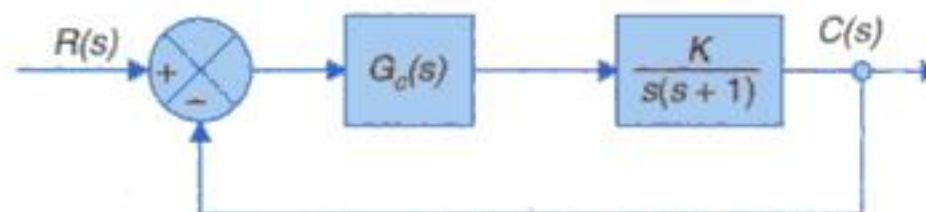


Fig. P-10.6

- 10.7.** Design a phase-lead compensator for the system shown in Fig. P-10.6, to satisfy the following specifications :

(i) The phase margin of the system must be greater than 45° .

(ii) Steady-state error for a unit step input should be less than 1/15 deg per deg/sec of the final output velocity.

(iii) The gain cross-over frequency of the system must be less than 7.5 rad/sec.

- 10.8.** A unity feedback system has an open-loop transfer function

$$G(s) = \frac{K}{s(s + 1)(0.2s + 1)}$$



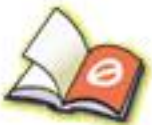
You have either reached a page that is unavailable for viewing or reached your viewing limit for this book.



You have either reached a page that is unavailable for viewing or reached your viewing limit for this book.



You have either reached a page that is unavailable for viewing or reached your viewing limit for this book.



You have either reached a page that is unavailable for viewing or reached your viewing limit for this book.



You have either reached a page that is unavailable for viewing or reached your viewing limit for this book.



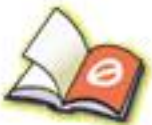
You have either reached a page that is unavailable for viewing or reached your viewing limit for this book.



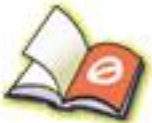
You have either reached a page that is unavailable for viewing or reached your viewing limit for this book.



You have either reached a page that is unavailable for viewing or reached your viewing limit for this book.



You have either reached a page that is unavailable for viewing or reached your viewing limit for this book.



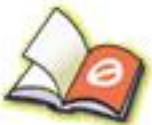
You have either reached a page that is unavailable for viewing or reached your viewing limit for this book.



You have either reached a page that is unavailable for viewing or reached your viewing limit for this book.



You have either reached a page that is unavailable for viewing or reached your viewing limit for this book.



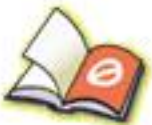
You have either reached a page that is unavailable for viewing or reached your viewing limit for this book.



You have either reached a page that is unavailable for viewing or reached your viewing limit for this book.



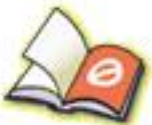
You have either reached a page that is unavailable for viewing or reached your viewing limit for this book.



You have either reached a page that is unavailable for viewing or reached your viewing limit for this book.



You have either reached a page that is unavailable for viewing or reached your viewing limit for this book.



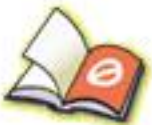
You have either reached a page that is unavailable for viewing or reached your viewing limit for this book.



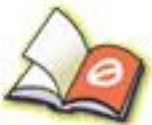
You have either reached a page that is unavailable for viewing or reached your viewing limit for this book.



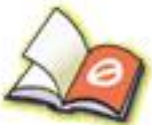
You have either reached a page that is unavailable for viewing or reached your viewing limit for this book.



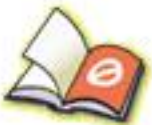
You have either reached a page that is unavailable for viewing or reached your viewing limit for this book.



You have either reached a page that is unavailable for viewing or reached your viewing limit for this book.



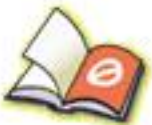
You have either reached a page that is unavailable for viewing or reached your viewing limit for this book.



You have either reached a page that is unavailable for viewing or reached your viewing limit for this book.



You have either reached a page that is unavailable for viewing or reached your viewing limit for this book.



You have either reached a page that is unavailable for viewing or reached your viewing limit for this book.



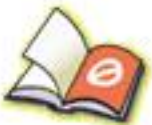
You have either reached a page that is unavailable for viewing or reached your viewing limit for this book.



You have either reached a page that is unavailable for viewing or reached your viewing limit for this book.



You have either reached a page that is unavailable for viewing or reached your viewing limit for this book.



You have either reached a page that is unavailable for viewing or reached your viewing limit for this book.



You have either reached a page that is unavailable for viewing or reached your viewing limit for this book.



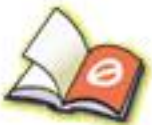
You have either reached a page that is unavailable for viewing or reached your viewing limit for this book.



You have either reached a page that is unavailable for viewing or reached your viewing limit for this book.



You have either reached a page that is unavailable for viewing or reached your viewing limit for this book.



You have either reached a page that is unavailable for viewing or reached your viewing limit for this book.

Heuristically, the Bode plots and gain and phase margin concepts of the frequency domain could be applied once the bilinear transformation has been carried out (see Section 11.12).

Example 11.17: Consider the sampled-data system of Fig. 11.36. Determine its characteristic equation in the z -domain and ascertain its stability via the bilinear transformation.

$$G(z) = Z \left[\frac{5}{s(s-1)(s+2)} \right] = 5Z \left[\frac{1}{2s} - \frac{1}{s+1} + \frac{1}{2(s+2)} \right]$$

$$= 5 \left[\frac{z}{2(z-1)} - \frac{z}{z-e^{-1}} + \frac{z}{2(z-e^{-2})} \right] = \frac{5z(0.4z + 0.594)}{2(z-1)(z-0.368)(z-0.135)}$$

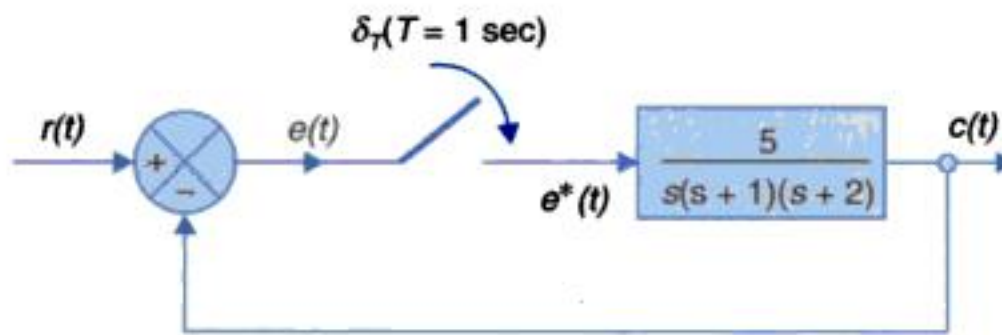


Fig. 11.36

The characteristic equation is

$$1 + G(z) = 2(z-1)(z-0.368)(z-0.135) + 5z(0.4z + 0.594) = 0$$

or

$$z^3 - 0.5z^2 + 2.49z - 0.496 = 0$$

Substituting (11.90), we get

$$\left(\frac{1+r}{1-r} \right)^3 - 0.5 \left(\frac{1+r}{1-r} \right)^2 + 2.49 \left(\frac{1+r}{1-r} \right) - 0.496 = 0$$

which upon simplification yields

$$3.5r^3 - 2.5r^2 + 0.5r + 2.5 = 0$$

The changes in sign of the characteristic polynomial indicate that the system is unstable. We therefore need not proceed to form the Routh array.

Let us check the stability if the system was linear continuous, *i.e.*,

$$1 + G(s) = 0$$

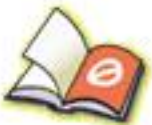
$$1 + \frac{5}{s(s+1)(s+2)} = 0$$

$$s^3 + 3s^2 + 2s + 5 = 0$$

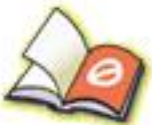
The Routh array is

| | | |
|-------|---------------|---|
| s^3 | 1 | 2 |
| s^2 | 3 | 5 |
| s^1 | $\frac{1}{3}$ | 0 |
| s^0 | 5 | |

It indicates a stable system.



You have either reached a page that is unavailable for viewing or reached your viewing limit for this book.



You have either reached a page that is unavailable for viewing or reached your viewing limit for this book.



You have either reached a page that is unavailable for viewing or reached your viewing limit for this book.

$$F(z) = \frac{b_0 z^{-(n-m)} + b_1 z^{-(n-m-1)} + \dots + b_m z^{-n}}{1 + a_1 z^{-1} + \dots + a_n z^{-n}}; n - m \geq 0 \quad \dots(11.96)$$

From Fig. 11.41

$$E(z) = R(z) - C(z) = [1 - T(z)]R(z) \quad \dots(11.97)$$

The steady-state error is given by

$$e(\infty) = \lim_{z \rightarrow 1} (1 - z^{-1})[1 - T(z)]R(z) \quad \dots(11.98)$$

For input of type $A(kT)^q$,

$$R(z) = \frac{B(z)}{(1 - z^{-1})^{q+1}} \quad \dots(11.99)$$

where $B(z)$ is a finite degree polynomial in z^{-1} (see Table 11.2 for $q = 0, 1, 2$).

$$\therefore e(\infty) = \lim_{z \rightarrow 1} (1 - z^{-1})[1 - T(z)] \frac{B(z)}{(1 - z^{-1})^{q+1}} \quad \dots(11.100)$$

It immediately follows from eqn. (11.100) that $e(\infty) = 0$, if

$$1 - T(z) = (1 - z^{-1})^{q+1}$$

or

$$T(z) = 1 - (1 - z^{-1})^{q+1} \quad \dots(11.101)$$

Now

$$E(z) = B(z) = \text{a finite degree polynomial in } z^{-1}.$$

This further ensures that $e(kT)$ goes to zero in a finite number of sampling intervals which are also the least in number of a specified q .

With $T(z)$ specified as in (11.101), we can obtain $D(z)$ from (11.95) as follows

$$D(z) = \frac{1 - (1 - z^{-1})^{q+1}}{(1 - z^{-1})^{q+1} Z[G_0(s)G(s)]} \quad \dots(11.102)$$

Equation (11.102) also ensures that if $Z[G_0(s)G(s)]$ is non-anticipative, $D(z)$ will also be nonanticipative.

Consider now the system response to three standard inputs wherein the system is compensated with appropriate $D(z)$ (see eqn. (11.97) in each case.

1. Step input (i.e., $q = 0$)

$$E(z) = (1 - z^{-1}) \frac{A}{(1 - z^{-1})} = A$$

Therefore

$$e(0) = A$$

$$e(kT) = 0 \quad \text{for } k = 1, 2, \dots$$

2. Ramp input (i.e., $q = 1$)

$$E(z) = (1 - z^{-1})^2 \frac{ATz^{-1}}{(1 - z^{-1})^2} = ATz^{-1}$$

Therefore

$$e(0) = 0$$

$$e(T) = AT$$

$$e(kT) = 0 \quad \text{for } k = 2, 3, 4, \dots$$



You have either reached a page that is unavailable for viewing or reached your viewing limit for this book.



You have either reached a page that is unavailable for viewing or reached your viewing limit for this book.



You have either reached a page that is unavailable for viewing or reached your viewing limit for this book.

11.14. A sampled-data control system is shown in Fig. P-11.14. Show that the output of the system at sampling instants is zero.

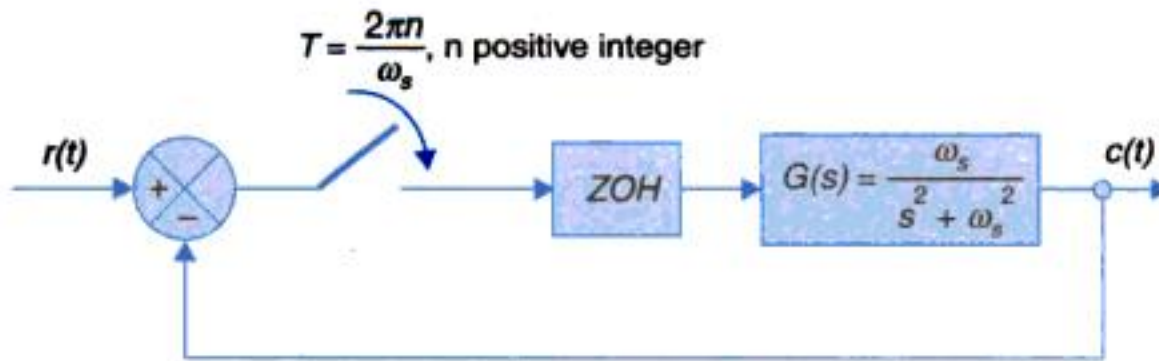


Fig. P-11.14

[Hint : $G(z) = 0$ which indicates that the sampled output of the system is zero but the continuous output is not zero.]

11.15. Find $C(z)/R(z)$ for the sampled-data closed-loop system of Fig. P-11.15. Assume both the samples to be of impulse type.

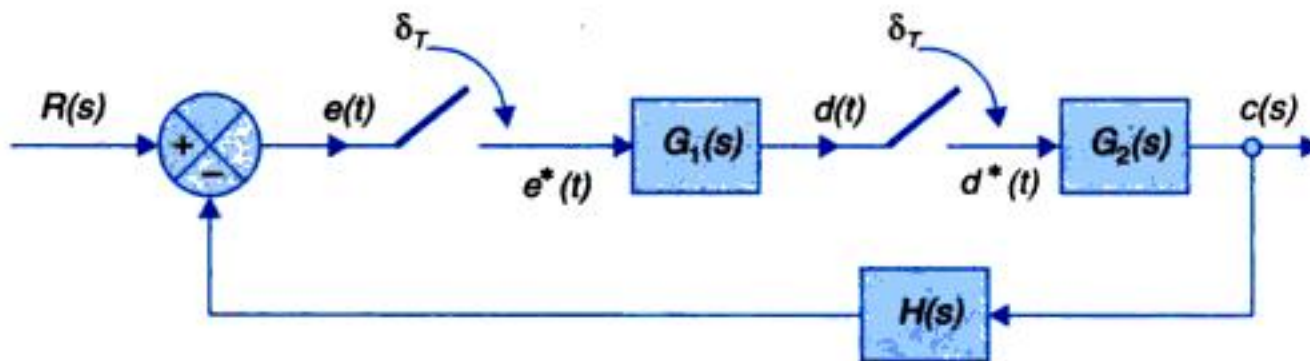


Fig. P-11.15

11.16. For the sampled-data feedback system with a digital network in the feedback path as shown in Fig. P-11.16, find $C(z)/R(z)$.

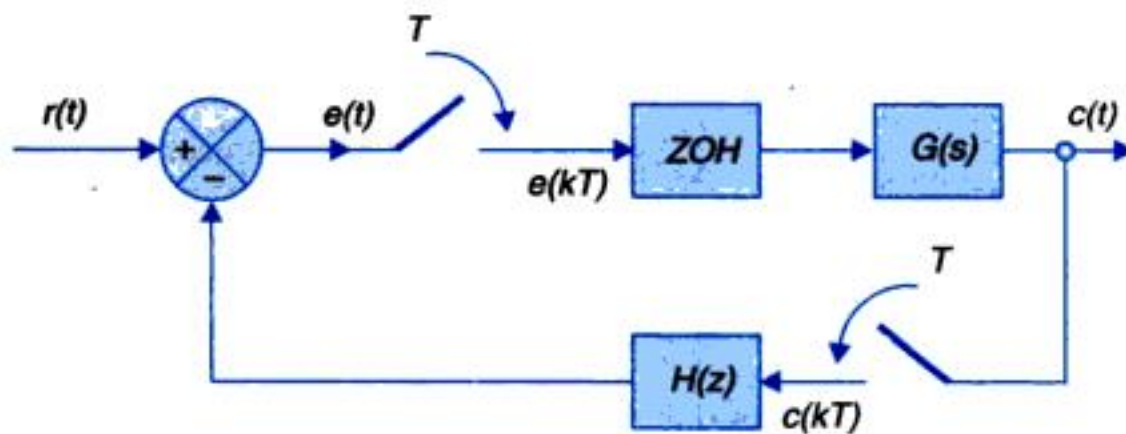


Fig. P-11.16

11.17. For the sampled-data system of Fig. P-11.17, find the response to unit step input

Given: $G(s) = \frac{1}{s+1}$

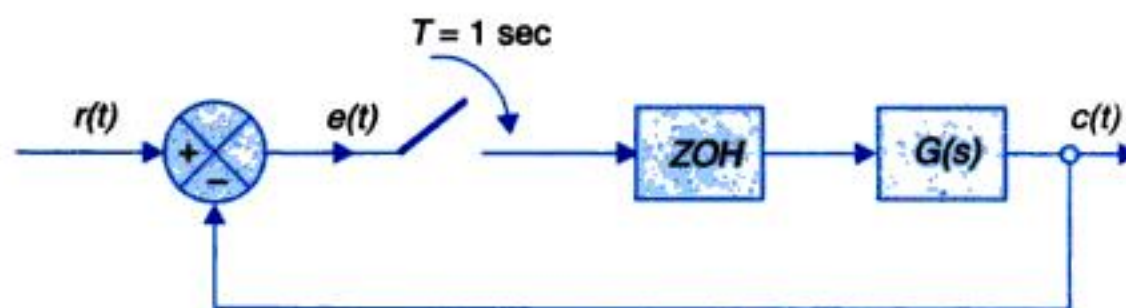
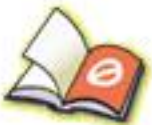


Fig. P-11.17



You have either reached a page that is unavailable for viewing or reached your viewing limit for this book.



You have either reached a page that is unavailable for viewing or reached your viewing limit for this book.



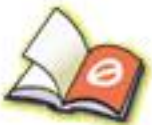
You have either reached a page that is unavailable for viewing or reached your viewing limit for this book.



You have either reached a page that is unavailable for viewing or reached your viewing limit for this book.



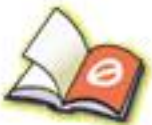
You have either reached a page that is unavailable for viewing or reached your viewing limit for this book.



You have either reached a page that is unavailable for viewing or reached your viewing limit for this book.



You have either reached a page that is unavailable for viewing or reached your viewing limit for this book.



You have either reached a page that is unavailable for viewing or reached your viewing limit for this book.



You have either reached a page that is unavailable for viewing or reached your viewing limit for this book.

The output being $y = x_1$, the output equation is given by

$$y = \mathbf{C}\mathbf{x} \quad \dots(12.29b)$$

where $\mathbf{C} = [1 \ 0 \ \dots \ 0]$.

The initial conditions on y give rise to the initial conditions $x_1(0), x_2(0), \dots, x_n(0)$ on the state variables as per the definition of the state variables given in eqns. (12.27). Figure 12.10 shows the block diagram representation of the state model derived above.

It is important to note that assuming the initial time equal to zero does not create any loss of generality. Since the system under the discussion is time-invariant, the charge of state does not depend on initial time but depends only on the length of time during which the control force is applied.

It follows from the above that for the transfer functions with poles only, the derivation of the state model through the differential equation is quite straightforward. However, when a transfer function has zeros as well, the resulting differential equation contains terms which are derivatives of the control force u and the method discussed above can no longer be applied as such. An alternate method using signal flow graphs is presented below.

Phase variable formulations for transfer function with poles and zeros

Let us consider a third order transfer function

$$\frac{Y(s)}{U(s)} = T(s) = \frac{b_0s^3 + b_1s^2 + b_2s + b_3}{s^3 + a_1s^2 + a_2s + a_3} \quad \dots(12.30)$$

We identify three state variables x_1, x_2 and x_3 . The signal flow graph must have at least three integrators. Equation (12.30) may be rearranged as

$$T(s) = \frac{b_0 + b_1/s + b_2/s^2 + b_3/s^3}{1 - (-a_1/s - a_2/s^2 - a_3/s^3)} \quad \dots(12.31)$$

In chapter 2, it was shown that the transfer function and signal flow graphs are related by Mason's gain formula, reproduced below.

$$T(s) = \frac{1}{\Delta} \sum_k P_k \Delta_k \quad \dots(12.32)$$

where P_k = Path gain of the k^{th} forward path; $\Delta = 1 - (\text{sum of loop gains of all individual loops}) + (\text{sum of gain products of all possible combinations of two non-touching loops}) - (\text{sum of gain products of all possible combinations of three non-touching loops}) + \dots$; Δ_k = the value of Δ for that part of the graph not touching the k^{th} forward path.

Comparing eqn. (12.30) with (12.31) we observe that a signal flow graph of eqn. (12.29) may consist of

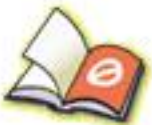
- (i) three feedback loops (touching each other) with gains $-a_1/s, -a_2/s^2$ and a_3/s^3 ;
- (ii) four forward paths which touch the loops and have gains $b_0, b_1/s, b_2/s^2$ and b_3/s^3

A signal flow graph configuration which satisfies the above requirements is shown in Fig. 12.11. From this figure, we have

$$y = x_1 + b_0u$$



You have either reached a page that is unavailable for viewing or reached your viewing limit for this book.



You have either reached a page that is unavailable for viewing or reached your viewing limit for this book.



You have either reached a page that is unavailable for viewing or reached your viewing limit for this book.

| | |
|------------------------------|---------------------|
| $\mathbf{x}(k) = n \times 1$ | state vector |
| $\mathbf{u}(k) = m \times 1$ | input vector |
| $\mathbf{y}(k) = p \times 1$ | output vector |
| $\mathbf{A} = n \times n$ | system matrix |
| $\mathbf{B} = n \times m$ | input matrix |
| $\mathbf{C} = p \times n$ | output matrix |
| $\mathbf{D} = p \times m$ | transmission matrix |

State Models from Linear Difference Equations/z-transfer Functions

Consider a third order system with the following z-transfer function

$$T(z) = \frac{Y(z)}{U(z)} = \frac{b_0z^3 + b_1z^2 + b_2z + b_3}{z^3 + a_1z^2 + a_2z + a_3} \quad \dots(i)$$

$$= \frac{b_0 + b_1z^{-1} + b_2z^{-2} + b_3z^{-3}}{1 + a_1z^{-1} + a_2z^{-2} + a_3z^{-3}} \quad \dots(ii)$$

The implementation of this transfer function by a digital computer can be done in many ways. Two methods are illustrated in terms of state diagrams in the following:

Method 1: The signal flow graph for $T(z)$ of eqn. (i) is shown in Fig. 12.19 (z^{-1} represents a time delay of T sec).

Taking the output of the delay elements as state variables we write

$$\begin{aligned} x_1(k+1) &= x_2(k) \\ x_2(k+1) &= x_3(k) \\ x_3(k+1) &= -a_3x_1(k) - a_2x_2(k) - a_1x_3(k) + u(k) \\ y(k) &= (b_3 - a_3b_0)x_1(k) + (b_2 - a_2b_0)x_2(k) + (b_1 - a_1b_0)x_3(k) + b_0u(k) \end{aligned} \quad \dots(iii)$$

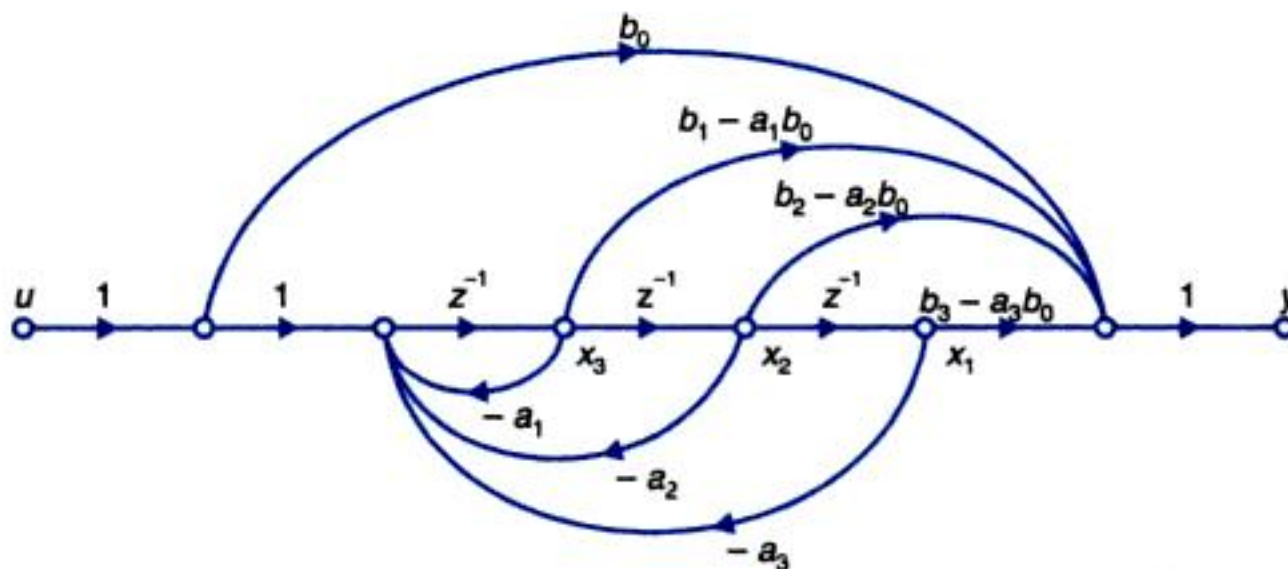


Fig. 12.19

These equations can be written as

$$\begin{aligned} \mathbf{x}(k+1) &= \mathbf{A}\mathbf{x}(k) + \mathbf{B}u(k) \\ y(k) &= \mathbf{C}\mathbf{x}(k) + b_0u(k) \end{aligned} \quad \dots(iv)$$



You have either reached a page that is unavailable for viewing or reached your viewing limit for this book.



You have either reached a page that is unavailable for viewing or reached your viewing limit for this book.



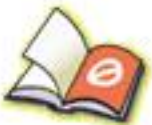
You have either reached a page that is unavailable for viewing or reached your viewing limit for this book.



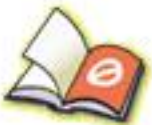
You have either reached a page that is unavailable for viewing or reached your viewing limit for this book.



You have either reached a page that is unavailable for viewing or reached your viewing limit for this book.



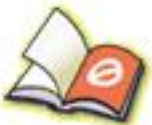
You have either reached a page that is unavailable for viewing or reached your viewing limit for this book.



You have either reached a page that is unavailable for viewing or reached your viewing limit for this book.



You have either reached a page that is unavailable for viewing or reached your viewing limit for this book.



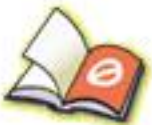
You have either reached a page that is unavailable for viewing or reached your viewing limit for this book.



You have either reached a page that is unavailable for viewing or reached your viewing limit for this book.



You have either reached a page that is unavailable for viewing or reached your viewing limit for this book.



You have either reached a page that is unavailable for viewing or reached your viewing limit for this book.

Then

$$\mathbf{AB} = \begin{bmatrix} 0 & 1 \\ -1 & -2 \end{bmatrix} \begin{bmatrix} 1 \\ -1 \end{bmatrix} = \begin{bmatrix} -1 \\ 1 \end{bmatrix}$$

The composite matrix defined in eqn. (12.90) is given by

$$\mathbf{Q}_c = [\mathbf{B} : \mathbf{AB}] = \begin{bmatrix} 1 & -1 \\ -1 & 1 \end{bmatrix}$$

The rank of r of this matrix is 1. The system is therefore not completely controllable. One state of the system is uncontrollable (r out of n states are controllable).

By the methods discussed in Section 12.3, the given differential equation can be transformed to the following controllable phase variable model:

$$\begin{bmatrix} \dot{x}_1 \\ \dot{x}_2 \end{bmatrix} = \begin{bmatrix} 0 & -1 \\ -1 & 2 \end{bmatrix} \begin{bmatrix} x_1 \\ x_2 \end{bmatrix} + \begin{bmatrix} 0 \\ 1 \end{bmatrix} u$$

$$y = [1 \quad 1] \begin{bmatrix} x_1 \\ x_2 \end{bmatrix}$$

Thus state controllability depends on how the state variables are defined for a given system.

Observability

Consider the state model of an n th order single-output linear time-invariant system,

$$\begin{aligned} \dot{\mathbf{x}} &= \mathbf{Ax} + \mathbf{Bu} \\ y &= \mathbf{Cx} \end{aligned}$$

The state equation may be transformed to the canonical form by the linear transformation $\mathbf{x} = \mathbf{Mv}$. The resulting state and output equations are

$$\dot{\mathbf{v}} = \mathbf{\Lambda v} + \tilde{\mathbf{B}}u \quad \dots(12.95a)$$

$$\begin{aligned} y &= \tilde{\mathbf{C}}\mathbf{v} \\ &= \tilde{c}_1 v_1 + \tilde{c}_2 v_2 + \dots + \tilde{c}_n v_n \quad \dots(12.95b) \end{aligned}$$

Since diagonalization decouples the states, no state now contains any information regarding any other state, *i.e.*, each state must be independently observable. It therefore follows that for a state to be observed through the output y , its corresponding coefficient in eqn. (12.95b) should be nonzero.

If any particular \tilde{c}_i is zero, the corresponding v_i can have any value without its effect showing up in the output y . Thus the necessary (it is also sufficient) condition for complete state observability is that none of the \tilde{c}_i 's (*i.e.*, none of the elements of $\tilde{\mathbf{C}} = \mathbf{CM}$) should be zero.

The result may be extended to the case of multi-input-multi-output systems where the output vector, after canonical transformation is given by

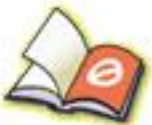
$$\begin{bmatrix} y_1 \\ y_2 \\ \vdots \\ y_p \end{bmatrix} = \begin{bmatrix} \tilde{c}_{11} & \tilde{c}_{12} & \cdots & \tilde{c}_{1n} \\ \tilde{c}_{21} & \tilde{c}_{22} & \cdots & \tilde{c}_{2n} \\ \vdots & \vdots & \ddots & \vdots \\ \tilde{c}_{p1} & \tilde{c}_{p2} & \cdots & \tilde{c}_{pn} \end{bmatrix} \begin{bmatrix} v_1 \\ v_2 \\ \vdots \\ v_n \end{bmatrix}$$



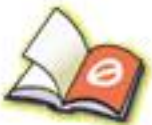
You have either reached a page that is unavailable for viewing or reached your viewing limit for this book.



You have either reached a page that is unavailable for viewing or reached your viewing limit for this book.



You have either reached a page that is unavailable for viewing or reached your viewing limit for this book.



You have either reached a page that is unavailable for viewing or reached your viewing limit for this book.



You have either reached a page that is unavailable for viewing or reached your viewing limit for this book.



You have either reached a page that is unavailable for viewing or reached your viewing limit for this book.



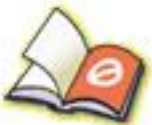
You have either reached a page that is unavailable for viewing or reached your viewing limit for this book.



You have either reached a page that is unavailable for viewing or reached your viewing limit for this book.



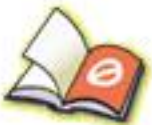
You have either reached a page that is unavailable for viewing or reached your viewing limit for this book.



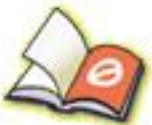
You have either reached a page that is unavailable for viewing or reached your viewing limit for this book.



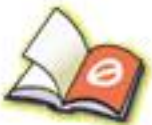
You have either reached a page that is unavailable for viewing or reached your viewing limit for this book.



You have either reached a page that is unavailable for viewing or reached your viewing limit for this book.



You have either reached a page that is unavailable for viewing or reached your viewing limit for this book.



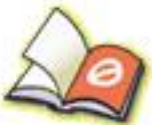
You have either reached a page that is unavailable for viewing or reached your viewing limit for this book.



You have either reached a page that is unavailable for viewing or reached your viewing limit for this book.



You have either reached a page that is unavailable for viewing or reached your viewing limit for this book.



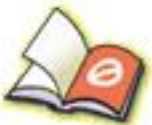
You have either reached a page that is unavailable for viewing or reached your viewing limit for this book.



You have either reached a page that is unavailable for viewing or reached your viewing limit for this book.



You have either reached a page that is unavailable for viewing or reached your viewing limit for this book.



You have either reached a page that is unavailable for viewing or reached your viewing limit for this book.



You have either reached a page that is unavailable for viewing or reached your viewing limit for this book.

14

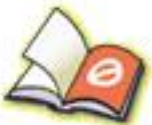
OPTIMAL CONTROL SYSTEMS

14.1 INTRODUCTION

There are, as discussed in Chapter 10, basically two approaches to the design of control systems. In one approach we select the configuration of the overall system by introducing compensators and then choose the parameters of the compensators to meet the given specifications on performance. In the other approach, for a given plant we find an overall system that meets the given specifications and then compute the necessary compensators.

The classical design method based on first approach mentioned above, has already been discussed at length in earlier chapters. This method relies heavily on the Laplace transform and z -transform. The designer is given a set of specifications in time domain or in frequency domain and system configuration. Peak overshoot, settling time, gain margin, phase margin, steady-state error, etc., are among most commonly used specifications. These design specifications are selected because of convenience in graphical interpretation with respect to root locus or frequency plots. Compensators are selected that give as closely as possible, the desired system performance. In general, it may not be possible to satisfy all the desired specifications. Then, through a trial and error procedure, an acceptable system performance (within certain tolerable error) is achieved. There are generally many designs that can yield this acceptable performance, *i.e.*, the solution is not unique. This trial and error design procedure works satisfactorily for single-input-single-output systems. The gap between the classical design procedure and its application to multi-input-multi-output systems has been bridged recently.

The trial and error uncertainties are eliminated in the parameter optimization method. The point of departure in the parameter optimization procedure is that the performance specifications consist of a single performance index. Integral square error performance index is very common but other performance indices can be used as well (refer Chapter 5). For a fixed system configuration, parameters that minimize the performance index are selected.



You have either reached a page that is unavailable for viewing or reached your viewing limit for this book.



You have either reached a page that is unavailable for viewing or reached your viewing limit for this book.



You have either reached a page that is unavailable for viewing or reached your viewing limit for this book.



You have either reached a page that is unavailable for viewing or reached your viewing limit for this book.



You have either reached a page that is unavailable for viewing or reached your viewing limit for this book.



You have either reached a page that is unavailable for viewing or reached your viewing limit for this book.



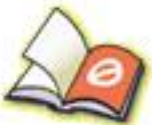
You have either reached a page that is unavailable for viewing or reached your viewing limit for this book.



You have either reached a page that is unavailable for viewing or reached your viewing limit for this book.



You have either reached a page that is unavailable for viewing or reached your viewing limit for this book.



You have either reached a page that is unavailable for viewing or reached your viewing limit for this book.



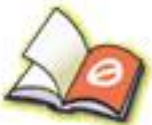
You have either reached a page that is unavailable for viewing or reached your viewing limit for this book.



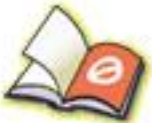
You have either reached a page that is unavailable for viewing or reached your viewing limit for this book.



You have either reached a page that is unavailable for viewing or reached your viewing limit for this book.



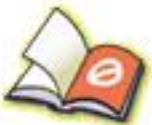
You have either reached a page that is unavailable for viewing or reached your viewing limit for this book.



You have either reached a page that is unavailable for viewing or reached your viewing limit for this book.



You have either reached a page that is unavailable for viewing or reached your viewing limit for this book.



You have either reached a page that is unavailable for viewing or reached your viewing limit for this book.



You have either reached a page that is unavailable for viewing or reached your viewing limit for this book.



You have either reached a page that is unavailable for viewing or reached your viewing limit for this book.

Find the control law $\mathbf{u}^*(t)$, so that quadratic performance index (eqn. (14.56))

$$J = \frac{1}{2} \int_0^{\infty} (\mathbf{x}^T(t) \mathbf{Q} \mathbf{x}(t) + \mathbf{u}^T(t) \mathbf{R} \mathbf{u}(t)) dt; \quad \dots(14.85)$$

\mathbf{Q} and \mathbf{R} are positive definite matrices, is minimized, subject to the initial condition

$$\mathbf{x}(0) = \mathbf{x}_0$$

Let us discuss the salient points of the infinite-time state regulator problem.

(i) For many applications, the final time t_f has no special significance and there exist no obvious values of t_f which should be specified in the performance index. In such cases, we are satisfied to let $t_f \rightarrow \infty$, as is done in eqn. (14.85).

(ii) When $t_f \rightarrow \infty$, $\mathbf{x}(\infty) \rightarrow \mathbf{0}$ for the optimal system to be stable. Therefore the terminal penalty term (in eqn. (14.55)) has no significance; consequently it does not appear in eqn. (14.85). *i.e.*, we have set $\mathbf{H} = \mathbf{0}$ in the general quadratic performance index (14.55).

(iii) In the finite-time regulator problem, there is no restriction on the controllability of the plant. This is because J is always finite and instability does not impose any problems in finite-interval control. This may not be so in the infinite-interval case. J can become infinite if

- (a) one or more states of the plant are uncontrollable,
- (b) the uncontrollable states are unstable, and
- (c) the unstable states are reflected in system performance index.

The performance index J would be infinite for all controls; we can not, therefore, distinguish the optimal control from other controls. J will be finite (*i.e.*, the solution to the infinite-time regulator problem will exist) if the states that are not asymptotically stable, are controllable (note that controllable unstable states of the plant can be stabilized by the feedback controller) or broadly, we may say that the controlled process given by eqn. (14.84) should satisfy the conditions of controllability.

(iv) Consider the matrix Riccati equation (eqn. (14.80)),

$$\dot{\mathbf{P}}(t) + \mathbf{Q} - \mathbf{P}(t) \mathbf{B} \mathbf{R}^{-1} \mathbf{B}^T \mathbf{P}(t) + \mathbf{P}(t) \mathbf{A} + \mathbf{A}^T \mathbf{P}(t) = \mathbf{0}$$

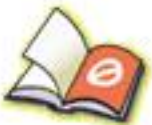
with the boundary condition $\mathbf{P}(t_f) = \mathbf{0}$.

We solve the Riccati equation backward in time with t_f as the starting time and $\mathbf{P}(t_f)$ as the initial condition. At time $t = t_f - \epsilon$, where ϵ is a small positive number, the transient due to initial condition will dominate the solution $\mathbf{P}(t)$; the transient will die out for large values of ϵ resulting in steady-state solution of Riccati equation for some interval of time. This time interval increases as t_f becomes large. As $t_f \rightarrow \infty$, the time interval of steady-state solution of Riccati equation grows without bound, *i.e.*, $\mathbf{P}(t) \rightarrow$ a constant \mathbf{P}^0 for all finite time t .

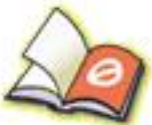
Consider the system of Example 14.7. For terminal time t_f ; the solution of the Riccati equation is (eqn (14.82))

$$p(t) = \frac{\frac{3}{2} (1 - e^{8(t-t_f)})}{1 + 3e^{8(t-t_f)}}$$

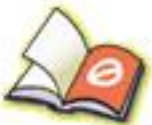
$p(t)$ is plotted in Fig. 14.13 for $t_f = 1$ sec and 10 sec.



You have either reached a page that is unavailable for viewing or reached your viewing limit for this book.



You have either reached a page that is unavailable for viewing or reached your viewing limit for this book.



You have either reached a page that is unavailable for viewing or reached your viewing limit for this book.



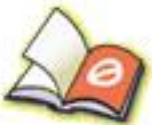
You have either reached a page that is unavailable for viewing or reached your viewing limit for this book.



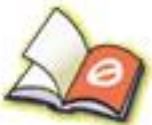
You have either reached a page that is unavailable for viewing or reached your viewing limit for this book.



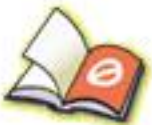
You have either reached a page that is unavailable for viewing or reached your viewing limit for this book.



You have either reached a page that is unavailable for viewing or reached your viewing limit for this book.



You have either reached a page that is unavailable for viewing or reached your viewing limit for this book.



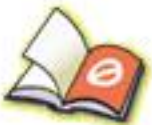
You have either reached a page that is unavailable for viewing or reached your viewing limit for this book.



You have either reached a page that is unavailable for viewing or reached your viewing limit for this book.



You have either reached a page that is unavailable for viewing or reached your viewing limit for this book.



You have either reached a page that is unavailable for viewing or reached your viewing limit for this book.



You have either reached a page that is unavailable for viewing or reached your viewing limit for this book.



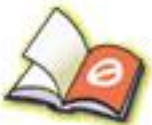
You have either reached a page that is unavailable for viewing or reached your viewing limit for this book.



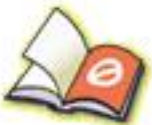
You have either reached a page that is unavailable for viewing or reached your viewing limit for this book.



You have either reached a page that is unavailable for viewing or reached your viewing limit for this book.



You have either reached a page that is unavailable for viewing or reached your viewing limit for this book.



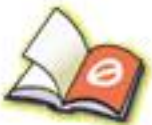
You have either reached a page that is unavailable for viewing or reached your viewing limit for this book.



You have either reached a page that is unavailable for viewing or reached your viewing limit for this book.



You have either reached a page that is unavailable for viewing or reached your viewing limit for this book.



You have either reached a page that is unavailable for viewing or reached your viewing limit for this book.

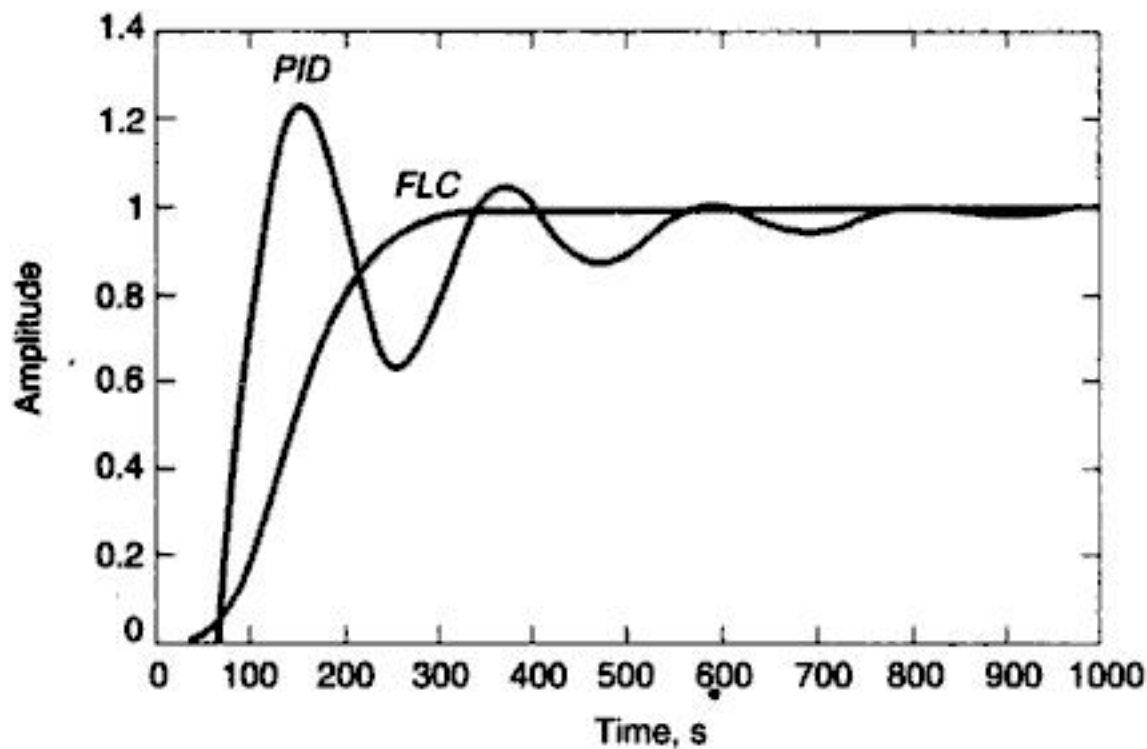


Fig. 15.25. Step input response : *FLC Vs PID*.

15.4 NEURAL NETWORKS

Artificial neural networks have emerged from the studies of how brain performs. The human brain is made up of many millions of individual processing elements, called *neurons*, that are highly interconnected. A schematic diagram of a single biological neuron is shown in Fig. 15.26. Information from the outputs of the other neurons, in the form of electrical pulses, are received by the cell at connections called *synapses*. The synapses connect to the cell inputs, or *space dendrites*, and the single output of the neuron appears at the *axon*. An electrical pulse is sent down the axon when the total input stimuli from all of the dendrites exceeds a certain threshold.

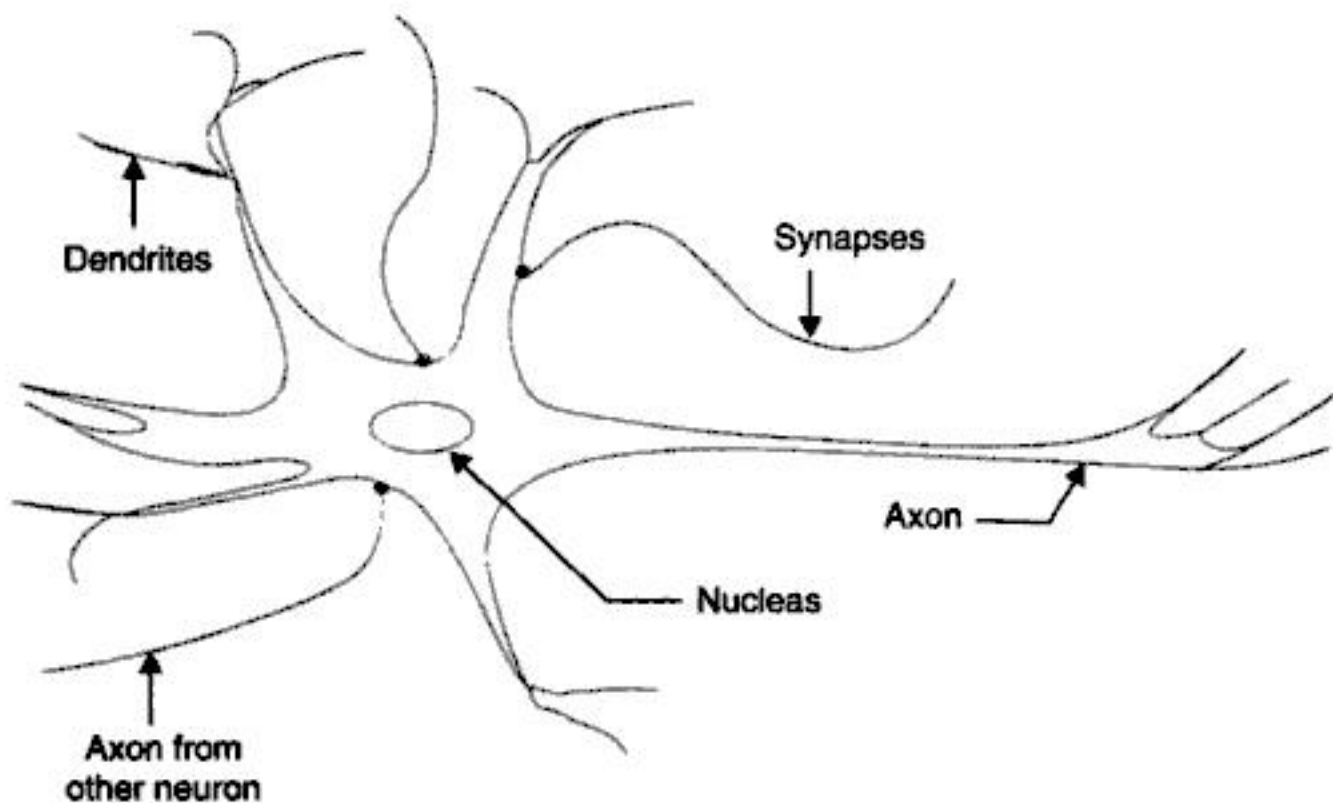


Fig. 15.26. A biological neuron.



You have either reached a page that is unavailable for viewing or reached your viewing limit for this book.



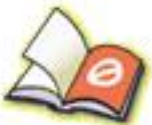
You have either reached a page that is unavailable for viewing or reached your viewing limit for this book.



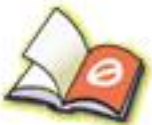
You have either reached a page that is unavailable for viewing or reached your viewing limit for this book.



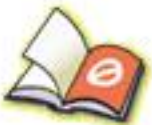
You have either reached a page that is unavailable for viewing or reached your viewing limit for this book.



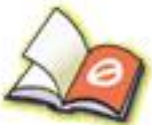
You have either reached a page that is unavailable for viewing or reached your viewing limit for this book.



You have either reached a page that is unavailable for viewing or reached your viewing limit for this book.



You have either reached a page that is unavailable for viewing or reached your viewing limit for this book.



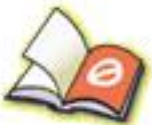
You have either reached a page that is unavailable for viewing or reached your viewing limit for this book.



You have either reached a page that is unavailable for viewing or reached your viewing limit for this book.



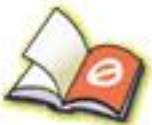
You have either reached a page that is unavailable for viewing or reached your viewing limit for this book.



You have either reached a page that is unavailable for viewing or reached your viewing limit for this book.



You have either reached a page that is unavailable for viewing or reached your viewing limit for this book.



You have either reached a page that is unavailable for viewing or reached your viewing limit for this book.



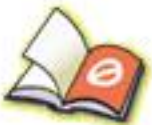
You have either reached a page that is unavailable for viewing or reached your viewing limit for this book.



You have either reached a page that is unavailable for viewing or reached your viewing limit for this book.



You have either reached a page that is unavailable for viewing or reached your viewing limit for this book.



You have either reached a page that is unavailable for viewing or reached your viewing limit for this book.

Principal minor. A minor of $|\mathbf{A}|$ whose diagonal elements are also diagonal elements of $|\mathbf{A}|$, is called a principal minor of $|\mathbf{A}|$.

Laplace expansion formula. The value of determinant of a matrix \mathbf{A} can be obtained by the so-called Laplace expansion formula.

$$|\mathbf{A}| = \sum_{j=1}^n (-1)^{i+j} a_{ij} M_{ij} \text{ for any integer } i; 1 \leq i \leq n$$

$$= \sum_{i=1}^n (-1)^{i+j} a_{ij} M_{ij} \text{ for any integer } j; 1 \leq j \leq n$$

where M_{ij} is the minor of element a_{ij} .

Cofactor. The cofactor C_{ij} of element a_{ij} of the matrix \mathbf{A} is defined as

$$C_{ij} = (-1)^{i+j} M_{ij}$$

Adjoint matrix. The adjoint matrix of a square matrix \mathbf{A} is found by remaining each element a_{ij} of matrix \mathbf{A} by its cofactor C_{ij} and then transposing. For example, if \mathbf{A} is given by (II.2), then

$$\text{adj } \mathbf{A} = \begin{bmatrix} \begin{vmatrix} 6 & 4 \\ 4 & 8 \end{vmatrix} & - \begin{vmatrix} -2 & 4 \\ 1 & 8 \end{vmatrix} & \begin{vmatrix} -2 & 6 \\ 1 & 4 \end{vmatrix} \\ - \begin{vmatrix} -2 & 1 \\ 4 & 8 \end{vmatrix} & \begin{vmatrix} 3 & 1 \\ 1 & 8 \end{vmatrix} & - \begin{vmatrix} 3 & -2 \\ 1 & 4 \end{vmatrix} \\ \begin{vmatrix} -2 & 1 \\ 6 & 4 \end{vmatrix} & - \begin{vmatrix} 3 & 1 \\ -2 & 4 \end{vmatrix} & \begin{vmatrix} 3 & -2 \\ -2 & 6 \end{vmatrix} \end{bmatrix}^T$$

$$= \begin{bmatrix} 32 & 20 & -14 \\ 20 & 23 & -14 \\ -14 & -14 & 14 \end{bmatrix}^T = \begin{bmatrix} 32 & 20 & -14 \\ 20 & 23 & -14 \\ -14 & -14 & 14 \end{bmatrix} \quad \dots(\text{II.4})$$

Singular and nonsingular matrices. A square matrix is called singular if its associated determinant is zero and nonsingular if its associated determinant is non-zero.

Rank of a matrix. A matrix \mathbf{A} is said to have rank r if there exists an $r \times r$ submatrix of \mathbf{A} which is nonsingular and all other $q \times q$ submatrices (where $q \geq r + 1$) are singular.

For example, consider a 4×4 matrix

$$\mathbf{A} = \begin{bmatrix} 1 & 2 & 3 & 4 \\ 0 & 1 & -1 & 0 \\ 1 & 0 & 1 & 2 \\ 1 & 1 & 0 & 2 \end{bmatrix}$$

$$\det \mathbf{A} = 0$$

and

$$\begin{vmatrix} 1 & 2 & 3 \\ 0 & 1 & -1 \\ 1 & 0 & 1 \end{vmatrix} \neq 0$$

Hence the rank of matrix \mathbf{A} is 3.

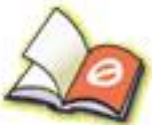
Conjugate matrix. The conjugate of a matrix \mathbf{A} (denoted as \mathbf{A}^*) is the matrix whose each element is the complex conjugate of the corresponding element of \mathbf{A} .



You have either reached a page that is unavailable for viewing or reached your viewing limit for this book.



You have either reached a page that is unavailable for viewing or reached your viewing limit for this book.



You have either reached a page that is unavailable for viewing or reached your viewing limit for this book.



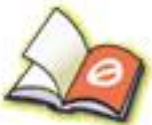
You have either reached a page that is unavailable for viewing or reached your viewing limit for this book.



You have either reached a page that is unavailable for viewing or reached your viewing limit for this book.



You have either reached a page that is unavailable for viewing or reached your viewing limit for this book.



You have either reached a page that is unavailable for viewing or reached your viewing limit for this book.



You have either reached a page that is unavailable for viewing or reached your viewing limit for this book.

```
iu = 1 ;
[z, p, k] = ss2zp(a, b, c, d, iu) ;
```

The values computed are the following :

$$z = [1], p = \begin{bmatrix} -1 \\ -3 \end{bmatrix}, k = [10] \quad \dots(\text{III.23})$$

Thus, the transfer function is

$$H(s) = \frac{10}{(s+1)(s+3)} \quad \dots(\text{III.24})$$

III.3 DESIGN AND ANALYSIS FUNCTIONS

MATLAB has several functions for designing and analyzing linear systems both in the time and frequency domains. Some of the functions frequently used are tabulated in Table III.2 :

Table III.2 : Design and Analysis Functions

| <i>Function</i> | <i>Purpose</i> |
|-----------------|-------------------------------------|
| bode | magnitude and phase-frequency plots |
| nyquist | Nyquist frequency plots |
| rlocus | Root-locus plots |
| step | Unit step time response |
| lqe | linear-quadratic estimator |
| lqr | linear-quadratic regulator |

Step Response

The format for calling this function is as given below :

```
[y, x, t] = step (num, den) ;
[y, x, t] = step (num, den, t) ;
[y, x, t] = step (a, b, c, d) ;
[y, x, t] = step (a, b, c, d, iu) ;
[y, x, t] = step (a, b, c, d, iu, t) ;
```

The arguments of these functions are dependent on the model you have chosen for the system. For example lets take the step response of a third-transfer function :

$$H(s) = \frac{1}{s(s+1)(s+2)} \quad \dots(\text{III.25})$$

can be generated using the following statements :

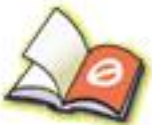
```
num = [1] ;
den = poly ([0 - 1 - 2]) ;
k = [0.25 0.4 1.5 6 8] ;      % Range of the gain of
                             % proportional controller
```



You have either reached a page that is unavailable for viewing or reached your viewing limit for this book.



You have either reached a page that is unavailable for viewing or reached your viewing limit for this book.



You have either reached a page that is unavailable for viewing or reached your viewing limit for this book.

The statements below will produce the same plot as shown in Fig. III.3:

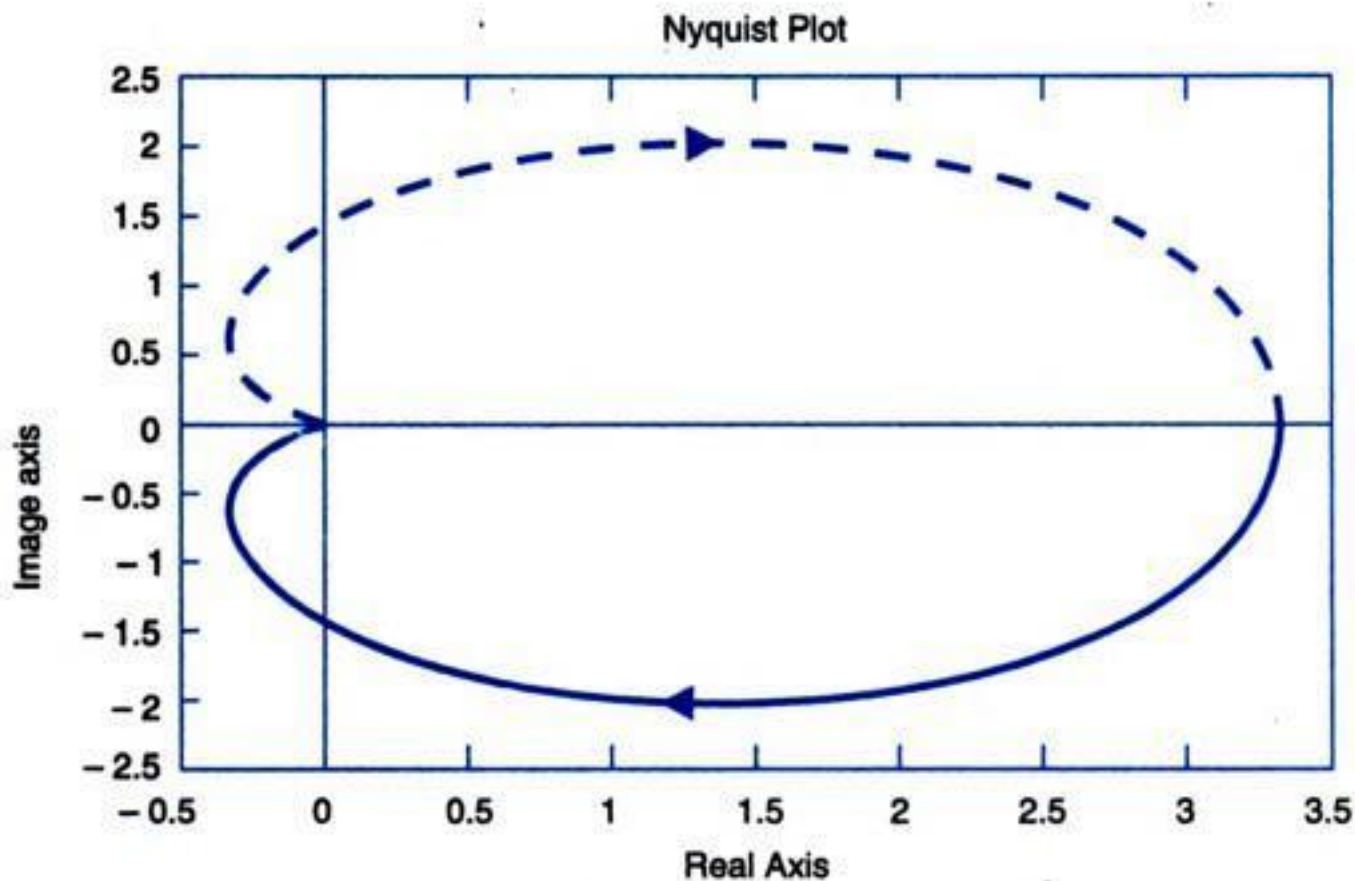


Fig. III.3. Nyquist plot.

a = [0 1 ; -3 -1] ;

b = [0 1]' ;

c = [10 0] ;

d = 0 ;

nyquist (a, b, c, d), title ('Nyquist Plot')

Root Locus Plots

The root locus is an useful tool for single-input/single-output systems. It helps in assessing the stability and transient response of a system and for determining ways to improve the system performance. The plot shows the location of roots of the characteristic equation of a system. The roots of the characteristic equation determine the stability of the system. By analysing the root-locus the system designer can improve the system performance.

In the equation below $G(s)$ represents the forward path transfer function and $H(s)$ is the feedback path transfer function :

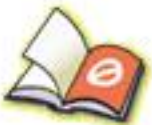
$$\frac{y(s)}{u(s)} = \frac{G(s)}{1 + G(s)H(s)} \quad \dots(\text{III.33})$$

The root locus is obtained by setting the denominator of the closed-loop transfer function equal to zero, which gives the characteristic equation of the system

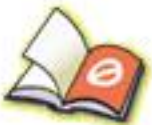
$$1 + G(s)H(s) = 0 \quad \dots(\text{III.34})$$

$$G(s)H(s) = -1 \quad \dots(\text{III.35})$$

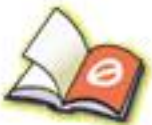
The roots of the characteristic equation are then computed as some parameter, usually the forward path gain, is varied from zero to infinity.



You have either reached a page that is unavailable for viewing or reached your viewing limit for this book.



You have either reached a page that is unavailable for viewing or reached your viewing limit for this book.



You have either reached a page that is unavailable for viewing or reached your viewing limit for this book.

In the component form we can write

$$\begin{aligned} v_1(t) &= p_{11}x_1 + p_{12}x_2 + \dots + p_{1n}x_n \\ &= \mathbf{P}_1 \mathbf{x}(t) \end{aligned}$$

Taking derivative on both sides of this equation, we have

$$\dot{v}_1(t) = \mathbf{P}_1 \dot{\mathbf{x}} = \mathbf{P}_1 \mathbf{A} \mathbf{x} + \mathbf{P}_1 \mathbf{B} u$$

But $\dot{v}_1 = v_2$ is a function of \mathbf{x} only as per transformation (V.3). Therefore $\mathbf{P}_1 \mathbf{B} = \mathbf{0}$ and

$$v_2 = \mathbf{P}_1 \mathbf{A} \mathbf{x}$$

Taking derivative on both sides once again, we have

$$\dot{v}_2 = v_3 = \mathbf{P}_1 \mathbf{A}^2 \mathbf{x} \text{ and } \mathbf{P}_1 \mathbf{A} \mathbf{B} = \mathbf{0}$$

This process gives

$$\dot{v}_{n-1} = v_n = \mathbf{P}_1 \mathbf{A}^{n-1} \mathbf{x} \text{ with } \mathbf{P}_1 \mathbf{A}^{n-2} \mathbf{B} = \mathbf{0}$$

Thus

$$v(t) = \mathbf{P} \mathbf{x} = \begin{bmatrix} \mathbf{P}_1 \\ \mathbf{P}_1 \mathbf{A} \\ \vdots \\ \mathbf{P}_1 \mathbf{A}^{n-1} \end{bmatrix} \mathbf{x} \quad \dots(\text{V.5})$$

and \mathbf{P}_1 should satisfy the conditions

$$\mathbf{P}_1 \mathbf{B} = \mathbf{P}_1 \mathbf{A} \mathbf{B} = \dots = \mathbf{P}_1 \mathbf{A}^{n-2} \mathbf{B} = \mathbf{0} \quad \dots(\text{V.6})$$

The transformation (V.3) transforms (V.2) to

$$\dot{\mathbf{v}} = \mathbf{P} \mathbf{A} \mathbf{P}^{-1} \mathbf{v} + \mathbf{P} \mathbf{B} u$$

Comparing this with (V.2), we get

$$\begin{aligned} & \mathbf{B} \quad \mathbf{P} \mathbf{B} \\ \text{or} \quad & \begin{bmatrix} 0 \\ 0 \\ \vdots \\ 1 \end{bmatrix} = \begin{bmatrix} \mathbf{P}_1 \mathbf{B} \\ \mathbf{P}_1 \mathbf{A} \mathbf{B} \\ \vdots \\ \mathbf{P}_1 \mathbf{A}^{n-1} \mathbf{B} \end{bmatrix} \\ \text{or} \quad & \mathbf{P}_1 [\mathbf{B} : \mathbf{A} \mathbf{B} : \dots : \mathbf{A}^{n-1} \mathbf{B}] = [0 \ 0 \ \dots \ 1] \quad \dots(\text{V.7}) \end{aligned}$$

This gives

$$\mathbf{P}_1 = [0 \ 0 \ \dots \ 1] [\mathbf{B} : \mathbf{A} \mathbf{B} : \dots : \mathbf{A}^{n-1} \mathbf{B}]^{-1}$$

The matrix $\mathbf{Q}_c = [\mathbf{B} : \mathbf{A} \mathbf{B} : \dots : \mathbf{A}^{n-1} \mathbf{B}]$ is nonsingular since the state model is controllable.

Therefore, the controllable state model can be transformed to the form (V.2) by the transformation

$$\mathbf{z} = \mathbf{P} \mathbf{x}$$

$$\text{where} \quad \mathbf{P} = \begin{bmatrix} \mathbf{P}_1 \\ \mathbf{P}_1 \mathbf{A} \\ \vdots \\ \mathbf{P}_1 \mathbf{A}^{n-1} \end{bmatrix}; \quad \mathbf{P}_1 = [0 \ 0 \ \dots \ 1] \mathbf{Q}_c^{-1} \quad \dots(\text{V.8})$$

The state variable form (V.2) is said to be in the *controlled phase variable form*.



You have either reached a page that is unavailable for viewing or reached your viewing limit for this book.



You have either reached a page that is unavailable for viewing or reached your viewing limit for this book.



You have either reached a page that is unavailable for viewing or reached your viewing limit for this book.

where $\Delta = 1 - (G_1H_3 + G_2H_4 + G_3H_2 + G_4H_1 + G_1G_2H_1H_2 + G_3G_4H_3H_4) + G_1H_3G_2H_4 + G_3H_2G_4H_1$

C_1 is independent of R_2 if $H_2 = \frac{-G_4}{G_1G_2 - G_3G_4}$

C_2 is independent of R_1 if $H_1 = \frac{-G_3}{G_1G_2 - G_3G_4}$

2.16. $\frac{X(s)}{U(s)} = \frac{\beta_3(s^2 + \alpha_1s + \alpha_2) + \beta_2s + \beta_1}{s^2 + \alpha_1s + \alpha_2}$

3.1. 0.001, -1, -10

3.2. (b) 0.1, -15 volts, 53 volts (c) 25 volts, -30 volts

3.3. $|S_G^T| = 0.029, |S_H^T| = 1.02$

3.4. (a) 10% (b) 0.2%

3.6. (a) $\frac{5}{s^2(s+6)+10}$ (b) 0.5

3.7. 0.04 sec, $K = 0.1$

3.8. (a) $\omega_0(t) = 9.62(1 - e^{-130t})$

(b) $\omega_0(t) = 9.62(1 - e^{-5t})$

(c) For all ω ,

$$|S_{KA}^{\omega_0(\text{with fb})}| < |S_{KA}^{\omega_0(\text{without fb})}|$$

$$|S_{\omega_s}^{\omega_0(\text{with fb})}| < |S_{\omega_s}^{\omega_0(\text{without fb})}|$$

3.9. $\frac{K}{sRC + 1 + K}$; for all ω , $|S_R^T| \leq |S_R^G|$; time constant reduced by a factor $(1 + K)$ with feedback.

3.10. (i) $\frac{KK_c C_i / V}{s + (Q_0 + KK_c C_i) / V}$

(ii) Steady-state error is reduced by a factor $(Q_0 + KK_c C_i) / Q_0$ with feedback.

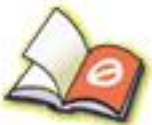
(iii) Steady-state error is reduced by a factor $(Q_0 + KK_c C_i^0) / Q_0$ with feedback.

3.12. (a) $\frac{-K_R K_f}{K_2 + K_f K_R}$

3.15. (a) 2×10^{-4} (b) -0.01 rad



You have either reached a page that is unavailable for viewing or reached your viewing limit for this book.



You have either reached a page that is unavailable for viewing or reached your viewing limit for this book.



You have either reached a page that is unavailable for viewing or reached your viewing limit for this book.

13.3. $x_1^2 + x_2^2 \leq 1$

13.4. The origin is asymptotically stable in-the-large.

13.5. $K > 0$

13.6. $-1 < K < 8$

13.7. The origin is asymptotically stable in-the-large.

13.8. The origin is asymptotically stable in-the-large

13.9. Nonlinear function is restricted to first and third quadrants.

14.1. $\alpha = 2$

14.2. $K_1 = 2, K_2 = 20$

14.3. $K = 4.63$

14.4. (i) $E(z) = \frac{z^3 - (a+1)z^2 + az}{z^3 + z^2(K-a-2) + z(1-K) - a}$

Use Table 13.2 to obtain J

(ii) $K > 0, -1 + \frac{K}{2} < a < 1$

14.5. $T^*(s) = \frac{200}{s^2 + 20s + 200}$

14.6. $D^*(z) = \frac{1.32(z - 0.368)}{(z + 3.33)}$

14.7. $u^*(z) = -0.236[x_1(t) + x_2(t)]$

14.8. (i) $K = 2$

(ii) $J_{\min} = 1.5$

(iii) $S_k^{\text{opt}} = 0.1$

14.10. (i) $K = \infty, J_{\min} = 0.5$

(ii) $K = 1, J_{\min} = 1$

14.11. (i) $K_1 = K_2 = \infty$

(ii) $K_1 = 1, K_2 = \sqrt{3}$

14.12. $u^*(k) = -[0.395 \quad 0.687] \begin{bmatrix} x_1(k) \\ x_2(k) \end{bmatrix}$

14.13. $u^*(0) = -0.177x(0)$

$u^*(1) = -0.177x(1)$

$u^*(2) = -0.177x(2)$

$u^*(3) = -0.164x(3)$

$u^*(k) = -0.177x(k)$ when $N \rightarrow \infty$

14.14. $u^*(0) = -0.8, u^*(1) = 0, u^*(2) = 0$



You have either reached a page that is unavailable for viewing or reached your viewing limit for this book.



You have either reached a page that is unavailable for viewing or reached your viewing limit for this book.

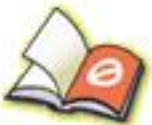


You have either reached a page that is unavailable for viewing or reached your viewing limit for this book.

INDEX



You have either reached a page that is unavailable for viewing or reached your viewing limit for this book.



You have either reached a page that is unavailable for viewing or reached your viewing limit for this book.

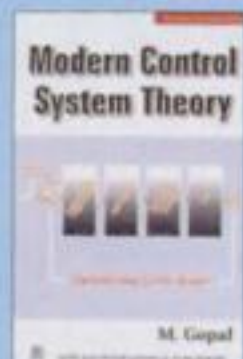


You have either reached a page that is unavailable for viewing or reached your viewing limit for this book.

Control Systems Engineering

FOURTH EDITION

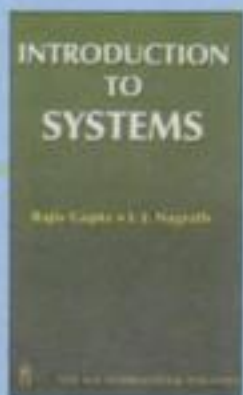
I.J. NAGRATH • M. GOPAL



ISBN 81-224-0503-7
Rs. 220.00



ISBN 0-85226-308-2
Rs. 220.00



ISBN 81-224-1599-7
Rs. 250.00

Modern Control System Theory (M. Gopal)

The book covers mainly two areas of modern control theory, namely; system theory, and multivariable and optimal control. Practical control problems from various engineering disciplines have been drawn to illustrate the potential concepts. Most of the theoretical results have been presented in a manner suitable for digital computer programming along with necessary algorithms for numerical computations.

Digital Control Engineering (M. Gopal)

The book presents control theory that is relevant to the analysis and design of Computer-Controlled Systems.

It also includes:

- Computer-aided-design package.
- Discusses basic characteristics of stepping motors and their associated drives.
- Three case studies on microprocessor-based control.

Introduction to Systems. (Rajiv Gupta, I.J. Nagrath)

Designed for an introductory course encompassing a wide variety of systems-physical, nonphysical and combination there of.

The salient features of the book are:

- Stress throughout on systems approach and systems thinking
- Modeling of all types of systems, a commonality of approach
- Analytico-qualitative approach for social systems
- Coverage extended to man-machines systems, expert systems, MIS, e-commerce, systems reliability

ISBN 81-224-1775-2



9 788122 417753



NEW AGE INTERNATIONAL (P) LIMITED, PUBLISHERS

(formerly Wiley Eastern Ltd.)

New Delhi • Bangalore • Chennai • Cochin • Guwahati • Hyderabad
Jalandhar • Kolkata • Lucknow • Mumbai • Ranchi

PUBLISHING FOR ONE WORLD

Visit us at www.newagepublishers.com